NTNU – Trondheim
Norwegian University of
Science and Technology

Disturbance Attenuation in Linear 2 x 2 Hyperbolic Systems

With Application to the Heave Problem in
Managed Pressure Drilling

Henrik Anfinsen

Master of Science in Engineering Cybernetics
Submission date: June 2013
Supervisor: Ole Morten Aamo, ITK

Norwegian University of Science and Technology
Department of Engineering Cybernetics

Problem Description

Many interesting problems in the oil and gas industry face the challenge of responding to disturbances from afar. Typically, the disturbance occurs at the inlet of a pipeline or at the bottom of an oil well, while sensing and actuation equipment is installed at the outlet, only. A new method for removing the effect of the disturbance at the inlet boundary by co-located output feedback control at the outlet boundary was recently derived in [1]. The topic of this project is to develop the method further in a number of directions. The following points should be addressed by the student:

Tasks:

1. Review relevant literature on the methods exploited in [1].
2. Extend the method in [1] to remove the effect of the disturbance at an arbitrary point in the domain.
3. Script an efficient code for computation of feedback and observer gains.
4. Apply the results to a model of the heave disturbance in managed pressure drilling.
5. Consider the resulting controller in the frequency domain, and consider model reduction schemes for obtaining rational approximations to it. Simulate to demonstrate performance.
6. Write a report.

Assignment given: 14. January 2013

Supervisor: Professor Ole Morten Aamo, ITK

[1] Aamo, O. M.: Disturbance rejection in 2 x 2 linear hyperbolic systems. *IEEE Transactions on Automatic Control*, Vol. 58, Issue 5, pages 1095-1106, 2013.

Problem Description

Preface

This Master Thesis is the final result from my five-year study at the Master of Technology program at the Norwegian University of Science and Technology (NTNU).

I would like to thank my supervisor Professor Ole Morten Aamo for suggesting the assignment and for his guidance throughout the semester. In addition, I would like to thank Associate Professor Rafael Vazquez at the Aerospace Engineering Department, University of Seville for valuable input and suggestions on solving the kernel equations, Torstein Thode Kristoffersen for feedback and Eli Johanne Mjellem for proofreading.

Trondheim, June 2013
Henrik Anfinsen

Abstract

Many physical systems can be modelled using linear 2×2 hyperbolic partial differential equations. The act of stabilizing systems of this type has therefore been subject to extensive research, and a number of techniques and feedback laws have been proposed in the literature. In this thesis, a full state feedback law for disturbance attenuation in such systems is derived, with actuation limited to the right boundary. The disturbance is modelled using an autonomous, finite dimensional linear system affecting the partial differential equation's left boundary. The effect of the disturbance is attenuated at an arbitrary given point in the domain. Two controller formulations of the feedback law is given, along with a considerable simplified controller derived subject to a few assumptions. The three controllers may be combined with an observer generating full state and disturbance estimates from sensing limited to the same boundary as actuation. Using the Laplace transform, the transfer functions of the three controllers combined with the observer are derived. A model reduction technique based on the Laguerre series representation is also given, so that rational, simple transfer function approximations can be found. The results are applied to the heave problem in Managed Pressure Drilling and tested through simulations. Both versions of the full state feedback law and the simplified one showed significant attenuation properties, both when using the system states directly, and when using the observer generated states. The attenuation properties of the reduced order transfer function approximations were also satisfactory in most cases. However, achieving a good transfer function match for the two full state feedback controllers deemed challenging, probably due to the apparent resonance terms observed in the original transfer functions. Rational transfer functions that approximated the original transfer functions well for the frequencies of interest were eventually found after some tuning. However, finding a good transfer function match when using the simplified controller was generally much easier, and a good match was quickly found for both the cases tested, without much tuning.

ABSTRACT

Sammendrag

Mange fysiske systemer kan modelleres ved hjelp av lineære 2×2 hyperbolske partielle differensiallikninger. Som følge av dette har det blitt skrevet mye om stabilisering av slike systemer, og flere metoder og reguleringslover har blitt foreslått. I denne mastertesen uteledes det en reguleringslov for støyundertrykkelse i slike systemer når regulatoren kun påvirker differensiallikningens høyre side. Forstyrrelsen modelleres som et autonomt, endeligdimensionelt lineært system som påvirker differensiallikninges venstre side. Støyen undertrykkes på et vilkårlig gitt punkt i domenet. To formuleringer av reguleringsloven blir gitt, i tillegg til en forenklet versjon som er gyldig under visse forutsetninger. De tre regulatorene kan så kombineres med en estimator som genererer system- og forstyrrelsesestimater fra målinger begrenset til samme side av den partielle differensiallikningen som aktuering. Ved hjelp av Laplacetransformasjon utledes transferfunksjonene til de tre kontrollerne sammen med estimatoren. En modellreduksjonsteknikk basert på Laguerre-rekker blir også presentert, slik at enkle, rasjonelle transferfunksjoner kan bli funnet. Resultatene anvendes så på hiv-problemet i Managed Pressure Drilling, og testes via simuleringer. Begge versjonene av reguleringsloven, samt den forenklede regulatoren, klarte å undertrykke støyen kraftig, både når systemtilstandene ble brukt direkte, og når tilstandene fra estimatoren ble brukt. De forenklede, rasjonelle tilpasningene ytet også tilfredsstillende, mens transferfunksjonstilpasningen for de to fulle reguleringslovene var vanskelig grunnet noe som så ut som resonans i systemet. Gode tilpasninger ble til slutt funnet etter en del parameterjusteringer. Å anvende modellreduksjonsalgoritmen på den forenklede regulatoren var derimot en del enklere, og gode tilpasninger ble funnet uten særlige parameterjusteringer.

SAMMENDRAG

Contents

List of Figures

List of Symbols

Sets

Variable	Description
C	Continuous functions.
C^1	Functions with continuous first derivatives.
$\mathbb{R}$	Real numbers.
$\mathbb{R}^+$	Positive real numbers, including zero.
$\mathbb{C}$	Complex numbers.
$\mathbb{Z}$	Integers.
$\mathbb{Z}^+$	Positive integers, including zero.

Hyperbolic system variables and parameters

Variable	Description
x	Domain variable.
t	Time variable.
$u(x,t), v(x,t)$	State variables.
$X(t)$	Disturbance variable.
$\epsilon_1(x)$, $\epsilon_2(x)$	System parameters.
$c_1(x)$, $c_2(x)$	System parameters.
A, C	Disturbance parameters.
q	Boundary condition constant.
$U(t)$	Actuation.
r	Controller objective constant.
$\bar{x}$	Disturbance attenuation coordinate.

Backstepping transformation variables and parameters

Variable	Description
$\alpha(x,t), \beta(x,t)$	Backstepping variables.
$V(t)$	Controller input.
$K^{ij}(x,\xi), \quad i,j \in \{u,v\}$	Forward transform kernels.
$L^{ij}(x,\xi), \quad i,j \in \{\alpha,\beta\}$	Backward transform kernels.

$\mathcal{T}$	Domain; $\{(x,\xi) \ : \ 0 \leq \xi \leq x \leq 1\}$.
$\mathcal{T}_0$	Domain; $\{(x,\xi) \ : \ 0 \leq x \leq \xi \leq 1\}$.

Controller parameters and functions

Variable	Description
$\phi_\alpha(z),\ \phi_\beta(z)$	Propagation time functions.
$\Phi_\beta(y,z),\ \Phi_\alpha(y,z)$	Functions relating two arbitrary points in the domain.
$\Psi_\beta(y),\ \Psi_\alpha(y)$	Functions relating the actuation to an arbitrary point in the domain.
$K_{psf}(\bar{x})$	Controller gain, pure state feedback controller.
$K_{rec}(\bar{x})$	Controller gain, recursive controller.
$K_\infty(\bar{x})$	Controller gain, simplified controller.
$\kappa_\alpha(x,\xi),\ \kappa_\beta(x,\xi)$	Time shift functions used in the pure state feedback controller.
$d_\alpha(\xi,\bar{x}),\ d_\beta(\xi,\bar{x}),\ d_{rec}(\bar{x})$	Time shift functions used in the recursive controller.
$\eta_\alpha(y),\ \eta_\beta(y)$	Time shift functions for relation to actuation.
$\Omega_\alpha(\xi,\bar{x}),\ \Omega_\beta(\xi,\bar{x})$	Disturbance shift functions, pure state feedback controller.
$L^\alpha(\bar{x},\xi),\ L^\beta(\bar{x},\xi)$	Linear combinations of the backward transform kernels.
$\delta(\xi,\bar{x},t)$	Conditional state variable.

Observer variables and parameters

Variable	Description
$\hat{u}(x,t), \hat{v}(x,t)$	State estimates.
$\hat{X}(t)$	Disturbance estimate.
$Y(t)$	Measurement; $u(1,t)$.
$P^{ij}(x,\xi),\ i,j \in \{u,v\}$	Observer kernels.
L	Gain matrix.
$p_1(x),\ p_2(x)$	Gain functions.

Transfer functions of hyperbolic systems

Variable	Description
$w(x,s)$	$\begin{bmatrix}\hat{u}(x,s) & \hat{v}(x,s)\end{bmatrix}^T$
$h_{XY}(s)$	Transfer function from $X(s)$ to $Y(s)$.
$D(s)$	Disturbance transfer function.

$\Theta(x,s)$	State space matrix for Laplace transformed observer states.
$\Upsilon(x)$	State space vector for Laplace transformed observer states.
$\Xi(x,x_0,s)$	Fundamental matrix.
$P(x,s)$	$\Xi(x,1,s)$
$Q(x,s)$	$\int_x^1 \Xi(x,\xi,s)\Upsilon(\xi)d\xi$
$M(s)$	$P(0,s)$
$N(s)$	$Q(0,s)$
μ	$\begin{bmatrix}1 & -q\end{bmatrix}^T$
$\varphi(s)$	$\mu^T M(s)/(CD(s)+\mu^T(M_1(s)+N(s)))$
$g_{rec}(\bar{x},s)$	Transfer function from $K_{rec}(\bar{x})X(s)$ to $V(s)$.

Laguerre-Gram algorithm

Variable	Description
α,γ	Algorithm parameters.
σ	$\frac{\gamma}{2}-\alpha$.
$\varpi(t)$	Exponential weighting function; $e^{-2\sigma}$.
$\langle f,g\rangle_\varpi$	Inner product; $\int_0^\infty \varpi(t)f(t)g(t)dt$.
$\|\|f\|\|_\varpi$	Norm; $\sqrt{\langle f,f\rangle_\varpi}$.
$L^2(\mathbb{R}^+)$	Space of square integrable function.
$L^2_\varpi(\mathbb{R}^+)$	Space derived from $\langle f,g\rangle_\varpi$.
$L_n(x)$	The nth Laguerre polynomial.
$l_n(t;\alpha,\gamma)$	The nth Laguerre function.
$q_n(\alpha,\gamma)$	Laguerre coefficients.
ϵ_N	Error emerging from truncating the Laguerre series after N terms.
$\mathcal{H}_\alpha$	A linear operator on orthogonal functions.
$\lambda(n)$	Nonnegative, monotonously increasing function related to $\mathcal{H}_\alpha$.
$G_\epsilon(\alpha)$	A function estimating the error.
w	Möbius transformation; $(s-\gamma+\alpha)/(s-\alpha)$.
r	Desired order for the reduced order model.

MPD system parameters

Variable	Description
z	Domain variable.
t	Time variable.
$p(z,t)$	Pressure.

$q(z,t)$	Volumetric flow.
$Z(t)$	Heave disturbance.
β	Bulk modulus.
A_1	Annulus' cross sectional area.
A_2	Drill bit's cross sectional area.
ρ	Mud density.
l	Length of well.
F_1	Friction factor.
g	Gravity constant.
$p_l(t)$	Actuation.
n	Number of frequency components in disturbance.
$\omega_i,\ i \in \{1,\ldots,n\}$	Angular velocities in the heave disturbance.
$\bar{A}, \bar{C}$	Heave motion parameters.
p_{sp}	Pressure set point.
$\bar{z}$	Coordinate of pressure fluctuation attenuation.

MPD ported to standard form

Variable	Description
ϵ	$\frac{1}{l}\sqrt{\beta/\rho}$
γ	$\frac{lF_1}{\sqrt{\beta\rho}}$
c_0	$-\frac{1}{2}\frac{F_1}{\rho}$
a_0	$c_0 e^{-\gamma\bar{x}}$
b_0	$c_0 e^{\gamma\bar{x}}$

Transfer functions of MPD system

Variable	Description
$H(x)$	Exponential scaling matrix; diag$\{e^{-\frac{\gamma}{2}x}, e^{\frac{\gamma}{2}x}\}$.
V	Scaling matrix; diag$\{-1, 1\}$.
$\Theta_0(s)$	Simplified state space matrix; $\Theta(x,s) = H(x)\Theta_0(s)H^{-1}(x)$.
$\bar{w}(x,s)$	Scaled observer states; $H(x)w(x,s)$.

List of Abbreviations

ABP	Applied Back Pressure
BC	Boundary Condition
BHP	Bottom Hole Pressure
BVP	Boundary Value Problem
DAE	Differential Algebraic Equation
DFT	Discrete Fourier Transform
FFT	Fast Fourier Transform
IVP	Initial Value Problem
MPD	Managed Pressure Drilling
ODE	Ordinary Differential Equation
PDE	Partial Differential Equation
p.s.f.	Pure state feedback

Subscripts

psf	Pure state feedback
rec	Recursive
sp	Set point

LIST OF ABBREVIATIONS

Part I

Background

Chapter 1

Introduction

1.1 Motivation

The specific class of systems described by linear 2×2 partial differential equations (PDEs) of hyperbolic type has attracted considerable attention due to the many examples of physical systems that can be modelled that way. Among such systems are open channels (Gugat and Leugering (2003) de Halleux, Prieur, Coron, d'Andrea Novel, and Bastin (2003)), road traffic (Goatin (2006)), gas flow pipelines (Gugat and Dick (2011)) and transmission lines (Curró, Fusco, and Manganaro (2011)). Although the theory concerned in this thesis has many potential areas of applications, the main motivations are those faced during drilling operations in the oil and gas industry. During these operations, the act of responding to disturbances is frequently a highly challenging task, due to the often very long distances between the entering point of the disturbance and the actuation and sensing equipment. An example is *the heave problem in Managed Pressure Drilling*, which can be modelled using linear 2×2 hyperbolic PDEs.

When drilling, a drilling fluid called "mud" is pumped down through the drill string, through the drill bit at the bottom of the well and up the annulus around the drill string. The mud does not only carry cuttings out of the system, but it also cools down the drill bit and works keeps pressure in the annulus at a desired level. This latter function is crucial, as the pressure needs to be kept within certain bounds to avoid a fracturing of the formation and a possible collapse of the well. *Managed Pressure Drilling* (MPD) is an umbrella term for technologies developed with the aim of improving the pressure control throughout the well. One of the most common MPD technology is Applied Back Pressure (ABP) drilling (Hannegan (2006)), which is characterized through that it closes the annulus section of the well and controls

the pressure within by restricting the return flow, using a choke. The back pressure can easily be changed by adjusting the choke opening, and a back pressure pump allows the pressure to be controlled even when the main mud pump is stopped.

The heave problem in MPD emerges when drilling offshore from a floating rig. The rig will naturally move up and down with the waves, and during drilling, an active mechanism is used to decouple the drill string from the rig, to prevent the string from moving with the waves. However, every 27-29 metres, it is necessary to extend the drill string by a drill string connection. During this procedure, the drilling is stopped, the heave compensation mechanism is deactivated and the string is rigidly attached to the rig. The drill string is therefore forced to move with the rig, acting as a piston on the mud in the well. Left uncompensated, this piston effect results in severe pressure fluctuations throughout the well, often exceeding the standard limits for pressure regulation accuracy in MPD, which are about ± 2.5 bar according to Godhavn (2010). It should, however, be possible to compensate the pressure fluctuation in the annulus by adjusting the pressure using ABP technology. The main problem is that sensing and actuation equipment is situated topside, while the disturbance and the control point of interest is situated down the well, potentially several kilometres from the actuation and sensing point. This complicates the control problem greatly, since the pressure and flow dynamics in the well will have to be modelled and taken account for in the control law.

Traditional MPD has focused on maintaining a constant bottom hole pressure (BHP), and active compensation for attenuation of the BHP fluctuations caused by heaving has already been achieved in Aamo (2013). This was achieved through modelling the oil well as a transmission line, and applying an infinite-dimensional backstepping transformation originally derived for the general class of systems described by linear 2×2 hyperbolic PDEs. There may, however, be situations where the pressure regulation at *other points in the well* is of interest, e.g. at the bottom of a casing string (also known as a *casing-shoe*).

Although the main motivation for this thesis is the heave problem in MPD, the disturbance attenuation problem - mathematically posed in Section 3.1 - is addressed for the general class of systems described by linear 2×2 hyperbolic partial differential equations.

1.2 Previous work

Linear 2×2 hyperbolic PDEs have, due to the wide range of practical applications, been subject to extensive research, and a number of techniques for controlling them have been proposed in the literature. Methods include using control Lyapunov functions (Coron, d'Andrea Novel, and Bastin (2007)), Riemann invariants (Greenberg and Tsien (1984)) and frequency domain approaches (Litrico and Fromion (2006)).

A more recently developed method for control of PDEs is the *Backstepping method*. The backstepping method in finite dimensions is a well known method from nonlinear control theory (Khalil (2002, Sec. 14.3), Kokotović (1992)) and is based on the design of diffeomorphisms to transform the problem into a new equivalent system with a nested structure that is far easier to stabilize. The backstepping method proceeds by designing a controller which stabilized the inner subsystems, and gradually "backs out", designing new controllers that in turn stabilize the outer subsystems before the overall system is stabilized. The backstepping method applied to partial differential equations, on the other hand, was first developed for PDEs of the parabolic type (Krstić and Smyshlyaev (2008)). A backstepping-like transformation was developed and used to stabilize an unstable heat equation in Bosković, Krstić, and Liu (2001). It was based on the same principles as in the finite-dimensional case, with the nested subsystems emerging from discretization of the PDE into a finite number of control volumes. A controller was designed for the innermost control volume, before gradually "backing out" and simultaneously extending the controller for stabilization of the remaining control volumes. The method derived in Bosković et al. (2001) was, however, restricted to systems with a number of open-loop unstable eigenvalues no more than one. This was stressed further in Balogh and Krstić (2002), where an arbitrary level of instability was allowed by using the backstepping method on a semi-discretized version of the system making the close loop system stable. The method involved recursively solving a series of equations for the unknown controller gains - frequently referred to as *kernels* - used in the backstepping, but numerical computations showed that the kernels contained discontinuities as an artifact of the discretization method used. The number of discontinuities would tend towards infinity as the discretization grid cell size approached zero.

In Liu (2003), the first version of the backstepping method in its *infinite-dimensional* form was presented. The method from Balogh and Krstić (2002) was here improved by expressing the integration kernels as solutions to PDEs. (On the other hand, the boundary conditions for the kernel PDEs were, inby Liu's own words, *strange*.) The method has since then been applied to, among

others, fluid flows (Aamo, Smyshlyaev, Krstić, and Foss (2004)) and nonlinear parabolic equations (Vazquez and Krstić (2008a) and Vazquez and Krstić (2008b)), and has even been extended to adaptive versions (Smyshlyaev and Krstić (2010)).

The method has later been derived for application on hyperbolic systems: in Krstić and Smyshlyaev (2008) on first order hyperbolic systems; in Smyshlyaev, Cerpa, and Krstić (2010) on second order systems; and in Vazquez, Krstić, and Coron (2011b) on two coupled first order equations. Most relevant to this thesis are the results in Krstić and Smyshlyaev (2008) and Vazquez et al. (2011b), which were used in Aamo (2013) to derive a full state feedback law for disturbance attenuation on the left boundary by control actuation from the right boundary, for the same type of systems considered in this thesis. The full state feedback law was combined with a state observer to create an output feedback law, with sensing also limited to the right boundary. The extension of the method from Aamo (2013) for disturbance attenuation in the interior domain has, to the best of our knowledge, not previously been addressed.

The heave problem in MPD in itself has been addressed in Landet, Pavlov, and Aamo (2013), using a lumped model and simplifying assumptions with regards to available measurements. It was also investigated in Mahdianfar, Aamo, and Pavlov (2012), where a linearization technique that neglected the friction terms, omitting the need to perform a backstepping transformation, was used.

1.3 Scope and emphasis

Firstly, we will seek to derive a control law for disturbance attenuation at an arbitrary point in the interior domain of 2×2 linear hyperbolic PDEs with spatially varying coefficients. The control law will also be combined with an observer that generates estimates of the states in the system from sensing on one end only, for practical implementation where sensing is often limited to the same boundary as actuation. Secondly, when considered as one single unit, the controller and observer together constitutes to one system with a single input; the measurement, and a single output; the control signal. By considering the lumped controller and observer in the frequency domain, a transfer function linking the input and output is derived. A Laguerre-Gram based model order reduction technique is then presented for generating rational approximations from irrational transfer functions, with the purpose of finding rational approximations of the combined controller and observer transfer functions.

The results are applied to and tested through simulations on the heave problem from Managed Pressure Drilling.

1.4 Outline and notation

Clarification of notations used throughout the thesis is in order. Firstly, by default, all vectors are column vectors. The exceptions are some controller gains which share notion with previous literature. Definitions are stated using a colon and an equality sign; $a := b$ means that a, by definition, equals b. The term *kernel* is a function acting as a gain, and is often evaluated through an integral. A function's Laplace transform is usually denoted using the same notation as the original time-dependent function, i.e. denoting $f(t)$ and $f(s)$ for the time domain and frequency domain representations of the function f, respectively. When this is the case, it should be obvious from the independent variable whether it is the time domain or frequency domain function. Derivatives are interchangeably denoted using subscripts or the standard Leibniz notation (i.e. x_t and dx/dt, respectively). For monovariable functions, the derivative is usually denoted using primes (i.e. $f'(t)$ and $f''(t)$ for the first and second order derivative, respectively), or a dot when the derivative is taken with respect to time (i.e. $\dot{x}$). For some general set $\mathbb{F}$, the notation $\mathbb{F}^n$ means the set of vectors of dimension n with components from $\mathbb{F}$. Similarly, the notation $\mathbb{F}^{m\times n}$ means the set of matrices with m rows and n columns, with elements from $\mathbb{F}$.

The thesis is separated into four parts. The first part consists of Chapters 1–2 and acts as an introduction. In Chapter 2, a short introduction to partial differential equations is given. Some common solution methods are also briefly presented. For readers familiar with partial differential equations, this chapter may be omitted. Part II consists of Chapters 3–6 and contains the theoretical contributions. Controllers with the desired properties are derived in Chapter 3, while a state observer is presented in Chapter 4. In Chapter 5, the transfer functions of the controllers, observer and combined system are derived, with a model order reduction algorithm presented in Chapter 6. The theory derived in part II is applied to the heave problem in Managed Pressure Drilling in Part III, which consists of Chapter 7–8. In Chapter 7, the theory is ported to a model for the heave problem in MPD, before simulations are performed in Chapter 8. The results are discussed and commented as they are presented. Part IV offers some concluding remarks and some suggested areas for further work in its Chapter 9. The appendices offer some additional lemmas, material, transfer function approximations and plots from simulations. A description of the folders and files on the

accompanying disc is also given, as well as a journal paper based on material derived in Chapter 3.

Chapter 2

An introduction to PDEs

2.1 Introduction

This chapter presents some relevant background material concerning partial differential equations, with emphasis on the type of PDEs encountered in this thesis. A brief overview of common solution methods is also given.

2.2 What are PDEs?

A *partial differential equation* (PDE) is an equation involving one or more partial derivatives of a function u, that depends on two or more *independent* variables (Kreyszig (2010, Sec. 12.1)) An *ordinary* differential equation (ODE), on the other hand, depends on a single variable only. Partial differential equations can generally be stated

$$F\left(x_1, x_2, \dots x_n, u, u_{x_1}, u_{x_2}, \dots u_{x_n}, u_{x_1x_1}, u_{x_1x_2}, \dots u_{x_1x_n}, \dots\right) = 0. \tag{2.1}$$

for some function u in the independent variables x_1, ..., x_n. A simple example of a PDE can be

$$u_t + u_{xx} = 0 \tag{2.2}$$

for some function $u(x,t)$ in two variables x and t.

The *order* of a differential equation is that of the highest order derivative that appears in the equation. The example PDE in (2.2) is of order 2. By a *domain*, we mean the set of independent variables on which the unknown function is defined. By a *boundary*, we mean the set of values at the domain's border. The boundary is often denoted $\partial\mathcal{D}$ for a domain $\mathcal{D}$. By the *interior domain*, we mean the whole domain except the boundary. By a *solution* of a PDE over some region $\mathcal{H}$ contained in $\mathcal{D}$, we mean a function u that has all

the partial derivatives appearing in the PDE in the domain $\mathcal{H}$, and satisfies the PDE everywhere in $\mathcal{H}$. A solution to (2.2) could for instance be

$$u(x,t) = 2t - x^2. \tag{2.3}$$

We call a PDE problem *well-posed* if (Renardy and Rogers (2004, Sec. 1.1.5)):

1. There exists a solution.
2. The solution is unique.
3. The solution depends continuously on the data.

where the phrase "depends continuously on the data" means that the solution's behaviour do not make a discontinuous change following a slight change in the initial conditions. If the problem fails to be well-posed, it is said to be *ill-posed*.

2.3 Boundary and initial conditions

PDEs generally have lots of solutions. The solutions of interest are usually singled out by imposing *initial conditions*, that is, conditions the solution must to satisfy at some given point (or set of points) in the domain. The PDE problem is then usually termed an *initial value problem* (IVP), a term also commonly used for ODEs. An example of an initial condition for (2.2) could be

$$u(x,0) = f(x) \tag{2.4}$$

for some monovariable function $f(x)$.

A *boundary condition* (BC) is an additional restraint the solution must satisfy at the domain's boundary. This forms *boundary value problems* (BVPs). Consider a function $u(x,t)$ defined over some domain $\mathcal{D}$. The three most common types of BCs, are (Kreyszig (2010, p. 564)):

1. A *Dirichlet* BC specifies the values a solution needs to take on the boundary of the domain, for instance

$$u(0,t) = 0, \quad t \geq 0. \tag{2.5}$$

2. A *Neumann* BC specifies the values the derivative of a solution needs to take on the boundary of the domain, e.g.

$$u_x(0,t) = 0, \quad t \geq 0. \tag{2.6}$$

3. *Robin* (or *mixed*) BCs are combinations of the Direchlet and Neumann type BCs, for instance

$$u(0,t) + u_x(0,t) = 0, \quad t \geq 0. \tag{2.7}$$

The Dirichlet type BC is the one most relevant for this thesis.

2.4 Linearity, quasilinearity and nonlinearity

As with common algebraic equations, differential equations are often categorized into linear and nonlinear. A PDE (2.1) is termed *linear* if F is a function linear in $u(x_1 \dots x_n)$ and it's derivatives. As an example; a linear PDE of order one for a function $u(x,t)$ may be written on the form:

$$a(x,t)u_x + b(x,t)u_t + c(x,t)u + d(x,t) = 0 \tag{2.8}$$

An example is the PDE

$$u + e^x(1 + \sin(t))u_x + u_t = 0. \tag{2.9}$$

Note here that the coefficients preceding u or its derivatives can be functions nonlinear in the *independent variables*. The PDE

$$(u_x)^2 + u_t = 0 \tag{2.10}$$

however, is not linear. If a PDE of order k is linear in its kth derivatives, with coefficients allowed to be functions of u and the less-than-kth derivatives of u, then the PDE is said to be *quasilinear*. An example is the inviscid Burgers' equation (Olver, 2013, Eq. (9.64))

$$u_t + uu_x = 0 \tag{2.11}$$

A PDE which is neither linear nor quasi-linear is said to be *nonlinear*.

2.5 Systems of PDEs

By a system of PDEs, we mean a collection of one or more partial differential equations where all the functions depend on the same set of variables. The order of the system is the highest order derivative occurring in *any* of its equations (Olver (2013, p. 3)). Systems of first order PDEs are common, and when referring to systems of first order PDEs being of a certain *dimension*, we mean the number of first order PDEs in the overall system. A system of

n first order linear PDEs with independent variables x and t can be stated in matrix form

$$A(x,t)u_t(x,t) + B(x,t)u_x(x,t) = C(x,t)u(x,t) + F(x,t) \tag{2.12}$$

for the vector of system states

$$u(x,t) = \begin{bmatrix} u_1(x,t) & u_2(x,t) & \dots & u_n(x,t) \end{bmatrix}^T \tag{2.13}$$

and a function $f(x,t)$ independent of the states in $u(x,t)$. When referring to a system of PDEs being $n \times n$ linear, the $n \times n$ refers to size of the matrix $A(x,t)$ (or $B(x,t)$) in (2.12).

2.6 Classes of second order PDEs

Second-order PDEs are often categorized into different classes telling something about its general behaviour. Consider the general form for a second order linear PDE for a function $u(x,y)$ in two variables x and y as follows

$$a(x,t)u_{xx} + 2b(x,t)u_{xt} + c(x,t)u_{tt} = f(x,t,u_x,u_t). \tag{2.14}$$

Define the quantity *discriminant* as (Kreyszig (2010, p. 555))

$$\Delta(x,t) := b^2(x,t) - a(x,t)c(x,t). \tag{2.15}$$

At the point (x,t), the PDE is called

1. *Hyperbolic* if $\Delta(x,t) > 0$. An example is the *one-dimensional wave equation*
$$u_{tt} = c^2 u_{xx}. \tag{2.16}$$

2. *Parabolic* if $\Delta(x,t) = 0$ and $a(x,t)$, $b(x,t)$, $a(x,t)$ are not all zero. An example of a PDE of the parabolic type is the *one-dimensional heat equation*
$$u_t = k \cdot u_{xx}. \tag{2.17}$$

3. *Elliptic* if $\Delta(x,t) < 0$. An example is the *two-dimensional Poisson equation*
$$u_{xx} + u_{yy} = -f \tag{2.18}$$
where $f = f(x,y)$ is a function. For the special case of $f \equiv 0$, this equation reduces to *two-dimensional Laplace's equation.*

4. *Singular* if $a(x,t) = b(x,t) = c(x,t) = 0$.

I these examples, taken from Kreyszig (2010, Eq. (1)-(4), Sec. 12.6), the term *dimension* refer to the number of coordinates (time t not included). As the discriminant generally can vary with the independent variables, the class may change throughout the domain. The PDE is then said to be of *mixed type*.

Equation (2.14) can be written as a 2×2 linear system of first order PDEs by defining

$$v := \begin{bmatrix} u_t \\ u_x \end{bmatrix} \tag{2.19}$$

with

$$A(x,t) := \begin{bmatrix} a(x,t) & b(x,t) \\ 0 & -1 \end{bmatrix} \tag{2.20}$$

and

$$B(x,t) := \begin{bmatrix} b(x,t) & c(x,t) \\ 1 & 0 \end{bmatrix}. \tag{2.21}$$

This yields

$$A(x,t)v_t(x,t) + B(x,t)v_x(x,t) = f(x,t,v). \tag{2.22}$$

The class is then determined from the expression of the solutions λ to (Byrne (2012, Eq. (2.20)))

$$\det(\lambda A - B) = 0, \tag{2.23}$$

where the discriminant (2.15) appears under the square root.

2.7 Solution methods

Finding an analytical solution to a given PDE is not a trivial task, it is often even impossible. There are, however, a few special cases where the exact solution may be found. We will here present the most common methods, as well as some numerical methods.

2.7.1 Separation of variables

This method (Kreyszig (2010, Sec. 12.3)) is also known as the product method, and is based on the assumption that the solution can be separated to be the product of monovariable functions from which simple ODEs can be formed. As an example, consider the heat equation (2.17)

$$u_t = k \cdot u_{xx}. \tag{2.24}$$

By the separation of variables method, we assume $u(x,t)$ can be written as a product

$$u(x,t) = F(x)G(t). \tag{2.25}$$

Inserting (2.25) into (2.24) and rearranging, we obtain

$$\frac{F''(x)}{F(x)} = \frac{1}{k}\frac{G'(t)}{G(t)} \tag{2.26}$$

As both the left and right hand sides are functions of independent variables, both expressions must equal the same constant, say $-\lambda$, yielding

$$\frac{F''(x)}{F(x)} = -\lambda, \quad \frac{1}{k}\frac{G'(t)}{G(t)} = -\lambda. \tag{2.27}$$

Thus, we've reduced the single PDE (2.24) into two ODEs. The solution (2.24) is thus found from the solutions to (2.27) as

$$u(x,t) = e^{-k\lambda t}(A\sin(\sqrt{\lambda}x) + B\cos(\sqrt{\lambda}x)) \tag{2.28}$$

for some constants A and B.

2.7.2 Method of Characteristics

The method of characteristics discovers curves, often named the *characteristic curves* or just *characteristics*, along which the PDE becomes an ordinary differential equation (ODE). The resulting ODEs can be integrated to find the solution, or to form integral-equations. As an example, consider the following linear PDE with constant coefficients in the derivatives

$$au_t + bu_x = f(x)u(x,t) \tag{2.29}$$

with initial condition $u(x,0) = u_0(x)$ where $f(x,t)$ and $u_0(x)$ are given, known functions. Consider the characteristic curves, or actually *lines* in this case, $x_u(x,t,s)$ and $t_u(x,t,s)$ of x and t is s, respectively, chosen so that

$$\frac{\partial x_u}{\partial s} = a, \quad \frac{\partial t_u}{\partial s} = b, \tag{2.30}$$

the derivative of $u(x,t)$ with respect to s then can be written

$$\frac{d}{ds}u(x_u(x,t,s), x_u(x,t,s)) = u_t\frac{\partial t_u}{\partial s} + u_x\frac{\partial x_u}{\partial s} = au_t + bu_x. \tag{2.31}$$

Hence

$$\frac{d}{ds}u(x_u(x,t,s), x_u(x,t,s)) = f(x_u(x,t,s))u(x_u(x,t,s), x_u(x,t,s)) \tag{2.32}$$

Thus, the PDE has be reduced to an ODE. Integration from $s = s_1$ to $s = s_2$ yields

$$u(x_u(x,t,s_2),t_u(x,t,s_2)) = u(x_u(x,t,s_1),t_u(x,t,s_1)) + \int_{s_1}^{s_2} f(x_u(x,t,s))u(x_u(x,t,s),t_u(x,t,s))ds \quad (2.33)$$

By additionally choosing the characteristic lines so that $x_u(x,t,s_2) = x$ and $t_u(x,t,s_2) = t$ for some s_2, and $t_u(x,t,s_1) = 0$ for some s_1, we obtain

$$u(x,t) = u_0(x_u(x,t,s_1)) + \int_{s_1}^{s_2} f(x_u(x,t,s))u(x_u(x,t,s),t_u(x,t,s))ds \quad (2.34)$$

which, generally is an inhomogeneous Volterra (or possibly Fredholm) equation of the second kind (see Appendix (B.1)). Several numerical methods for solving equations like these exist in the literature, including forming Taylor series (Yalçinbaş (2002)), homotopy perturbations (Ghasemi, Kajani, and Babolian (2007)), block pulse functions (Jiang and Schaufelberger (1992)) or, more recently, triangular functions (Babolian, Masouri, and Hatamzadeh-Varmazyar (2009)).

Another method is based on forming a sequence of successive approximations, which, for instance, was used by Vazquez, Coron, Krstić, and Bastin (2011a) in conjunction with Banach's fixed point Theorem (Banach (1922), Ciesielski (2007)) to prove existence of solutions for a family of PDEs. The method goes as follows; assume one has an integral equation on the form

$$u(x,t) = f(x,t) + F[u](x,t) \quad (2.35)$$

where $f(x,t)$ is a known function, and F is an operator on u involving integrals. One proceed by forming a sequence

$$u^0(x,t) = f(x,t) \quad (2.36)$$

$$u^{n+1}(x,t) = f(x,t) + F[u^n](x,t) \quad n \geq 0. \quad (2.37)$$

Provided (2.35) has a unique solution, the sequence formed by (2.37) will converge to it as $n \to \infty$. (See e.g. Kreyszig (2010, p. 42) or Tricomi (1957, p. 53).)

2.7.3 Laplace transform

The well-known Laplace transform may be used to solve PDEs. When applying the Laplace transform to one of the two variables (usually time t)

of a dual-variable PDE, the system of PDEs is transformed to a system of ODEs. The ODEs may for instance be solved using the variation of constants method as stated in Lemma A.4 in Appendix A.4. Taking the inverse Laplace transform of this solution yields the solution to the original problem. As an example, consider the very simple PDE

$$z_t(x,t) = -z_x(x,t), \quad x \in [0,L], \quad t \geq 0 \tag{2.38}$$

with boundary condition

$$z(0,t) = f(t) \tag{2.39}$$

for some known function $f(t)$ which Laplace transform $f(s) := \mathcal{L}\{f(t)\}$ is assumed to exist. Laplace transforming (2.38) with respect to t yields

$$sz(x,s) = -z_x(x,s). \tag{2.40}$$

This equation is an ODE in the variable x, which may be integrated to yield

$$\ln|z(x,s)| = -sx(x,s) + C \tag{2.41}$$

for some constant C. Solving this with respect to $z(x,s)$ and inserting the boundary condition (2.39) gives

$$z(x,s) = f(s)e^{-xs}. \tag{2.42}$$

Taking the inverse Laplace transform of this yields

$$z(x,t) = f(t-x) \tag{2.43}$$

hence, the PDE (2.38) holds time-delayed versions of the signal $f(t)$.

2.7.4 Numerical methods

A brief overview of common numerical methods is given here. Consult the accompanying references for more information.

2.7.4.1 Finite Element methods

The Finite Element method (Babuška, Banerjee, and Osborn (2004)) is an umbrella term for all methods dividing the domain into several smaller subdomains, termed finite elements, with many simple element equations to approximate the solution over a larger domain.

2.7.4.2 Finite Difference method

The Finite Difference method (Strikwerda (2004)) splits the domain into a finite dimensional grid, and approximate the derivatives by finite differences of the grid values. The results are a series of algebraic equations which may be solved using standard methods.

2.7.4.3 The Method of Lines

When using The Method of Lines (Schiesser (1991), Hamdi, Schiesser, and Griffiths (2007)), all but one (usually time) spatial variables are discretized using a finite difference method. The resulting system of ODEs and Differential Algebraic equations (DAEs) can be solved using standard numerical methods on a computer. The method requires the PDE to be well-posed as an initial value problem, as ODE and DAE solvers are IVP solvers.

Part II

Disturbance attenuation

Chapter 3

Controller design

3.1 Introduction

In this thesis, we consider systems described by linear 2×2 first order hyperbolic PDEs with spatially varying coefficients of the same type as considered in Aamo (2013). They can be states as

$$u_t(x,t) = -\epsilon_1(x)u_x(x,t) + c_1(x)v(x,t) \tag{3.1a}$$
$$v_t(x,t) = \epsilon_2(x)v_x(x,t) + c_2(x)u(x,t) \tag{3.1b}$$
$$u(0,t) = qv(0,t) + CX(t) \tag{3.1c}$$
$$v(1,t) = U(t) \tag{3.1d}$$
$$\dot{X}(t) = AX(t) \tag{3.1e}$$

where $x \in [0,\ 1]$, $t \geq 0$, $0 < \epsilon_1(x), \epsilon_2(x) \in C^1([0,1])$, $c_1(x), c_2(x) \in C([0,1])$ and $q \neq 0$. $X(t) \in \mathbb{R}^n$ can be considered a disturbance described by $A \in \mathbb{R}^{n\times n}$, $C \in \mathbb{R}^{1\times n}$, with the pair (A, C) observable. $U(t)$ is the actuation and $u(1,t)$ is assumed measured. With $x = 0$ denoted the *left boundary* and $x = 1$ the *right boundary*, the variable $u(x,t)$ represents information that travels from left to right, and $v(x,t)$ information that travels from right to left. The system is well posed since $u(x,t)$ has a boundary condition on the left and $v(x,t)$ has a boundary condition on the right (Russell (1978)). The control objective is to design $U(t)$ so that

$$u(\bar{x},t) = rv(\bar{x},t) \tag{3.2}$$

is achieved for some given, fixed $\bar{x} \in (0,\ 1)$.

We will start in Section 3.2 by decoupling (3.1a)–(3.1b) into two new subsystems only connected through a boundary condition (and not in the PDEs). In Sections 3.3 and 3.4 we establish properties of the solutions, before

the main controller for disturbance attenuation at an arbitrary point in the domain, assuming full state information is available, is derived in Section 3.5. In Section 3.6, an alternative formulation of the controller that facilitates for frequency analysis later in this thesis is derived, before a considerably simplified controller is derived subject to a few assumptions in Section 3.7.

3.2 Decoupling

We seek a coordinate transformation decoupling (3.1a)–(3.1b) into two new, decoupled subsystems. This was achieved in Aamo (2013) using the following infinite-dimensional backstepping transformation

$$\alpha(x,t) = u(x,t) - \int_0^x K^{uu}(x,\xi)u(\xi,t)d\xi - \int_0^x K^{uv}(x,\xi)v(\xi,t)d\xi \tag{3.3a}$$
$$\beta(x,t) = v(x,t) - \int_0^x K^{vu}(x,\xi)u(\xi,t)d\xi - \int_0^x K^{vv}(x,\xi)v(\xi,t)d\xi \tag{3.3b}$$

in conjunction with the controller

$$U(t) = \int_0^1 K^{vu}(1,\xi)u(\xi,t)d\xi + \int_0^1 K^{vv}(1,\xi)v(\xi,t)d\xi + V(t), \tag{3.4}$$

yielding the following decoupled system

$$\alpha_t(x,t) = -\epsilon_1(x)\alpha_x(x,t) - \epsilon_1(0)K^{uu}(x,0)CX(t) \tag{3.5a}$$
$$\beta_t(x,t) = \epsilon_2(x)\beta_x(x,t) - \epsilon_1(0)K^{vu}(x,0)CX(t) \tag{3.5b}$$
$$\alpha(0,t) = q\beta(0,t) + CX(t) \tag{3.5c}$$
$$\beta(1,t) = V(t) \tag{3.5d}$$
$$\dot{X}(t) = AX(t). \tag{3.5e}$$

The kernels in (3.3), (3.5a), (3.5b) were given as the solution to the following system of PDEs

$$\epsilon_1(x)K^{uu}_x(x,\xi) + \epsilon_1(\xi)K^{uu}_\xi(x,\xi) = -\epsilon_1'(\xi)K^{uu}(x,\xi) - c_2(\xi)K^{uv}(x,\xi) \tag{3.6a}$$
$$\epsilon_1(x)K^{uv}_x(x,\xi) - \epsilon_2(\xi)K^{uv}_\xi(x,\xi) = \epsilon_2'(\xi)K^{uv}(x,\xi) - c_1(\xi)K^{uu}(x,\xi) \tag{3.6b}$$
$$\epsilon_2(x)K^{vu}_x(x,\xi) - \epsilon_1(\xi)K^{vu}_\xi(x,\xi) = \epsilon_1'(\xi)K^{vu}(x,\xi) + c_2(\xi)K^{vv}(x,\xi) \tag{3.6c}$$
$$\epsilon_2(x)K^{vv}_x(x,\xi) + \epsilon_2(\xi)K^{vv}_\xi(x,\xi) = -\epsilon_2'(\xi)K^{vv}(x,\xi) + c_1(\xi)K^{vu}(x,\xi) \tag{3.6d}$$

with boundary conditions

$$K^{uu}(x,0) = \frac{\epsilon_2(0)}{q\epsilon_1(0)} K^{uv}(x,0) \tag{3.7a}$$

$$K^{uv}(x,x) = \frac{c_1(x)}{\epsilon_1(x)+\epsilon_2(x)} \tag{3.7b}$$

$$K^{vu}(x,x) = -\frac{c_2(x)}{\epsilon_1(x)+\epsilon_2(x)} \tag{3.7c}$$

$$K^{vv}(x,0) = \frac{q\epsilon_1(0)}{\epsilon_2(0)} K^{vu}(x,0) \tag{3.7d}$$

defined over the triangular domain

$$\mathcal{T} = \{(x,\xi) \ : \ 0 \le \xi \le x \le 1\}. \tag{3.8}$$

The transformation (3.3) was originally derived in Vazquez et al. (2011b) and used for state feedback stabilization of (3.1) in the case without disturbance ($X(t) \equiv 0$). The inverse of (3.3) was also given in Vazquez et al. (2011b) as

$$u(x,t) = \alpha(x,t) + \int_0^x L^{\alpha\alpha}(x,\xi)\alpha(\xi,t)d\xi + \int_0^x L^{\alpha\beta}(x,\xi)\beta(\xi,t)d\xi \tag{3.9a}$$

$$v(x,t) = \beta(x,t) + \int_0^x L^{\beta\alpha}(x,\xi)\alpha(\xi,t)d\xi + \int_0^x L^{\beta\beta}(x,\xi)\beta(\xi,t)d\xi \tag{3.9b}$$

where the kernels were given as the solution to the system of PDEs

$$\epsilon_1(x)L_x^{\alpha\alpha}(x,\xi) + \epsilon_1(\xi)L_\xi^{\alpha\alpha}(x,\xi) = -\epsilon_1'(\xi)L^{\alpha\alpha}(x,\xi) + c_1(x)L_\xi^{\beta\alpha}(x,\xi) \tag{3.10a}$$

$$\epsilon_1(x)L_x^{\alpha\beta}(x,\xi) - \epsilon_2(\xi)L_\xi^{\alpha\beta}(x,\xi) = \epsilon_2'(\xi)L^{\alpha\beta}(x,\xi) + c_1(x)L_\xi^{\beta\beta}(x,\xi) \tag{3.10b}$$

$$\epsilon_2(x)L_x^{\beta\alpha}(x,\xi) - \epsilon_1(\xi)L_\xi^{\beta\alpha}(x,\xi) = \epsilon_1'(\xi)L^{\beta\alpha}(x,\xi) - c_2(x)L_\xi^{\alpha\alpha}(x,\xi) \tag{3.10c}$$

$$\epsilon_2(x)L_x^{\alpha\beta}(x,\xi) + \epsilon_2(\xi)L_\xi^{\beta\beta}(x,\xi) = -\epsilon_2'(\xi)L^{\beta\beta}(x,\xi) - c_2(x)L_\xi^{\alpha\beta}(x,\xi) \tag{3.10d}$$

with boundary conditions

$$L^{\alpha\alpha}(x,0) = \frac{\epsilon_2(0)}{q\epsilon_1(0)} L^{\alpha\beta}(x,0) \tag{3.11a}$$

$$L^{\alpha\beta}(x,x) = \frac{c_1(x)}{\epsilon_1(x)+\epsilon_1(x)} \tag{3.11b}$$

$$L^{\beta\alpha}(x,x) = -\frac{c_2(x)}{\epsilon_1(x)+\epsilon_1(x)} \tag{3.11c}$$

$$L^{\beta\beta}(x,0) = \frac{q\epsilon_1(0)}{\epsilon_2(0)} L^{\beta\alpha}(x,0) \tag{3.11d}$$

defined over the triangular domain (3.8). Proofs of existence and uniqueness of solutions of (3.6)–(3.7) and (3.10)–(3.11) were given in Vazquez et al. (2011b), and it was also proved that the solutions are continuous over $\mathcal{T}$. As the transform (3.3) is invertible, the stability properties of (3.1) and (3.5) are equivalent. This was utilized in Aamo (2013) to derive a controller achieving (3.2) for $\bar{x} = 0$, and will in this thesis be utilized in a similar manner to derive a controller that achieves (3.2) for some arbitrary $\bar{x} \in (0, 1)$.

3.3 Relationships in domain and time

The aim of this section is to derive algebraic expressions relating the solutions α and β of (3.5a)-(3.5b) at two arbitrary points in the domain. We start by stating relationships between two arbitrary points in the domain for the solution of a simple PDE on the form we will encounter throughout subsequent sections.

Lemma 3.1. *For a PDE on the form*

$$u_t(x,t) + \epsilon(x)u_x(x,t) = f(x)g(t), \quad x \in (-\infty, \infty),\ t \in [0, \infty) \tag{3.12}$$

with $\epsilon(x) > 0 \ \ \forall x$*, the following relationship apply to two arbitrary points* $y, z \in (-\infty, \infty)$

$$u(y, t - \phi(y)) - u(z, t - \phi(z)) = \int_{\phi(y)}^{\phi(z)} f(\phi^{-1}(\tau))g(t - \tau)d\tau \tag{3.13}$$

for $t \geq \max\{\phi(y), \phi(z)\}$*, where*

$$\phi(z) = \int_z^1 \frac{d\gamma}{\epsilon(\gamma)}. \tag{3.14}$$

Proof. Using Lemma A.1 in the appendix, we derive the following relationships between two arbitrary points y and z

$$u(y,t) = u_0(\phi^{-1}(t + \phi(y))) + \int_0^t f(\phi^{-1}(t - \gamma + \phi(y)))g(\gamma)d\gamma \tag{3.15a}$$

$$u(z,t) = u_0(\phi^{-1}(t + \phi(z))) + \int_0^t f(\phi^{-1}(t - \gamma + \phi(z)))g(\gamma)d\gamma. \tag{3.15b}$$

Assuming $t \geq \max\{\phi(y), \phi(z)\}$, we shift time in both equations to obtain

$$u(y, t - \phi(y)) = u_0(\phi^{-1}(t)) + \int_0^{t-\phi(y)} f(\phi^{-1}(t - \gamma))g(\gamma)d\gamma \tag{3.16a}$$

$$u(z, t - \phi(z)) = u_0(\phi^{-1}(t)) + \int_0^{t-\phi(z)} f(\phi^{-1}(t - \gamma))g(\gamma)d\gamma. \tag{3.16b}$$

Thus, the initial condition can be eliminated by subtracting (3.16b) from (3.16a), yielding

$$u(y, t-\phi(y)) - u(z, t-\phi(z)) = \int_{t-\phi(z)}^{t-\phi(y)} f(\phi^{-1}(t-\gamma))g(\gamma)d\gamma. \tag{3.17}$$

An appropriate substitution $\tau = t-\gamma$ in the integral yields the desired result (3.13). □

Next, we state a valuable lemma, which will show great significance in the rest of the controller design.

Lemma 3.2. *For two arbitrary points $y, z \in [0,\ 1]$, the following relationships apply to the solutions α and β of* (3.5)

$$\alpha(y, t-\phi_\alpha(y)) - \alpha(z, t-\phi_\alpha(z)) = \Phi_\alpha(y, z)X(t) \tag{3.18a}$$

for $t \geq \max\{\phi_\alpha(y), \phi_\alpha(z)\}$, and

$$\beta(y, t-\phi_\beta(y)) - \beta(z, t-\phi_\beta(z)) = \Phi_\beta(y, z)X(t) \tag{3.18b}$$

for $t \geq \max\{\phi_\beta(y), \phi_\beta(z)\}$, where

$$\Phi_\alpha(y, z) = -\epsilon_1(0)\int_{\phi_\alpha(y)}^{\phi_\alpha(z)} K^{uu}(\phi_\alpha^{-1}(\tau), 0)Ce^{-A\tau}d\tau \tag{3.19a}$$

$$\Phi_\beta(y, z) = -\epsilon_1(0)\int_{\phi_\beta(y)}^{\phi_\beta(z)} K^{vu}(\phi_\beta^{-1}(\tau), 0)Ce^{-A\tau}d\tau \tag{3.19b}$$

with

$$\phi_\alpha(z) = \int_z^1 \frac{d\gamma}{\epsilon_1(\gamma)} \tag{3.20a}$$

$$\phi_\beta(z) = \int_0^z \frac{d\gamma}{\epsilon_2(\gamma)}. \tag{3.20b}$$

Proof. The proof of Lemma 3.2 follows from application of Lemma 3.1. The proof for (3.18a) is independent from (3.18b), and for clarity of presentation, these two equations will be proven in sequence.

The α-subsystem

The subsystem (3.5a) has the form required by Lemma 3.1 with $u(x,t) = \alpha(x,t)$, $\epsilon(x) = \epsilon_1(x)$, $f(x) = -\epsilon_1(0)K^{uu}(x,0)$ and $g(t) = CX(t)$. The result (3.18a) with (3.19a) and (3.20a) therefore follows by Lemma 3.1 and the *semigroup property* of (3.5e), i.e. $X(t-\tau) = e^{-A\tau}X(t)$, as stated in Lemma A.5.

The β-subsystem

Application of Lemma 3.1 is not straight forward to use on the subsystem (3.5b) since the sign preceding $\epsilon_2(x)$ is not as required by the lemma. We will resolve this by a change of variables. Define $\bar{\beta}(x,t)$ and $\bar{\epsilon}_2(x)$ as

$$\bar{\beta}(x,t) := \beta(1-x,t) \Leftrightarrow \beta(x,t) = \bar{\beta}(1-x,t) \tag{3.21}$$

and

$$\bar{\epsilon}_2(x) := \epsilon_2(1-x) \Leftrightarrow \epsilon_2(x,t) = \bar{\epsilon}_2(1-x,t) \tag{3.22}$$

respectively. From the following properties

$$\bar{\beta}_t(x,t) = \beta_t(1-x,t) \tag{3.23}$$

and

$$\bar{\beta}_x(x,t) = -\beta_x(1-x,t), \tag{3.24}$$

and a substitution $x \to 1-x$, the subsystem (3.5b) can be written in the new variables as

$$\bar{\beta}_t(x,t) + \bar{\epsilon}_2(x)\bar{\beta}_x(x,t) = -\epsilon_1(0)K^{vu}(1-x,0)CX(t) \tag{3.25}$$

which is on the form required by Lemma 3.1. With $u(x,t) = \bar{\beta}(x,t)$, $\epsilon(x) = \bar{\epsilon}_2(x)$, $f(x) = -\epsilon_1(0)K^{vu}(1-x,0)$ and $g(t) = CX(t)$, Lemma 3.1 yields

$$\begin{aligned}&\bar{\beta}(y,t-h_\beta(y)) - \bar{\beta}(z,t-h_\beta(z)) \\ &\qquad = -\epsilon_1(0)\int_{h_\beta(y)}^{h_\beta(z)} K^{vu}(1-h_\beta^{-1}(\tau))CX(t-\tau)d\tau\end{aligned} \tag{3.26}$$

for $t \geq \max\{h_\beta(y), h_\beta(z)\}$, where $h_\beta(z)$ is defined as

$$h_\beta(z) := \int_z^1 \frac{d\tau}{\epsilon(\tau)}. \tag{3.27}$$

Inserting back in for β in (3.21) followed by the substitutions $y \to 1-y$ and $z \to 1-z$ yields

$$\begin{aligned}&\beta(y,t-h_\beta(1-y)) - \beta(z,t-h_\beta(1-z)) \\ &\qquad = -\epsilon_1(0)\int_{h_\beta(1-y)}^{h_\beta(1-z)} K^{vu}(1-h_\beta^{-1}(\tau))CX(t-\tau)d\tau\end{aligned} \tag{3.28}$$

for $t \geq \max\{h_\beta(1-y), h_\beta(1-z)\}$.

The strictly *increasing* and hence invertible function in (3.20b) has the following property

$$\phi_\beta(z) = \int_0^z \frac{d\gamma}{\epsilon_2(\gamma)} = \int_{1-z}^1 \frac{d\tau}{\epsilon_2(1-\tau)} = \int_{1-z}^1 \frac{d\tau}{\overline{\epsilon}_2(\tau)} = h_\beta(1-z). \tag{3.29}$$

Additionally, we have

$$\phi_\beta^{-1}(z) = 1 - h_\beta^{-1}(z). \tag{3.30}$$

This can be seen as follows; let τ denote the following

$$\tau = \phi_\beta(z) = h_\beta(1-z) \tag{3.31}$$

then

$$z = \phi_\beta^{-1}(\tau) \tag{3.32}$$

and

$$1 - z = h_\beta^{-1}(\tau) \tag{3.33}$$

substituting (3.32) into (3.33), we obtain (3.30). Substituting (3.29) and (3.30) into (3.28), using the semigroup property of (3.5e) and using (3.19b) finally proves the lemma's second half. □

3.4 Relationships to the control input

By utilizing the results in Lemma 3.2, we will characterize the solutions α and β of (3.5) in terms of the actuation $V(t) = \beta(1,t)$ for any arbitrary point y in the domain.

Lemma 3.3. *For an arbitrary point y in the domain, the solutions α and β of* (3.5)*, satisfy*

$$\alpha(y,t) = qV(t - \eta_\alpha(y)) + \Psi_\alpha(y)X(t) \tag{3.34a}$$

for $t \geq \eta_\alpha(y)$ and

$$\beta(y,t) = \ \ V(t - \eta_\beta(y)) + \Psi_\beta(y)X(t) \tag{3.34b}$$

for $t \geq \eta_\beta(y)$, where

$$\Psi_\alpha(y) = \Phi_\alpha(y,0)e^{A\phi_\alpha(y)} + (q\Phi_\beta(0,1) + C)e^{A(\phi_\alpha(y) - \phi_\alpha(0))} \tag{3.35a}$$

$$\Psi_\beta(y) = \Phi_\beta(y,1)e^{A\phi_\beta(y)} \tag{3.35b}$$

and

$$\eta_\alpha(y) = \phi_\beta(1) + \phi_\alpha(0) - \phi_\alpha(y) \tag{3.36a}$$

$$\eta_\beta(y) = \phi_\beta(1) - \phi_\beta(y). \tag{3.36b}$$

Proof. Again, we will split the proof in two, dealing with the α and β subsystems separately.

The α-subsystem

From (3.18a) in Lemma 3.2, with $z = 0$ and time shifting $\phi_\alpha(y)$ units, we find

$$\alpha(y,t) = \alpha(0, t - \phi_\alpha(0) + \phi_\alpha(y)) + \Phi_\alpha(y,0)X(t + \phi_\alpha(y)) \tag{3.37}$$

for $t \geq \phi_\alpha(0) - \phi_\alpha(y)$. Substituting for the boundary condition (3.5c) yields

$$\begin{aligned}\alpha(y,t) = q\beta(0, t - \phi_\alpha(0) + \phi_\alpha(y)) + CX(t - \phi_\alpha(0) + \phi_\alpha(y)) \\ + \Phi_\alpha(y,0)X(t + \phi_\alpha(y))\end{aligned} \tag{3.38}$$

From (3.18b) in Lemma 3.2, with $y = 0$, $z = 1$ and noticing that $\phi_\beta(0) = 0$, we obtain

$$\beta(0,t) = \beta(1, t - \phi_\beta(1)) + \Phi_\beta(0,1)X(t) \tag{3.39}$$

for $t \geq \phi_\beta(1)$. Shifting time $\phi_\alpha(y) - \phi_\alpha(0)$ units, assuming $t \geq \phi_\beta(1) + \phi_\alpha(0) - \phi_\alpha(y) = \eta_\alpha(y)$, we find

$$\begin{aligned}\beta(0, t - \phi_\alpha(0) + \phi_\alpha(y)) = \beta(1, t - \eta_\alpha(y)) \\ + \ \Phi_\beta(0,1)X(t - \phi_\alpha(0) + \phi_\alpha(y)).\end{aligned} \tag{3.40}$$

where (3.36a) has been used. Inserting (3.40) into (3.38) results in

$$\begin{aligned}\alpha(y,t) = q\beta(1, t - \eta_\alpha(y)) \\ + q\Phi_\beta(0,1)X(t - \phi_\alpha(0) + \phi_\alpha(y)) \\ + CX(t - \phi_\alpha(0) + \phi_\alpha(y)) \\ + \Phi_\alpha(y,0)X(t + \phi_\alpha(y))\end{aligned} \tag{3.41}$$

for $t \geq \eta_\alpha(y)$. Using the semigroup property of (3.5e) we get rid of the time delayed disturbance terms and find

$$\begin{aligned}\alpha(y,t) = q\beta(1, t - \eta_\alpha(y)) \\ + q\Phi_\beta(0,1)e^{A(\phi_\alpha(y) - \phi_\alpha(0))}X(t) \\ + Ce^{A(\phi_\alpha(y) - \phi_\alpha(0))}X(t) \\ + \Phi_\alpha(y,0)e^{A\phi_\alpha(y)}X(t)\end{aligned} \tag{3.42}$$

for $t \geq \eta_\alpha(y)$. By inserting for the boundary condition (3.5d) and using (3.35a) and (3.36a), the first part of the lemma is verified.

The β-subsystem

From (3.18b) in Lemma 3.2, with $z = 1$ we find

$$\beta(y, t - \phi_\beta(y)) = \beta(1, t - \phi_\beta(1)) + \Phi_\beta(y, 1)X(t) \tag{3.43}$$

for $t \geq \max\{\phi_\beta(y), \phi_\beta(1)\}$. When time shifting $\phi_\beta(y)$ units, assuming $t \geq \phi_\beta(1) - \phi_\beta(y) = \eta_\beta(y)$, to arrive at

$$\beta(y, t) = \beta(1, t - \eta_\beta(y)) + \Phi_\beta(y, 1)X(t + \phi_\beta(y)). \tag{3.44}$$

where (3.36b) has been used. Again using the semigroup property of (3.5e), inserting for the boundary condition (3.5d) and using (3.35b), the lemma's second half is proved. □

3.5 Pure state feedback controller

The results of Lemma 3.2 and Lemma 3.3 finally facilitates for the main controller design. We start by substituting (3.3) into (3.2) to state the controller objective in the backstepping variables α and β

$$\begin{aligned}\alpha(\bar{x}, t) + \int_0^{\bar{x}} L^{\alpha\alpha}(\bar{x}, \xi)\alpha(\xi, t)d\xi + \int_0^{\bar{x}} L^{\alpha\beta}(\bar{x}, \xi)\beta(\xi, t)d\xi \\ = r\left(\beta(\bar{x}, t) + \int_0^{\bar{x}} L^{\beta\alpha}(\bar{x}, \xi)\alpha(\xi, t)d\xi + \int_0^{\bar{x}} L^{\beta\beta}(\bar{x}, \xi)\beta(\xi, t)d\xi\right)\end{aligned} \tag{3.45}$$

for $r \neq 0$. We seek a controller $V(t)$ so that (3.45) is achieved for some given, fixed $\bar{x} \in (0, 1)$.

Theorem 3.1 (Pure state feedback controller)**.** *Assume $r \neq 0$, and let*

$$\begin{aligned}V(t) = &\frac{1}{r}K_{psf}(\bar{x})X(t) + \frac{1}{r}\delta(\bar{x}, \bar{x}, t) \\ &+ \frac{1}{r}\int_0^{\bar{x}} L^\alpha(\bar{x}, \xi)\delta(\xi, \bar{x}, t)d\xi \\ &+ \frac{1}{r}\int_0^{\bar{x}} L^\beta(\bar{x}, \xi)\beta(\phi_\beta^{-1}(\kappa_\beta(\xi, \bar{x})), t)d\xi\end{aligned} \tag{3.46}$$

where

$$\begin{aligned}K_{psf}(\bar{x}) = &\Omega_\alpha(\bar{x}, \bar{x}) - r\Psi_\beta(\bar{x})e^{A\eta_\alpha(\bar{x})} \\ &+ \int_0^{\bar{x}} L^\alpha(\bar{x}, \xi)\Omega_\alpha(\xi, \bar{x})d\xi + \int_0^{\bar{x}} L^\beta(\bar{x}, \xi)\Omega_\beta(\xi, \bar{x})d\xi\end{aligned} \tag{3.47}$$

$$\delta(\xi,\bar{x},t)=\begin{cases}\alpha(\phi_\alpha^{-1}(\kappa_\alpha(\xi,\bar{x})),t) & \text{if } \kappa_\alpha(\xi,\bar{x})\le\phi_\alpha(0)\\ q\beta(\phi_\beta^{-1}(\kappa_\alpha(\xi,\bar{x})-\phi_\alpha(0)),t) & \text{otherwise}\end{cases} \tag{3.48}$$

and

$$\Omega_{\alpha\alpha}(\xi,\bar{x})=\Phi_\alpha(\xi,\phi_\alpha^{-1}(\kappa_\alpha(\xi,\bar{x})))e^{A\kappa_\alpha(\xi,\bar{x})} \tag{3.49a}$$

$$\Omega_{\alpha\beta}(\xi,\bar{x})=(q\Phi_\beta(0,\phi_\beta^{-1}(\kappa_\alpha(\xi,\bar{x})-\phi_\alpha(0)))+C)e^{A\kappa_\beta(\xi,\bar{x})} + \Phi_\alpha(\xi,0)e^{A\kappa_\alpha(\xi,\bar{x})} \tag{3.49b}$$

$$\tag{3.49c}$$

$$\Omega_\alpha(\xi,\bar{x})=\begin{cases}\Omega_{\alpha\alpha}(\xi,\bar{x}) & \text{if } \kappa_\alpha(\xi,\bar{x})\le\phi_\alpha(0)\\ \Omega_{\alpha\beta}(\xi,\bar{x}) & \text{otherwise}\end{cases} \tag{3.50a}$$

$$\Omega_\beta(\xi,\bar{x})=\Phi_\beta(\xi,\phi_\beta^{-1}(\kappa_\beta(\xi,\bar{x})))e^{A\kappa_\beta(\xi,\bar{x})} \tag{3.50b}$$

$$\kappa_\alpha(\xi,\bar{x})=\phi_\alpha(\xi)+\eta_\beta(\bar{x}) \tag{3.51a}$$

$$\kappa_\beta(\xi,\bar{x})=\phi_\beta(\xi)+\eta_\beta(\bar{x}) \tag{3.51b}$$

with

$$L^\alpha(\bar{x},\xi)=L^{\alpha\alpha}(\bar{x},\xi)-rL^{\beta\alpha}(\bar{x},\xi) \tag{3.52a}$$

$$L^\beta(\bar{x},\xi)=L^{\alpha\beta}(\bar{x},\xi)-rL^{\beta\beta}(\bar{x},\xi) \tag{3.52b}$$

where $L^{\alpha\alpha}(\bar{x},\xi), L^{\alpha\beta}(\bar{x},\xi), L^{\beta\alpha}(\bar{x},\xi), L^{\beta\beta}(\bar{x},\xi)$ *is the solution to* (3.9)–(3.10)*, then the control law* (3.4) *will guarantee* (3.45) *for all* $t\ge\eta_\beta(\bar{x})$*.*

Note that $\alpha(x,t)$ and $\beta(x,t)$ in (3.46) and (3.48) must be evaluated from $u(x,t)$ and $v(x,t)$ using the backstepping transformation (3.3).

Proof. With (3.52a) and (3.52b), the controller objective (3.45) can be stated as

$$r\beta(\bar{x},t)=\alpha(\bar{x},t)+\int_0^{\bar{x}}L^\alpha(\bar{x},\xi)\alpha(\xi,t)d\xi+\int_0^{\bar{x}}L^\beta(\bar{x},\xi)\beta(\xi,t)d\xi. \tag{3.53}$$

Using (3.34b) in Lemma 3.3, we can derive

$$rV(t-\eta_\beta(\bar{x}))+r\Psi_\beta(\bar{x})X(t)=\alpha(\bar{x},t)+\int_0^{\bar{x}}L^\alpha(\bar{x},\xi)\alpha(\xi,t)d\xi+\int_0^{\bar{x}}L^\beta(\bar{x},\xi)\beta(\xi,t)d\xi \tag{3.54}$$

for $t \geq \eta_\beta(\bar{x})$. Time shifting $\eta_\beta(\bar{x})$ units and rearranging, we obtain

$$\begin{aligned} rV(t) = &-r\Psi_\beta(\bar{x})X(t+\eta_\beta(\bar{x})) + \alpha(\bar{x}, t+\eta_\beta(\bar{x})) \\ &+ \int_0^{\bar{x}} L^\alpha(\bar{x},\xi)\alpha(\xi, t+\eta_\beta(\bar{x}))d\xi \\ &+ \int_0^{\bar{x}} L^\beta(\bar{x},\xi)\beta(\xi, t+\eta_\beta(\bar{x}))d\xi \end{aligned} \tag{3.55}$$

for $t \geq 0$.

We will have to find expressions for $\alpha(\xi, t+\eta_\alpha(\bar{x}))$ and $\beta(\xi, t+\eta_\beta(\bar{x}))$ that does not include time shifts.

The α-subsystem

The α-part is a bit tricky, as the signal conditionally will have to be propagated through the boundary condition (3.5c), for certain values of ξ and $\bar{x}$. From (3.18a), solutions to (3.5a) satisfy

$$\alpha(\xi, t-\phi_\alpha(\xi)) - \alpha(z, t-\phi_\alpha(z)) = \Psi_\alpha(\xi, z)X(t) \tag{3.56}$$

Shifting time by $\phi_\alpha(\xi) + \eta_\alpha(\bar{x})$ units, we find

$$\begin{aligned} \alpha(\xi, t+\eta_\beta(\bar{x})) = &\alpha(z, t-\phi_\alpha(z)+\kappa_\alpha(\xi,\bar{x})) \\ &+ \Phi_\alpha(\xi, z)X(t+\kappa_\alpha(\xi,\bar{x})) \end{aligned} \tag{3.57}$$

where (3.51a) has been used. We would now like to select $z \in [0,1]$ so that $\phi_\alpha(z) = \kappa_\alpha(\xi,\bar{x})$. As the inverse of $\phi_\alpha(z)$ is defined on $[\phi_\alpha(1)=0, \phi_\alpha(0)]$ and $\kappa_\alpha(\xi,\bar{x})$ is nonnegative, this is possible if

$$\kappa_\alpha(\xi,\bar{x}) \leq \phi_\alpha(0). \tag{3.58}$$

In this case, we choose $z = \phi_\alpha^{-1}(\kappa_\alpha(\xi,\bar{x}))$ and (3.57) becomes

$$\begin{aligned} \alpha(\xi, t+\eta_\beta(\bar{x})) = &\alpha(\phi_\alpha^{-1}(\kappa_\alpha(\xi,\bar{x})), t) \\ &+ \Phi_\alpha(\xi, \phi_\alpha^{-1}(\kappa_\alpha(\xi,\bar{x})))X(t+\phi_\alpha(z_{\alpha\alpha}(\xi,\bar{x}))). \end{aligned} \tag{3.59}$$

Using the semigroup property of (3.5e) and using (3.49a), (3.59) can be written

$$\alpha(\xi, t+\eta_\beta(\bar{x})) = \alpha(\phi_\alpha^{-1}(\kappa_\alpha(\xi,\bar{x}))), t) + \Omega_{\alpha\alpha}(\xi,\bar{x},t)X(t). \tag{3.60}$$

If however, the requirement (3.58) does not hold, the signal has to be propagated through the boundary condition (3.5c). We then let $z=0$ in (3.57) and find

$$\begin{aligned} \alpha(\xi, t+\eta_\beta(\bar{x})) = &\alpha(0, t-\phi_\alpha(0)+\kappa_\alpha(\xi,\bar{x})) \\ &+ \Phi_\alpha(\xi, 0)X(t+\kappa_\alpha(\xi,\bar{x})). \end{aligned} \tag{3.61}$$

Inserting for the boundary condition (3.5c), we end up with

$$\begin{aligned}\alpha(\xi, t+\eta_\beta(\bar{x})) = q\beta(0, t-\phi_\alpha(0)+\kappa_\alpha(\xi,\bar{x})) \\ + CX(t-\phi_\alpha(0)+\kappa_\alpha(\xi,\bar{x})) \\ + \Phi_\alpha(\xi,0)X(t+\kappa_\alpha(\xi,\bar{x})).\end{aligned} \tag{3.62}$$

By inserting $y = 0$ into (3.18b) in Lemma 3.2, we have

$$\beta(0,t) = \beta(z, t-\phi_\beta(z)) + \Psi_\beta(0,z)X(t). \tag{3.63}$$

Shifting time $\kappa_\alpha(\xi,\bar{x}) - \phi_\alpha(0)$ units, we obtain

$$\begin{aligned}\beta(0, t+\kappa_\alpha(\xi,\bar{x})-\phi_\alpha(0)) = \beta(z, t-\phi_\beta(z)-\phi_\alpha(0)+\kappa_\alpha(\xi,\bar{x})) \\ + \Psi_\beta(0,z)X(t-\phi_\alpha(0)+\kappa_\alpha(\xi,\bar{x})).\end{aligned} \tag{3.64}$$

Substituting (3.64) into (3.62) gives

$$\begin{aligned}\alpha(\xi, t+\eta_\beta(\bar{x})) = q\beta(z, t-\phi_\beta(z)-\phi_\alpha(0)+\kappa_\alpha(\xi,\bar{x})) \\ + q\Phi_\beta(0,z)X(t-\phi_\alpha(0)+\kappa_\alpha(\xi,\bar{x})) \\ + CX(t-\phi_\alpha(0)+\kappa_\alpha(\xi,\bar{x})) \\ + \Phi_\alpha(\xi,0)X(t+\kappa_\alpha(\xi,\bar{x})).\end{aligned} \tag{3.65}$$

We now choose $z = \phi_\beta^{-1}(\kappa_\alpha(\xi,\bar{x}) - \phi_\alpha(0))$ which is well defined since $0 < \kappa_\alpha(\xi,\bar{x}) - \phi_\alpha(0) = \phi_\alpha(\xi) - \phi_\alpha(0) + \phi_\beta(1) - \phi_\beta(\bar{x}) \leq \phi_\beta(1)$, and find

$$\begin{aligned}\alpha(\xi, t+\eta_\beta(\bar{x})) = q\beta(\phi_\beta^{-1}(\kappa_\alpha(\xi,\bar{x})-\phi_\alpha(0)), t) \\ + q\Phi_\beta(0, \phi_\beta^{-1}(\kappa_\alpha(\xi,\bar{x})-\phi_\alpha(0)))X(t+\kappa_\alpha(\xi,\bar{x})-\phi_\alpha(0)) \\ + CX(t+\kappa_\alpha(\xi,\bar{x})-\phi_\alpha(0)) \\ + \Phi_\alpha(\xi,0)X(t+\kappa_\alpha(\xi,\bar{x})).\end{aligned} \tag{3.66}$$

Again using the semigroup property of (3.5e) and using (3.49b), (3.66) can be stated as

$$\alpha(\xi, t+\eta_\beta(\bar{x})) = q\beta(\phi_\beta^{-1}(\kappa_\alpha(\xi,\bar{x})-\phi_\alpha(0)), t) + \Omega_{\alpha\beta}(\xi,\bar{x})X(t). \tag{3.67}$$

The above results (3.60) and (3.67) can be combined into a single expression by using $\delta(\xi,\bar{x},t)$ and $\Omega_\alpha(\xi,\bar{x})$ as given from (3.48) and (3.50a) respectively, yielding

$$\alpha(\xi, t+\eta_\alpha(\bar{x})) = \delta(\xi,\bar{x},t) + \Omega_\alpha(\xi,\bar{x})X(t). \tag{3.68}$$

The β-subsystem

From (3.18b) in Lemma 3.1, we find that solutions to (3.5b) satisfy

$$\beta(\xi, t = \phi_\beta(\xi)) - \beta(z, t - \phi_\beta(z)) + \Phi_\beta(\xi, z)X(t). \tag{3.69}$$

Shifting time $\phi_\beta(\xi) + \eta_\beta(\bar{x})$ units, we obtain

$$\beta(\xi, t + \eta_\beta(\bar{x})) = \beta(z, t - \phi_\beta(z) + \kappa_\beta(\xi, \bar{x})) = \Phi_\beta(\xi, z)X(t + \kappa_\beta(\xi, \bar{x})) \tag{3.70}$$

where (3.51b) has been used. As $0 < \kappa_\beta(\xi, \bar{x}) = \phi_\beta(\xi) + \phi_\beta(1) - \phi_\beta(\bar{x}) \leq \phi_\beta(1)$, the selection $z = \phi_\beta^{-1}(\kappa_\beta(\xi, \bar{x}))$ is well defined and we obtain

$$\begin{aligned}\beta(\xi, t + \eta_\beta(\bar{x})) = \beta(\phi_\beta^{-1}(\kappa_\beta(\xi, \bar{x})), t) \\ + \Phi_\beta(\xi, \phi_\beta^{-1}(\kappa_\beta(\xi, \bar{x}))X(t + \kappa_\beta(\xi, \bar{x})).\end{aligned} \tag{3.71}$$

Lastly using the semigroup property of (3.5e) and using (3.50b), we find

$$\beta(\xi, t + \eta_\beta(\bar{x})) = \beta(\phi_\beta^{-1}(\kappa_\beta(\xi, \bar{x})), t) + \Omega_\beta(\xi, \bar{x})X(t). \tag{3.72}$$

Substituting (3.68) and (3.72) into (3.55), we obtain

$$\begin{aligned}rV(t) = -r\Psi_\beta(\bar{x})X(t + \eta_\beta(\bar{x})) + \delta(\bar{x}, \bar{x}, t) + \Omega_\alpha(\xi, \bar{x})X(t) \\ + \int_0^{\bar{x}} L^\alpha(\bar{x}, \xi)\delta(\xi, \bar{x}, t) + \Omega_\alpha(\xi, \bar{x})X(t)d\xi \\ + \int_0^{\bar{x}} L^\beta(\bar{x}, \xi)\beta(\phi_\beta^{-1}(\kappa_\beta(\xi, \bar{x})), t) + \Omega_\beta(\xi, \bar{x})X(t)d\xi.\end{aligned} \tag{3.73}$$

Equation (3.46) now follows from the semigroup property of (3.5e), using the definitions (3.47)–(3.51) and dividing by r.

The disturbance will be cancelled in finite time, and the time required is the propagation time from $x = 1$ to $x = \bar{x}$. By inserting $\xi = \bar{x}$ into (3.72), we find this time to be $\eta_\beta(\bar{x})$. □

3.6 Recursive controller

The controller derived in the previous section is complex and involves evaluation of integrals of functions defined differently throughout the domain, as well as requiring the evaluation of α and β online by means of the transformation (3.3). Using Lemma 3.3, which relates the system states to the controller input, it is possible to replace system states by past inputs to form a control law for $V(t)$ that does not include the system states. This should also better facilitate for the derivation of the controller transfer function later in this thesis.

Theorem 3.2 (Recursive controller)**.** *Assume $r \neq 0$ and let*

$$\begin{aligned} V(t) = \frac{q}{r}V(t-d_r(\bar{x})) &+ \frac{q}{r}\int_0^{\bar{x}} L^\alpha(\bar{x},\xi)V(t-d_\alpha(\xi,\bar{x}))d\xi \\ &+ \frac{1}{r}\int_0^{\bar{x}} L^\beta(\bar{x},\xi)V(t-d_\beta(\xi,\bar{x}))d\xi \\ &+ \frac{1}{r}K_{rec}(\bar{x})X(t) \end{aligned} \tag{3.74}$$

where

$$d_\alpha(\xi,\bar{x}) = \eta_\alpha(\xi) - \eta_\beta(\bar{x}) \tag{3.75}$$

$$d_\beta(\xi,\bar{x}) = \eta_\beta(\xi) - \eta_\beta(\bar{x}) \tag{3.76}$$

$$d_{rec}(\bar{x}) = d_\alpha(\bar{x},\bar{x}) \tag{3.77}$$

and

$$\begin{aligned} K_{rec}(\bar{x}) = &\left(\Psi_\alpha(\bar{x}) - r\Psi_\beta(\bar{x}) + \int_0^{\bar{x}} (L^\alpha(\bar{x},\xi)\Psi_\alpha(\xi) + L^\beta(\bar{x},\xi)\Psi_\beta(\xi))d\xi\right) \\ &\times e^{A\eta_\beta(\bar{x})} \end{aligned} \tag{3.78}$$

then the control law (3.4) *will guarantee* (3.45) *for all $t \geq \eta_\alpha(\bar{x})$.*

Proof. We begin the proof with a rearranged version of (3.53) as follows

$$r\beta(\bar{x},t) = \alpha(\bar{x},t) + \int_0^{\bar{x}} L^\alpha(\bar{x},\xi)\alpha(\xi,t)d\xi + \int_0^{\bar{x}} L^\beta(\bar{x},\xi)\beta(\xi,t)d\xi. \tag{3.79}$$

Using both (3.34a) and (3.34b) in Lemma 3.3 successively with $y = \bar{x}$ and $y = \xi$, we find

$$\begin{aligned} qV(t-\eta_\alpha(\bar{x})) + \Psi_\alpha(\bar{x})X(t) - rV(t-\eta_\beta(\bar{x})) - r\Psi_\beta(\bar{x})X(t) \\ = -\int_0^{\bar{x}} L^\alpha(\bar{x},\xi)\left[qV(t-\eta_\alpha(\xi)) + \Psi_\alpha(\xi)X(t)\right]d\xi \\ -\int_0^{\bar{x}} L^\beta(\bar{x},\xi)\left[V(t-\eta_\beta(\xi)) + \Psi_\beta(\xi)X(t)\right]d\xi \end{aligned} \tag{3.80}$$

which is valid for $t \geq \eta_\alpha(\bar{x})$. Rearranging this and time shifting $\eta_\beta(\bar{x})$ units, we obtain

$$\begin{aligned} rV(t) = &qV(t-\eta_\alpha(\bar{x})+\eta_\beta(\bar{x})) + (\Psi_\alpha(\bar{x}) - r\Psi_\beta(\bar{x}))X(t+\eta_\beta(\bar{x})) \\ &+ \int_0^{\bar{x}} L^\alpha(\bar{x},\xi)\left[qV(t-\eta_\alpha(\xi)+\eta_\beta(\bar{x})) + \Psi_\alpha(\xi)X(t+\eta_\beta(\bar{x}))\right]d\xi \\ &+ \int_0^{\bar{x}} L^\beta(\bar{x},\xi)\left[V(t-\eta_\beta(\xi)+\eta_\beta(\bar{x})) + \Psi_\beta(\xi)X(t+\eta_\beta(\bar{x}))\right]d\xi \end{aligned} \tag{3.81}$$

for $t \geq \max\{\eta_\alpha(\bar{x})-\eta_\beta(\bar{x}), \eta_\beta(0)-\eta_\beta(\bar{x})\} = \max\{\phi_\alpha(0)-\phi_\alpha(\bar{x})+\phi_\beta(\bar{x}),\ \phi_\beta(\bar{x})\} = \phi_\alpha(0) - \phi_\alpha(\bar{x}) + \phi_\beta(\bar{x}) = \eta_\alpha(\bar{x}) - \eta_\beta(\bar{x})$. A slight rearranging of the terms in the integrals yields

$$\begin{aligned} rV(t) = {} & qV(t - \eta_\alpha(\bar{x}) + \eta_\beta(\bar{x})) + (\Psi_\alpha(\bar{x}) - r\Psi_\beta(\bar{x}))X(t + \eta_\beta(\bar{x})) \\ & + \int_0^{\bar{x}} \left[L^\alpha(\bar{x}, \xi)\Psi_\alpha(\xi) + L^\beta(\bar{x}, \xi)\Psi_\beta(\xi)\right] d\xi X(t + \eta_\beta(\bar{x})) \\ & + \int_0^{\bar{x}} L^\alpha(\bar{x}, \xi) qV(t - \eta_\alpha(\xi) + \eta_\beta(\bar{x}))d\xi \\ & + \int_0^{\bar{x}} L^\beta(\bar{x}, \xi) V(t - \eta_\beta(\xi) + \eta_\beta(\bar{x}))d\xi. \end{aligned} \tag{3.82}$$

Lastly, using the semigroup property of (3.5e), using (3.75)–(3.78) and dividing by r, we end up with the control law (3.74).

The time constraint is derived as follows: $d_{rec}(\bar{x})$ is the time needed for any initial conditions in the time-delayed controller inputs to be driven out of the system. An additional $\eta_\beta(\bar{x})$ of time, as derived in the proof of Theorem 3.1, is required for the signal to propagate to $x = \bar{x}$. Hence, after a maximum time of $d_{rec}(\bar{x}) + \eta_\beta(\bar{x}) = \eta_\alpha(\bar{x}) - \eta_\beta(\bar{x}) + \eta_\beta(\bar{x}) = \eta_\alpha(\bar{x})$, the control objective is achieved. □

The controller of Theorem 3.2 was considerably easier to derive then the controller of Theorem 3.1, but has the disadvantage that it requires storage of past control inputs in the time interval $[t, t - d_{rec}(\bar{x})]$; an infinite amount of data on a continuous time system. As the controller relies on stored inputs rather than the actual system states, this is also a potential robustness issue. The controller of Theorem 3.1 avoids these drawbacks, but is generally more complex.

3.7 Simplified controller

Subject to a few assumptions, it turns out that the controller of Theorem 3.2 can be significantly simplified.

Theorem 3.3. *Under the assumption that the quantities added by terms in the integrals of the controller in Theorem 3.2 are small, that $|q/r| < 1$, and that $I - \frac{q}{r}e^{-Ad_r(\bar{x})}$ is nonsingular, then if we let*

$$V(t) = \frac{1}{r}K_\infty(\bar{x})X(t) \tag{3.83}$$

where

$$K_\infty(\bar{x}) = K_{rec}(\bar{x})\left[I - \frac{q}{r}e^{-A\cdot d_{rec}(\bar{x})}\right]^{-1}, \tag{3.84}$$

the control law (3.4) *will approximately achieve* (3.45) *for* $t \geq \eta_\alpha(\bar{x})$.

How well the controller objective (3.45) is approximated will depend on how much information is lost by neglecting the integral terms in the controller of Theorem 3.2.

Proof. By neglecting the integral terms in the controller of Theorem 3.2, we are left with

$$V(t) = \frac{q}{r}V(t - d_{rec}(\bar{x})) + \frac{1}{r}K_{rec}(\bar{x})X(t). \tag{3.85}$$

Time shifting this expression $-d_{rec}(\bar{x})$ units, we find

$$V(t - d_{rec}(\bar{x})) = \frac{q}{r}V(t - 2d_{rec}(\bar{x})) + \frac{1}{r}K_{rec}(\bar{x})X(t - d_{rec}(\bar{x})). \tag{3.86}$$

Inserting this into (3.85) yields

$$V(t) = \frac{q^2}{r^2}V(t - 2d_{rec}(\bar{x})) + \frac{q}{r^2}K_{rec}(\bar{x})X(t - d_{rec}(\bar{x})) + \frac{1}{r}K_{rec}(\bar{x})X(t). \tag{3.87}$$

From repeated substitution, and using $|(q/r)^k| \to 0$ as $k \to \infty$ due to the assumption $|q/r| < 1$, we find

$$V(t) = \frac{1}{r}K_{rec}(\bar{x}) \sum_{k=0}^{\infty} e^{-Akd_{rec}(\bar{x})}X(t) \tag{3.88}$$

where the semigroup property of (3.5e), as stated in Lemma A.5, has been used. By the assumption of having $I - \frac{q}{r}e^{-Ad_{rec}(\bar{x})}$ nonsingular, we find an exact expression for the infinite sum by using the results in Lemma A.2, thus

$$V(t) = \frac{1}{r}K_{rec}(\bar{x}) \left[I - \frac{q}{r}e^{-Ad_{rec}(\bar{x})} \right]^{-1} X(t). \tag{3.89}$$

Lastly using (3.84), we find (3.83).

As the controller assumes the current control law has been applied "an infinite amount of time" and no information regarding past inputs or current system states is used in the control law, the applied control law will not be the correct one before both the solutions α and β in (3.5a)–(3.5b) have achieved their steady-state values. Hence, the time needed is the propagation time from $x = 1$ to $x = \bar{x}$ *via* $x = 0$. By inserting $y = \bar{x}$ into (3.34a), we find this time to be $\eta_\alpha(\bar{x})$. □

The key strength of the controller formulation in Theorem 3.3 is that $V(t)$ is a function purely in the disturbance term $X(t)$. However, knowledge of $u(x,t)$ and $v(x,t)$ are still needed in (3.4). Justification of the assumption

of having integral terms approximately zero can for instance be when the kernel terms are small, that is $|L^{\alpha}(x,\xi)| \ll 1$ and $|L^{\beta}(x,\xi)| \ll 1$ for all pairs of $(x,\xi) \in \mathcal{T}$, where $\mathcal{T}$ is as given in (3.8). From the kernel equations (3.10)–(3.11), it is observed that $c_1(x) \equiv 0$ and $c_2(x) \equiv 0$ yields the trivial solution $L^{\alpha\alpha}(x,\xi) = L^{\alpha\beta}(x,\xi) = L^{\beta\alpha}(x,\xi) = L^{\beta\beta}(x,\xi) = 0 \ \forall (x,\xi) \in \mathcal{T}$. Hence, it is reasonable to assume that if the magnitude of the cross terms coefficients $c_1(x)$ and $c_2(x)$ in (3.1a)–(3.1b) are considerably smaller in magnitude than $\epsilon_1(x)$ and $\epsilon_2(x)$, the kernel terms are small and the simplification of Theorem (3.3) is justified.

Chapter 4

Observer design

4.1 Introduction

The control laws derived in Chapter 3 require full knowledge of the system states $u(x,t)$, $v(x,t)$ as well as the disturbance $X(t)$. With practical problems often limited to sensing at $x = 1$, this is obviously an assumption that will limit the control laws from being implemented in practice. If, however, we assume *estimates* of $u(x,t)$, $v(x,t)$ and $X(t)$ are available and rely on the certainty equivalence principle (that is; neglect uncertainty and treat estimates as if they are true values (Åström (1996))), the controllers can be implemented using the estimates instead of the real states. The estimates will have to be generated from the only signals available; the sensing at $x = 1$ and the generated controller input $U(t)$.

4.2 Observer equations

An observer estimating the states of the system using only sensing at $x = 1$ was derived in Vazquez et al. (2011b). The authors proved that the estimation errors converged exponentially to zero. A slight modification of the observer from Vazquez et al. (2011b) was done in Aamo (2013) to accommodate the disturbance term entering at the right boundary. The observer takes the applied input $U(t)$ and one measurement from the system as inputs, and estimates the states of the system as well as the disturbance. The observer

is formulated using PDEs, and is given as

$$\hat{u}_t(x,t) = -\epsilon_1(x)\hat{u}_x(x,t) + c_1(x)\hat{v}(x,t) + p_1(x)(Y(t) - \hat{u}(1,t)) \tag{4.1a}$$
$$\hat{v}_t(x,t) = \epsilon_2(x)\hat{v}_x(x,t) + c_2(x)\hat{u}(x,t) + p_2(x)(Y(t) - \hat{u}(1,t)) \tag{4.1b}$$
$$\hat{u}(0,t) = q\hat{v}(0,t) + C\hat{X}(t) \tag{4.1c}$$
$$\hat{v}(1,t) = U(t) \tag{4.1d}$$
$$\dot{\hat{X}}(t) = A\hat{X}(t) + e^{A\phi_\alpha(0)}L(Y(t) - \hat{u}(1,t)) \tag{4.1e}$$

where

$$Y(t) = u(1,t) \tag{4.2}$$

is the measurement. The matrix L is a gain matrix chosen so that $(A - LC)$ is Hurwitz (i.e all eigenvalues have negative real part). The functions $p_1(x)$ and $p_2(x)$ are injection gains, given as

$$p_1(x) = Ce^{A\phi_\alpha(x)}L - \epsilon_1(1)P^{uu}(x,1) - \int_x^1 P^{uu}(x,1)Ce^{A\phi_\alpha(\xi)}Ld\xi \tag{4.3a}$$
$$p_2(x) = -\epsilon_1(1)P^{vu}(x,1) - \int_x^1 P^{vu}(x,1)Ce^{A\phi_\alpha(\xi)}Ld\xi \tag{4.3b}$$

where the kernels are the solution to[1]

$$\epsilon_1(x)P^{uu}_x(x,\xi) + \epsilon_1(\xi)P^{uu}_\xi(x,\xi) = -\epsilon_1'(\xi)P^{uu}(x,\xi) + c_1(x)P^{vu}(x,\xi) \tag{4.4a}$$
$$\epsilon_1(x)P^{uv}_x(x,\xi) - \epsilon_2(\xi)P^{uv}_\xi(x,\xi) = \epsilon_2'(\xi)P^{uv}(x,\xi) + c_1(x)P^{vv}(x,\xi) \tag{4.4b}$$
$$\epsilon_2(x)P^{vu}_x(x,\xi) - \epsilon_1(\xi)P^{vu}_\xi(x,\xi) = \epsilon_1'(\xi)P^{vu}(x,\xi) - c_2(x)P^{uu}(x,\xi) \tag{4.4c}$$
$$\epsilon_2(x)P^{vv}_x(x,\xi) + \epsilon_2(\xi)P^{uv}_\xi(x,\xi) = -\epsilon_2'(\xi)P^{vv}(x,\xi) - c_2(x)P^{uv}(x,\xi) \tag{4.4d}$$

with boundary conditions

$$P^{uu}(0,\xi) = qP^{vu}(0,\xi) \tag{4.5a}$$
$$P^{uv}(x,x) = \frac{c_1(x)}{\epsilon_1(x) + \epsilon_2(x)} \tag{4.5b}$$
$$P^{vu}(x,x) = -\frac{c_2(x)}{\epsilon_1(x) + \epsilon_2(x)} \tag{4.5c}$$
$$P^{vv}(0,\xi) = \frac{1}{q}P^{uv}(0,\xi) \tag{4.5d}$$

defined over the triangular domain

$$\mathcal{T}_0 = \{(x,\xi) \ : \ 0 \le x \le \xi \le 1\}. \tag{4.6}$$

[1]Apparently, the kernel equations stated in Vazquez et al. (2011b) contained some typos. The kernel equations stated here are the ones found in Aamo (2013).

It was in Vazquez et al. (2011b) proved that there exist a unique solution to (4.4)-(4.5), and that the solution is continuous over $\mathcal{T}_0$.

For proofs of exponential convergence of the estimates, the interested reader is referred to the proofs in Aamo (2013).

Chapter 5

Transfer function derivations

5.1 Introduction

The current structure of the system, observer and controller is as stated in Figure 5.1a. By considering the controller and observer as a single unit in the frequency domain, it should be possible to derive a single transfer function relating the measurement to the controller output as illustrated in Figure 5.1b. Being an infinite dimensional controller and observer, the resulting transfer function is likely to be irrational and complicated, but by using model reduction techniques, simple approximations may be found. This is the subject of Chapter 6.

We will start the derivations in this chapter by deriving the transfer functions for the observer in Section 5.2, then for the controllers of Theorems 3.1–3.3 in Sections 5.3–5.5.

5.2 Observer

We derive the transfer functions that links the observer states $\hat{u}(x,s)$ and $\hat{v}(x,s)$ as well as the estimated disturbance $\hat{X}(s)$ to the Laplace transforms of the measurement $Y(s) = \mathcal{L}(Y(t))$ and applied controller input $U(s) = \mathcal{L}(U(t))$. Thus, we seek transfer functions $h_{\hat{u}Y}(x,s)$, $h_{\hat{u}U}(x,s)$, $h_{\hat{v}Y}(x,s)$, $h_{\hat{v}U}(x,s)$, $h_{\hat{X}Y}(s)$ and $h_{\hat{X}U}(s)$ so that

$$\hat{u}(x,s) = h_{\hat{u}Y}(x,s)Y(s) + h_{\hat{u}U}(x,s)U(s) \tag{5.1a}$$

$$\hat{v}(x,s) = h_{\hat{v}Y}(x,s)Y(s) + h_{\hat{v}U}(x,s)U(s) \tag{5.1b}$$

$$\hat{X}(s) = h_{\hat{X}Y}(s)Y(s) + h_{\hat{X}U}(s)U(s). \tag{5.1c}$$

We will do this by initially solving the Laplace transformed (4.1), using the result to derive the transfer functions in (5.1c) and use these results to derive

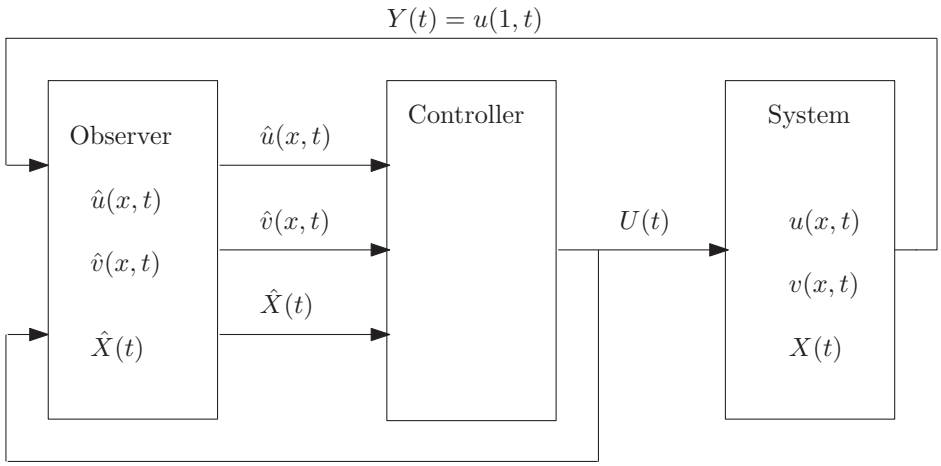

(a) System with controller and observer.

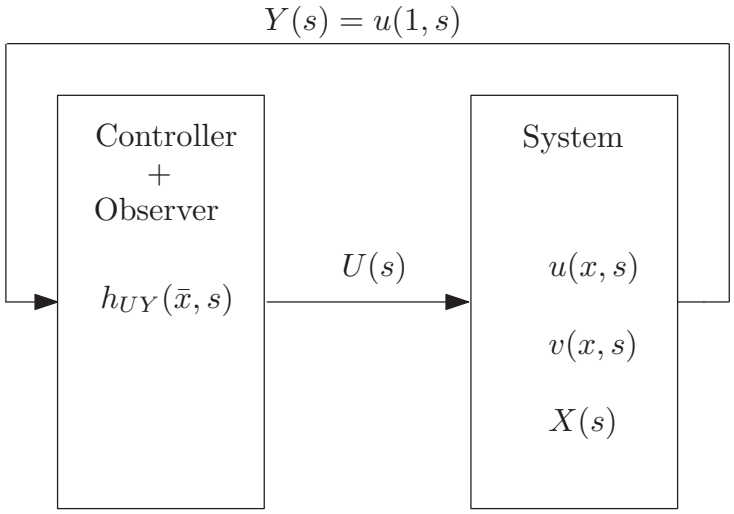

(b) System an controller combined with observer in the Laplace domain.

Figure 5.1: System structure.

the transfer functions in (5.1a) and (5.1b).

5.2.1 Solving the observer equations

Ignoring initial conditions, we apply the Laplace transform to the observer (4.1). After a slight rearranging of the terms, we obtain

$$\hat{u}_x(x,s) = \frac{1}{\epsilon_1(x)}(-s\hat{u}(x,s) + c_1(x)\hat{v}(x,s) + p_1(x)(Y(s) - \hat{u}(1,s)) \tag{5.2a}$$

$$\hat{v}_x(x,s) = \frac{1}{\epsilon_2(x)}(s\hat{v}(x,s) - c_2(x)\hat{u}(x,s) - p_2(x)(Y(s) - \hat{u}(1,s)) \tag{5.2b}$$

$$\hat{u}(0,s) = q\hat{v}(0,s) + C\hat{X}(s) \tag{5.2c}$$

$$\hat{v}(1,s) = U(s) \tag{5.2d}$$

$$\hat{X}(s) = D(s)(Y(s) - \hat{u}(1,s)) \tag{5.2e}$$

where

$$D(s) := (sI - A)^{-1}e^{A\phi_\alpha(0)}L \tag{5.3}$$

has been defined. The subsystem consisting of (5.2a)–(5.2b) can be written more compactly by introducing the vector of observer states

$$w(x,s) := \begin{bmatrix}\hat{u}(x,s)\\ \hat{v}(x,s)\end{bmatrix}, \tag{5.4}$$

the matrix

$$\Theta(x,s) := \begin{bmatrix}-\frac{s}{\epsilon_1(x)} & \frac{c_1(x)}{\epsilon_1(x)}\\ -\frac{c_2(x)}{\epsilon_2(x)} & \frac{s}{\epsilon_2(x)}\end{bmatrix} \tag{5.5}$$

and the vector

$$\Upsilon(x) := \begin{bmatrix}\frac{p_1(x)}{\epsilon_1(x)}\\ -\frac{p_2(x)}{\epsilon_2(x)}\end{bmatrix}. \tag{5.6}$$

We may then write (5.2a)–(5.2b) as

$$w_x(x,s) = \Theta(x,s)w(x,s) + \Upsilon(x)(Y(s) - \hat{u}(1,s)). \tag{5.7}$$

We proceed by applying the variation of constants formula as stated in Lemma A.4. We assume that there exists a fundamental matrix $\Xi(x,x_0,s)$ with the desired properties, and find the solution of (5.7) as

$$w(x,s) = \Xi(x,x_0,s)w(x_0,s) + \int_{x_0}^{x}\Xi(x,\xi,s)\Upsilon(\xi)d\xi(Y(s) - \hat{u}(1,s)). \tag{5.8}$$

By additionally defining

$$P(x,s) = \begin{bmatrix} P_1(x,s) & P_2(x,s) \end{bmatrix} := \Xi(x,1,s) \tag{5.9}$$

and

$$Q(x,s) := \int_x^1 \Xi(x,\xi,s)\Upsilon(\xi)d\xi, \tag{5.10}$$

we find the following relationship between any arbitrary point x in the domain, and the actuation and sensing boundary at $x = 1$

$$w(x,s) = P(x,s)w(1,s) - Q(x,s)(Y(s) - \hat{u}(1,s)). \tag{5.11}$$

5.2.2 Estimated disturbance

By utilizing the above results, we will now derive the transfer functions $h_{\hat{X}Y}(s)$ and $h_{\hat{X}U}(s)$ in (5.1c). Let $x = 0$ in (5.11) and define

$$M(s) = \begin{bmatrix} M_1(s) & M_2(s) \end{bmatrix} = \begin{bmatrix} m_{11}(s) & m_{12}(s) \\ m_{21}(s) & m_{22}(s) \end{bmatrix} := P(0,s) \tag{5.12}$$

and

$$N(s) = \begin{bmatrix} n_1(s) \\ n_2(s) \end{bmatrix} := Q(0,s) \tag{5.13}$$

then we obtain

$$w(0,s) = M(s)w(1,s) - N(s)(Y(s) - \hat{u}(1,s)) \tag{5.14}$$

or, when written out in full

$$\hat{u}(0,s) = (m_{11}(s) + n_1(s))\hat{u}(1,s) + m_{12}(s)\hat{v}(1,s) - n_1(s)Y(s) \tag{5.15a}$$
$$\hat{v}(0,s) = (m_{21}(s) + n_2(s))\hat{u}(1,s) + m_{22}(s)\hat{v}(1,s) - n_2(s)Y(s). \tag{5.15b}$$

Inserting for the boundary conditions (5.2c) and (5.2d), and multiplying (5.15b) by q, we find

$$\begin{aligned} q\hat{v}(0,s) + C\hat{X}(s) = (m_{11}(s) + n_1(s))\hat{u}(1,s) \\ + m_{12}(s)U(s) - n_1(s)Y(s) \end{aligned} \tag{5.16}$$
$$\begin{aligned} q\hat{v}(0,s) = q(m_{21}(s) + n_2(s))\hat{u}(1,s) \\ + qm_{22}(s)U(s) - qn_2(s)Y(s). \end{aligned} \tag{5.17}$$

Subtracting (5.17) from (5.16), inserting (5.2e) and defining

$$\mu := \begin{bmatrix} 1 & -q \end{bmatrix}^T \tag{5.18}$$

we find the following relationship between the measurement $Y(s)$, actuation $U(s)$ and $\hat{u}(1,s)$

$$\begin{aligned} CD(s)(Y(s)-\hat{u}(1,s)) &= \mu^T(M_1(s)+N(s))\hat{u}(1,s) \\ &\quad + \mu^T M_2(s)U(s) - \mu^T N(s)Y(s). \end{aligned} \tag{5.19}$$

Now solving (5.19) for $\hat{u}(1,s)$, we find

$$\begin{aligned} \hat{u}(1,s) &= \frac{(CD(s)+\mu^T N(s))Y(s) - \mu^T M_2(s)U(s)}{CD(s)+\mu^T(M_1(s)+N(s))} \\ &= Y(s) - \frac{\mu^T M_1(s)Y(s) + \mu^T M_2(s)U(s)}{CD(s)+\mu^T(M_1(s)+N(s))}. \end{aligned} \tag{5.20}$$

By defining

$$\varphi(s) := \frac{\mu^T M(s)}{CD(s)+\mu^T(M_1(s)+N(s))}, \tag{5.21}$$

equation (5.20) can compactly be written

$$\hat{u}(1,s) = Y(s) - \varphi(s)\begin{bmatrix} Y(s) \\ U(s) \end{bmatrix}. \tag{5.22}$$

Substituting (5.22) into (5.2e), we finally find the transfer functions $h_{\hat{X}Y}(s)$ and $h_{\hat{X}U}(s)$ in (5.1c) as the elements of the following row vector

$$H_{\hat{X}YU}(s) = \begin{bmatrix} h_{\hat{X}Y}(s) & h_{\hat{X}U}(s) \end{bmatrix} := D(s)\varphi(s) \tag{5.23}$$

with $\varphi(s)$ given from (5.21).

5.2.3 Estimated states

We will now use the result of the previous two subsections to derive the transfer functions relating the observer states $\hat{u}(x,s)$ and $\hat{v}(x,s)$ to $Y(s)$ and $U(s)$. From (5.11), when writing $P(x,s)$ out in its columns, we have

$$w(x,s) = P_1(x,s)\hat{u}(1,s) + P_2(x,s)\hat{v}(1,s) - Q(x,s)(Y(s)-\hat{u}(1,s)). \tag{5.24}$$

Inserting (5.22) and the boundary condition (5.2d), we obtain

$$\begin{aligned} w(x,s) &= P_1(x,s)\left(Y(s) - \varphi(s)\begin{bmatrix} Y(s) \\ U(s) \end{bmatrix}\right) \\ &\quad + P_2(x,s)U(s) - Q(x,s)\varphi(s)\begin{bmatrix} Y(s) \\ U(s) \end{bmatrix}. \end{aligned} \tag{5.25}$$

A slight rearrangement of the terms yields

$$w(x,s) = (P(x,s) - (Q(x,s) + P_1(x,s))\varphi(s)) \begin{bmatrix} Y(s) \\ U(s) \end{bmatrix}. \tag{5.26}$$

Hence, the transfer functions from the measurement $Y(s)$ and actuation $U(s)$ to the estimated states $\hat{u}(x,s)$ and $\hat{v}(x,s)$ in (5.1a) and (5.1b) can be read out as the elements of the following matrix

$$\begin{aligned} H_{wYU}(x,s) &= \begin{bmatrix} h_{\hat{u}Y}(x,s) & h_{\hat{u}U}(x,s) \\ h_{\hat{v}Y}(x,s) & h_{\hat{v}U}(x,s) \end{bmatrix} \\ &:= P(x,s) - (Q(x,s) + P_1(x,s))\varphi(s) \end{aligned} \tag{5.27}$$

with $\varphi(s)$ defined in (5.21).

5.3 Pure state feedback controller

We will now use the results from the previous section to derive the transfer function from the measurement to the actuation when using the controller of Theorem 3.1 in conjunction with the observer (4.1).

Theorem 5.1. *The relationship between the measurement $Y(s) = \mathcal{L}\{Y(t)\}$ and the actuation $U(s) = \mathcal{L}\{U(t)\}$ when using the controller of Theorem 3.1 in conjunction with the observer* (4.1) *is*

$$U(s) = h_{YU_{psf}}(\bar{x}, s)Y(s) \tag{5.28}$$

where

$$\begin{aligned} &h_{YU_{psf}}(\bar{x}, s) \\ &= \frac{\int_0^1 (K^{vu}(\bar{x},\xi)h_{\hat{u}Y}(\xi,s) + K^{vv}(\bar{x},\xi)h_{\hat{v}Y}(\xi,s))d\xi + h_{VY_{psf}}(\bar{x},s)}{1 - \int_0^1 (K^{vu}(\bar{x},\xi)h_{\hat{u}U}(\xi,s) + K^{vv}(\bar{x},\xi)h_{\hat{v}U}(\xi,s))d\xi - h_{VU_{psf}}(\bar{x},s)} \end{aligned} \tag{5.29}$$

and

$$\begin{aligned} h_{VY_{psf}}(\bar{x},s) &:= \frac{1}{r}K_{psf}(\bar{x})h_{\hat{X}Y}(s) + \frac{1}{r}h_{\hat{\delta}Y}(\bar{x},\bar{x},s) + \frac{1}{r}\int_0^{\bar{x}} L^{\alpha}(\bar{x},\xi)h_{\hat{\delta}Y}(\xi,\bar{x},s)d\xi \\ &\quad + \frac{1}{r}\int_0^{\bar{x}} L^{\beta}(\bar{x},\xi)h_{\hat{\beta}Y}(\phi_{\beta}^{-1}(\kappa_{\beta}(\xi,\bar{x})),s)d\xi \end{aligned} \tag{5.30a}$$

$$\begin{aligned} h_{VU_{psf}}(\bar{x},s) &:= \frac{1}{r}K_{psf}(\bar{x})h_{\hat{X}U}(s) + \frac{1}{r}h_{\hat{\delta}U}(\bar{x},\bar{x},s) + \frac{1}{r}\int_0^{\bar{x}} L^{\alpha}(\bar{x},\xi)h_{\hat{\delta}U}(\xi,\bar{x},s)d\xi \\ &\quad + \frac{1}{r}\int_0^{\bar{x}} L^{\beta}(\bar{x},\xi)h_{\hat{\beta}U}(\phi_{\beta}^{-1}(\kappa_{\beta}(\xi,\bar{x})),s)d\xi \end{aligned} \tag{5.30b}$$

$$h_{\hat{\delta}Y}(\xi,\bar{x},s) := \begin{cases} h_{\hat{\alpha}Y}(\phi_\alpha^{-1}(\kappa_\alpha(\xi,\bar{x})),s) & \text{if } \kappa_\alpha(\xi,\bar{x}) \le \phi_\alpha(0) \\ qh_{\hat{\beta}Y}(\phi_\beta^{-1}(\kappa_\alpha(\xi,\bar{x})-\phi_\alpha(0)),s) & \text{otherwise} \end{cases} \tag{5.31a}$$

$$h_{\hat{\delta}U}(\xi,\bar{x},s) := \begin{cases} h_{\hat{\alpha}U}(\phi_\alpha^{-1}(\kappa_\alpha(\xi,\bar{x})),s) & \text{if } \kappa_\alpha(\xi,\bar{x}) \le \phi_\alpha(0) \\ qh_{\hat{\beta}U}(\phi_\beta^{-1}(\kappa_\alpha(\xi,\bar{x})-\phi_\alpha(0)),s) & \text{otherwise} \end{cases} \tag{5.31b}$$

with

$$\begin{aligned} h_{\hat{\alpha}Y}(x,s) &:= h_{\hat{u}Y}(x,s) - \int_0^x K^{uu}(x,\xi)h_{\hat{u}Y}(\xi,s)d\xi \\ &\quad - \int_0^x K^{uv}(x,\xi)h_{\hat{v}Y}(\xi,s)d\xi \end{aligned} \tag{5.32a}$$

$$\begin{aligned} h_{\hat{\alpha}U}(x,s) &:= h_{\hat{u}U}(x,s) - \int_0^x K^{uu}(x,\xi)h_{\hat{u}U}(\xi,s)d\xi \\ &\quad - \int_0^x K^{uv}(x,\xi)h_{\hat{v}U}(\xi,s)d\xi \end{aligned} \tag{5.32b}$$

$$\begin{aligned} h_{\hat{\beta}Y}(x,s) &:= h_{\hat{v}Y}(x,s) - \int_0^x K^{vu}(x,\xi)h_{\hat{u}Y}(\xi,s)d\xi \\ &\quad - \int_0^x K^{vv}(x,\xi)h_{\hat{v}Y}(\xi,s)d\xi \end{aligned} \tag{5.32c}$$

$$\begin{aligned} h_{\hat{\beta}U}(x,s) &:= h_{\hat{v}U}(x,s) - \int_0^x K^{vu}(x,\xi)h_{\hat{u}U}(\xi,s)d\xi \\ &\quad - \int_0^x K^{vv}(x,\xi)h_{\hat{v}U}(\xi,s)d\xi \end{aligned} \tag{5.32d}$$

where $K^{uu}(x,\xi)$, $K^{uv}(x,\xi)$, $K^{vu}(x,\xi)$, $K^{vv}(x,\xi)$ *is the solution to* (3.6)–(3.7).

Proof. We start the proof by using (3.3) to derive the transfer functions relating the estimated backstepping variables $\hat{\alpha}$ and $\hat{\beta}$ emerging from replacing u and v with their estimates $\hat{u}$ and $\hat{v}$ in (3.3), to the measurement $Y(s)$ and actuation $U(s)$. Inserting (5.1a) and (5.1b) for u and v, respectively into a Laplace transformed (3.3) with estimates replacing the real states, we obtain

$$\begin{aligned} \hat{\alpha}(x,s) &= (h_{\hat{u}Y}(x,s)Y(s) + h_{\hat{u}U}(x,s)U(s)) \\ &\quad - \int_0^x K^{uu}(x,\xi)(h_{\hat{u}Y}(\xi,s)Y(s) + h_{\hat{u}U}(\xi,s)U(s))d\xi \\ &\quad - \int_0^x K^{uv}(x,\xi)(h_{\hat{v}Y}(\xi,s)Y(s) + h_{\hat{v}U}(\xi,s)U(s))d\xi \end{aligned} \tag{5.33a}$$

$$\begin{aligned} \hat{\beta}(x,s) &= (h_{\hat{v}Y}(x,s)Y(s) + h_{\hat{v}U}(x,s)U(s)) \\ &\quad - \int_0^x K^{vu}(x,\xi)(h_{\hat{u}Y}(\xi,s)Y(s) + h_{\hat{u}U}(\xi,s)U(s))d\xi \\ &\quad - \int_0^x K^{vv}(x,\xi)(h_{\hat{v}Y}(\xi,s)Y(s) + h_{\hat{v}U}(\xi,s)U(s))d\xi. \end{aligned} \tag{5.33b}$$

By rearranging terms, we find

$$\begin{aligned}\hat{\alpha}(x,s) = [&h_{\hat{u}Y}(x,s) - \int_0^x K^{uu}(x,\xi)h_{\hat{u}Y}(\xi,s)d\xi \\ &- \int_0^x K^{uv}(x,\xi)h_{\hat{v}Y}(\xi,s)d\xi]Y(s) \\ &+ [h_{\hat{u}U}(x,s) - \int_0^x K^{uu}(x,\xi)h_{\hat{u}U}(\xi,s)d\xi \\ &- \int_0^x K^{uv}(x,\xi)h_{\hat{v}U}(\xi,s)d\xi]U(s) \qquad (5.34a)\\ \hat{\beta}(x,s) = [&h_{\hat{v}Y}(x,s) - \int_0^x K^{vu}(x,\xi)h_{\hat{u}Y}(\xi,s)d\xi \\ &- \int_0^x K^{vv}(x,\xi)h_{\hat{v}Y}(\xi,s)d\xi]Y(s) \\ &+ [h_{\hat{v}U}(x,s) - \int_0^x K^{vu}(x,\xi)h_{\hat{u}U}(\xi,s)d\xi \\ &- \int_0^x K^{vv}(x,\xi)h_{\hat{v}U}(\xi,s)d\xi]U(s). \qquad (5.34b)\end{aligned}$$

Thus, by using (5.32) we may write (5.34) as

$$\hat{\alpha}(x,s) = h_{\hat{\alpha}Y}(x,s)Y(s) + h_{\hat{\alpha}U}(x,s)U(s) \qquad (5.35a)$$
$$\hat{\beta}(x,s) = h_{\hat{\beta}Y}(x,s)Y(s) + h_{\hat{\beta}U}(x,s)U(s). \qquad (5.35b)$$

Next, we apply the Laplace transform to (3.46) of Theorem 3.1 and obtain

$$\begin{aligned}V(s) = &\frac{1}{r}K_{psf}(\bar{x})X(s) + \frac{1}{r}\delta(\bar{x},\bar{x},s) \\ &+ \frac{1}{r}\int_0^{\bar{x}} L^{\alpha}(\bar{x},\xi)\delta(\xi,\bar{x},s)d\xi \\ &+ \frac{1}{r}\int_0^{\bar{x}} L^{\beta}(\bar{x},\xi)\beta(\phi_{\beta}^{-1}(\kappa_{\beta}(\xi,\bar{x})),s)d\xi \qquad (5.36)\end{aligned}$$

where $\delta(\xi,\bar{x},s)$ is obtained by Laplace transforming (3.48), yielding

$$\delta(\xi,\bar{x},s) = \begin{cases} \alpha(\phi_{\alpha}^{-1}(\kappa_{\alpha}(\xi,\bar{x})),s) & \text{if } \kappa_{\alpha}(\xi,\bar{x}) \le \phi_{\alpha}(0) \\ q\beta(\phi_{\beta}^{-1}(\kappa_{\alpha}(\xi,\bar{x}) - \phi_{\alpha}(0)),s) & \text{otherwise.} \end{cases} \qquad (5.37)$$

By substituting (5.35) into (5.37), and using (5.31), we immediately obtain an expression for $\hat{\delta}(\xi,\bar{x},s)$ by means of $Y(s)$ and $U(s)$

$$\hat{\delta}(\xi,\bar{x},s) = h_{\hat{\delta}Y}(\xi,\bar{x},s)Y(s) + h_{\hat{\delta}U}(\xi,\bar{x},s)U(s). \qquad (5.38)$$

Substituting (5.1c), (5.35b) and (5.38) into (5.36) we find

$$V(s) = \frac{1}{r}K_{psf}(\bar{x})(h_{\hat{X}Y}(s)Y(s) + h_{\hat{X}U}(s)U(s)) \tag{5.39}$$
$$+ \frac{1}{r}(h_{\hat{\delta}Y}(\bar{x},\bar{x},s)Y(s) + h_{\hat{\delta}U}(\bar{x},\bar{x},s)U(s))$$
$$+ \frac{1}{r}\int_0^{\bar{x}} L^{\alpha}(\bar{x},\xi)[h_{\hat{\delta}Y}(\xi,\bar{x},s)Y(s) + h_{\hat{\delta}U}(\xi,\bar{x},s)U(s)]d\xi$$
$$+ \frac{1}{r}\int_0^{\bar{x}} L^{\beta}(\bar{x},\xi)[h_{\hat{\beta}Y}(\phi_{\beta}^{-1}(\kappa_{\beta}(\xi,\bar{x})),s)Y(s)$$
$$+ h_{\hat{\beta}U}(\phi_{\beta}^{-1}(\kappa_{\beta}(\xi,\bar{x})),s)U(s)]d\xi \tag{5.40}$$

By grouping terms in $Y(s)$ and $U(s)$ and using (5.30) we obtain

$$V(s) = h_{VY_{psf}}(\bar{x},s)Y(s) + h_{VU_{psf}}(\bar{x},s)U(s). \tag{5.41}$$

From Laplace transforming (3.4) and substituting u nad v with their estimates $\hat{u}$ and $\hat{v}$, we find

$$U(s) = \int_0^1 K^{vu}(1,\xi)\hat{u}(\xi,s)d\xi + \int_0^1 K^{vv}(1,\xi)\hat{v}(\xi,s)d\xi + V(s). \tag{5.42}$$

The result (5.28) follows from (5.42) by inserting (5.1a), (5.1b) and (5.41), solving for $U(s)$ and finally using (5.29). □

5.4 Recursive controller

The transfer function of the controller of Theorem 3.2 in conjunction with the observer (4.1) will here be derived.

Theorem 5.2. *The relationship between the measurement $Y(s) = \mathcal{L}\{Y(t)\}$ and the actuation $U(s) = \mathcal{L}\{U(t)\}$ when using the controller of Theorem 3.2 in conjunction with the observer* (4.1) *is*

$$U(s) = h_{YU_{rec}}(\bar{x},s)Y(s) \tag{5.43}$$

where

$$h_{YU_{rec}}(\bar{x},s) = \frac{\int_0^1 (K^{vu}(\bar{x},\xi)h_{\hat{u}Y}(\xi,s) + K^{vv}(\bar{x},\xi)h_{\hat{v}Y}(\xi,s))d\xi + h_{VY_{rec}}(\bar{x},s)}{1 - \int_0^1 (K^{vu}(\bar{x},\xi)h_{\hat{u}U}(\xi,s) + K^{vv}(\bar{x},\xi)h_{\hat{v}U}(\xi,s))d\xi - h_{VU_{rec}}(\bar{x},s)} \tag{5.44}$$

and

$$h_{VY_{rec}}(\bar{x}, s) = g_{rec}(\bar{x}, s)K_{rec}(\bar{x})h_{\hat{X}Y}(s) \tag{5.45a}$$
$$h_{VU_{rec}}(\bar{x}, s) = g_{rec}(\bar{x}, s)K_{rec}(\bar{x})h_{\hat{X}U}(s) \tag{5.45b}$$

with

$$g_{rec}(\bar{x}, s) = \frac{1}{r - qe^{-sd_{rec}(\bar{x})} - q\int_0^{\bar{x}} L^{\alpha}(\bar{x}, \xi)e^{-sd_{\alpha}(\xi,\bar{x})}d\xi - \int_0^{\bar{x}} L^{\beta}(\bar{x}, \xi)e^{-sd_{\beta}(\xi,\bar{x})}d\xi}. \tag{5.46}$$

Proof. By Laplace transforming (3.74) from Theorem 3.2, we obtain

$$\begin{aligned} V(s) = \frac{q}{r}V(s)e^{-sd_{rec}(\bar{x})} &+ \frac{q}{r}\int_0^{\bar{x}} L^{\alpha}(\bar{x}, \xi)e^{-sd_{\alpha}(\xi,\bar{x})}d\xi V(s) \\ &+ \frac{1}{r}\int_0^{\bar{x}} L^{\beta}(\bar{x}, \xi)e^{-sd_{\beta}(\xi,\bar{x})}d\xi V(s) \\ &+ \frac{1}{r}K_{rec}(\bar{x})X(s) \end{aligned} \tag{5.47}$$

which is straightforwardly solved for $V(s)$, resulting in

$$V(s) = g_{rec}(\bar{x}, s)K_{rec}(\bar{x})X(s) \tag{5.48}$$

where (5.46) has been used. Substituting for the estimate $\hat{X}(s)$ instead of the actual $X(s)$ and using (5.1c) we obtain

$$V(s) = g_{rec}(\bar{x}, s)K_{rec}(\bar{x})(h_{\hat{X}Y}(s)Y(s) + h_{\hat{X}U}(s)U(s)) \tag{5.49}$$

The result (5.43) follows from substituting (5.49) into (5.42), solving for $U(s)$ and using (5.45). □

As predicted, the transfer function in Theorem 5.2 is much easier to derive than the transfer function in Theorem 5.1.

5.5 Simplified controller

Lastly, the transfer function of the controller of Theorem 3.3 in conjunction with the observer (4.1) is derived.

Theorem 5.3. *The relationship between the measurement* $Y(s) = \mathcal{L}\{Y(t)\}$ *and the actuation* $U(s) = \mathcal{L}\{U(t)\}$ *when using the controller of Theorem 3.3 in conjunction with the observer* (4.1) *is*

$$U(s) = h_{YU_{\infty}}(\bar{x}, s)Y(s) \tag{5.50}$$

where

$$h_{YU_\infty}(\bar{x},s) = \frac{\int_0^1 (K^{vu}(\bar{x},\xi)h_{\hat{u}Y}(\xi,s) + K^{vv}(\bar{x},\xi)h_{\hat{v}Y}(\xi,s))d\xi + h_{VY_\infty}(\bar{x},s)}{1 - \int_0^1 (K^{vu}(\bar{x},\xi)h_{\hat{u}U}(\xi,s) + K^{vv}(\bar{x},\xi)h_{\hat{v}U}(\xi,s))d\xi - h_{VU_\infty}(\bar{x},s)}. \quad (5.51)$$

and

$$h_{VY_\infty}(\bar{x},s) = \frac{1}{r}K_\infty(\bar{x})h_{\hat{X}Y}(s) \quad (5.52a)$$

$$h_{VU_\infty}(\bar{x},s) = \frac{1}{r}K_\infty(\bar{x})h_{\hat{X}U}(s). \quad (5.52b)$$

Proof. By taking the Laplace transform of (3.83) from Theorem 3.3, and inserting for the disturbance estimate, using (5.1c) we obtain

$$V(s) = \frac{1}{r}K_\infty(\bar{x})(h_{\hat{X}Y}(s)Y(s) + h_{\hat{X}U}(s)U(s)). \quad (5.53)$$

By inserting (5.53) into (5.42), solving for $U(s)$ and using (5.51)–(5.52), we find (5.50). □

Chapter 6

Model reduction: Obtaining rational transfer function approximations

6.1 Introduction

In order to implement the transfer functions of Theorems 5.1–5.3 on a computer, we will have to find their time domain equivalents, that is; their inverse Laplace transforms. The inverse Laplace transform for some function $F(s)$ which inverse is $f(t)$ is generally given by the line integral (Abramowitz and Stegun (1975, Eq. (29.2.2)))

$$f(t) = \frac{1}{2\pi j} \int_{\sigma_0 - j\infty}^{\sigma_0 + j\infty} F(s) e^{st} ds \tag{6.1}$$

where σ_0 must be larger than the real part of all singularities of $F(s)$. The integral (6.1) is also known as the *Bromwich integral*, with the line $\Re(s) = \sigma_0$ along which the integration is taken known as the *Bromwich contour*. The inversion formula (6.1) is an example of the so-called "ill-posed problem". Numerically, one is faced with the question of numerical instabilities: small perturbations of the data produce large fluctuations in the output data, and there is no universal algorithm to evaluate the integral, according to Cunha and Viloche (1992).

In this section, we present a model reduction scheme based on a series expansion using a type of functions known as Laguerre functions. The use of Laguerre functions for inverting Laplace transforms is an old established method, dating back to 1935 (Tricomi (1935), Widder (1935)). In Amghayrir, Tanguy, Bréhonnet, Vilbé, and Calvez (2005), the Laguerre series representation was used to derive a model reduction technique using a transfer-function

formalism. The method allowed reduction of irrational transfer functions into rational approximations, and found the approximation that minimized the error in the least squares sense. A rational approximation is highly desirable for implementation on a computer as it allows for state space implementation and realization using standard, linear ODEs. The method from Amghayrir et al. (2005) was also applied to an irrational transfer function in Mahdianfar et al. (2012), proving very good results.

6.2 Laguerre representation

We will in this section show how a wide class of functions can be represented using an infinite sum of so-called Laguerre functions. The representation is based on inner product and Hilbert space theory, but as this is a vast and complex field in mathematics, the theory will be superficially touched and only the relevant properties of such spaces will be presented. However, the reader is expected to be somewhat familiar with basic vector space theory, inner products and norms. For more information, consult e.g. Kreyszig (2010, Sec. 7.9) or Axler (1997).

6.2.1 The extended space of square integrable functions

We start by defining an inner product space $L^2_\varpi(\mathbb{R}^+)$ of functions that are square integrable after an exponential weighting. Given two time varying functions $f(t)$ and $g(t)$ defined for $t \geq 0$. Define the weighted inner product

$$\langle f, g \rangle_\varpi := \int_0^\infty \varpi(t) f(t) g(t) dt \tag{6.2}$$

with associated norm

$$||f||_\varpi = \sqrt{\langle f, f \rangle_\varpi} \tag{6.3}$$

where the weighting

$$\varpi(t) := e^{-(\gamma - 2\alpha)t} \tag{6.4}$$

is determined using two parameters γ and α. Next, let $L^2_\varpi(\mathbb{R}^+)$ denote the space of measurable real valued functions $f(t)$ which has a well-defined norm in the sense of (6.2), viz.

$$f \in L^2_\varpi(\mathbb{R}^+) \Leftrightarrow ||f||_\varpi < \infty. \tag{6.5}$$

The space $L^2_\varpi(\mathbb{R}^+)$ is a *Hilbert space* according to Amghayrir et al. (2005). As the well known space of square integrable functions $L^2(\mathbb{R}^+)$ can be obtained

from $L^2_\varpi(\mathbb{R}^+)$ by choosing $\gamma = 2\alpha$, $L^2_\varpi(\mathbb{R}^+)$ can be considered an extension of $L^2_\varpi(\mathbb{R}^+)$. The space $L^2_\varpi(\mathbb{R}^+)$ allows for exponential weighting of functions, in that $f(t)$ belongs to $L^2_\varpi(\mathbb{R}^+)$ if the exponentially weighted function $g(t) = e^{-\sigma t} f(t)$, where

$$\sigma := \frac{\gamma}{2} - \alpha \tag{6.6}$$

belongs to $L^2(\mathbb{R}^+)$.

6.2.2 Laguerre polynomials and functions

The Laguerre polynomials $L_n(x), x \geq 0,\ n \in \mathbb{Z}^+$ are the solutions to the Laguerre equation

$$xL_n''(x) + (1-x)L_n'(x) + nL_n(x) = 0 \tag{6.7}$$

for $n \in \mathbb{Z}^+$. An alternative formulation is given by the *Rodrigues formula* (Weideman (1999, p. 114))

$$L_n(x) = \frac{e^x}{n!}\frac{d^n}{dx^n}\left(e^{-x}x^n\right), x \geq 0 \tag{6.8}$$

or as the binomial series (Abate, Choudhury, and Whitt (1996))

$$L_n(x) = \sum_{k=0}^{n} \binom{n}{k} \frac{(-x)^k}{k!}, x \geq 0. \tag{6.9}$$

The Laguerre functions are mixed polynomial and exponential functions generated from the Laguerre polynomials. There exist several variations in the literature on how these functions are generated from the Laguerre polynomials (see e.g. Steiglitz (1965), Weideman (1999), Malti, Maquin, and Ragot (1999) and Kano, Brio, and Moloney (2005) for a few). We will focus on the one presented in Amghayrir et al. (2005) which are parametrized using two parameters $\gamma > 0$ and $\alpha > 0$ and is given as

$$l_n(t; \alpha, \gamma) := \sqrt{\gamma} e^{-\alpha t} L_n(\gamma t). \tag{6.10}$$

An important property of the Laguerre functions (6.10) is that they form a so-called *orthonormal basis* (Hochstrasser (1975, Sec. 22.1.1)) for $L^2_\varpi(\mathbb{R}^+)$ for any set of parameters $0 < \gamma, \alpha \in \mathbb{R}$. This means, among many other properties, that the inner product (6.2) applied to a pair of Laguerre functions is

$$\langle l_n, l_m \rangle_\varpi = \delta_{nm}, \quad \text{where} \quad \delta_{nm} = \begin{cases} 1 & \text{if } n = m \\ 0 & \text{otherwise.} \end{cases} \tag{6.11}$$

6.2.3 Laguerre expansions

As the Laguerre functions (6.10) form an orthonormal basis for the Hilbert space $L^2_\varpi(\mathbb{R}^+)$, it follows that *any* function $f(t) \in L_\varpi(\mathbb{R}^+)$ can be written as an infinite sum of weighted Laguerre functions (Axler (1997, Theorem 6.17)) as follows

$$f(t) = \sum_{n=0}^{\infty} q_n(\alpha, \gamma) l_n(t; \alpha, \gamma) \tag{6.12}$$

for some set of (real) coefficients $\{q_n(\alpha, \gamma)\}_{0 \leq n \in \mathbb{Z}^+}$. From Parseval's Formula (Debnath and Mikusinski (1990, Thrm. 3.8.5)), we also have that

$$||f|| = \sum_{n=0}^{\infty} q_n^2(\alpha, \gamma) < \infty \tag{6.13}$$

from which it follows that

$$\lim_{n \to \infty} q_n(\alpha, \gamma) = 0. \tag{6.14}$$

The set of Laguerre coefficients $\{q_n(\alpha, \gamma)\}_{n \in \mathbb{Z}^+}$ is often referred to as the function's *Laguerre Spectrum*. One can find the Laguerre spectrum $\{q_n(\alpha, \gamma)\}_{n \in \mathbb{Z}^+}$ by evaluation of the inner product

$$q_n(\alpha, \gamma) = \langle f, l_n \rangle_\varpi = \int_0^\infty \varpi(t) f(t) l_n(t)\, dt. \tag{6.15}$$

This can be seen from applying the inner product (6.2) to (6.12) and the Laguerre functions (6.10), and using (6.11).

6.3 Laguerre-Gram based model order reduction

A model order reduction scheme based on the Laguerre expansion of the function is here presented. The algorithm was originally presented in Amghayrir et al. (2005), and takes the function's Laguerre spectrum as input, solves a linear set of equations from a pair of matrices generated from the Laguerre spectrum, and uses the result to construct the numerator and denominator of the rational approximation. In practice, an N-order truncated Laguerre spectrum is used, and it is assumed that the truncation error is sufficiently small the model reduction will give a good approximation of the original transfer function.

The algorithm takes the following inputs:

1. A desired order r for the rational approximation,
2. The truncated Laguerre spectrum $\{q_n(\alpha,\gamma)\}_{n\in\mathbb{Z},\, 0\le n\le N+r}$ for some $N \gg r$, for the function f to be approximated,
3. The design variables α, γ used to find the Laguerre spectrum,

and produces a rational approximation $\hat{f}$ in the following steps:

1. Form the following matrix (known as a Gram matrix)

$$\Psi := \begin{bmatrix} \psi_{0,0} & \psi_{0,1} & \dots & \psi_{0,r-1} \\ \psi_{1,0} & \psi_{1,1} & \dots & \psi_{1,r-1} \\ \vdots & \vdots & \ddots & \vdots \\ \psi_{r-1,0} & \psi_{r-1,1} & \dots & \psi_{r-1,r-1} \end{bmatrix} \tag{6.16}$$

   and the vector

$$b := \begin{bmatrix} \psi_{0,r} & \psi_{1,r} & \dots & \psi_{r-1,r} \end{bmatrix}^T. \tag{6.17}$$

   where the coefficients $\psi_{i,j}$ are computed from the truncated Laguerre spectrum as

$$\psi_{i,j} = \sum_{n=0}^{N} q_{n+i} q_{n+j}. \tag{6.18}$$

2. Solve the system of equations

$$\Psi a = -b \tag{6.19}$$

   for the vector of coefficients

$$a := \begin{bmatrix} a_0 & a_1 & \dots & a_{r-1} \end{bmatrix}^T. \tag{6.20}$$

3. Form the reduced order model using

$$\hat{f}(s) = \frac{\sqrt{\gamma}\sum_{i=1}^{r} a_i \sum_{j=0}^{i-1} q_j (s+\alpha)^{i-j-1}(s-\gamma+\alpha)^{r-i+j}}{\sum_{i=0}^{r} a_i (s+\alpha)^i (s-\gamma+\alpha)^{r-i}} \tag{6.21}$$

   where $a_r = 1$ has been defined.

For derivation of the algorithm, analysis and proofs, the interested reader is referred to Amghayrir et al. (2005). Note that the computational speed needed for computing the quantities $\psi_{i,j}$ in (6.18) can be drastically reduced using recursion and symmetry properties, as $\psi_{i,j} = \psi_{i-1,j-1} - q_{i-1}q_{j-1}$ for $i = 1, 2, ..., r-1$ and $j = i, i+1, ..., r$, and that $\psi_{i,j} = \psi_{j,i}$.

6.4 Determination of the Laguerre spectrum

An immediate problem with the algorithm in the previous section, is the determination of the (truncated) Laguerre spectrum $\{q_n(\alpha,\gamma)\}_{n\in\mathbb{Z}^+}$. The expression (6.15) requires the knowledge of $f(t)$, but finding an approximation to this unknown function is precisely the intention of introducing the Laguerre coefficients in the first place. This issue was not addressed in Amghayrir et al. (2005).

An expression stating the Laguerre spectrum of a function $f(t)$ with Laguerre functions given from (6.10) with the knowledge of it's Laplace transform $F(s)$ will here be derived. This has previously been addressed by several authors (Steiglitz (1965), Garbow, Giunta, and Murli (1988), Abate et al. (1996), Weideman (1999)). However, to the best of our knowledge, is has not been derived for the Laguerre functions of the kind given from (6.10). We will base our derivation on the one found in Kano et al. (2005), which is a variation of Weeks' method (Weeks (1966)).

The Laguerre functions $l_n(t;\alpha,\gamma)$ as given in (6.10) have Laplace transforms (Amghayrir et al. (2005))

$$l_n(s) = \mathcal{L}(l_n(t;\alpha,\gamma)) = \frac{\sqrt{\gamma}}{s+\alpha}\left(\frac{s-\gamma+\alpha}{s+\alpha}\right)^n. \tag{6.22}$$

Taking the Laplace transform of (6.12), we find

$$F(s) = \sum_{n=0}^{\infty} q_n(\alpha,\gamma) l_n(s) = \frac{\sqrt{\gamma}}{s+\alpha}\sum_{n=0}^{\infty} q_n(\alpha,\gamma)\left(\frac{s-\gamma+\alpha}{s+\alpha}\right)^n. \tag{6.23}$$

where $F(s) = \mathcal{L}\{f(t)\}$. Consider the transformation[1]

$$w := \frac{s-\gamma+\alpha}{s+\alpha} \tag{6.24}$$

which inverse is

$$s = \frac{\gamma}{1-w} - \alpha. \tag{6.25}$$

The transformation (6.24) maps the domain $\Re(s) > \sigma = \frac{\gamma}{2} - \alpha$ in the complex plane to the interior of the unit circle. This can be seen by substituting

$$s = \frac{\gamma}{2} - \alpha + h + j\omega \tag{6.26}$$

[1]This is a so-called Möbious Transformation. Consult e.g. Kreyszig (2010, Sec. 17.2) for more information.

for some $h \in \mathbb{R}$ into (6.24), yielding

$$w = \frac{\frac{\gamma}{2} - \alpha + h + j\omega - \gamma + \alpha}{\frac{\gamma}{2} - \alpha + h + j\omega + \alpha} = \frac{h - \frac{\gamma}{2} + j\omega}{h + \frac{\gamma}{2} + j\omega}. \tag{6.27}$$

The norm of w is

$$|w| = \sqrt{\frac{(h - \frac{\gamma}{2})^2 + \omega^2}{(h + \frac{\gamma}{2})^2 + \omega^2}} \tag{6.28}$$

If $h > 0$ (and $\gamma > 0$), clearly $(h - \frac{\gamma}{2})^2 < (h + \frac{\gamma}{2})^2$, and the denominator is larger then the numerator. Hence $|w| < 1$ for $\Re(s) > \frac{\gamma}{2} - \alpha$.

Inserting (6.24) into (6.23), we find

$$\sum_{n=0}^{\infty} q_n(\alpha, \gamma) w^n = \frac{\sqrt{\gamma}}{1 - w} F\left(\frac{\gamma}{1 - w} - \alpha\right) \tag{6.29}$$

which is a complex MacLaurin series. The radius of convergence is greater than one following the way the transformation (6.24) was chosen. Multiplying both sides of (6.29) with w^{-m-1} for $m \in \mathbb{Z}$, we obtain

$$\sum_{n=0}^{\infty} q_n(\alpha, \gamma) w^{n-m-1} = \sqrt{\gamma} \frac{w^{-m-1}}{1 - w} F\left(\frac{\gamma}{1 - w} - \alpha\right) \tag{6.30}$$

By integrating along the contour $|w| = 1$ it follows from Lemma A.3 in the appendix that every term in the left hand side sum to $2\pi j$ for $m = n$, and zero otherwise, hence

$$q_n(\alpha, \gamma) = \frac{\sqrt{\gamma}}{2\pi j} \oint_{|w|=1} \frac{w^{-n-1}}{1 - w} F\left(\frac{\gamma}{1 - w} - \alpha\right) dw \tag{6.31}$$

which is an equation explicitly expressing the Laguerre coefficients. Lastly, inserting for $w = e^{j\theta}$ we obtain

$$q_n(\alpha, \gamma) = \frac{\sqrt{\gamma}}{2\pi} \int_{-\pi}^{\pi} \frac{e^{-jn\theta}}{1 - e^{j\theta}} F\left(\frac{\gamma}{1 - e^{j\theta}} - \alpha\right) d\theta. \tag{6.32}$$

This expression can be evaluated using a numerical integration scheme. Care must be taken, as $1 - e^{j\theta}$ is zero when $\theta = 0$, which would require the evaluation of the integrand in (6.32) at infinity. One could circumvent this by substituting $w = Re^{j\theta}$ for $0 < R < 1$ instead, as was done in Lyness and Giunta (1986), or for instance, using the midpoint rule (see Appendix B.2) which misses out the point $\theta = 0$. This was for instance done in Weideman (1999).

Another interesting observation, is that if one defines the function

$$G(\theta) := \frac{\sqrt{\gamma}}{1 - e^{j\theta}} F\left(\frac{\gamma}{1 - e^{j\theta}} - \alpha\right) \tag{6.33}$$

the expression (6.32) becomes

$$q_n(\alpha, \gamma) = \frac{1}{2\pi} \int_{-\pi}^{\pi} G(\theta) e^{-jn\theta} d\theta \tag{6.34}$$

which can be recognized as Fourier series coefficients for the function $G(\theta)$. Now using the midpoint rule (see Appendix B.2) with $2N$ intervals, one can compute an estimate of q_n as

$$\hat{q}_n(\alpha, \gamma) = \frac{e^{-jn\frac{\pi}{2N}}}{2N} \sum_{k=-N}^{N-1} G\left(\frac{\pi}{N}(k + 1/2)\right) e^{-j\pi nk/N}, \quad n = 0, \ldots, N-1 \tag{6.35}$$

which, from inspection, can be recognized as a shifted and scaled version of the Discrete Fourier Transform (DFT) of $G(\theta)$. The efficient Fast Fourier Transform (FFT) (Kreyszig (2010, p. 531)) may therefore be applied for computing the Laguerre spectrum $\{q_n(\alpha, \gamma)\}_{0 \leq n \in \mathbb{Z}}$ from a set of cleverly sampled points of the Laplace Transform $F(s)$.

6.5 Optimum choice of parameters

A natural question related to the method presented above arises; how does one choose the parameters α and γ? This was addressed in Tanguy, Vilbé, and Calvez (1995), where a method for determination of the free parameters in orthogonal bases so that the error is minimized in a least squares sense was proposed. The method was also said to be used for choosing α and γ in the examples in Amghayrir et al. (2005), but the details were left out. The main clues, ported to the orthogonal Laguerre functions (6.10), are here presented. The method is presented under the assumption of having a single free variable. We will denote this as α, and assume a relationship to γ is given, that is $\gamma = \gamma(\alpha)$, so that $q_n(\alpha, \gamma) = q_n(\alpha)$ and $l_n(t; \alpha, \gamma) = l_n(t; \alpha)$.

Consider the approximation, created by truncating the infinite series (6.12) after N terms

$$\hat{f}(t) = \sum_{n=0}^{N-1} q_n(\alpha) l_n(t; \alpha) \tag{6.36}$$

and denote the relative weighted, quadratic error emerging by truncating the series as

$$\epsilon_N(\alpha) = \frac{||\hat{f} - f||^2}{||f||^2} = \frac{||\sum_{n=N}^{\infty} q_n(\alpha) l_n(t; \alpha)||^2}{||f||^2}. \tag{6.37}$$

It is observed that $0 \leq \epsilon_N(\alpha) \leq 1$. According to Tanguy et al. (1995) does, due to the orthogonality property of the functions $l_n(t;\alpha)$, the following hold

$$\epsilon_N(\alpha) = \frac{1}{||f||^2} \sum_{n=N}^{\infty} q_n^2(\alpha) \tag{6.38}$$

where the norm $||f||$ can be expressed from (6.13). This expression for the quadratic error can usually be reduced by a proper choice of α.

Many set of continuous orthogonal functions satisfy the noteworthy equation

$$\mathcal{H}_\alpha l_n(t;\alpha) = \lambda(n) l_n(t;\alpha) \tag{6.39}$$

where $\mathcal{H}_\alpha$ is a linear operator on the form

$$\mathcal{H}_\alpha f(t) = A(t;\alpha) f''(t) + B(t;\alpha) f'(t) + C(t;\alpha) f(t). \tag{6.40}$$

The term $\lambda(n)$ is a strictly increasing function independent of t, satisfying

$$\lambda(0) = 0 < \lambda(1) < \lambda(2) < \lambda(3) < \dots \tag{6.41}$$

and $y_n(t;\alpha),\ n \in \mathbb{Z}^+$ are the orthogonal functions. If we apply this operator $\mathcal{H}$ to the Laguerre expansion (6.12), we find

$$\mathcal{H}_\alpha f(t) = \sum_{n=0}^{\infty} q_n(\alpha) \mathcal{H}_\alpha l_n(t;\alpha) = \sum_{n=0}^{\infty} q_n(\alpha) \lambda(n) l_n(t;\alpha) \tag{6.42}$$

By applying the inner product to $f(t)$ and $\mathcal{H}_\alpha f(t)$ and using the linearity property of inner products (i.e. $\langle af + bg, l_n \rangle = a\langle f, l_n \rangle + b\langle g, l_n \rangle$ for functions f, g and constants a, b) we find

$$\langle f, \mathcal{H}_\alpha f \rangle = \sum_{n=0}^{\infty} \lambda(n) q_n^2(\alpha) \geq \lambda(N) \sum_{n=N}^{\infty} q_n^2(\alpha). \tag{6.43}$$

Thus, by comparing (6.43) with the error term (6.38), we find an upper bound for the error $\epsilon_N(\alpha)$ as

$$\epsilon_N(\alpha) \leq \frac{1}{\lambda(N)} \frac{\langle f, \mathcal{H}_\alpha f \rangle}{||f||^2} = \frac{1}{\lambda(N)} G_\epsilon(\alpha) \tag{6.44}$$

where

$$G_\epsilon(\alpha) := \frac{\langle f, \mathcal{H}_\alpha f \rangle}{||f||^2} \tag{6.45}$$

has been defined. Thus, the best choice of the parameter α is the $\alpha = \alpha_0$ which minimizes $G_\epsilon(\alpha)$ in (6.45). Also note that $G_\epsilon(\alpha)$ in (6.45) is independent of N. Thus, α_0 can be computed first and N can be chosen afterwards,

but note that in order to get a useful bound, N must be large enough so that $N > G_\epsilon(\alpha)$, or else the error term $\epsilon_N(\alpha)$ that is upper bounded by 1, may exceed unity. When the signal $f(t)$ is known via experimental data, $G_\epsilon(\alpha)$ can be readily determined by computer.

For the Laguerre functions defined in (6.10), the operator $\mathcal{H}_\alpha$ can be taken as[1]

$$\begin{aligned}\mathcal{H}_\alpha f(t) = &-\frac{1}{\gamma(\alpha)} t f''(t) + \frac{1}{\gamma(\alpha)}((\gamma(\alpha) - 2\alpha)t - 1) f'(t) \\ &- \frac{1}{\gamma(\alpha)}(\alpha + \alpha(\alpha - \gamma(\alpha))t) f(t)\end{aligned} \tag{6.46}$$

with

$$\lambda(n) = n, \tag{6.47}$$

and the error function becomes

$$G_\epsilon(\alpha) = \frac{\langle f, \mathcal{H}_\alpha f \rangle}{||f||^2} = \frac{\sum_{n=0}^{\infty} n q_n^2(\alpha)}{\sum_{n=0}^{\infty} q_n^2(\alpha)} \tag{6.48}$$

The act of finding the α minimizing $G_\epsilon(\alpha)$ in (6.48) can for instance be performed using extremum seeking numerically on a computer.

[1]This can be verified by direct computations.

Part III

Application and Simulation

Chapter 7

Application to the heave problem in MPD

7.1 Introduction

We will demonstrate the theory derived in Part II on the heave problem in Managed Pressure Drilling. The following model was used in used in Aamo (2013) to model the heave problem in MPD

$$p_t(z,t) = -\frac{\beta}{A_1} q_z(z,t) \tag{7.1a}$$

$$q_t(z,t) = -\frac{A_1}{\rho} p_z(z,t) - \frac{F_1}{\rho} q(z,t) - A_1 g \tag{7.1b}$$

$$q(0,t) = -A_2 \bar{C} Z(t) \tag{7.1c}$$

$$p(l,t) = p_l(t) \tag{7.1d}$$

$$\dot{Z} = \bar{A} Z, \qquad Z(0) = Z_0 \tag{7.1e}$$

where l is the well depth, $z \in [0,l]$, $t \geq 0$, $p(z,t)$ is the pressure, $q(z,t)$ is the volumetric flow, β is the mud's bulk modulus, ρ is the mud density, A_1 is the cross sectional area of annulus, A_2 is the cross sectional area of the drill bit, F_1 is the friction factor and g is the gravity constant. $p_l(t)$ is the actuation, and its actuation device is assumed to have significantly faster dynamics than the rest of the system so that actuation dynamics can be ignored. Also, $q(1,t) = q_l(t)$ is assumed measured. A desired constant pressure at $z = \bar{z} \in (0,l)$ is stated as

$$p(\bar{z},t) = p_{sp}. \tag{7.2}$$

The disturbance $Z(t)$ is assumed to be an autonomously driven harmonic oscillator, parametrized by a finite set $\{\omega_1, \omega_2, \ldots, \omega_n\}$ of n known frequencies

and has the following form

$$\bar{A} = \text{diag}\left(\begin{bmatrix} 0 & \omega_1 \\ -\omega_1 & 0 \end{bmatrix}, \dots \begin{bmatrix} 0 & \omega_n \\ -\omega_n & 0 \end{bmatrix}\right) \tag{7.3}$$

$$\bar{C} = \begin{bmatrix} 0 & 1 & 0 & 1 & \dots & 0 & 1 \end{bmatrix}. \tag{7.4}$$

Note that the pair $(\bar{A}, \bar{C})$ is observable. The model (7.1) was originally presented in Landet et al. (2013), with the disturbance model (7.3)–(7.4) added in Aamo (2013).

Firstly, we will in Section 7.2 pose a coordinate transformation to bring the model (7.1)–(7.4) to the form (3.1). In Section 7.3, the results from Chapter 3 as well as the transformation in 7.2 are used to derive controllers for attenuation of heave induced pressure fluctuations in Managed Pressure Drilling assuming full state measurements are available. An expression for the signal $Y(t)$ required for implementation of the observer from Chapter 4 is also presented, for practical implementation where sensing usually is limited to the topside. A fundamental matrix needed to evaluate the transfer functions in Chapter 5 is derived in Section 7.4. In Section 7.5, numerics for solving the kernel equations (3.6)–(3.7), (3.10)–(3.11), and (4.4)–(4.5) is derived.

7.2 Feasibility of design

A transformation relating to drilling system (7.1)–(7.4) to (3.1) is here presented.

Lemma 7.1 (Modified from Lemma 10 in Aamo (2013))**.** *For a given $\bar{z}$ and p_{sp}, the transformation*

$$u(x,t) = \frac{1}{2}\left[q(xl,t) + \frac{A_1}{\sqrt{\beta\rho}}\left(p(xl,t) - p_{sp} + \rho g l(x-\bar{x})\right)\right] e^{\frac{lF_1}{2\sqrt{\beta\rho}}(x-\bar{x})} \tag{7.5a}$$

$$v(x,t) = \frac{1}{2}\left[q(xl,t) - \frac{A_1}{\sqrt{\beta\rho}}\left(p(xl,t) - p_{sp} + \rho g l(x-\bar{x})\right)\right] e^{-\frac{lF_1}{2\sqrt{\beta\rho}}(x-\bar{x})} \tag{7.5b}$$

where

$$\bar{x} = \frac{\bar{z}}{l}. \tag{7.6}$$

maps the system (7.1) *to the form* (3.1) *with*

$$X(t) = Z(t) \tag{7.7}$$

$$U(t) = \frac{1}{2}\left(q(l,t) - \frac{A_1}{\sqrt{\beta\rho}}(p_l(t) - p_{sp} + \rho g l(1-\bar{x}))\right) e^{-\frac{\gamma}{2}(1-\bar{x})} \tag{7.8}$$

$$\epsilon_1(x) = \epsilon_2(x) = \epsilon, \quad c_1(x) = a_0 e^{\gamma x}, \quad c_2(x) = b_0 e^{-\gamma x} \tag{7.9}$$

$$q = -e^{-\gamma \bar{x}} \tag{7.10}$$

$$A = \bar{A}, \quad C = -e^{\frac{\gamma}{2}\bar{x}} A_2 \bar{C} \tag{7.11}$$

where

$$\epsilon = \frac{1}{l}\sqrt{\frac{\beta}{\rho}}, \quad a_0 = c_0 e^{-\gamma \bar{x}}, \quad b_0 = c_0 e^{\gamma \bar{x}}, \quad c_0 = -\frac{1}{2}\frac{F_1}{\rho}, \quad \gamma = \frac{l F_1}{\sqrt{\beta \rho}}. \tag{7.12}$$

Moreover, the control objective (7.2) *is transformed to* (3.2) *with* $r = 1$ *and* $\bar{x}$ *as in* (7.6).

Proof. We remove the constant term and shift the origin by defining

$$\bar{p}(z,t) = p(z,t) - p_{sp} + \rho g(z - \bar{z}) \tag{7.13}$$

from which we find

$$\bar{p}_z(z,t) = p_z(z,t) + \rho g \tag{7.14}$$

and

$$\bar{p}_t(z,t) = p_t(z,t). \tag{7.15}$$

This yields the modified system

$$\bar{p}_t(z,t) = -\frac{\beta}{A_1} q_z(z,t) \tag{7.16a}$$

$$q_t(z,t) = -\frac{A_1}{\rho}\bar{p}_z(z,t) - \frac{F_1}{\rho} q(z,t) \tag{7.16b}$$

$$\bar{p}(l,t) = p_l(t) - p_{sp} + \rho g(l - \bar{z}). \tag{7.16c}$$

Consider now the diagonalizing change of variables

$$\bar{u}(z,t) = \frac{1}{2}\left(q(z,t) + \frac{A_1}{\sqrt{\beta\rho}}\bar{p}(z,t)\right) \tag{7.17a}$$

$$\bar{v}(z,t) = \frac{1}{2}\left(q(z,t) - \frac{A_1}{\sqrt{\beta\rho}}\bar{p}(z,t)\right) \tag{7.17b}$$

from which we find the partial derivatives with respect to z as

$$\bar{u}_z(z,t) = \frac{1}{2}\left(q_z(z,t) + \frac{A_1}{\sqrt{\beta\rho}}\bar{p}_z(z,t)\right) \tag{7.18a}$$

$$\bar{v}_z(z,t) = \frac{1}{2}\left(q_z(z,t) - \frac{A_1}{\sqrt{\beta\rho}}\bar{p}_z(z,t)\right) \tag{7.18b}$$

and with respect to t as (omitting the details regarding $\bar{v}_t(z,t)$)

$$\begin{aligned}
\bar{u}_t(z,t) &= \frac{1}{2}\left(-\frac{A_1}{\rho}\bar{p}_z(z,t) - \frac{F_1}{\rho}q(z,t) - \frac{A_1}{\sqrt{\beta\rho}}\frac{\beta}{A_1}q_z(z,t)\right) \\
&= -\frac{1}{2}\left(\frac{A_1}{\rho}\bar{p}_z(z,t) + \sqrt{\frac{\beta}{\rho}}q_z(z,t)\right) - \frac{1}{2}\frac{F_1}{\rho}q(z,t) \\
&= -\frac{1}{2}\sqrt{\frac{\beta}{\rho}}\left(\frac{A_1}{\sqrt{\rho\beta}}\bar{p}_z(z,t) + q_z(z,t)\right) - \frac{1}{2}\frac{F_1}{\rho}q(z,t) \\
&= -\sqrt{\frac{\beta}{\rho}}\bar{u}_z(z,t) - \frac{1}{2}\frac{F_1}{\rho}(\bar{u}(z,t) + \bar{v}(z,t)) \qquad (7.19a)
\end{aligned}$$

$$\bar{v}_t(z,t) = \sqrt{\frac{\beta}{\rho}}\bar{v}_z(z,t) - \frac{1}{2}\frac{F_1}{\rho}(\bar{u}(z,t) + \bar{v}(z,t)) \tag{7.19b}$$

where (7.18a) has been inserted into (7.19a). We get rid of the term in $\bar{u}$ in (7.19a) and in $\bar{v}$ in (7.19b), and scale the domain into $[0,1]$ by defining

$$u(x,t) = \bar{u}(xl,t)e^{\frac{lF_1}{2\sqrt{\beta\rho}}(x-\bar{x})} \tag{7.20a}$$

$$v(x,t) = \bar{v}(xl,t)e^{-\frac{lF_1}{2\sqrt{\beta\rho}}(x-\bar{x})} \tag{7.20b}$$

from which we find

$$u_t(x,t) = \bar{u}_t(xl,t)e^{\frac{lF_1}{2\sqrt{\beta\rho}}(x-\bar{x})} \tag{7.21a}$$

$$v_t(x,t) = \bar{v}_t(xl,t)e^{-\frac{lF_1}{2\sqrt{\beta\rho}}(x-\bar{x})} \tag{7.21b}$$

and

$$u_x(x,t) = \left(l\bar{u}_z(xl,t) + \frac{lF_1}{2\sqrt{\beta\rho}}\bar{u}(xl,t)\right)e^{\frac{lF_1}{2\sqrt{\beta\rho}}(x-\bar{x})} \tag{7.22a}$$

$$v_x(x,t) = \left(l\bar{v}_z(xl,t) - \frac{lF_1}{2\sqrt{\beta\rho}}\bar{v}(xl,t)\right)e^{-\frac{lF_1}{2\sqrt{\beta\rho}}(x-\bar{x})}. \tag{7.22b}$$

Substituting (7.19) into (7.21), we obtain

$$u_t(x,t) = \frac{1}{l}\sqrt{\frac{\beta}{\rho}}\left(-l\bar{u}_z(xl,t) - \frac{l}{2}\frac{F_1}{\sqrt{\rho\beta}}\bar{u}(xl,t) - \frac{l}{2}\frac{F_1}{\sqrt{\rho\beta}}\bar{v}(xl,t)\right) \times e^{\frac{lF_1}{2\sqrt{\beta\rho}}(x-\bar{x})} \tag{7.23a}$$

$$v_t(x,t) = \frac{1}{l}\sqrt{\frac{\beta}{\rho}}\left(l\bar{v}_z(xl,t) - \frac{l}{2}\frac{F_1}{\sqrt{\rho\beta}}\bar{u}(xl,t) - \frac{l}{2}\frac{F_1}{\sqrt{\rho\beta}}\bar{v}(xl,t)\right) \times e^{-\frac{lF_1}{2\sqrt{\beta\rho}}(x-\bar{x})}. \tag{7.23b}$$

When slightly rearranged, this turns into

$$u_t(x,t) = -\frac{1}{l}\sqrt{\frac{\beta}{\rho}}\left(l\bar{u}_z(xl,t) + \frac{l}{2}\frac{F_1}{\sqrt{\rho\beta}}\bar{u}(xl,t)\right)e^{\frac{lF_1}{2\sqrt{\beta\rho}}(x-\bar{x})} - \frac{1}{2}\frac{F_1}{\rho}\bar{v}(xl,t))e^{\frac{lF_1}{2\sqrt{\beta\rho}}(x-\bar{x})} \tag{7.24a}$$

$$v_t(x,t) = \frac{1}{l}\sqrt{\frac{\beta}{\rho}}\left(l\bar{v}_z(xl,t) - \frac{l}{2}\frac{F_1}{\sqrt{\rho\beta}}\bar{u}(xl,t)\right)e^{-\frac{lF_1}{2\sqrt{\beta\rho}}(x-\bar{x})} - \frac{1}{2}\frac{F_1}{\rho}\bar{v}(xl,t))e^{-\frac{lF_1}{2\sqrt{\beta\rho}}(x-\bar{x})}. \tag{7.24b}$$

Inserting (7.22) into (7.24), we finally obtain

$$u_t(x,t) = -\frac{1}{l}\sqrt{\frac{\beta}{\rho}}u_x(x,t) - \frac{1}{2}\frac{F_1}{\rho}v(z,t)e^{\frac{lF_1}{\sqrt{\beta\rho}}(x-\bar{x})} \tag{7.25}$$

$$v_t(x,t) = \frac{1}{l}\sqrt{\frac{\beta}{\rho}}v_x(x,t) - \frac{1}{2}\frac{F_1}{\rho}u(z,t)e^{-\frac{lF_1}{\sqrt{\beta\rho}}(x-\bar{x})} \tag{7.26}$$

which is on the form (3.1) with coefficients (7.9) and parameters (7.12).

Composing the transformations (7.20), (7.17) and (7.13), and using (7.6), we find (7.5). The connection between $p_l(t)$ and $U(t)$ given in (7.8) is verified by inserting $x = 1$ into (7.5b) and using (3.1d). The parameters in the boundary condition (3.1c) can be expressed by forming

$$u(0,t) + v(0,t)e^{-\frac{lF_1}{\sqrt{\beta\rho}}\bar{x}} = q(0,t)e^{-\frac{lF_1}{2\sqrt{\beta\rho}}\bar{x}} \tag{7.27}$$

and defining q and C as in (7.10) and (7.11), respectively. Lastly, by inserting $x = \bar{x} = \bar{z}/l$ into (7.5), we obtain

$$u(\bar{x},t) = \frac{1}{2}\left[q(\bar{x}l,t) + \frac{A_1}{\sqrt{\beta\rho}}\left(p(\bar{x}l,t) - p_{sp}\right)\right] \tag{7.28a}$$

$$v(\bar{x},t) = \frac{1}{2}\left[q(\bar{x}l,t) - \frac{A_1}{\sqrt{\beta\rho}}\left(p(\bar{x}l,t) - p_{sp}\right)\right]. \tag{7.28b}$$

Thus, by requiring $u(\bar{x},t) = v(\bar{x},t)$, we enforce $p(\bar{x}l,t) = p_{sp}$. Hence, $r = 1$ makes the controller objective (3.2) equivalent to (7.2). □

7.3 Attenuation of heave induced pressure fluctuations

Having established that the MPD model (7.12) admits the form (3.1), we can apply the results from Chapter 3.

Theorem 7.1. *Consider the MPD system* (7.1). *Given a desired setpoint* p_{sp} *and a chosen coordinate* $\bar{z} \in (0,l)$ *for pressure attenuation, and let*

$$p_l(t) = \frac{\sqrt{\beta\rho}}{A_1}\left(q_l(t) - 2U(t)e^{\frac{\gamma}{2}(1-\bar{x})}\right) + p_{sp} - \rho g l(1-\bar{x}) \tag{7.29}$$

where $\bar{x} = \bar{z}/l$, $\gamma = \frac{lF_1}{\sqrt{\beta\rho}}$ *and* $U(t)$ *is given by the control law of Theorem 3.1 with* $u(x,t)$ *and* $v(x,t)$ *needed by the control law acquired from* $q(z,t)$ *and* $p(z,t)$ *by means of the transformation* (7.5). *Then* (7.2) *is achieved for*

$$t \geq \sqrt{\frac{\rho}{\beta}}(l-\bar{z}). \tag{7.30}$$

Moreover, if $U(t)$ *in* (7.29) *is given by the control law of Theorem 3.2, then* (7.2) *is achieved for*

$$t \geq \sqrt{\frac{\rho}{\beta}}(l+\bar{z}). \tag{7.31}$$

Lastly, if $U(t)$ *is given by the control law in Theorem 3.3, and the assumptions therein holds, then* (7.2) *is approximately achieved within the time given by* (7.31).

Proof. As the system (7.12) admits the form (3.1) following the results of Lemma 7.1, it will suffice to show that the actuation $p_l(t)$ in (7.12) relates to the actuation $U(t)$ in (3.1) according to (7.29), and that the given time constraints corresponds to the respective time constraints of Theorems 3.1, 3.2 and 3.3. The expression (7.29) follows trivially from (7.8) by solving (7.8) for $p_l(t)$. The time constraint of Theorem 3.1 is $t \geq \eta_\beta(\bar{x})$, where $\eta_\beta(\bar{x})$ is given in 3.36b and (3.20b). For $\epsilon_1(x)$ and $\epsilon_2(x)$ constant and equal as in (7.12), we find

$$\begin{aligned}\eta_\beta(\bar{x}) &= \phi_\beta(1) - \phi_\beta(\bar{x}) = \int_0^1 \frac{d\gamma}{\epsilon} - \int_0^{\bar{x}} \frac{d\gamma}{\epsilon} \\ &= \frac{1}{\epsilon} - \frac{\bar{x}}{\epsilon} = \frac{1}{\epsilon}(1-\bar{x}).\end{aligned} \tag{7.32}$$

Inserting for the ϵ in (7.12) and using (7.6), we find the right hand side of (7.30). Similarly for Theorem 3.2 and Theorem 3.3 which share time constraints, we find

$$\begin{aligned}\eta_\alpha(\bar{x}) &= \phi_\beta(1) + \phi_\alpha(0) - \phi_\alpha(\bar{x}) = \int_0^1 \frac{d\gamma}{\epsilon} + \int_0^1 \frac{d\gamma}{\epsilon} - \int_{\bar{x}}^1 \frac{d\gamma}{\epsilon} \\ &= \frac{1}{\epsilon}(1+\bar{x}) \end{aligned} \tag{7.33}$$

Inserting for ϵ in (7.12) and using (7.6), we find the right hand side of (7.31). □

Note that the time constraints (7.30)–(7.31) actually are the distance travelled by the applied signal $(l \pm \bar{z})$ divided by the mud's speed of sound $(c = \sqrt{\frac{\beta}{\rho}}$ (White (2012, p. 39))).

Additionally, one can implement (7.29) and Theorems 3.1–3.3 with the observer from Chapter 4 by relating the measurement $Y(t)$ in (4.1) to the system (7.1). By inserting $x = 1$ into (7.5a), we find $Y(t)$ to be

$$Y(t) = \frac{1}{2}\left[q_l(t) + \frac{A_1}{\sqrt{\beta\rho}}\left(p_l(t) - p_{sp} + \rho g l(1-\bar{x})\right)\right] e^{\frac{\gamma}{2}(1-\bar{x})} \tag{7.34}$$

where (7.6) and γ in (7.12) have been used.

7.4 Finding a fundamental matrix

A fundamental matrix $\Xi(x, x_0, s)$ with all the properties required by Lemma A.4 is needed to evaluate the transfer functions derived in Chapter 5. If such a matrix is found, we can implement (7.29) with $U(t)$ generated from a rational approximation found from applying the method described in Chapter 6 on one of the transfer functions in Theorems 5.1–5.3. For the drilling system (7.1) ported to (3.1) by means of (7.5), the matrix $\Theta(x, s)$ in (5.5) has the simple form

$$\Theta(x,s) = \frac{1}{\epsilon}\begin{bmatrix} -s & a_0 e^{\gamma x} \\ -b_0 e^{-\gamma x} & s \end{bmatrix}. \tag{7.35}$$

Lemma 7.1. *A possible fundamental matrix needed in* (5.8) *for the drilling system* (7.1) *is*

$$\Xi(x, x_0, s) = H^{-1}(x) e^{(\Theta_0(s) + \frac{\gamma}{2}V)(x - x_0)} H(x_0). \tag{7.36}$$

where

$$\Theta_0(s) := \frac{1}{\epsilon}\begin{bmatrix} -s & a_0 \\ -b_0 & s \end{bmatrix}, \tag{7.37}$$

$$H(x) = \begin{bmatrix} e^{-\frac{\gamma}{2}x} & 0 \\ 0 & e^{\frac{\gamma}{2}x} \end{bmatrix} \tag{7.38}$$

and

$$V = \begin{bmatrix} -1 & 0 \\ 0 & 1 \end{bmatrix}. \tag{7.39}$$

Proof. We cannot use (A.31), as $\Theta(x, s)$ depends on x. We resolve this by a coordinate transformation. First off, we note that

$$\frac{d}{dx}H(x) = \frac{\gamma}{2}VH(x) = \frac{\gamma}{2}H(x)V \tag{7.40}$$

and

$$\frac{d}{dx}H^{-1}(x) = -\frac{\gamma}{2}VH^{-1}(x) = -\frac{\gamma}{2}H^{-1}(x)V. \tag{7.41}$$

Additionally, we note that $H(x)$, $H^{-1}(x)$ and V commute as they are all diagonal, and that $VV = V^2 = I$. Using (7.37) and (7.38), we may write (7.35) as

$$\Theta(x, s) = H^{-1}(x)\Theta_0(s)H(x). \tag{7.42}$$

Note that $\Theta_0(s)$ is independent of x. Next, define the new vector of exponentially scaled observer states

$$\bar{w}(x, s) = H(x)w(x, s) \Leftrightarrow w(x, s) = H^{-1}(x)\bar{w}(x, s). \tag{7.43}$$

Inserting (7.43) into (5.7) and using (7.41), we obtain

$$\begin{aligned} -\frac{\gamma}{2}H^{-1}(x)V\bar{w}(x, s) + H^{-1}(x)\bar{w}_x(x, s) & \\ = H^{-1}(x)\Theta_0(s)H(x)H^{-1}(x)\bar{w}(x, s) & \\ + \Upsilon(x)(Y(s) - \hat{u}(1, s)). & \end{aligned} \tag{7.44}$$

Premultiplication with $H(x)$ and rearranging, we find

$$\bar{w}_x(x, s) = \left(\Theta_0(s) + \frac{\gamma}{2}V\right)\bar{w}(x, s) + H(x)\Upsilon(x)(Y(s) - \hat{u}(1, s)). \tag{7.45}$$

Now (A.31) of Lemma A.4 may be applied, yielding

$$\bar{w}(x, s) = \bar{\Xi}(x, x_0, s)\bar{w}(x_0, s) + \int_{x_0}^{x} \bar{\Xi}(x, \xi, s)H(\xi)\Upsilon(\xi)d\xi \tag{7.46}$$

where

$$\bar{\Xi}(x, x_0, s) := e^{(\Theta_0(s)+\frac{\gamma}{2}V)(x-x_0)}. \tag{7.47}$$

Substituting (7.43) back into (7.46), we obtain

$$w(x,s) = H^{-1}(x)\bar{\Xi}(x,x_0,s)H(x_0)w(x_0,s) + \int_{x_0}^{x} H^{-1}(x)\bar{\Xi}(x,\xi,s)H(\xi)\Upsilon(\xi)d\xi. \tag{7.48}$$

Comparing (7.48) with (5.8), one observe that the fundamental matrix in (5.2) can be taken as $H^{-1}(x)\bar{\Xi}(x,\xi,s)H(\xi)$, which yields (7.36). □

Equation (7.36) satisfies all the requirements of Lemma A.4, easily verified by direct computation.

7.5 Solving the kernel equations

To implement the controller and system on a computer, the solutions to the kernel equations (3.6)–(3.7) and (3.10)–(3.11) are needed. Additionally, the solution to (4.4)–(4.5) is needed if the observer from Chapter 4 is to be implemented.

Recently, an explicit solution to the subsystem consisting of (3.6c)–(3.6d) and (3.7c)–(3.7d) was found in Vazquez and Krstić (2013), under the assumption of having constant coefficients. The solution is complex, and involves Bessel functions and generalized Marcum Q-functions of the first order. Although the solution derived in Vazquez and Krstić (2013) covers the kernel equations emerging when inserting (7.9), and performing a transformation, we still need the solution to (3.6a)–(3.6b) with (3.7a)–(3.7b), as well as (3.10)–(3.11) and (4.4)–(4.5).

Solving these equations using numerical methods is challenging, according to Vazquez (2013), which suggests two methods for solving the equations. By discretizing the PDEs, one faces the same numerical issues as was observed in Balogh and Krstić (2002), previously mentioned in Section 1.2, as the discretization method inserts discontinuities to the system, and the number of discontinuities tends towards infinity when the grid cell size approaches zero. One of the suggested methods is to modify the method derived in Smyshlyaev and Krstić (2004) which was based on the Ablowitz–Kruskal–Ladik scheme (Ablowitz, Kruskal, and Ladik (1979)). The key feature of the scheme was the use of a discretization method *averaging* certain terms, instead of using their exact values. The scheme, however, had to be modified to suit the geometry and boundary conditions of the kernel PDEs in Smyshlyaev and Krstić (2004); an apparently non-trivial task for the unusual boundary conditions of our kernel equations.

We will instead solve the equations using the other suggested method; the Method of Characteristics as presented in Section 2.7.2. This method

was in Vazquez et al. (2011b) used to prove existence and uniqueness for all the kernel equations appearing in this thesis. A part of the proof showed that the method is guaranteed to converge to the true, unique solution.

7.5.1 Statement and simplification

As $\epsilon_1(x)$ and $\epsilon_2(x)$ are constants, and equal, the overall complexity of the kernel equations is somewhat reduced. Inserting for (7.9) into (3.6)-(3.7), (3.10)-(3.11), (4.4)-(4.5) and defining

$$a := \frac{a_0}{\epsilon}, \quad b := \frac{b_0}{\epsilon} \tag{7.49}$$

we find the forward transform kernel equations

$$K_x^{uu}(x,\xi) + K_\xi^{uu}(x,\xi) = -be^{-\gamma\xi}K^{uv}(x,\xi) \tag{7.50a}$$
$$K_x^{uv}(x,\xi) - K_\xi^{uv}(x,\xi) = -ae^{\gamma\xi}K^{uu}(x,\xi) \tag{7.50b}$$
$$K_x^{vu}(x,\xi) - K_\xi^{vu}(x,\xi) = be^{-\gamma\xi}K^{vv}(x,\xi) \tag{7.50c}$$
$$K_x^{vv}(x,\xi) + K_\xi^{vv}(x,\xi) = ae^{\gamma\xi}K^{vu}(x,\xi) \tag{7.50d}$$

with boundary conditions

$$K^{uu}(x,0) = \frac{1}{q}K^{uv}(x,0) \tag{7.51a}$$
$$K^{uv}(x,x) = \frac{1}{2}ae^{\gamma x} \tag{7.51b}$$
$$K^{vu}(x,x) = -\frac{1}{2}be^{-\gamma x} \tag{7.51c}$$
$$K^{vv}(x,0) = qK^{vu}(x,0), \tag{7.51d}$$

the inverse transform kernel equations

$$L_x^{\alpha\alpha}(x,\xi) + L_\xi^{\alpha\alpha}(x,\xi) = ae^{\gamma x}L^{\beta\alpha}(x,\xi) \tag{7.52a}$$
$$L_x^{\alpha\beta}(x,\xi) - L_\xi^{\alpha\beta}(x,\xi) = ae^{\gamma x}L^{\beta\beta}(x,\xi) \tag{7.52b}$$
$$L_x^{\beta\alpha}(x,\xi) - L_\xi^{\beta\alpha}(x,\xi) = -be^{-\gamma x}L^{\alpha\alpha}(x,\xi) \tag{7.52c}$$
$$L_x^{\alpha\beta}(x,\xi) + L_\xi^{\beta\beta}(x,\xi) = -be^{-\gamma x}L^{\alpha\beta}(x,\xi) \tag{7.52d}$$

with boundary conditions

$$L^{\alpha\alpha}(x,0) = \frac{1}{q}L^{\alpha\beta}(x,0) \tag{7.53a}$$
$$L^{\alpha\beta}(x,x) = \frac{1}{2}ae^{\gamma x} \tag{7.53b}$$
$$L^{\beta\alpha}(x,x) = -\frac{1}{2}be^{-\gamma x} \tag{7.53c}$$
$$L^{\beta\beta}(x,0) = qL^{\beta\alpha}(x,0) \tag{7.53d}$$

and the observer kernel equations

$$P^{uu}_x(x,\xi) + P^{uu}_\xi(x,\xi) = ae^{\gamma x}P^{vu}(x,\xi) \tag{7.54a}$$
$$P^{uv}_x(x,\xi) - P^{uv}_\xi(x,\xi) = ae^{\gamma x}P^{vv}(x,\xi) \tag{7.54b}$$
$$P^{vu}_x(x,\xi) - P^{vu}_\xi(x,\xi) = -be^{-\gamma x}P^{uu}(x,\xi) \tag{7.54c}$$
$$P^{vv}_x(x,\xi) + P^{uv}_\xi(x,\xi) = -be^{-\gamma x}P^{uv}(x,\xi) \tag{7.54d}$$

with boundary conditions

$$P^{uu}(0,\xi) = qP^{vu}(0,\xi) \tag{7.55a}$$
$$P^{uv}(x,x) = \frac{1}{2}ae^{\gamma x} \tag{7.55b}$$
$$P^{vu}(x,x) = -\frac{1}{2}be^{-\gamma x} \tag{7.55c}$$
$$P^{vv}(0,\xi) = \frac{1}{q}P^{uv}(0,\xi). \tag{7.55d}$$

We will by defining a series of matrices and exponential weightings, further simplify the kernels. Define the following matrices of kernels

$$K(x,\xi) := \begin{bmatrix} K^{uu}(x,\xi) & K^{uv}(x,\xi) \\ K^{vu}(x,\xi) & K^{vv}(x,\xi) \end{bmatrix} \tag{7.56}$$

$$L(x,\xi) := \begin{bmatrix} L^{\alpha\alpha}(x,\xi) & L^{\alpha\beta}(x,\xi) \\ L^{\beta\alpha}(x,\xi) & L^{\beta\beta}(x,\xi) \end{bmatrix} \tag{7.57}$$

$$P(x,\xi) := \begin{bmatrix} P^{uu}(x,\xi) & P^{uv}(x,\xi) \\ P^{vu}(x,\xi) & P^{vv}(x,\xi) \end{bmatrix} \tag{7.58}$$

and matrices

$$Q_0 := \begin{bmatrix} 0 & q \\ 0 & 1 \end{bmatrix}, \quad C(x) := \begin{bmatrix} 0 & ae^{\gamma x} \\ be^{-\gamma x} & 0 \end{bmatrix} \tag{7.59}$$

then the kernel equations can compactly be stated

$$VK_x(x,\xi) + K_\xi(x,\xi)V = K(x,\xi)C(\xi) \tag{7.60}$$
$$VL_x(x,\xi) + L_\xi(x,\xi)V = -C(x)L(x,\xi) \tag{7.61}$$
$$VP_x(x,\xi) + P_\xi(x,\xi)V = -C(x)P(x,\xi) \tag{7.62}$$

with boundary conditions

$$K(x,0)VQ_0 = 0, \quad K(x,x)V - VK(x,x) = C(x) \tag{7.63}$$
$$L(x,0)VQ_0 = 0, \quad L(x,x)V - VL(x,x) = C(x) \tag{7.64}$$
$$Q_0^T VP(0,\xi) = 0, \quad P(x,x)V - VP(x,x) = C(x) \tag{7.65}$$

where the matrix V was given in (7.39). Additionally using the matrix $H(x)$ from (7.38), the exponential weighting matrix $C(x)$ can be split into terms in $H(x)$ and a constant term C_0 as follows

$$C(x) = H^{-1}(x)C_0H(x) \tag{7.66}$$

for the constant matrix

$$C_0 = \begin{bmatrix} 0 & a \\ b & 0 \end{bmatrix}. \tag{7.67}$$

Remember that V commute with $H(x)$ and $H^{-1}(x)$, and that $VV = V^2 = I$. Now consider the following exponential scaling

$$K(x,\xi) := H^{-1}(x)B^K(x,\xi)H(\xi) \tag{7.68}$$
$$L(x,\xi) := H^{-1}(x)B^L(x,\xi)H(\xi) \tag{7.69}$$
$$P(x,\xi) := H^{-1}(x)B^P(x,\xi)H(\xi) \tag{7.70}$$

for some new matrices $B^K(x,\xi)$, $B^L(x,\xi)$ and $B^P(x,\xi)$. Inserting (7.68)–(7.70) into the kernel equations (7.60)–(7.62) we end up with simpler versions of the original equations. Showing the calculations here only for $B^K(x,\xi)$, we find

$$V\left[\frac{d}{dx}(H^{-1}(x)B^K(x,\xi)H(\xi))\right] + \left[\frac{d}{d\xi}(H^{-1}(x)B^K(x,\xi)H(\xi))\right]V = H^{-1}(x)B^K(x,\xi)C_0H(\xi). \tag{7.71}$$

Application of the product rule yields

$$\begin{aligned} V\left[\frac{d}{dx}H^{-1}(x)\right]B^K(x,\xi)H(\xi) &+ VH^{-1}(x)B_x^K(x,\xi)H(\xi) \\ &+ H^{-1}(x)B_\xi^K(x,\xi)H(\xi)M \\ &+ H^{-1}(x)B^K(x,\xi)\left[\frac{d}{d\xi}H(\xi)\right]V \\ &= H^{-1}(x)B^K(x,\xi)C_0H(\xi). \end{aligned} \tag{7.72}$$

Using (7.40), we obtain

$$\begin{aligned} V\left[-\frac{\gamma}{2}MH^{-1}(x)\right]B^K(x,\xi)H(\xi) + VH^{-1}(x)B^K_x(x,\xi)H(\xi) \\ + H^{-1}(x)B^K_\xi(x,\xi)H(\xi)V \\ + H^{-1}(x)B^K(x,\xi)\left[\frac{\gamma}{2}H(\xi)V\right]V \\ = H^{-1}(x)B^K(x,\xi)C_0H(\xi). \end{aligned} \tag{7.73}$$

Using $VV = I$ and the commuting property of $H(x)$ and $H^{-1}(x)$ with V, we find

$$\begin{aligned} -\frac{\gamma}{2}H^{-1}(x)B^K(x,\xi)H(\xi) + H^{-1}(x)VB^K_x(x,\xi)H(\xi) \\ + H^{-1}(x)B^K_\xi(x,\xi)VH(\xi) \\ + \frac{\gamma}{2}H^{-1}(x)B^K(x,\xi)H(\xi) \\ = H^{-1}(x)B^K(x,\xi)C_0H(\xi). \end{aligned} \tag{7.74}$$

Cancelling the two equal terms on the left hand side, premultiplication with $H(x)$ and postmultiplication with $H^{-1}(\xi)$, we are left with the simplified kernel equations

$$VB^K_x(x,\xi) + B^K_\xi(x,\xi)V = B^K(x,\xi)C_0. \tag{7.75}$$

From the boundary condition (7.63), we find

$$H^{-1}(x)B^K(x,0)H(0)VQ_0 = 0 \tag{7.76}$$

$$H^{-1}(x)B^K(x,x)H(x)V - VH^{-1}(x)B^K(x,x)H(x) = H^{-1}(x)C_0H(x) \tag{7.77}$$

Again using the commuting property of M, that $H(0) = I$ and appropriate pre- and postmultiplication with $H(x)$ and $H^{-1}(x)$, respectively, we find the simplified BCs

$$B^K(x,0)VQ_0 = 0, \quad B^K(x,x)V - VB^K(x,x) = C_0. \tag{7.78}$$

Through similar derivations for $L(x,\xi)$ and $P(x,\xi)$, we obtain

$$VB^L_x(x,\xi) + B^L_\xi(x,\xi)V = -C_0B^L(x,\xi) \tag{7.79}$$

$$VB^P_x(x,\xi) + B^P_\xi(x,\xi)V = -C_0B^P(x,\xi) \tag{7.80}$$

with boundary conditions

$$B^L(x,0)MQ_0 = 0, \quad B^L(x,x)V - VB^L(x,x) = C_0 \tag{7.81}$$

$$Q_0^TMB^P(0,\xi) = 0, \quad B^P(x,x)V - VB^P(x,x) = C_0. \tag{7.82}$$

Note that the kernel equations have been reduced to PDEs with constant coefficients.

7.5.2 Transforming to integral equations

The next step of the Method of Characteristics is to define characteristic curves along which the PDEs turn to ODEs. The ODEs are then integrated to form integral equations. Let us initially focus on (7.75) with the corresponding BCs (7.78). Let the elements of $B^K(x,\xi)$ be stated as

$$B^K(x,\xi) := \begin{bmatrix} u^K(x,\xi) & v^K(x,\xi) \\ w^K(x,\xi) & z^K(x,\xi) \end{bmatrix} \tag{7.83}$$

then (7.75) when written out becomes

$$u_x^K(x,\xi) + u_\xi^K(x,\xi) = -bv^K(x,\xi) \tag{7.84a}$$
$$v_x^K(x,\xi) - v_\xi^K(x,\xi) = -au^K(x,\xi) \tag{7.84b}$$
$$w_x^K(x,\xi) - w_\xi^K(x,\xi) = bz^K(x,\xi) \tag{7.84c}$$
$$z_x^K(x,\xi) + z_\xi^K(x,\xi) = aw^K(x,\xi) \tag{7.84d}$$

with (7.78) becoming

$$u^K(x,0) = \frac{1}{q}v^K(x,0) \tag{7.85a}$$
$$v^K(x,x) = \frac{1}{2}a \tag{7.85b}$$
$$w^K(x,x) = -\frac{1}{2}b \tag{7.85c}$$
$$z^K(x,0) = qw^K(x,0). \tag{7.85d}$$

Define the following characteristic lines for u^K and z^K

$$x_{uz}(s) = x_{uz}(x,\xi,s) := x - \xi + s \tag{7.86a}$$
$$\xi_{uz}(s) = \xi_{uz}(x,\xi,s) := s \tag{7.86b}$$

and for v^K and w^K

$$x_{vw}(s) = x_{vw}(x,\xi,s) := \frac{1}{2}(x+\xi) + s \tag{7.87a}$$
$$\xi_{vw}(s) = \xi_{vw}(x,\xi,s) := \frac{1}{2}(x+\xi) - s. \tag{7.87b}$$

Differentiating (7.84) with respect to s along their corresponding characteristic lines yields

$$\frac{d}{ds}u^K(x_{uz}(s),\xi_{uz}(s)) = u_x^K(x_{uz}(s),\xi_{uz}(s)) + u_\xi^K(x_{uz}(s),\xi_{uz}(s)) \tag{7.88a}$$
$$\frac{d}{ds}v^K(x_{vw}(s),\xi_{vw}(s)) = v_x^K(x_{vw}(s),\xi_{vw}(s)) - v_\xi^K(x_{vw}(s),\xi_{vw}(s)) \tag{7.88b}$$
$$\frac{d}{ds}w^K(x_{vw}(s),\xi_{vw}(s)) = w_x^K(x_{vw}(s),\xi_{vw}(s)) - w_\xi^K(x_{vw}(s),\xi_{vw}(s)) \tag{7.88c}$$
$$\frac{d}{ds}z^K(x_{uz}(s),\xi_{uz}(s)) = z_x^K(x_{uz}(s),\xi_{uz}(s)) + z_\xi^K(x_{uz}(s),\xi_{uz}(s)). \tag{7.88d}$$

We recognize the right hand sides and substitute for (7.84), yielding

$$\frac{d}{ds}u^K(x_{uz}(s),\xi_{uz}(s)) = -bv^K(x_{uz}(s),\xi_{uz}(s)) \tag{7.89a}$$
$$\frac{d}{ds}v^K(x_{vw}(s),\xi_{vw}(s)) = -au^K(x_{vw}(s),\xi_{vw}(s)) \tag{7.89b}$$
$$\frac{d}{ds}w^K(x_{vw}(s),\xi_{vw}(s)) = bz^K(x_{vw}(s),\xi_{vw}(s)) \tag{7.89c}$$
$$\frac{d}{ds}z^K(x_{uz}(s),\xi_{uz}(s)) = aw^K(x_{uz}(s),\xi_{uz}(s)). \tag{7.89d}$$

Integrating (7.89a) and (7.89d) from $s = 0$ to $s = \xi$, and (7.89b) and (7.89c) from $s = 0$ to $s = \frac{1}{2}(x - \xi)$, we obtain

$$\begin{aligned} u^K(x_{uz}(\xi),\xi_{uz}(\xi)) &= u^K(x_{uz}(0),\xi_{uz}(0)) \\ &\quad - b\int_0^\xi v^K(x_{uz}(s),\xi_{uz}(s))ds \end{aligned} \tag{7.90a}$$
$$\begin{aligned} v^K(x_{vw}(\frac{1}{2}(x-\xi)),\xi_{vw}(\frac{1}{2}(x-\xi))) &= v^K(x_{vw}(0),\xi_{vw}(0)) \\ &\quad - a\int_0^{\frac{1}{2}(x-\xi)} u^K(x_{vw}(s),\xi_{vw}(s))ds \end{aligned} \tag{7.90b}$$
$$\begin{aligned} w^K(x_{vw}(\frac{1}{2}(x-\xi)),\xi_{vw}(\frac{1}{2}(x-\xi))) &= w^K(x_{vw}(0),\xi_{vw}(0)) \\ &\quad + b\int_0^{\frac{1}{2}(x-\xi)} z^K(x_{vw}(s),\xi_{vw}(s))ds \end{aligned} \tag{7.90c}$$
$$\begin{aligned} z^K(x_{uz}(\xi),\xi_{uz}(\xi)) &= z^K(x_{uz}(0),\xi_{uz}(0)) \\ &\quad + a\int_0^\xi w^K(x_{uz}(s),\xi_{uz}(s))ds \end{aligned} \tag{7.90d}$$

which, when inserting for the characteristic lines (7.86) and (7.87) simplifies to

$$u^K(x,\xi) = u^K(x-\xi,0) - b\int_0^\xi v^K(x-\xi+s,s)ds \tag{7.91a}$$

$$v^K(x,\xi) = v^K(\frac{1}{2}(x+\xi),\frac{1}{2}(x+\xi)) - a\int_0^{\frac{1}{2}(x-\xi)} u^K(\frac{1}{2}(x+\xi)+s,\frac{1}{2}(x+\xi)-s)ds \tag{7.91b}$$

$$w^K(x,\xi) = w^K(\frac{1}{2}(x+\xi),\frac{1}{2}(x+\xi)) + b\int_0^{\frac{1}{2}(x-\xi)} z^K(\frac{1}{2}(x+\xi)+s,\frac{1}{2}(x+\xi)-s)ds \tag{7.91c}$$

$$z^K(x,\xi) = z^K(x-\xi,0) + a\int_0^\xi w^K(x-\xi+s,s)ds. \tag{7.91d}$$

Now inserting for the boundary conditions (7.85), we substitute the leftmost terms on the right side of equations (7.91b)–(7.91c) with constants, to obtain

$$u^K(x,\xi) = \frac{1}{q}v^K(x-\xi,0) - b\int_0^\xi v^K(x-\xi+s,s)ds \tag{7.92a}$$

$$v^K(x,\xi) = v_0 - a\int_0^{\frac{1}{2}(x-\xi)} u^K(\frac{1}{2}(x+\xi)+s,\frac{1}{2}(x+\xi)-s)ds \tag{7.92b}$$

$$w^K(x,\xi) = w_0 + b\int_0^{\frac{1}{2}(x-\xi)} z^K(\frac{1}{2}(x+\xi)+s,\frac{1}{2}(x+\xi)-s)ds \tag{7.92c}$$

$$z^K(x,\xi) = qw^K(x-\xi,0) + a\int_0^\xi w^K(x-\xi+s,s)ds. \tag{7.92d}$$

Lastly, using (7.92b) and (7.92c) respectively, to insert for $v^K(x-\xi,0)$ and $w^K(x-\xi,0)$ in (7.92a) and (7.92d), we land on

$$u^K(x,\xi) = \frac{1}{q}v_0 - \frac{a}{q}\int_0^{\frac{1}{2}(x-\xi)} u^K(\frac{1}{2}(x-\xi)+s,\frac{1}{2}(x-\xi)-s)ds - b\int_0^\xi v^K(x-\xi+s,s)ds \tag{7.93a}$$

$$v^K(x,\xi) = v_0 - a\int_0^{\frac{1}{2}(x-\xi)} u^K(\frac{1}{2}(x+\xi)+s,\frac{1}{2}(x+\xi)-s)ds \tag{7.93b}$$

$$w^K(x,\xi) = w_0 + b\int_0^{\frac{1}{2}(x-\xi)} z^K(\frac{1}{2}(x+\xi)+s,\frac{1}{2}(x+\xi)-s)ds \tag{7.93c}$$

$$z^K(x,\xi) = qw_0 + qb\int_0^{\frac{1}{2}(x-\xi)} z^K(\frac{1}{2}(x-\xi)+s,\frac{1}{2}(x-\xi)-s)ds + a\int_0^\xi w^K(x-\xi+s,s)ds \tag{7.93d}$$

which is a set of four inhomogeneous Volterra equations of the second kind (see Appendix B.1). Several methods for solving these are described in the literature, as previously mentioned in Section 2.7.2.

A similar derivation for (7.79) and (7.81), using the same characteristic lines (7.86)–(7.87), and (7.80) and (7.82) using the characteristic lines

$$x_{uz} = s \tag{7.94}$$
$$\xi_{uz} = \xi - x + s \tag{7.95}$$
$$x_{vw} = \frac{1}{2}(x+\xi) + s \tag{7.96}$$
$$\xi_{vw} = \frac{1}{2}(x+\xi) - s. \tag{7.97}$$

with

$$B^L(x,\xi) := \begin{bmatrix} u^L(x,\xi) & v^L(x,\xi) \\ w^L(x,\xi) & z^L(x,\xi) \end{bmatrix} \tag{7.98}$$

and

$$B^P(x,\xi) := \begin{bmatrix} u^P(x,\xi) & v^P(x,\xi) \\ w^P(x,\xi) & z^P(x,\xi) \end{bmatrix} \tag{7.99}$$

yield the Volterra equations

$$u^L(x,\xi) = \frac{1}{q}v_0 + \frac{a}{q}\int_0^{\frac{1}{2}(x-\xi)} z^L(\frac{1}{2}(x-\xi)+s, \frac{1}{2}(x-\xi)-s)ds + a\int_0^{\xi} w^L(x-\xi+s,s)ds \tag{7.100a}$$
$$v^L(x,\xi) = v_0 + a\int_0^{\frac{1}{2}(x-\xi)} z^L(\frac{1}{2}(x+\xi)+s, \frac{1}{2}(x+\xi)-s)ds \tag{7.100b}$$
$$w^L(x,\xi) = w_0 - b\int_0^{\frac{1}{2}(x-\xi)} u^L(\frac{1}{2}(x+\xi)+s, \frac{1}{2}(x+\xi)-s)ds \tag{7.100c}$$
$$z^L(x,\xi) = qw_0 - qb\int_0^{\frac{1}{2}(x-\xi)} u^L(\frac{1}{2}(x-\xi)+s, \frac{1}{2}(x-\xi)-s)ds - b\int_0^{\xi} v^L(x-\xi+s,s)ds \tag{7.100d}$$

for the inverse transform kernels, and

$$u^P(x,\xi) = qw_0 + qb\int_0^{\frac{1}{2}(\xi-x)} u^P(\frac{1}{2}(\xi-x)-s, \frac{1}{2}(\xi-x)+s)\,ds + a\int_0^x w^P(s,\xi-x+s)\,ds \tag{7.101a}$$

$$v^P(x,\xi) = v_0 - a\int_0^{\frac{1}{2}(\xi-x)} z^P(\frac{1}{2}(x+\xi)-s, \frac{1}{2}(x+\xi)+s)\,ds \tag{7.101b}$$

$$w^P(x,\xi) = w_0 + b\int_0^{\frac{1}{2}(\xi-x)} u^P(\frac{1}{2}(x+\xi)-s, \frac{1}{2}(x+\xi)+s)\,ds \tag{7.101c}$$

$$z^P(x,\xi) = \frac{1}{q}v_0 - \frac{1}{q}a\int_0^{\frac{1}{2}(\xi-x)} z^P(\frac{1}{2}(\xi-x)-s, \frac{1}{2}(\xi-x)+s)\,ds - b\int_0^x v^P(s,\xi-x+s)\,ds \tag{7.101d}$$

for the observer kernels.

7.5.3 Numerical computations

We will solve the equations (7.93), (7.100) and (7.101) numerically on a computer using the method of successive approximations, as described in Section 2.7.2. In order to do that, we will have to discretize the domain $\mathcal{T}$ as given in (3.8) into a triangular equivalent. To ease the implementation on a computer, we construct a square equivalent of size $N \times N$, and use only the lower triangular part, constituting of $\frac{1}{2}N \times (N+1)$ discrete sample points with

$$\Delta = \frac{1}{N-1} \tag{7.102}$$

as the cell size. To simplify the notation in subsequent derivations, we introduce the notation

$$x_i := \Delta i \tag{7.103a}$$

$$\xi_j := \Delta j \tag{7.103b}$$

and

$$u^K_{i,j} := u^K(x_i,\xi_j) \tag{7.104a}$$

$$v^K_{i,j} := v^K(x_i,\xi_j) \tag{7.104b}$$

$$w^K_{i,j} := w^K(x_i,\xi_j) \tag{7.104c}$$

$$z^K_{i,j} := z^K(x_i,\xi_j). \tag{7.104d}$$

Using (7.103) and (7.104) on (7.93), we obtain

$$u^K_{i,j} = \frac{1}{q}v_0 - \frac{a}{q}\int_0^{\frac{1}{2}\Delta(i-j)} u^K(\frac{1}{2}\Delta(i-j)+s, \frac{1}{2}\Delta(i-j)-s)ds$$
$$- b\int_0^{\Delta j} v^K(\Delta(i-j)+s, s)ds \tag{7.105a}$$

$$v^K_{i,j} = v_0 - a\int_0^{\frac{1}{2}\Delta(i-j)} u^K(\frac{1}{2}\Delta(i+j)+s, \frac{1}{2}\Delta(i+j)-s)ds \tag{7.105b}$$

$$w^K_{i,j} = w_0 + b\int_0^{\frac{1}{2}\Delta(i-j)} z^K(\frac{1}{2}\Delta(i+j)+s, \frac{1}{2}\Delta(i+j)-s)ds \tag{7.105c}$$

$$z^K_{i,j} = qw_0 + qb\int_0^{\frac{1}{2}\Delta(i-j)} z^K(\frac{1}{2}\Delta(i-j)+s, \frac{1}{2}\Delta(i-j)-s)ds$$
$$+ a\int_0^{\Delta j} w^K(\Delta(i-j)+s, s)ds \tag{7.105d}$$

Now substitute $s \to \frac{1}{2}s$ in the leftmost integrals in (7.105a) and (7.105d), as well as the integrals in (7.105b) and (7.105c), followed by trapezoidal rule (see Appendix B.2) with

$$s_k = \Delta k, \tag{7.106}$$

we find

$$u^K_{i,j} = \frac{1}{q}v_0 - \frac{1}{q}\frac{a}{2}\Delta\sum_{k=0}^{i-j}\sigma_1(i,j,k)u^K(\frac{1}{2}\Delta(i-j+k), \frac{1}{2}\Delta(i-j-k))$$
$$- b\Delta\sum_{k=0}^{j}\sigma_2(j,k)v^K(\Delta(i-j+k), \Delta k) \tag{7.107a}$$

$$v^K_{i,j} = v_0 - \frac{a}{2}\Delta\sum_{k=0}^{i-j}\sigma_1(i,j,k)u^K(\frac{1}{2}\Delta(i+j+k), \frac{1}{2}\Delta(i+j-k)) \tag{7.107b}$$

$$w^K_{i,j} = w_0 + \frac{b}{2}\Delta\sum_{k=0}^{i-j}\sigma_1(i,j,k)z^K(\frac{1}{2}\Delta(i+j+k), \frac{1}{2}\Delta(i+j-k)) \tag{7.107c}$$

$$z^K_{i,j} = qw_0 + q\frac{b}{2}\Delta\sum_{k=0}^{i-j}\sigma_1(i,j,k)z^K(\frac{1}{2}\Delta(i-j+k), \frac{1}{2}\Delta(i-j-k))$$
$$+ a\Delta\sum_{k=0}^{j}\sigma_2(j,k)w^K(\Delta(i-j+k), \Delta k) \tag{7.107d}$$

where

$$\sigma_1(i,j,k) := \begin{cases} 0 & \text{if } i = j \\ \frac{1}{2} & \text{if } i \neq j \text{ and } (k = 0 \text{ or } k = i-j) \\ 1 & \text{otherwise} \end{cases} \tag{7.108}$$

and

$$\sigma_2(j,k) := \begin{cases} 0 & \text{if } j = 0 \\ \frac{1}{2} & \text{if } j \neq 0 \text{ and } (k = 0 \text{ or } k = j) \\ 1 & \text{otherwise} \end{cases} \tag{7.109}$$

have been defined. Equations (7.107) are straight forward to implement on a computer, with values at fractional indices computed using interpolation on the grid cells. Similar derivations for (7.100) and (7.101) yield

$$\begin{aligned} u^L_{i,j} &= \frac{1}{q}w_0 + \frac{a}{q}\Delta \sum_{k=0}^{i-j} \sigma_1(i,j,k) z(\frac{\Delta}{2}(i-j+k), \frac{\Delta}{2}(i-j-k)) \\ &\quad + a\Delta \sum_{k=0}^{j} \sigma_2(j,k) v(\Delta(k+i-j), \Delta k) \end{aligned} \tag{7.110a}$$

$$v^L_{i,j} = v_0 + a\Delta \sum_{k=0}^{i-j} \sigma_1(i,j,k) z(\frac{\Delta}{2}(i+j+k), \frac{\Delta}{2}(i+j-k)) \tag{7.110b}$$

$$w^L_{i,j} = w_0 + b\Delta \sum_{k=0}^{i-j} \sigma_1(i,j,k) u(\frac{\Delta}{2}(i+j+k), \frac{\Delta}{2}(i+j-k)) \tag{7.110c}$$

$$\begin{aligned} z^L_{i,j} &= qv_0 + qb\Delta \sum_{k=0}^{i-j} \sigma_2(j,k) u(\frac{\Delta}{2}(i-j+k), \frac{\Delta}{2}(i-j-k)) \\ &\quad + b\Delta \sum_{k=0}^{j} \sigma_1(i,j,k) w(\Delta(k+i-j), \Delta k) \end{aligned} \tag{7.110d}$$

and

$$\begin{aligned} u^P_{i,j} &= qw_0 + qb\Delta \sum_{k=0}^{j-i} \sigma_1(j,i,k) z(\frac{\Delta}{2}(j-i-k), \frac{\Delta}{2}(j-i+k)) \\ &\quad + a\Delta \sum_{k=0}^{i} \sigma_2(i,k) v(\Delta(k+j-i), \Delta k) \end{aligned} \tag{7.111a}$$

$$v^P_{i,j} = v_0 - a\Delta \sum_{k=0}^{j-i} \sigma_1(j,i,k) z(\frac{\Delta}{2}(i+j-k), \frac{\Delta}{2}(i+j+k)) \tag{7.111b}$$

$$w^P_{i,j} = w_0 + b\Delta \sum_{k=0}^{i-j} \sigma_1(j,i,k) u(\frac{\Delta}{2}(i+j-k), \frac{\Delta}{2}(i+j+k)) \tag{7.111c}$$

$$\begin{aligned} z^P_{i,j} &= \frac{1}{q}v_0 - \frac{1}{q}a\Delta \sum_{k=0}^{j-i} \sigma_1(j,i,k) u(\frac{\Delta}{2}(j-i-k), \frac{\Delta}{2}(j-i+k)) \\ &\quad + b\Delta \sum_{k=0}^{i} \sigma_2(i,k) w(\Delta(k+j-i), \Delta k), \end{aligned} \tag{7.111d}$$

respectively.

7.5.4 Code optimization

With each of the elements in (7.107), (7.110) and (7.111) consisting of $\frac{1}{2}N \times (N+1)$ elements, each involving a sum with a number of elements growing linearly with N, the number of calculations are $O(N^3)$ for each iteration[1]. The run time can be drastically reduced by a few steps, as will be showed next.

As the leftmost sum in (7.107a), the rightmost sum in (7.107a) and the sum in (7.107b) are equivalent in structure with the leftmost sum in (7.107d), the rightmost sum in (7.107d) and the sum in (7.107c), respectively, we will show the derivations for the sums in (7.107a)–(7.107b) only. The main ideas easily port to the other sums, as well as the sums in (7.110) and (7.111). Let

$$I_{u1}(i,j) := \sum_{k=0}^{i-j} \sigma_1(i,j,k) u^K(\frac{1}{2}\Delta(i-j+k), \frac{1}{2}\Delta(i-j-k)) \tag{7.112}$$

$$I_{u2}(i,j) := \sum_{k=0}^{j} \sigma_2(j,k) v^K(\Delta(i-j+k), \Delta k) \tag{7.113}$$

and

$$I_{v1}(i,j) := \frac{a}{2}\Delta \sum_{k=0}^{i-j} \sigma_1(i,j,k) u^K(\frac{1}{2}\Delta(i+j+k), \frac{1}{2}\Delta(i+j-k)) \tag{7.114}$$

denote the different sums. It is noted that for constant difference $i-j = m \geq 0$, we have for

$$I_{u1}(i,i-m) = \sum_{k=0}^{m} \sigma_1(i,i-m,k) u^K(\frac{1}{2}\Delta(m+k), \frac{1}{2}\Delta(m-k)) \tag{7.115}$$

hence, along the "lines" where $i-j=m$, the terms in the sum overlap, and thus

$$\begin{aligned} I_{u1}(i+1,i+1-m) &= \sum_{k=0}^{m} \sigma_1(i+1,i+1-m,k) u^K(\frac{1}{2}\Delta(m+k), \frac{1}{2}\Delta(m-k)) \\ &= \sum_{k=0}^{m} \sigma_1(i,i-m,k) u^K(\frac{1}{2}\Delta(m+k), \frac{1}{2}\Delta(m-k)) \\ &= I_{u1}(i,i-m) \end{aligned} \tag{7.116}$$

where the second equality sign follows from the definition of $\sigma_1(i,j,k)$ in (7.108). If we form a matrix with elements $I_{u1}(i,j)$, this matrix is the upper

[1]For details concerning the *big O* notation, consult e.g. Knuth (1976)

triangular part of a so-called *Toeplitz matrix* (Bini (1995)) and the total matrix consists of only N distinct entries. The full matrix can therefore be computed in only $O(N^2)$ time.

Similarly, along the lines $i - j = m$, we find for (7.113)

$$I_{u2}(m-j,j) = \sum_{k=0}^{j} \sigma_2(j,k) v^K(\Delta(m+k), \Delta k) \tag{7.117}$$

and

$$I_{u2}(m-j+1,j+1) = \sum_{k=0}^{j+1} \sigma_2(j+1,k) v^K(\Delta(m+k), \Delta k) \tag{7.118}$$

as $\sigma_2(j,k)$ equals 1 for all cases where $j \neq 0$, $k \neq 0$ and $k \neq j$, we find

$$\begin{aligned} I_{u2}(m-j+1,j+1) = I_{v1}(m-j,j) &+ \frac{1}{2} v^K(\Delta(m+j), \Delta j) \\ &+ \frac{1}{2} v^K(\Delta(m+j+1), \Delta(j+1)) \end{aligned} \tag{7.119}$$

Utilizing this overlapping structure, the computation time is reduced to $O(1)$ for each of the elements $I_{v1}(i,j)$. A similar derivation for (7.114) along the lines $i + j = m$ yields

$$\begin{aligned} I_{v1}(i+1,i+1-m) = I_{v1}(i,i-m) &+ \frac{1}{2} u^K(\frac{1}{2}\Delta(m+k), \frac{1}{2}\Delta(m-k)) \\ &+ \frac{1}{2} u^K(\frac{1}{2}\Delta(m+k+1), \frac{1}{2}\Delta(m-k+1)), \end{aligned} \tag{7.120}$$

and the computational time is reduced to only $O(1)$ for each of the elements $I_{v1}(i,j)$ as well.

Using the proposed numerical optimization techniques, the run time can be reduced from $O(N^3)$ at every iteration to only $O(N^2)$ for all kernel equations.

Chapter 8

Simulations

8.1 Introduction

The MPD system (7.1) was implemented in `MATLAB`. The numerical values used for the physical parameters are given in Table 8.1.

Parameter	Description	Value	Unit
β	Bulk modulus	$7317 \cdot 10^5$	Pa
A_1	Annulus cross sectional area	0.024	m^2
ρ	Mud density	1250	kg/m^3
F_1	Friction factor	10	kg/m^3
g	Gravity constant	9.81	m/s^2
A_2	Drill bit cross sectional area	0.02	m^2
l	Well length	2500	m
ω	Angular velocity	$\frac{2\pi}{16}$	
Z_0	The disturbance's initial value	$\begin{bmatrix}10 & 0\end{bmatrix}^T$	m

Table 8.1: Well and drill system parameters

The length of the well is 2500 meters, with the disturbance term modelled as a simple harmonic with period 16 seconds (≈ 0.39 rad / sec). This is a typical dominating swell wave period in the first peak of the Torsethaugen wave spectrum (Fossen (2011, Figure 8.11)), which is an empirically based wave spectrum developed from curve fitting experimental data from the North Sea. The amplitude of oscillation is chosen quite large to better see the attenuation properties of the controller. Additional parameter values are the same as was used for the simulations in Aamo (2013). The kernel equations were solved numerically using successive approximations with (7.105), (7.110) and (7.111), with the optimization techniques presented in Section 7.5.4. The resulting elements of $L^\alpha(\bar{x}, \xi)$ and $L^\beta(\bar{x}, \xi)$ in (3.52a)–(3.52b) are all upper bounded in magnitude by $1.1 \cdot 10^{-4}$, and it is therefore reasonable

to assume that the terms added by the integrals in (3.74) are small. As additionally $|q/r| < 1$, and A has only imaginary eigenvalues, the assumptions of Theorem 3.3 hold, and the simplified controller can be implemented as well.

The control law in Theorem 7.1 was tested, with $U(t)$ generated from the original controllers of Theorem 3.1–3.3 both when using the system states directly, and when using the observer generated states. Rational transfer function approximations found from applying the algorithm in Section 6.3 on the transfer functions of Theorems 5.1–5.3 were also tested out. All controllers were tested on the system through two different cases. The cases only differ in the depth of attenuation and the pressure set point. Case one will try to attenuate at a depth of 2000 meters, and case two at 1000 meters, with the pressure set point p_{sp} set to 450 bar and 300 bar, respectively. In both cases, the system is initially started in equilibrium and will be driven in open-loop by the disturbance term. The controller and observer, the latter only if included, will be turned on after $t = 40$ seconds. The observer (4.1) is then initiated with all zeroes, and will have to rely on the injection terms to converge to its true values.

By using the optimization technique presented in Section 6.5, the number of free parameter in the model reduction algorithm of Section 6.3 is reduced from two to one. It still leaves one free parameter that can be tuned. This free parameters was decided by choosing a value for the σ defined in (6.6), and determine α and γ using the optimization technique from Section 6.5. A value of $\sigma = 0.000$ was first tested out, with σ increased to 0.025 and 0.050 if the first value of σ did not yield satisfactory results. The fourth, sixth and tenth order approximations for the different values of σ can be found in Appendix C, with the one chosen for later simulations shown here. This choice is based on both the level of conformity with the original transfer function and the order of the transfer function, with emphasis on having a low order approximation.

To ease the implementation was, system (3.1) was the one actually implemented, with $p(z,t)$ and $q(z,t)$ calculated from (3.1a)–(3.1b) by inverting the transform (7.5). In all simulation cases, the system of PDEs was simulated using the Method of Lines, as described in Section 2.7.4.3, with the spatial derivatives in x approximated using a single step finite difference scheme as presented in section 2.7.4.2, and t left untouched. The explicit Runge-Kutta solver ode23 was used on the resulting IVP. A total of $N = 400$ discretization points were used for each system state $u(x,t)$ and $v(x,t)$, and their estimates. The time delayed $V(t)$ needed for the recursive controller is achieved using a transmission line as in Krstić and Smyshlyaev (2008) (and as illustrated in the example of Section 2.7.3), and implemented using the Method of Lines. A total of $N_{tr} = 400$ grid points were used. The transmission line is ini-

tialized and fed with some random signal (actually a sine wave with period 2π and amplitude 0.1) when not in use. The purpose of this is to ensure that the transmission line contains some erroneous signal when the recursive controller is turned on, and to illustrate that the initial conditions have to be driven out of the system before the recursive controller applies to correct signal. The simulation horizon was $t = 200$ for all simulation cases, while the observer poles were placed at $-0.15 \pm 0.02j$ using the `MATLAB` command `place()`. These are the same poles as were used in Aamo (2013).

We start each case by finding a transfer function approximation for each one of the controllers. The system is then simulated with all the controllers, and the results are displayed for comparison. The following figures are used to display the simulation results:

1. The first figure shows the pressure at the depth of attenuation, and a close up zoom of it from when the controller is turned of with the purpose of comparing the state feedback implementation with the full output feedback implementation. At the bottom is an additional plot comparing the model order reduced controller with the full output feedback implementation.

2. The second figure shows the applied controller signal $U(t)$ for all controllers used.

3. The third figure shows the pressure in the well as a function of time for selected depths. The depths are chosen distributed in the well with a uniform spacing of 500 meters. Two plots are shown, one for the state feedback case, and one for the output feedback case.

4. The fourth figure shows at the top a same type of plot as found in the third figure, but this time for the reduced order controller. At the bottom are two plots shown, each containing four plots of the pressure profile in the well for the state feedback case, sampled with a spacing of 1 second. This creates an stop-motion representation of the pressure distribution, with each subplot animating four seconds of simulation with the oldest sample in the lightest colour and newer samples plotted in a gradually darker colours. The purpose of these latter two plots is to capture the transients that occur when the controller is turned on after $t = 40$ seconds.

5. The fifth figure is only shown for the pure state feedback implementations. It shows a 3D representation of the pressure in the well, as well as the observer state errors $\tilde{u}(x,t) = u(x,t) - \hat{u}(x,t)$ and

$\tilde{v}(x,t) = v(x,t) - \hat{v}(x,t)$. At the bottom is the disturbance term with the observer's estimate shown. The purpose is to show the convergence properties of the observer and the overall behaviour of the well when the controller is turned on.

8.2 Case 1: Attenuation at a depth of 2000 metres

The depth of attenuation was for all the simulations shown in this section set to 2000 m. This corresponds to $\bar{x} = \frac{1}{5}$.

8.2.1 Transfer function approximations

8.2.1.1 Pure state feedback controller

The transfer function of Theorem 5.1 is plotted in Figure 8.1 alongside the sixth order rational transfer function approximation found using the method described in Sections 6.3 and 6.4 with $\sigma = 0.025$. The corresponding α and γ were found with the method described in Section 6.5. Additional approximations using $\sigma = 0.000$, $\sigma = 0.0250$ and $\sigma = 0.050$ of order 4, 6 and 10 can be found in Appendix C.1.1. Very little performance gain was achieved from choosing a higher order approximation.

From Figure 8.1, it is seen that the approximation fails to capture most of the characteristics for frequencies above 0.8 rad / sec, but that the approximation is reasonably good for frequencies below 0.8 rad / sec.

The original transfer function has unusually strange resonance peaks near 2 rad / sec and 7 rad / sec, and additionally it has an unexpected phase plot with a phase increasing with frequency. One could expect a falling phase, as the system contain a transmission line which would act as time delay. The phase plot was generated using the `MATLAB` function `phase()` on the sampled frequency response, and the odd phase plot may be caused by this function. Another source of the strange phase plot could be the `MATLAB` function `expm()`, used to evaluate the matrix exponential needed in (7.36), which is known to be numerically unstable when the matrix contains elements which have large spans in magnitude (Moler (2012)).

8.2.1.2 Recursive controller

The transfer function of Theorem 5.2 and its sixth order approximation with $\sigma = 0.025$ are plotted in Figure 8.2. The approximation was found using the

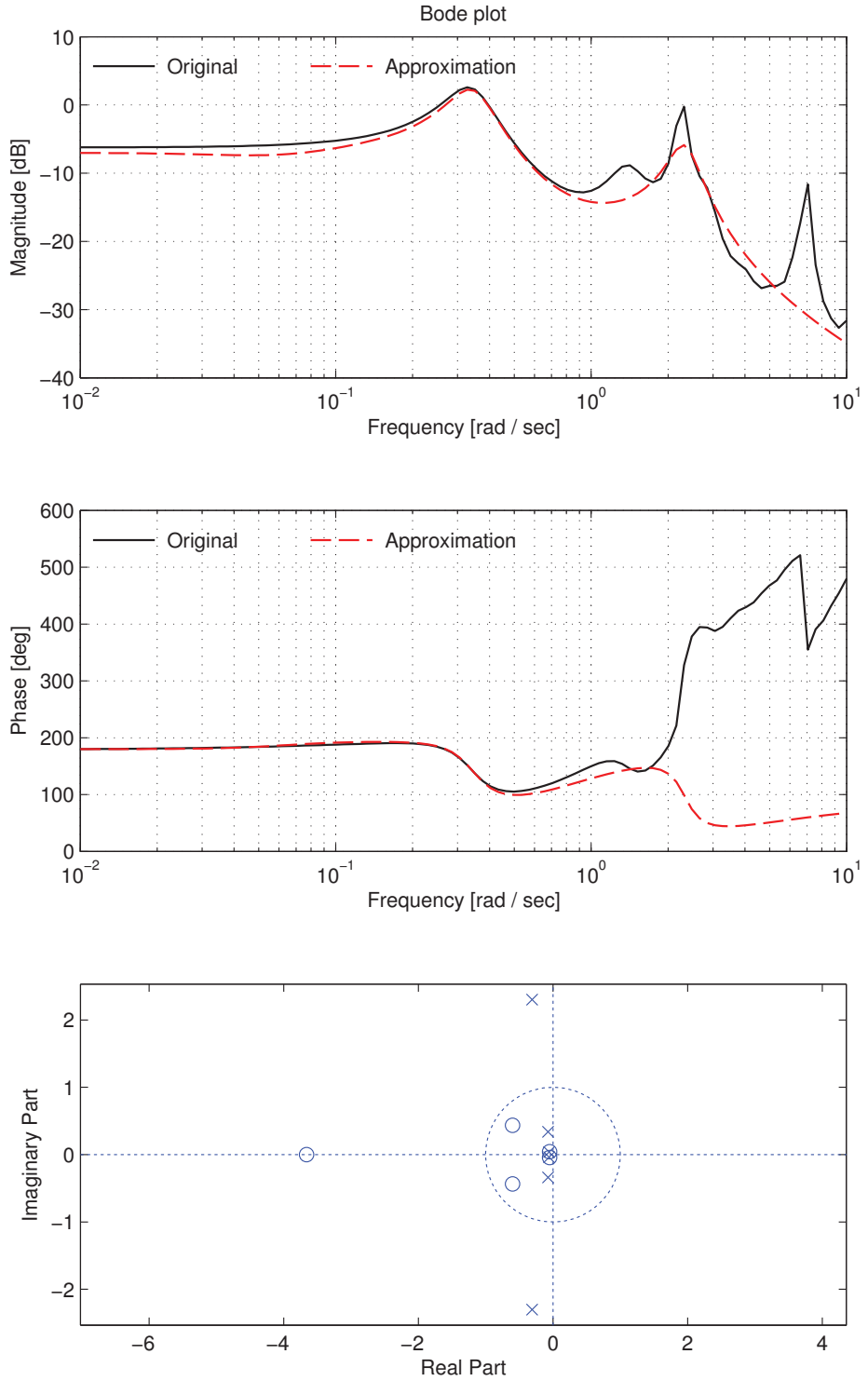

Figure 8.1: Transfer function approximation for Case 1: Pure state feedback controller.

same method as in the previous section. Additional approximations using $\sigma = 0.00$, $\sigma = 0.025$ and $\sigma = 0.05$ of order 4, 6 and 10 can be found in Appendix C.1.2. The similarity between the transfer functions of Theorem 5.1 and Theorem 5.2, as shown in figures 8.1 and 8.2, respectively, is remarkable. Except for a slightly larger peak near $\omega = 2$ rad / sec, the transfer functions are nearly indistinguishable, which should not be surprising as the controllers of Theorems 3.1 and 3.2 are in fact two different representations of the *same* control law. Naturally, the approximation in Figure 8.2 also fails to capture most of the characteristics for frequencies above 0.8 rad / sec, but the approximation is reasonably good for frequencies below 0.8 rad / sec.

From further inspection, it is evident that the source of strange resonance peaks and unusual phase plots is the term $g_{rec}(\bar{x}, s)$ in (5.46). By neglecting the terms added by the integrals (which are anyway small in magnitude), we find an approximation of $g_{rec}(\bar{x}, s)$ in (5.46) as

$$g_{rec}(\bar{x}, s) \approx \frac{1}{r - qe^{-sd_{rec}(\bar{x})}}. \tag{8.1}$$

As q is negative and close to $-r = -1$, we will experience a considerable resonance peak when $e^{-sd_{rec}(\bar{x})} = -1$. These happen at frequencies

$$\omega = \frac{\pi(1 + 2k)}{d_{rec}(\bar{x})} \tag{8.2}$$

for $k \in \mathbb{Z}^+$. Inserting for the numerical values of Table 8.1, the resonance peaks are found at

$$\omega = (2.40 + 4.81k) \text{ rad / sec.} \tag{8.3}$$

The peaks for $k = 0$ and $k = 1$ are clearly seen in Figure 8.2. These peaks, and the infinitely many more peaks at frequencies given by (8.3) for $2 \leq k \in \mathbb{Z}^+$, probably makes the transfer function matching difficult (or even impossible) and the method therefore fails to achieve a good approximation. However, these peaks are situated above the expected bandwidth of the controller (which should be around frequency of the disturbance), and one could probably achieve far better approximations by weighting the different frequencies prior to applying the model reduction algorithm, for instance by taking the actuator dynamics into account, or simply add a low pass filter.

8.2.1.3 Simplified controller

Figure 8.3 shows the sampled frequency response for transfer function in Theorem 5.3, alongside the sixth order transfer function approximation achieved from using $\sigma = 0.000$.

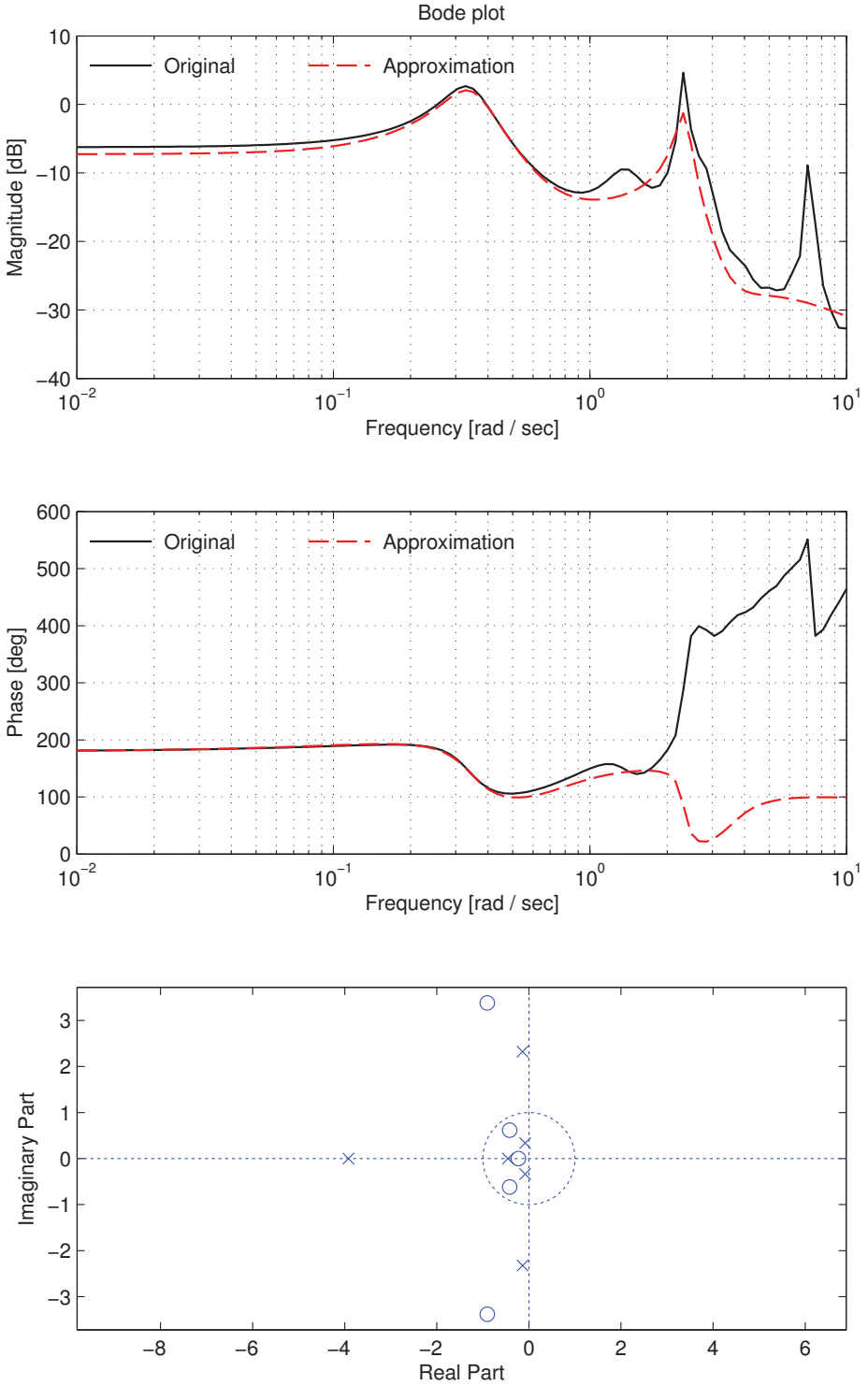

Figure 8.2: Transfer function approximation for Case 1: Recursive controller.

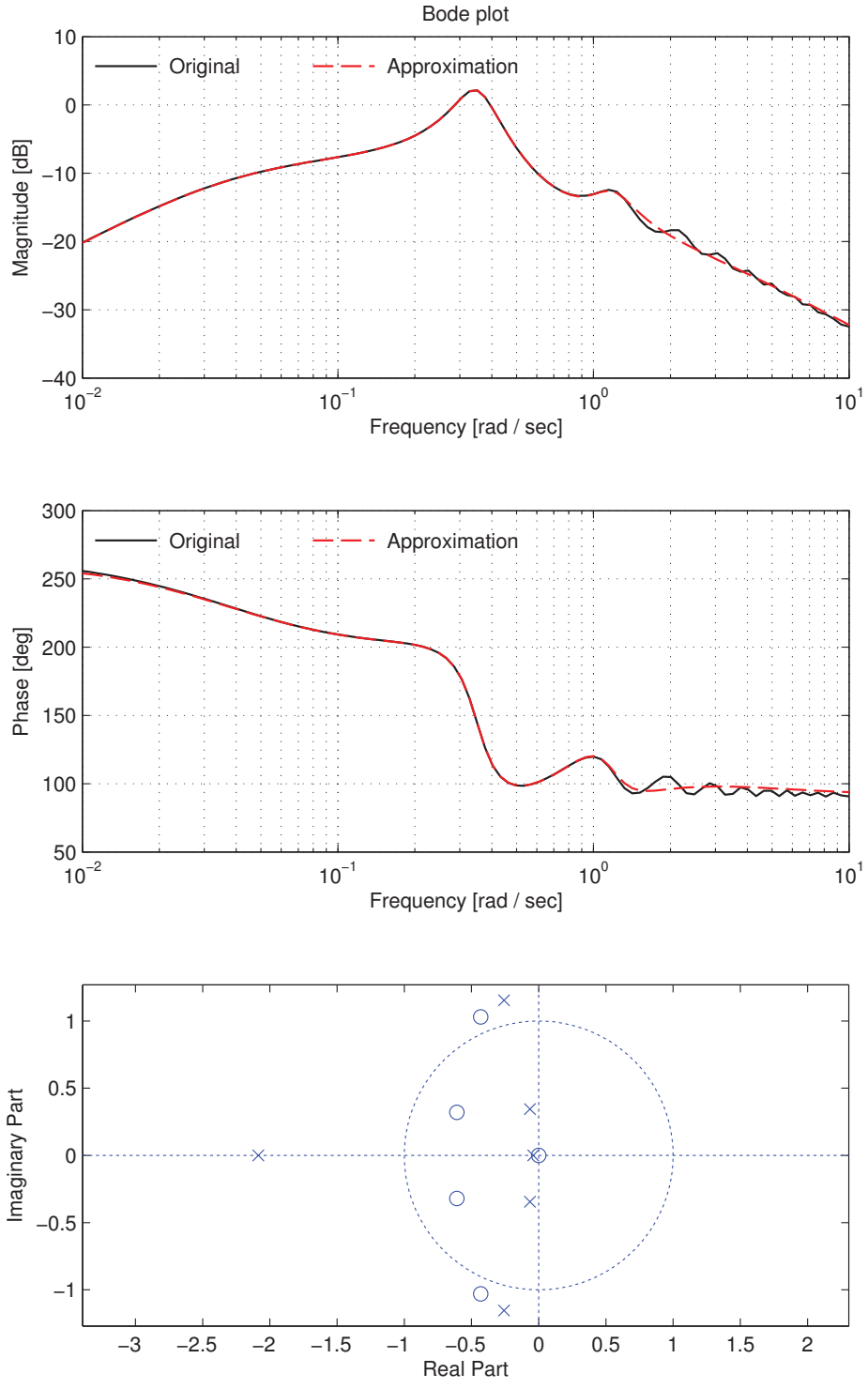

Figure 8.3: Transfer function approximation for Case 1: Simplified controller.

As observed in Figure 8.3, the sixth order approximation does fit the original transfer function extremely well for frequencies below 1 rad / sec. An additional fourth and a tenth order approximation is shown in Figure C.7 on page 164. The forth order approximation is underparametrized, while the tenth order approximation matches well for frequencies up to 2 rad / sec.

8.2.2 Simulations

8.2.2.1 Pure state feedback controller

The results from simulating the system with the control law of Theorem 3.1 are here given. Also given are the results from applying the same control law, but with the controller using the states estimated using (4.1), and when using the rational approximation found in Section 8.2.1.1. The simulation results can be found in figures 8.4–8.8 on pages 100–104.

From the 3D visualization in Figure 8.8a it can clearly be observed that the whole well is affected when the controller is turned on after $t = 40$ seconds. From figures 8.4a and 8.4b, it is seen that the amplitude of oscillations is reduced from approximately 75 bar to less than 0.15 bar, when using both the state feedback and the output feedback implementations. This constitutes to an attenuation factor of over 500. The output feedback implementation is somewhat slower, and an exponential decay is clearly observed from Figure 8.4a as expected from the properties of the observer (4.1), also illustrated in Figure 8.8. The estimated observer states converge to their real values after a few seconds. A similar result was observed from simulations with the same observer in Aamo (2013).

Several small, fast oscillating components can be observed from figures 8.6a and 8.6b when the controller triggers after $t = 40$ seconds. They can also be noted from the applied controller signals in Figure 8.5. The oscillations are somewhat damped for the output feedback case shown in Figure 8.6b. This can be expected, as all the signals are passed through the observer, somewhat damping them on their way. The oscillations gradually decay, and are practically zero in amplitude after about 120 seconds of active pressure attenuation for the state feedback case, and 60 seconds for the output feedback case. These oscillations are probably due to the initial conditions present in the system when the controller is turned on at $t = 40$, and may also be amplified due to the discretization method used.

From the left plot of Figure 8.7b, one can see the different pressure gradients travels down the well. The pressure at $z = \bar{z}$ reaches its setpoint as soon as the first pressure gradient reaches the depth, something that takes about 2.5 seconds from controller activation. By inserting numerical values of Table 8.1 into the expression (7.30), we find the predicted time constraint to be 2.61 seconds, which is in accordance with the observed regulation time.

The reduced order controller performs well, as seen from Figure 8.4c, comparing the pressure at a depth of 2000 metres from using the reduced order controller with the full, output feedback controller. The amplitude of oscillations is about 2 bar, which is within the standard MPD limits of 2.5

bar. When considering that the number of ODEs are reduced from 800 in the full output feedback case, to only 6, this is a satisfactory performance. The pressure oscillations in the well that were observed for all the previous simulation cases are almost not present when using the reduced order controller. A few oscillations with very small amplitudes can be observed for the first 20 seconds of controller action in Figure 8.7a, but the oscillations are considerably damped out compared with those observed in figures 8.6a and 8.6b.

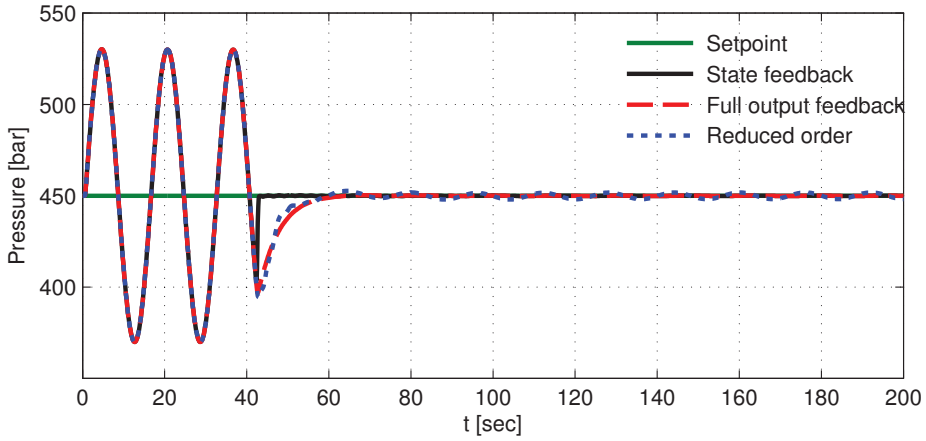

(a) Overview.

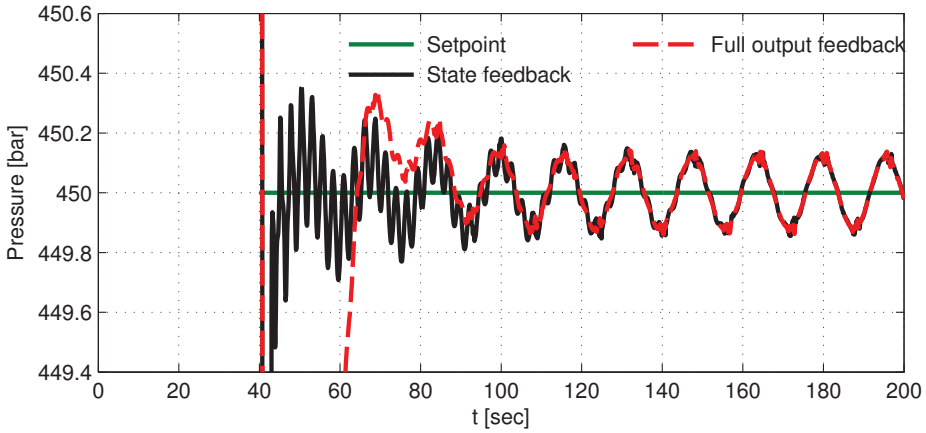

(b) State feedback vs full output feedback.

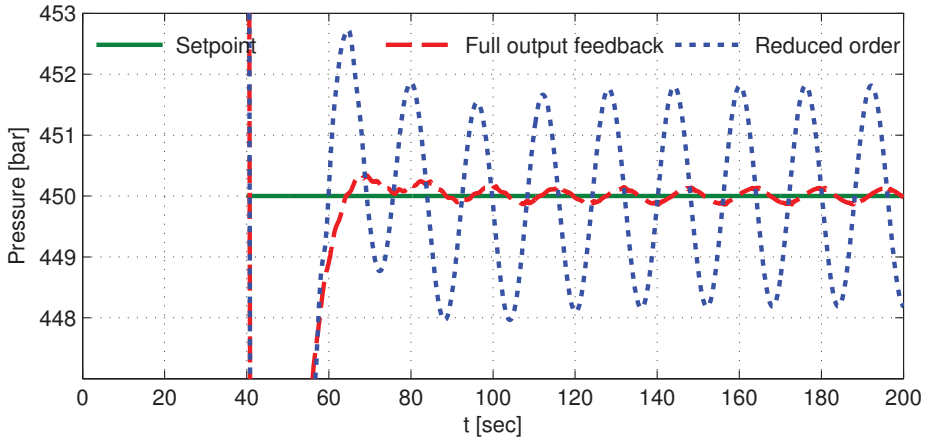

(c) Full vs reduced order output feedback.

Figure 8.4: Case 1: P.s.f. controller: Pressure at depth 2000 metres.

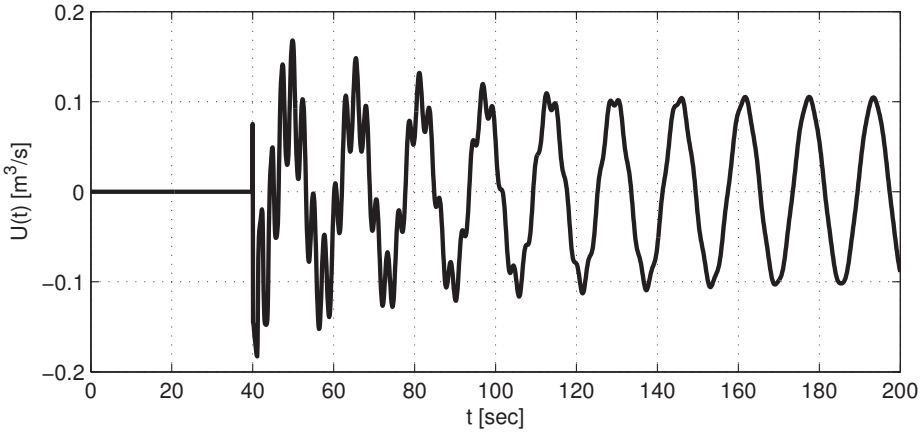

(a) State feedback.

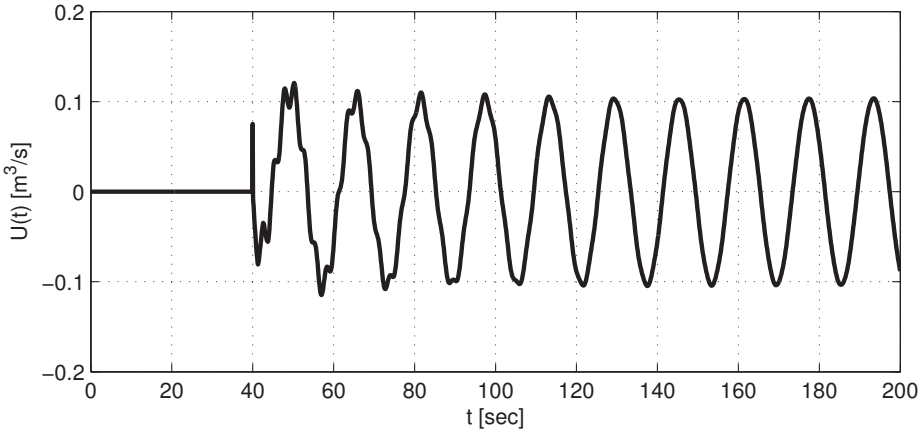

(b) Full order output feedback.

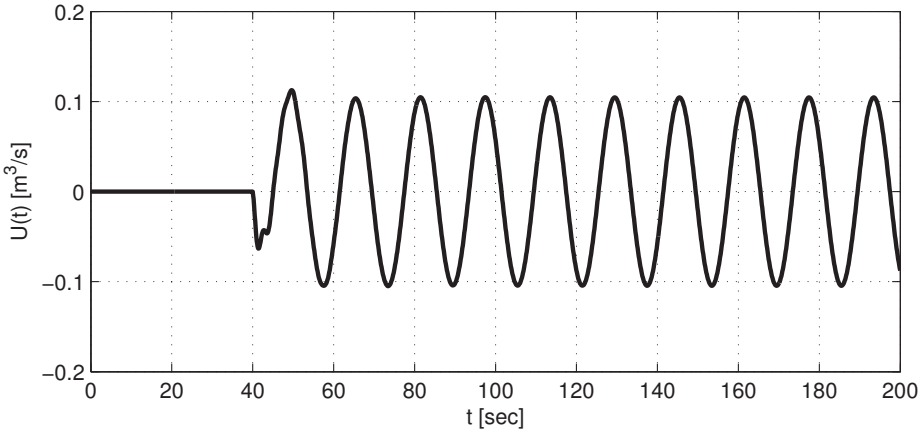

(c) Reduced order output feedback.

Figure 8.5: Case 1: P.s.f. controller: Applied controller signals.

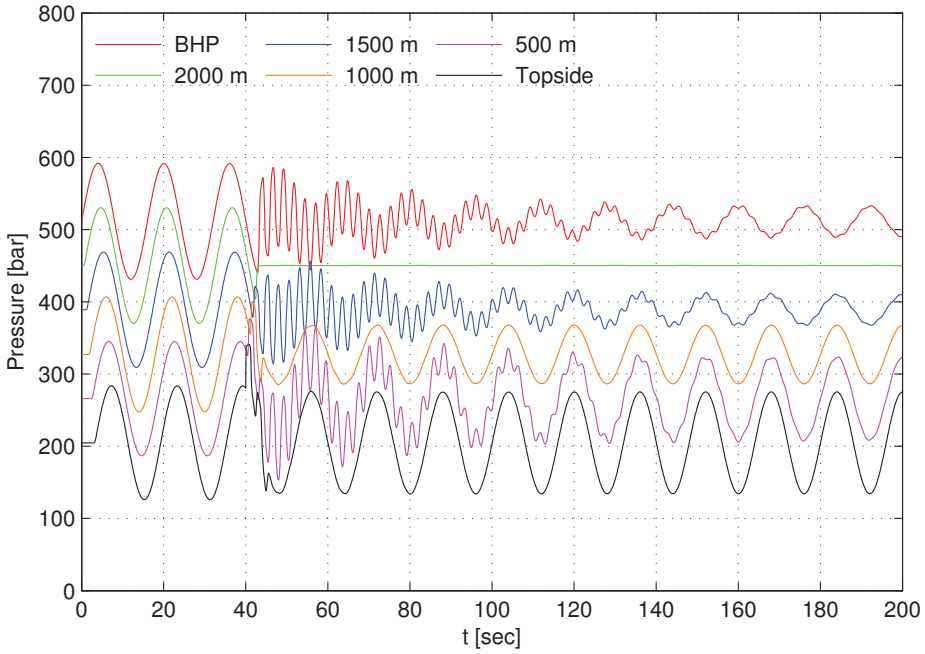

(a) State feedback.

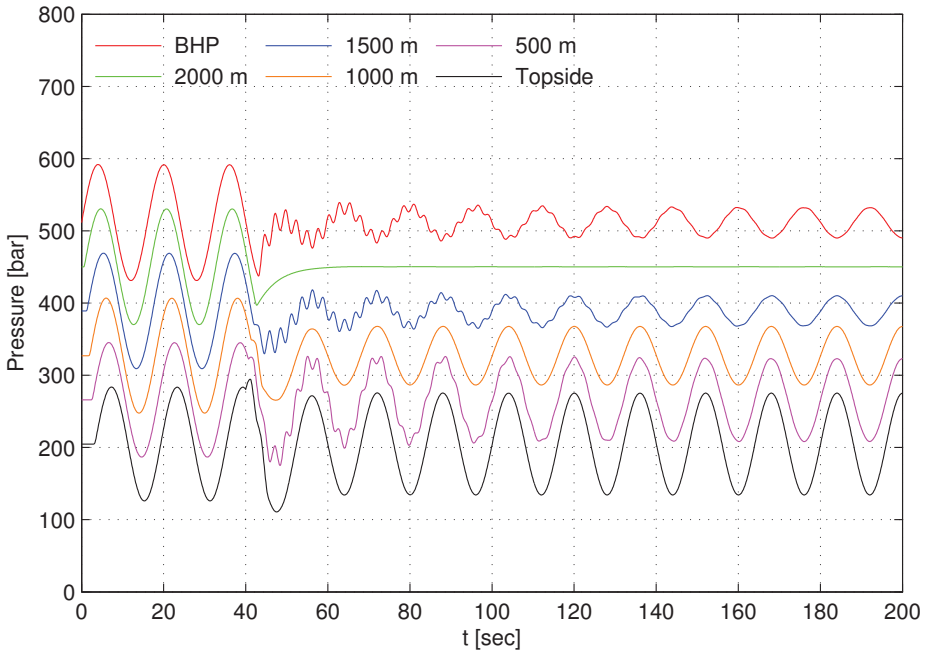

(b) Full order output feedback.

Figure 8.6: Case 1: P.s.f. controller: Pressure at selected depths.

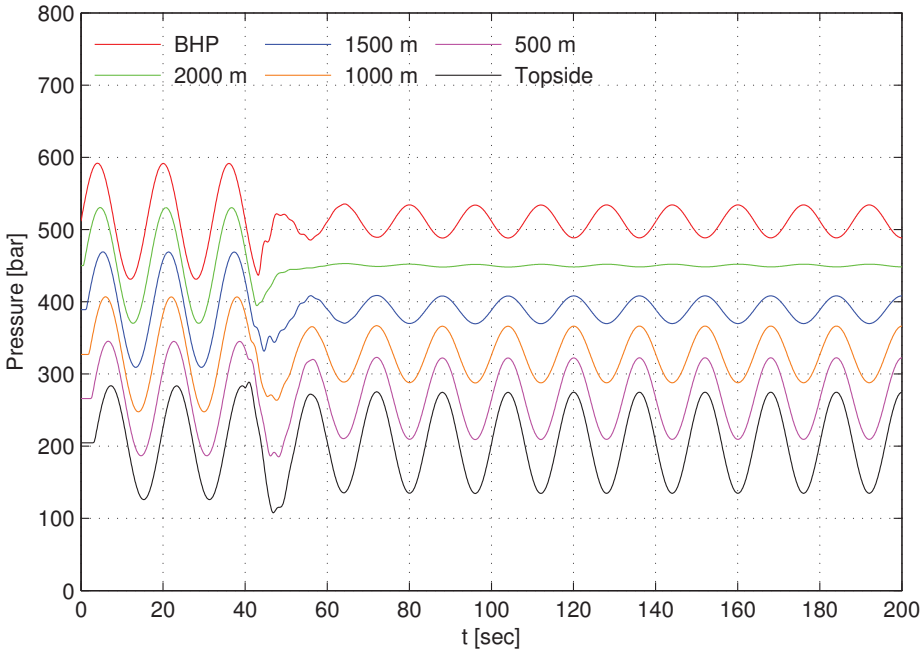

(a) Pressure at selected depths for reduced order controller.

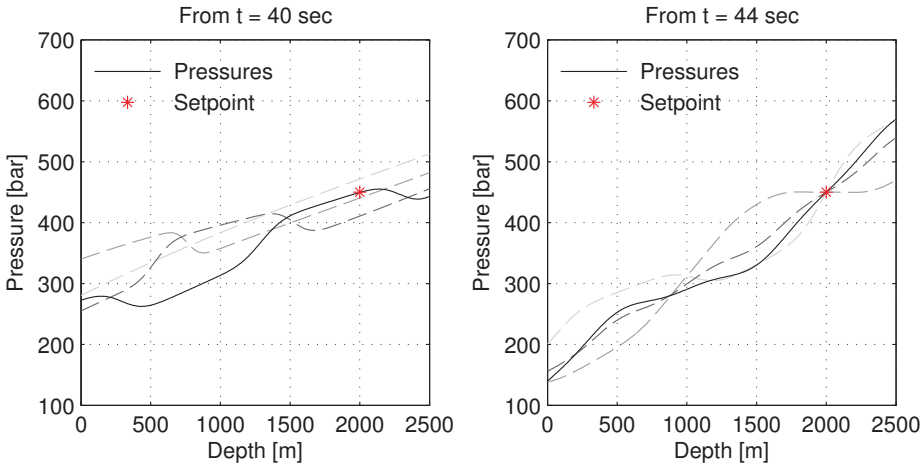

(b) Selected pressure profiles in the well, state feedback.

Figure 8.7: Case 1: P.s.f. controller: Pressure at selected depths and pressure profiles.

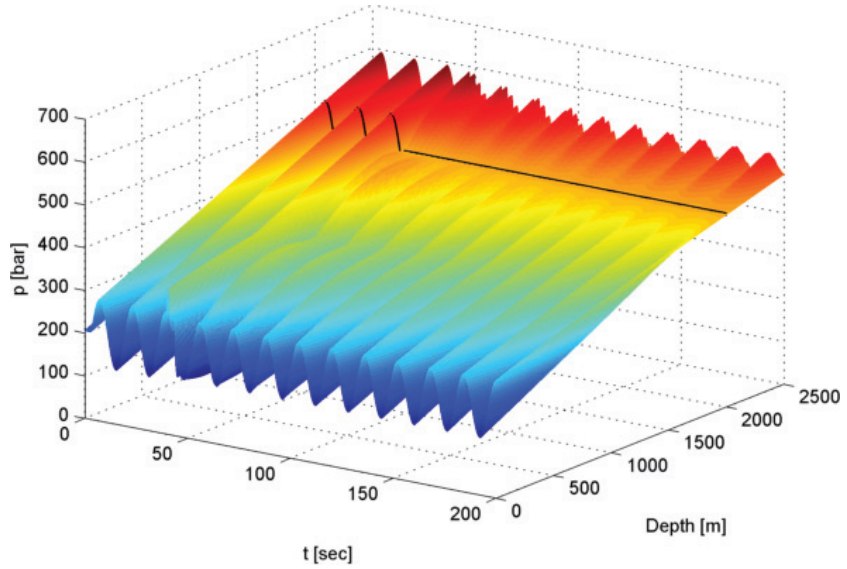

(a) Pressure distribution when using state feedback.

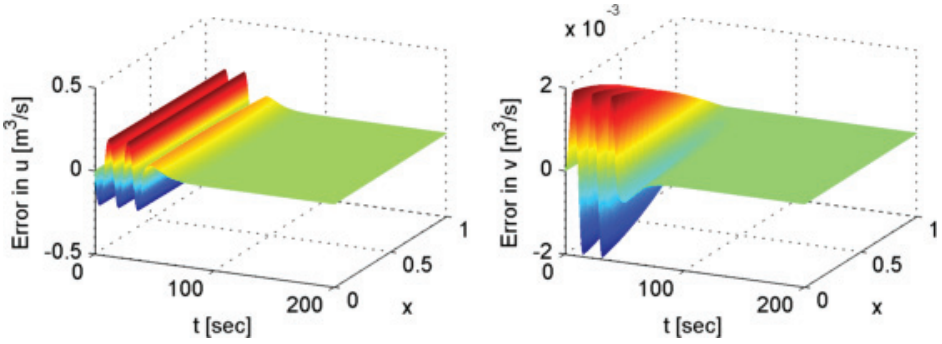

(b) System state estimation error.

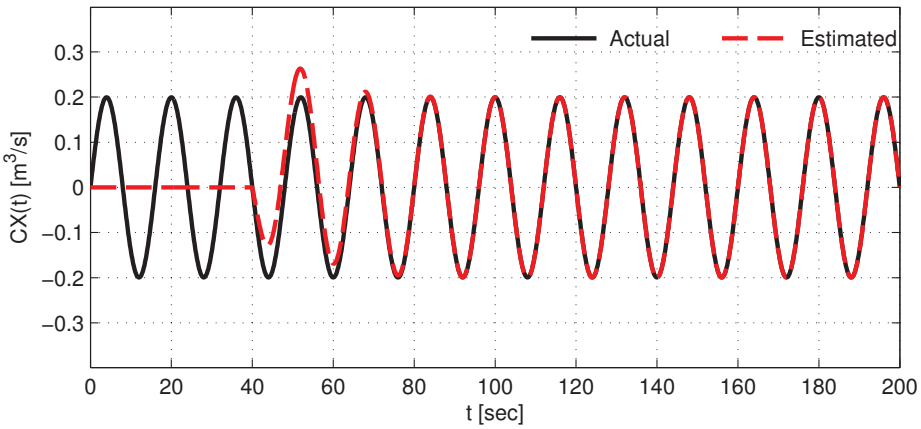

(c) Disturbance with estimated disturbance.

Figure 8.8: Case 1: P.s.f. controller: Disturbance and observer states, pressure distribution.

8.2.2.2 Recursive controller

The control law Theorem 3.2 was here implemented along with the observer (4.1) and the rational approximation found in Section 8.2.1.2. The simulation results can be found in figures 8.9–8.12 on pages 106–109.

The state feedback implementation of the recursive controller exhibits somewhat the same level of attenuation at depth 2000 as the pure state feedback controller. This can be seen from comparing figures 8.9a and 8.9b with their equivalents in figures 8.4a and 8.4b. The amplitude of oscillations is reduced to approximately 0.12 bar, actually slightly better than the pure state feedback controller in the previous section. However, the oscillations for the first 60 seconds after the controller has been turned on are much more excessive. The oscillations are probably amplified from the use of a transmission line and the initial conditions therein. The pure state feedback implementation in the previous section avoided this robustness issue by using the actual system states. The output feedback implementation shows the same tendency, with larger fluctuations around the set point for the first seconds of controller action. This is also observed from the increased amplitude of the pressure oscillations in the rest of the well, as can be seen from both Figure 8.11a and Figure 8.11b when comparing with the equivalents in Figure 8.6.

Figure 8.12b shows that the pressure at depth 2000 does not meet its set point as the first applied pressure gradient reaches the depth. The gradient has to be propagated back up again via the well's bottom before the set point is reached. This is precisely as predicted from theory, as the initial conditions in the transmission line have to be driven out of the system before the correct output is given. The total time seems to be around 4 seconds, which is in accordance with the value of 3.92 seconds found by inserting numerical values of Table 8.1 into (7.31).

As seen from Figure 8.9, does the reduced order controller perform, not surprisingly, much like the reduced order controller from the previous section. A slightly better attenuation level is achieved, with an amplitude of oscillation at 1 bar, quite acceptable as the number of ODEs are reduced from 1200 to 6. The slightly better performance than in the previous sections is probably a mere coincidence.

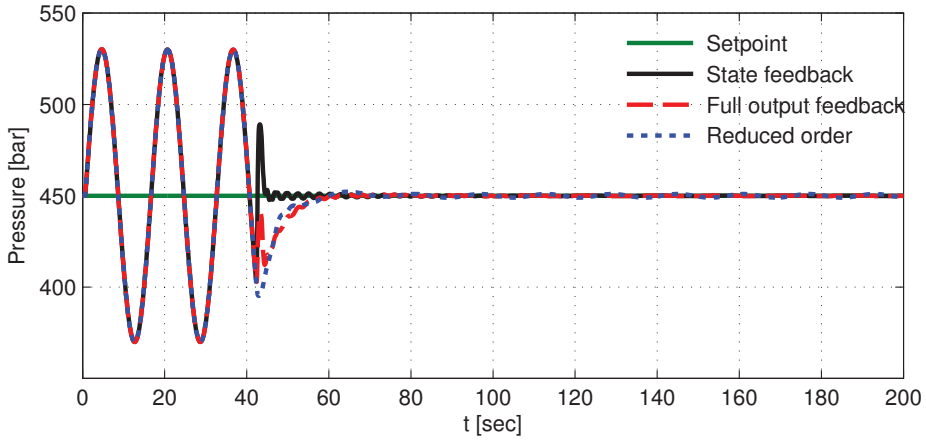

(a) Overview.

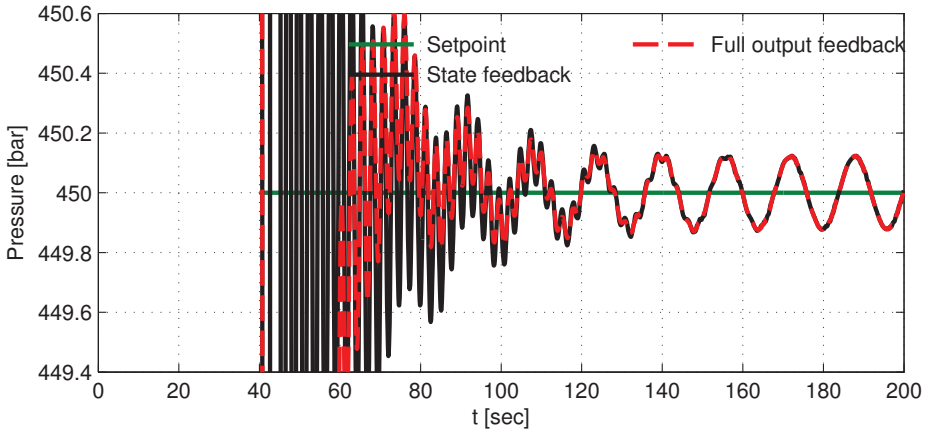

(b) State feedback vs full output feedback.

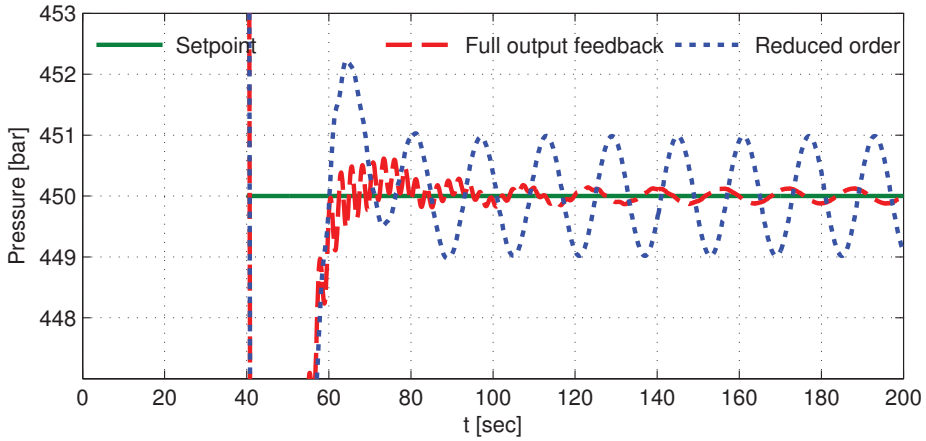

(c) Full vs reduced order output feedback.

Figure 8.9: Case 1: Recursive controller: Pressure at depth 2000 metres.

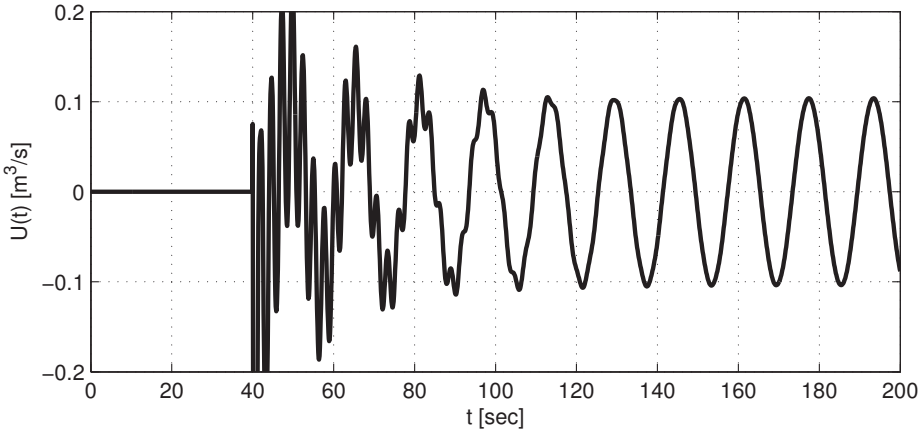

(a) State feedback.

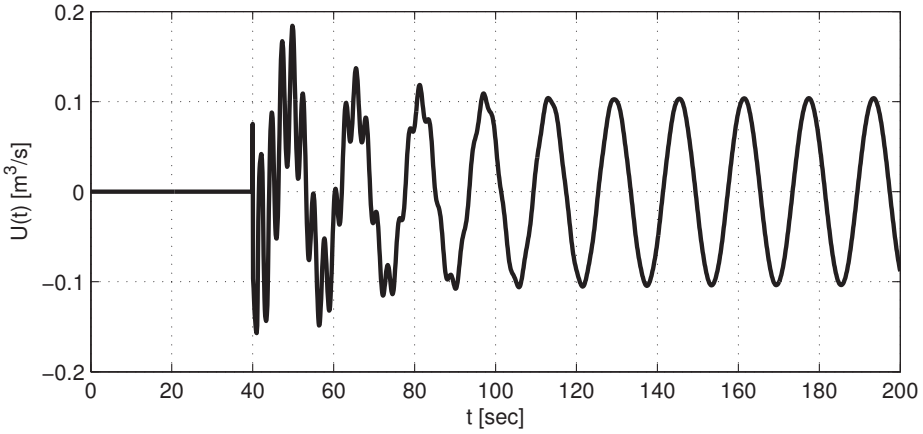

(b) Full order output feedback.

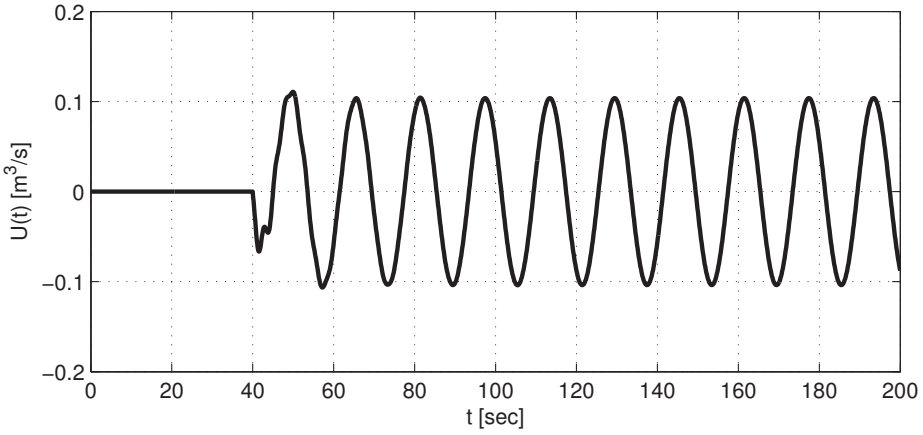

(c) Reduced order output feedback.

Figure 8.10: Case 1: Recursive controller: Applied controller signals.

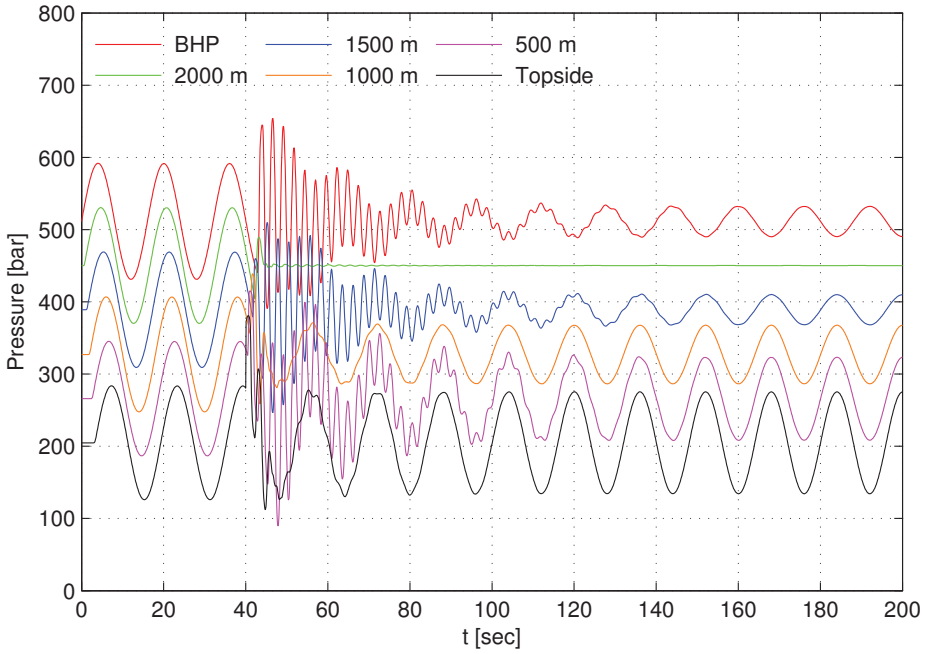

(a) State feedback.

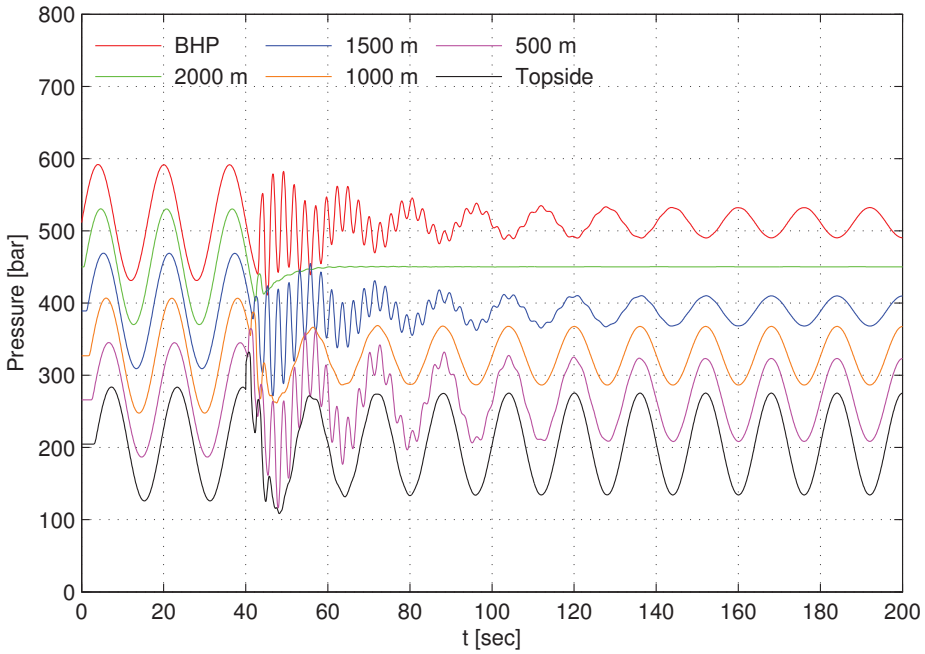

(b) Full order output feedback.

Figure 8.11: Case 1: Recursive controller: Pressure at selected depths.

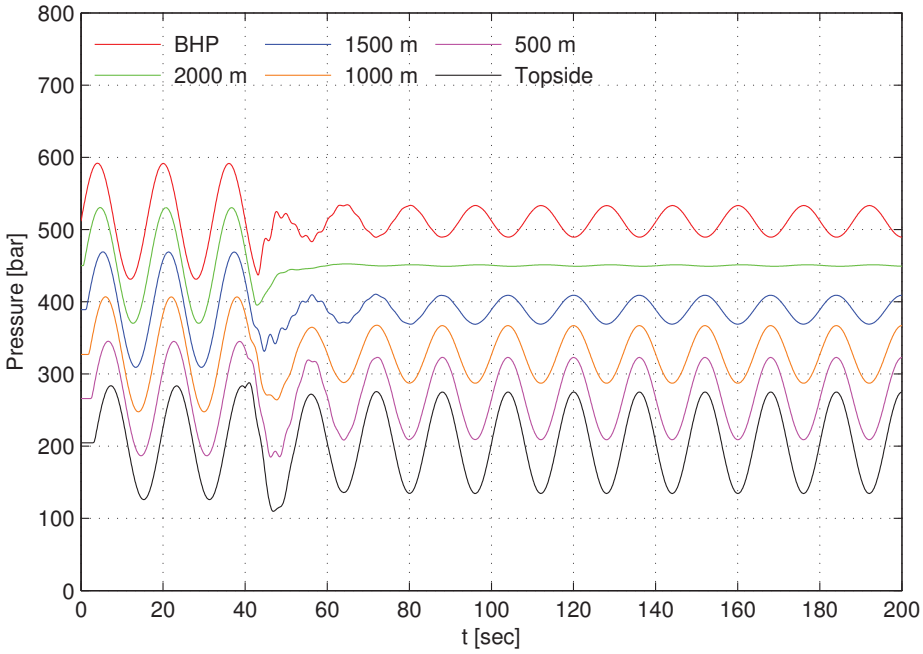

(a) Pressure at selected depths for reduced order controller.

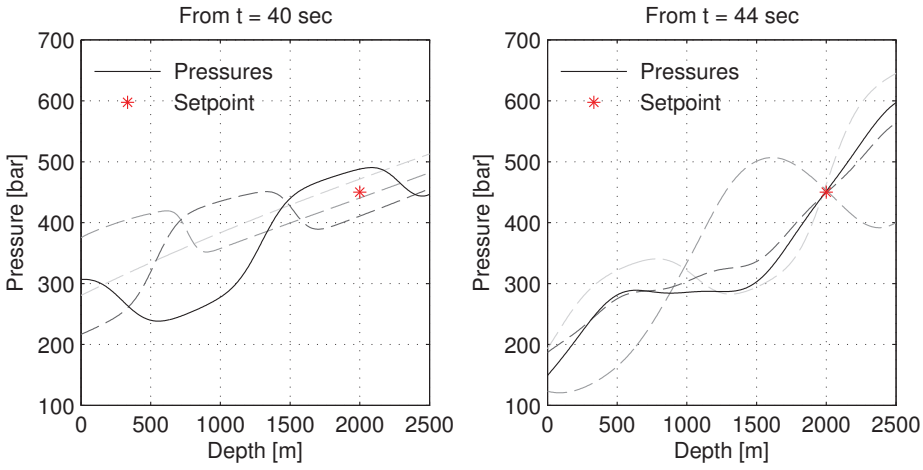

(b) Selected pressure profiles in the well, state feedback.

Figure 8.12: Case 1: Recursive controller: Pressure at selected depths and pressure profiles.

8.2.2.3 Simplified controller

The simplified controller of Theorem 3.3 was here implemented both when using the system states directly, and when using the observer generated states. Also implemented, was the rational approximation found in Section 8.3.1.3. The results are found in figures 8.13–8.16 on pages 111–114.

When comparing the pressure at depth 2000 metres shown in Figure 8.13b with those of figures 8.4b and 8.9b, it is observed that the attenuation factor is just as good as for the two previous simulations. This is not precisely as predicted from theory, since one should expect a deterioration, following the assumption of neglecting the integral terms in (3.74). However, as these terms turned out to be very small, the uncertainties due to e.g. discretization are probably a much larger source of error. The deterioration following the simplifications made during the derivation should become more apparent if the terms (3.52a)–(3.52b) had considerably larger values. This could for instance be if the friction factor in the system (7.1) was larger. (This is verified using a constructed simulation case in Appendix D.1).

Not easily observed from Figure 8.16b, but as predicted from theory, the first applied pressure gradient needs to be propagated via the well's bottom before the control objective is achieved. The control time seems to be the same as for the recursive controller in the previous section, as predicted. The controller in overall is much more predictive and less aggressive than the those in the two previous sections. This is particularly observed from the smooth control signals of figures 8.14a and 8.14b as opposed to the signals of figures 8.5a–8.5b and 8.10a–8.10b, as well as the lack of oscillations in figures 8.15a and 8.15b.

As expected from the extremely good match for the reduced order transfer function shown in Figure 8.3, the attenuation properties of the reduced order controller are extremely good, easily observed from Figure 8.13c. The amplitude of pressure fluctuations is only about 0.25 bar. The overall behaviour looks very much like the full output feedback controller, as one also can observe from the indistinguishable results of figures 8.15b and 8.16a.

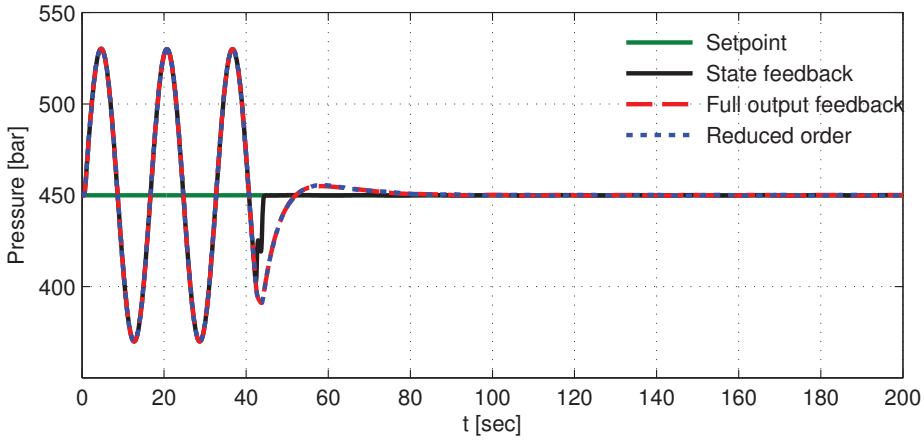

(a) Overview.

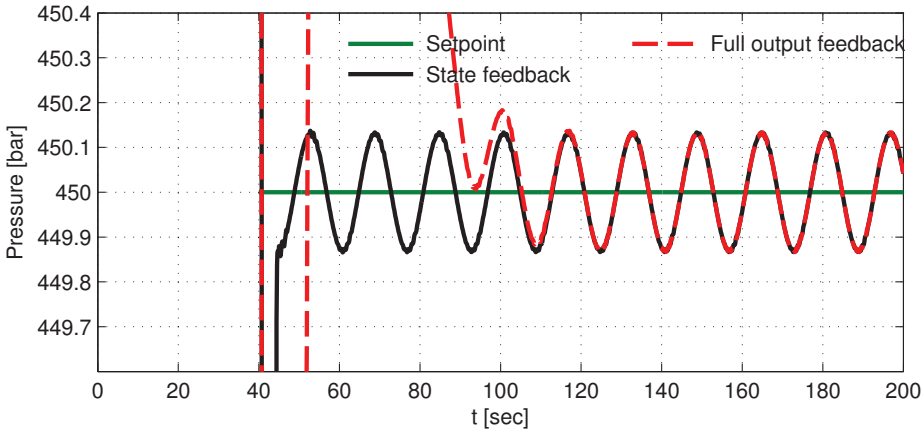

(b) State feedback vs full output feedback.

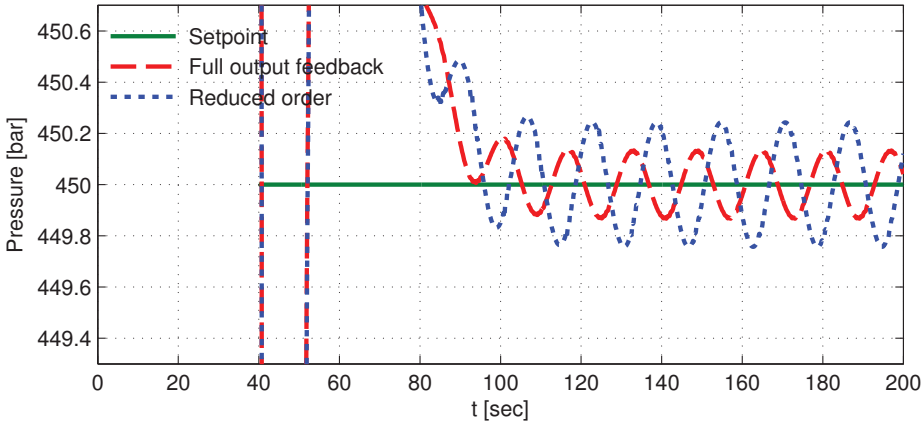

(c) Full vs reduced order output feedback.

Figure 8.13: Case 1: Simplified controller: Pressure at depth 2000 metres.

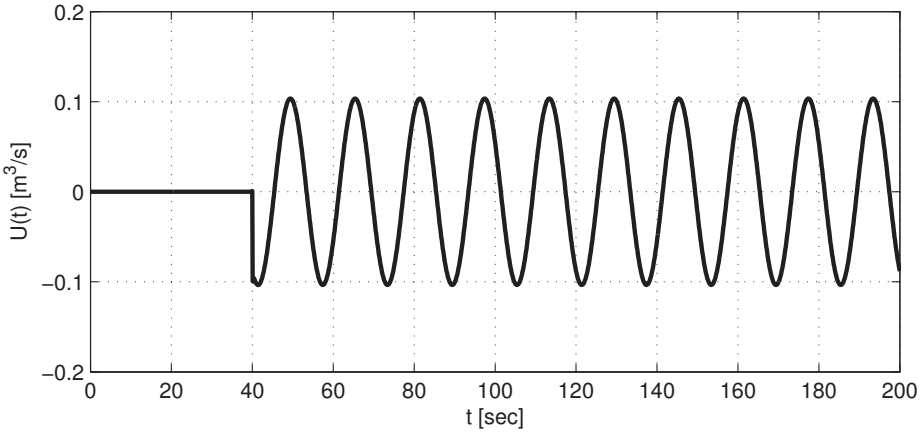

(a) State feedback.

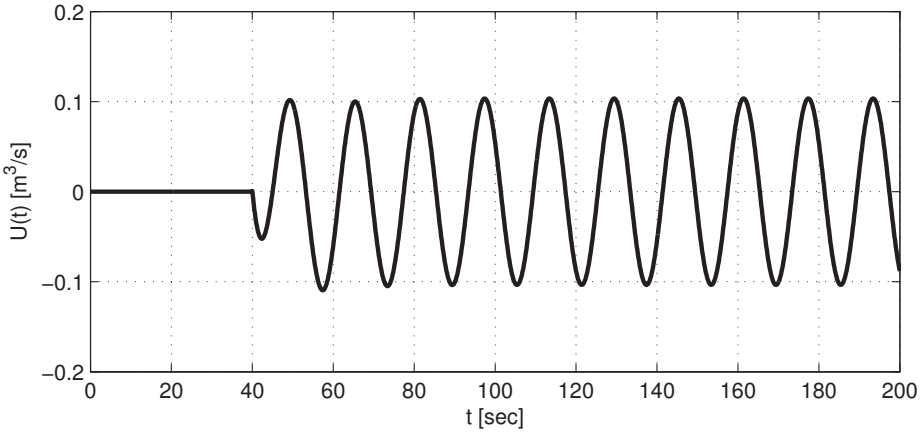

(b) Full order output feedback.

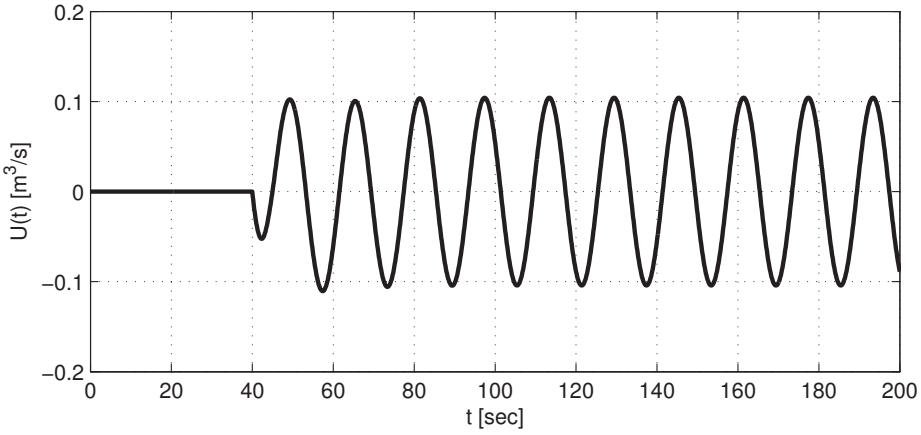

(c) Reduced order output feedback.

Figure 8.14: Case 1: Simplified controller: Applied controller signals.

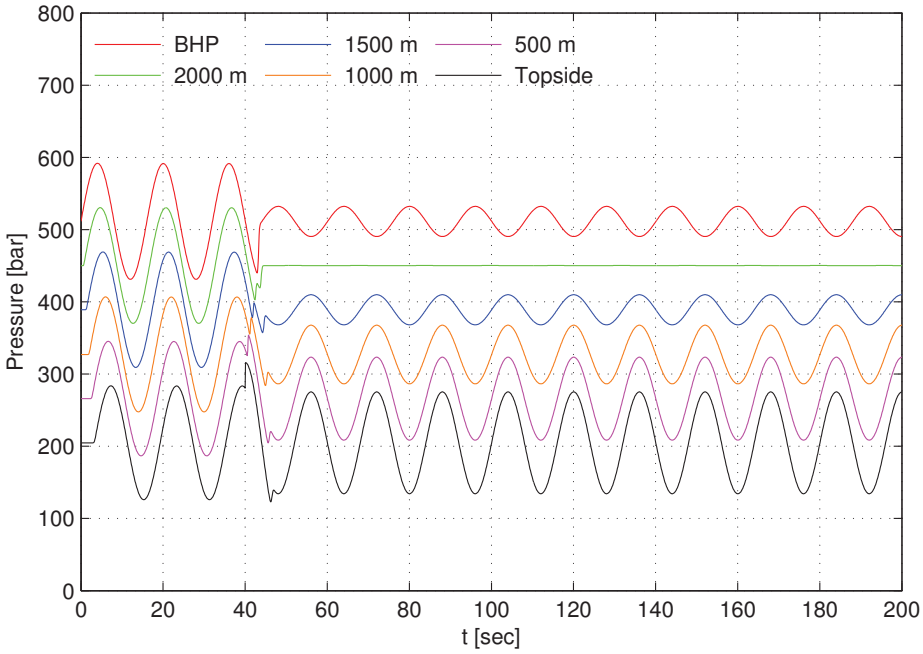

(a) State feedback.

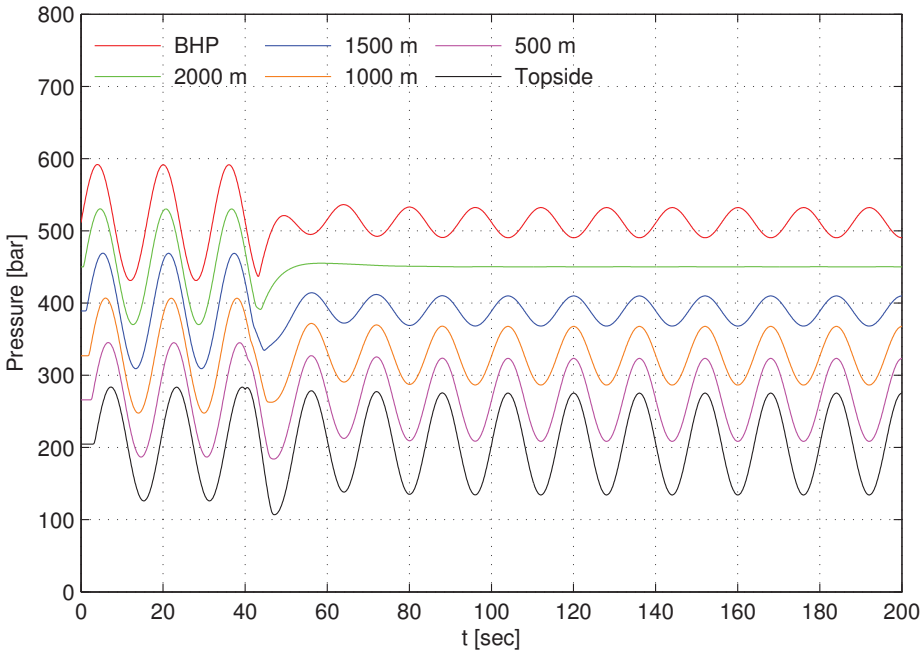

(b) Full order output feedback.

Figure 8.15: Case 1: Simplified controller: Pressure at selected depths.

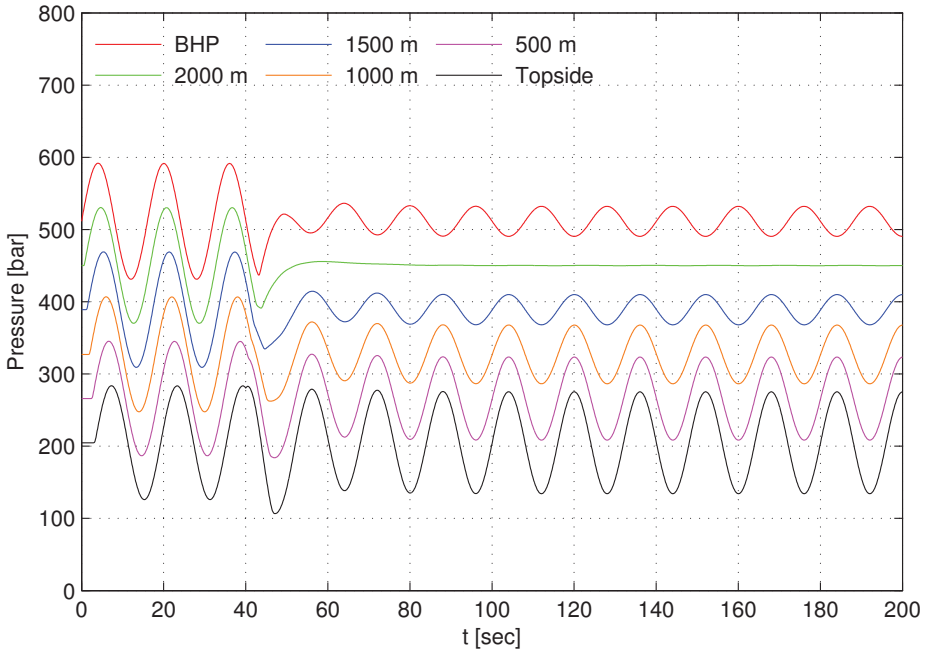

(a) Pressure at selected depths for reduced order controller.

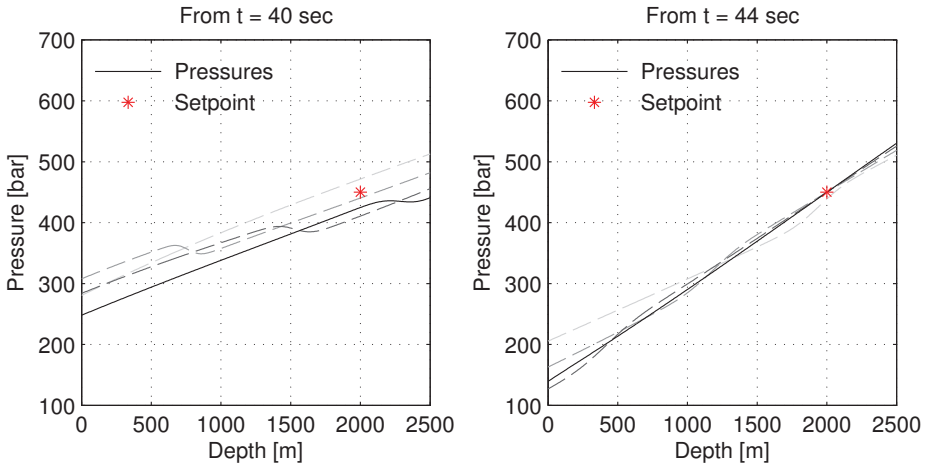

(b) Selected pressure profiles in the well, state feedback.

Figure 8.16: Case 1: Simplified controller: Pressure at selected depths and pressure profiles.

8.3 Case 2: Attenuation at a depth of 1000 metres

The depth of attenuation was this time set to 1000 m, which corresponds to $\bar{x} = \frac{3}{5}$.

8.3.1 Transfer function approximations

8.3.1.1 Pure state feedback controller

The transfer function of Theorem 5.1 for attenuation at depth 1000 metres is plotted in Figure 8.1 alongside the sixth order rational transfer function approximation, found using $\sigma = 0.025$. By using $\sigma = 0.000$, the approximation is not at all nearby the original transfer function, as can be seen from the fourth, sixth and tenth order approximations in Figure C.4 on page 161. The original transfer function shown in Figure 8.17 additionally has the strange resonance spikes as was previously observed in Section 8.2.1.2. The peaks are placed differently this time, as the value of $\bar{x}$ has changed. The phase plot once again has an *increasing* phase, and it seems as the plot has several discontinuities throughout.

The sixth and tenth order approximations shown in figures C.10b and C.10c match the original transfer function extremely well for frequencies below 0.7 rad / sec. However, the approximations have at least one pair of complex conjugated *unstable poles*. This is also present for the approximations achieved for $\sigma = 0.050$. Hence, the controller approximations are unstable and cannot be implemented as is. The unstable poles lie just within the right half plane, and by simply forcing them to the imaginary axis, we can artificially construct a (marginally) stable controller without too much distortion of the frequency response. It is this transfer function that is shown in Figure 8.18. It is observed that the differences compared to the original, unstable version are very small except for a slightly "sharper" phase change near $\omega = 0.3$ rad / sec.

Apart from the possible numerical issues mentioned in Section 8.2.1.1 that may cause these problems, the emergence of a complex conjugated pair of poles strongly indicates that the overall closed loop system is unstable for a certain set of parameters. In fact, no proofs of boundedness for the closed loop system has been given. In Aamo (2013) proof of boundedness for the closed loop system with observer was given for the attenuation point $\bar{x} = 0$, but nothing was stated about the behaviour of the rest of the system. Theoretically, the system may lead to oscillations with increasing amplitudes in the rest of the system even when the controller objective (7.2) is satisfied

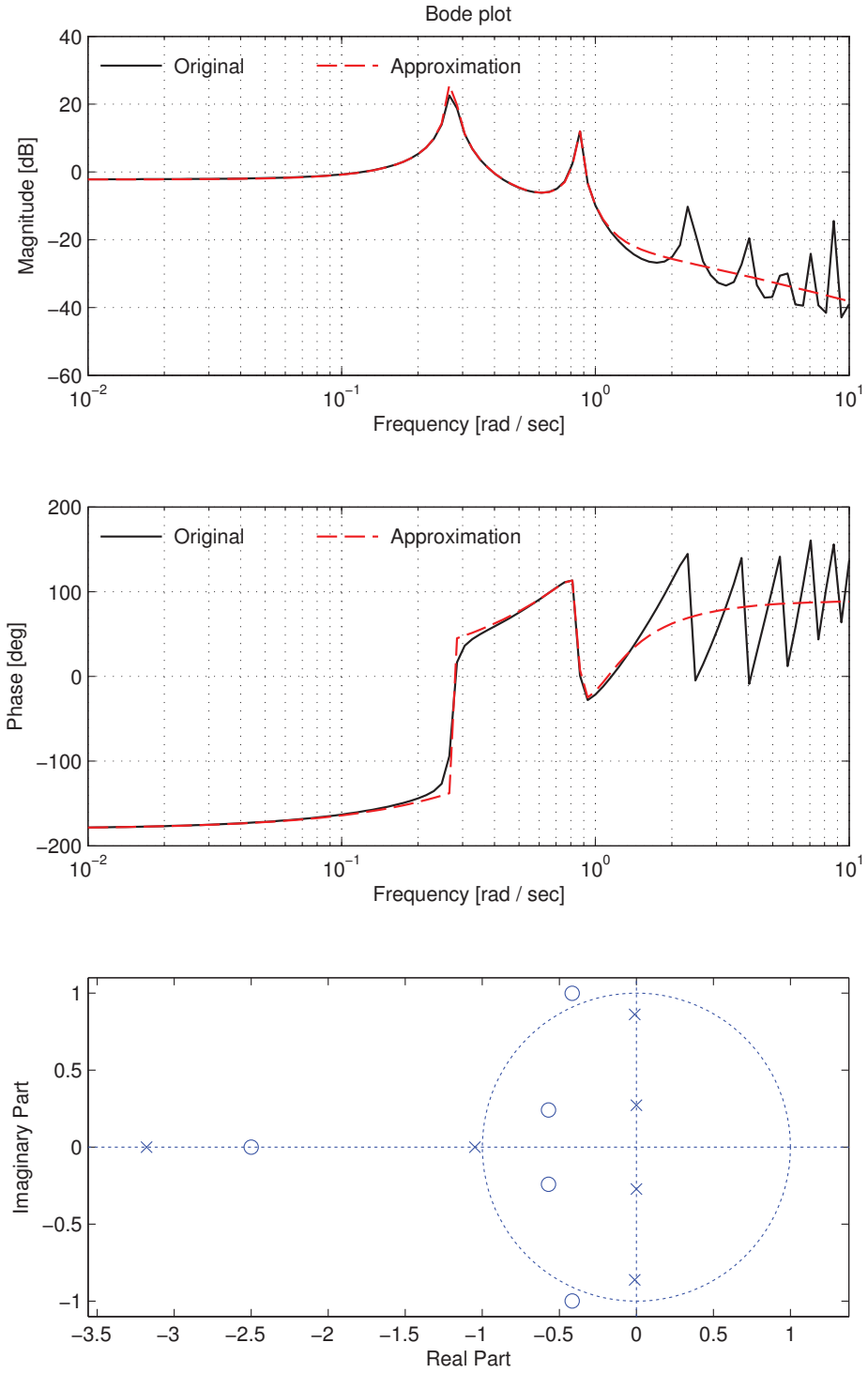

Figure 8.17: Transfer function approximation for Case 2: Pure state feedback controller.

at $\bar{x} = 0$.

8.3.1.2 Recursive controller

Figure 8.18 shows the sampled frequency response for transfer function of the recursive controller of Theorem 5.2 and the sixth order transfer function approximation achieved from using $\sigma = 0.025$. Once again the transfer functions of Theorems 5.1 and Theorem 5.2 are extremely similar, as can be easily observed from figures 8.18 and 8.17. Also this time, a complex conjugated pair of unstable poles emerged. They were forced to the imaginary axis, as in the previous section. This has been done in the approximation shown in Figure 8.18. The original transfer functions can be found in figures C.11–C.13. They closely resemble the approximations using the pure state feedback controller, found in Appendix C.2.1.

8.3.1.3 Simplified controller

Figure 8.19 shows the sampled frequency response for the transfer function in Theorem 5.3 along with the sixth order transfer function approximation achieved from using $\sigma = 0.000$. As observed from Figure 8.3, the approximation of the simplified controller matches the original transfer function extremely well for frequencies below a certain threshold; $\omega = 0.8$ rad / sec in this case. A tenth order approximation matches well up to 1 rad / sec, as can be seen from Figure C.14c in Appendix C.2.3, while the fourth order approximation match up to 0.4 rad / sec.

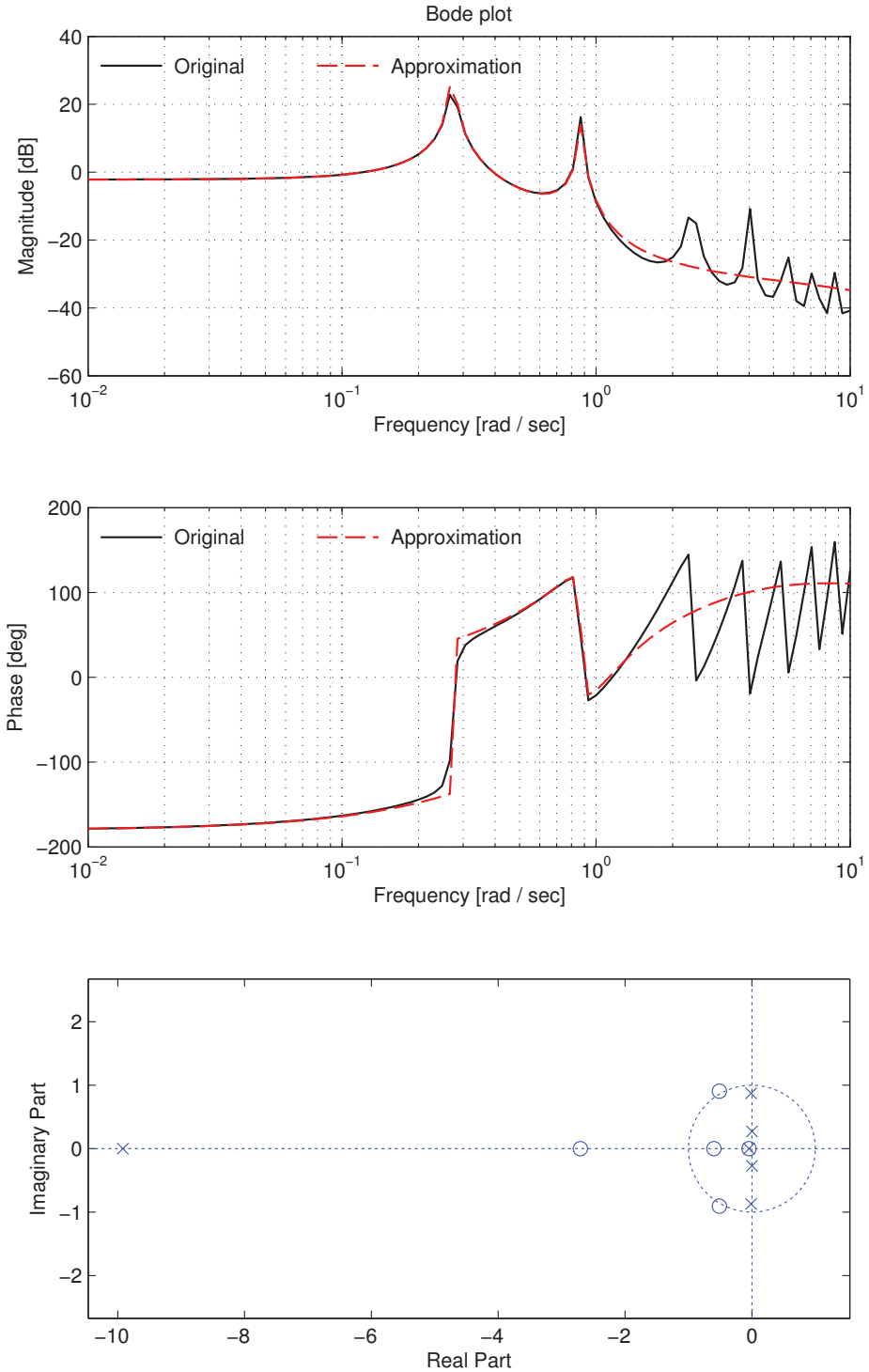

Figure 8.18: Transfer function approximation for Case 2: Recursive controller.

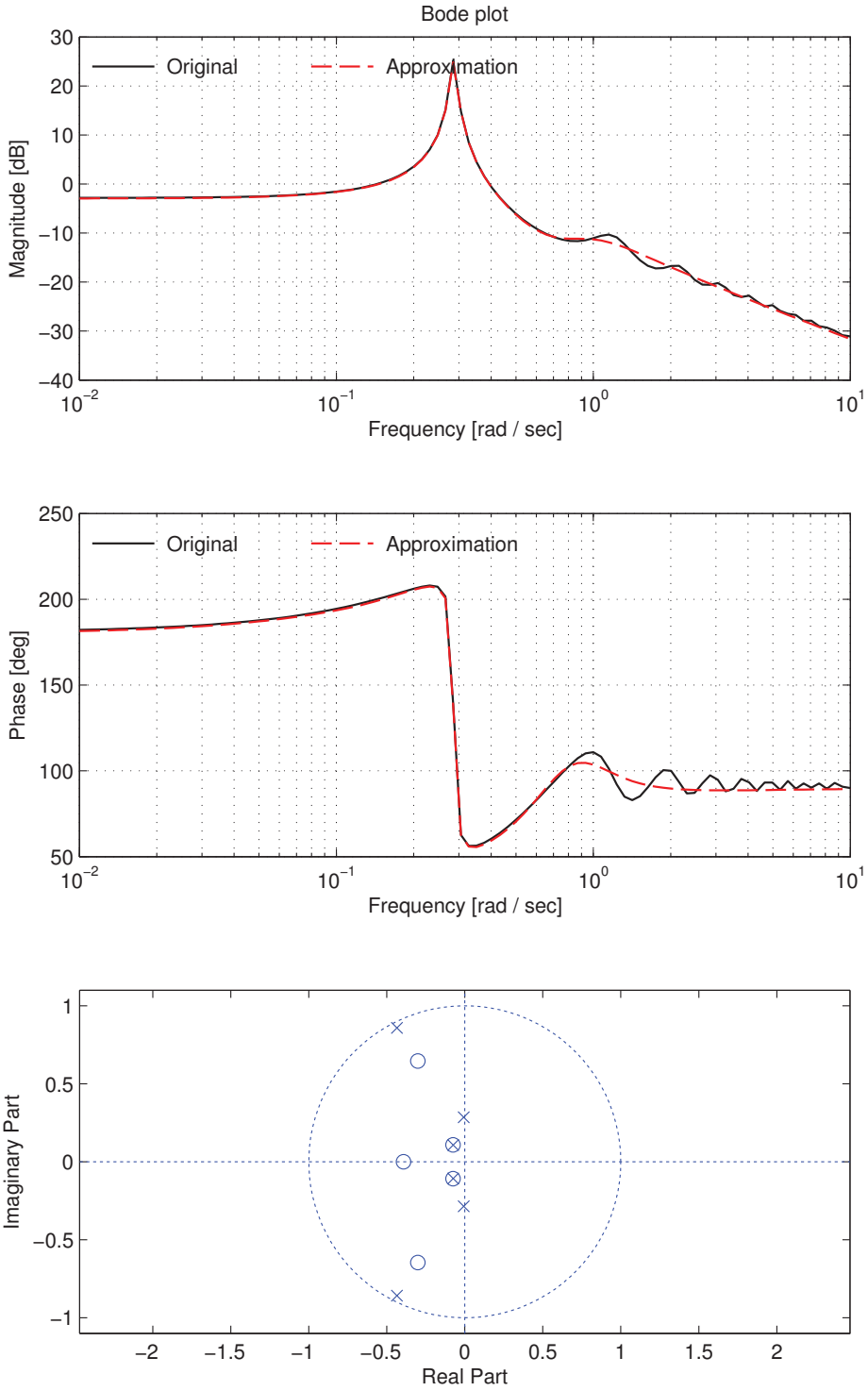

Figure 8.19: Transfer function approximation for Case 2: Simplified controller.

8.3.2 Simulations

8.3.2.1 Pure state feedback controller

The pure state feedback controller of Theorem 3.1 was once again implemented both when using the actual states and when using the observer generated states as input to the controller. Also implemented was the reduced order controller found in Section 8.3.1.1. Figures 8.20–8.24 on pages 121–125 display the simulation results. A clear attenuation of the pressure fluctuations for both the state feedback and the output feedback case is observed from Figure 8.20a, but the attenuation factor is not as good as for the previous case. The pressure at $z = \bar{z}$ now fluctuates with an amplitude of about 0.3 bar. This is still an considerable attenuation factor of about 250. Again, the set point is reached as soon as the first pressure gradient reaches the depth, as one can see from Figure 8.23b. The time needed is shorter (around 1.31 seconds according to (7.30)) as the distance from the actuation point to the depth of attenuation is shorter.

An interesting observation is made from Figure 8.22a, in that the fluctuations in BHP are drastically increased when the controller is turned on. This can also be observed from the 3D visualization in Figure 8.24a. However, the amplitude of fluctuations are decaying. Also in this case, the observer estimates converge to their correct values, as easily observed from Figure 8.24. The pressure at depth 1000 also has an exponential convergence rate to the set point when using full output feedback, as observed from figures 8.20a and 8.22b. Also new to this simulation is that the applied controller signals $U(t)$ in Figure 8.21a and 8.21b seem to fluctuate around a slowly moving bias that gradually converges towards zero.

The reduced order controller manages to keep the pressure at 1000 metres within the standard limits of ± 2.5 bar. This may be somewhat surprising, as the original, best fit transfer function was manually modified to force it stable, resulting in a slightly distorted frequency response. The control signal produced is considerably smoother, however, as seen when comparing Figure 8.21c with figures 8.21a and 8.21b, and so is the general response in the well, observed from Figure 8.23a.

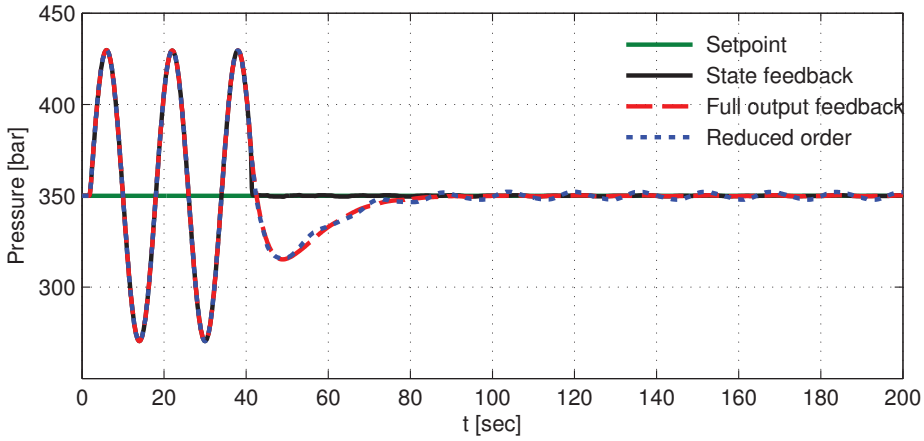

(a) Overview.

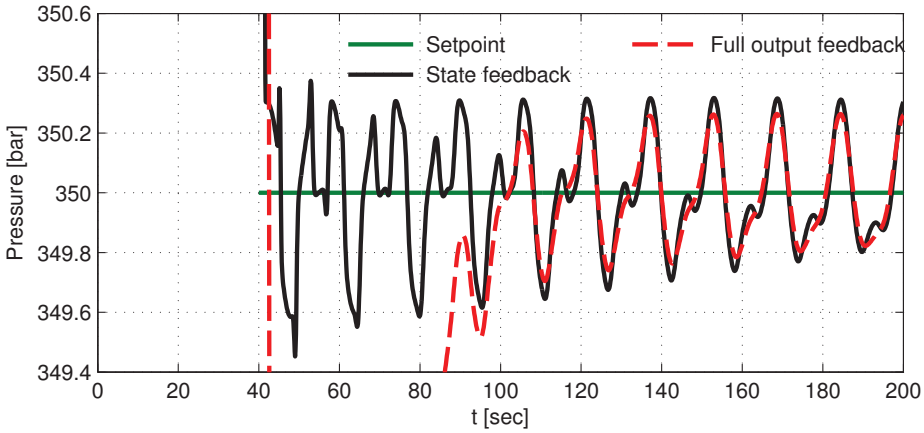

(b) State feedback vs full output feedback.

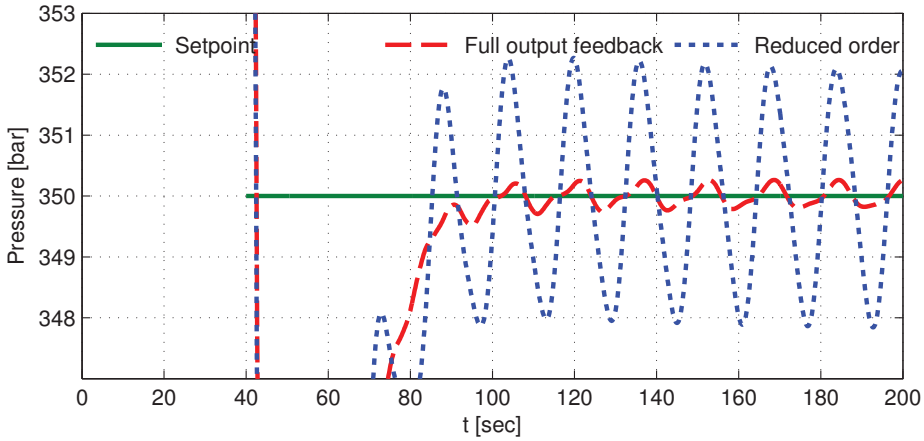

(c) Full vs reduced order output feedback.

Figure 8.20: Case 2: P.s.f. controller: Pressure at depth 1000 metres.

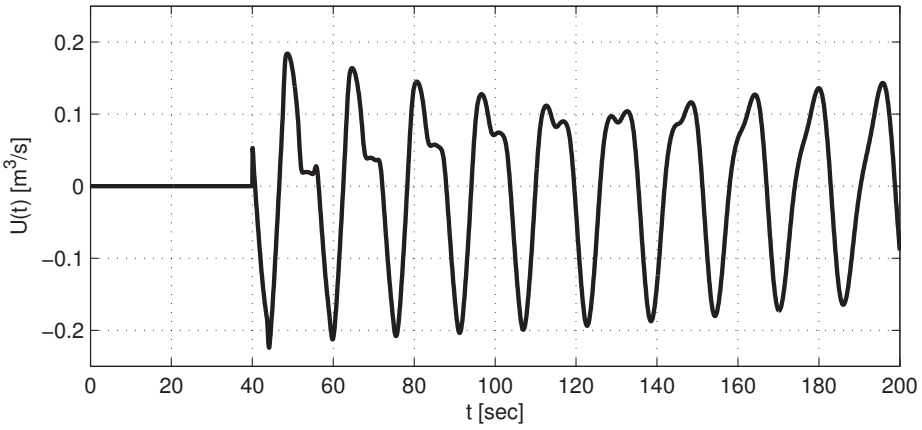

(a) State feedback.

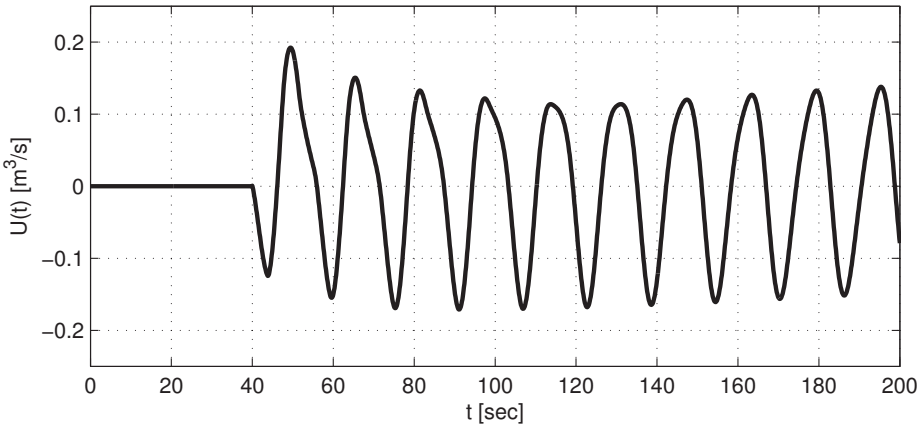

(b) Full order output feedback.

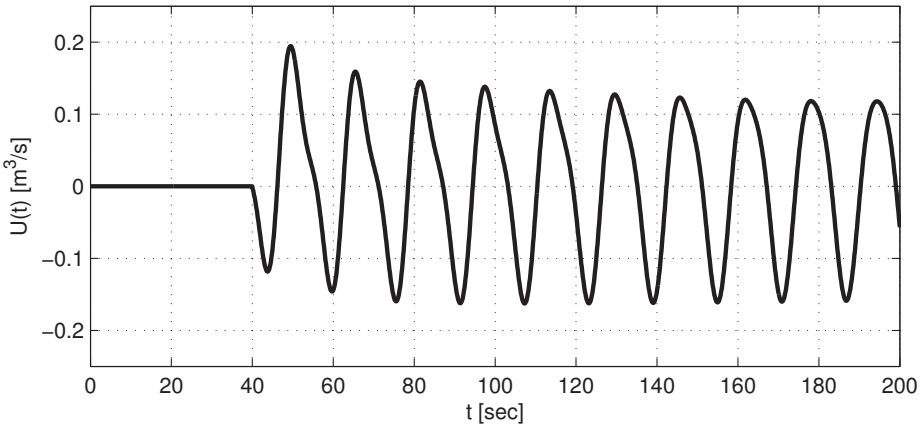

(c) Reduced order output feedback.

Figure 8.21: Case 2: P.s.f. controller: Applied controller signals.

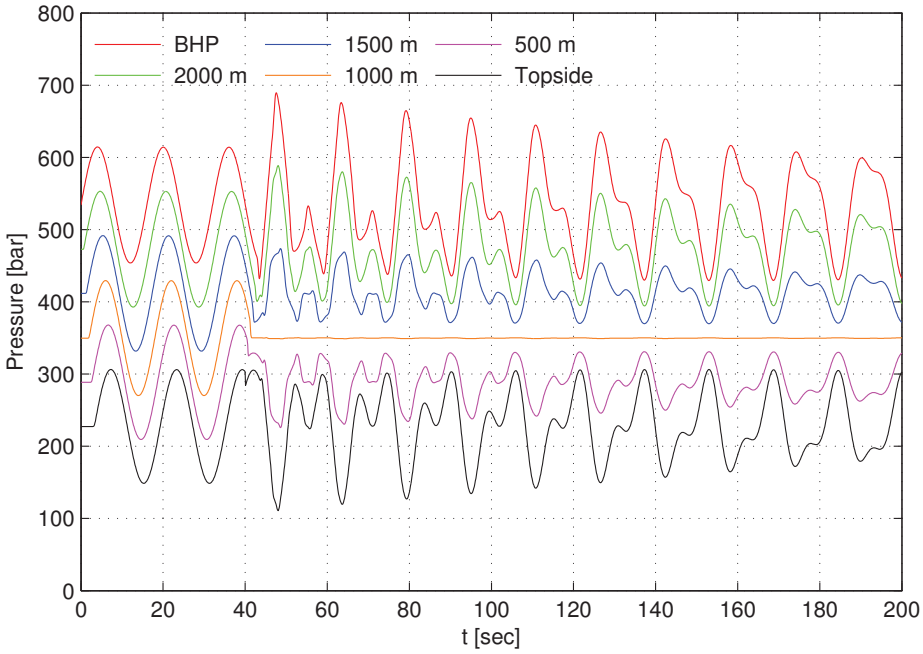

(a) State feedback.

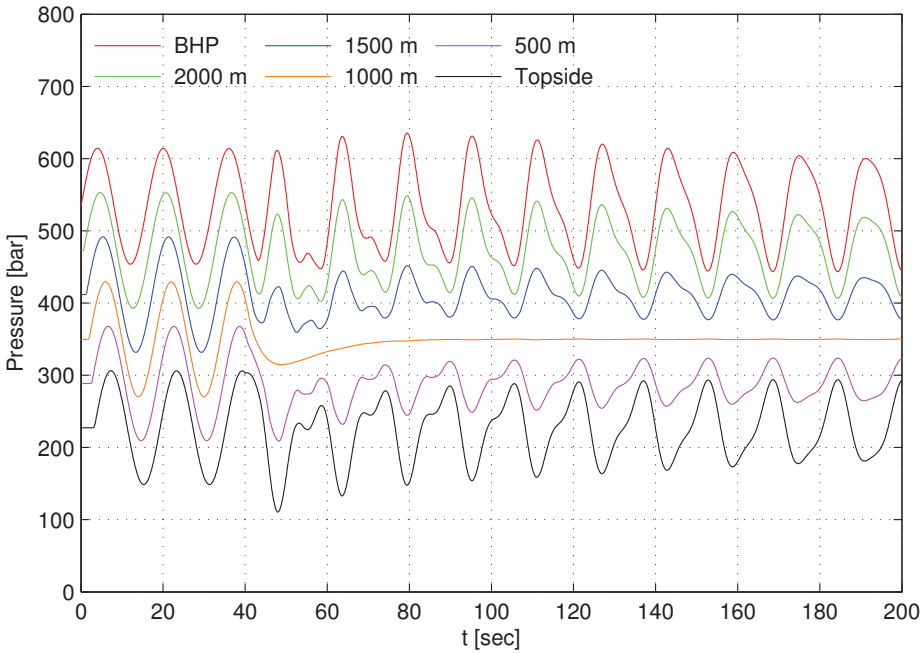

(b) Full order output feedback.

Figure 8.22: Case 2: P.s.f. controller: Pressure at selected depths.

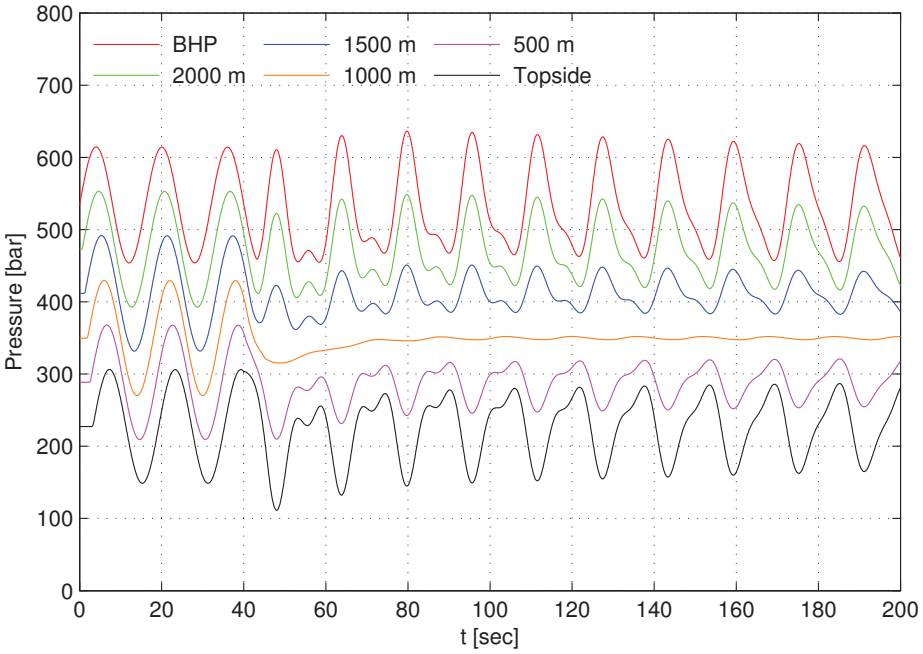

(a) Pressure at selected depths for reduced order controller.

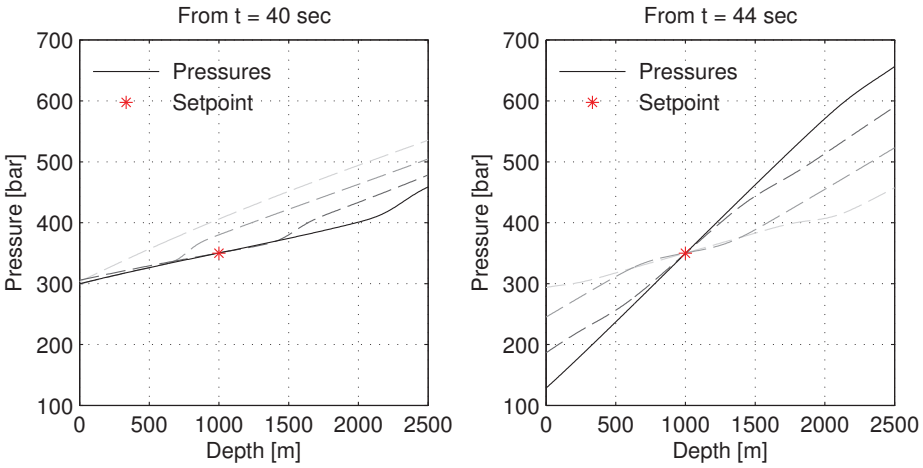

(b) Selected pressure profiles in the well, state feedback.

Figure 8.23: Case 2: P.s.f. controller: Pressure distribution in well.

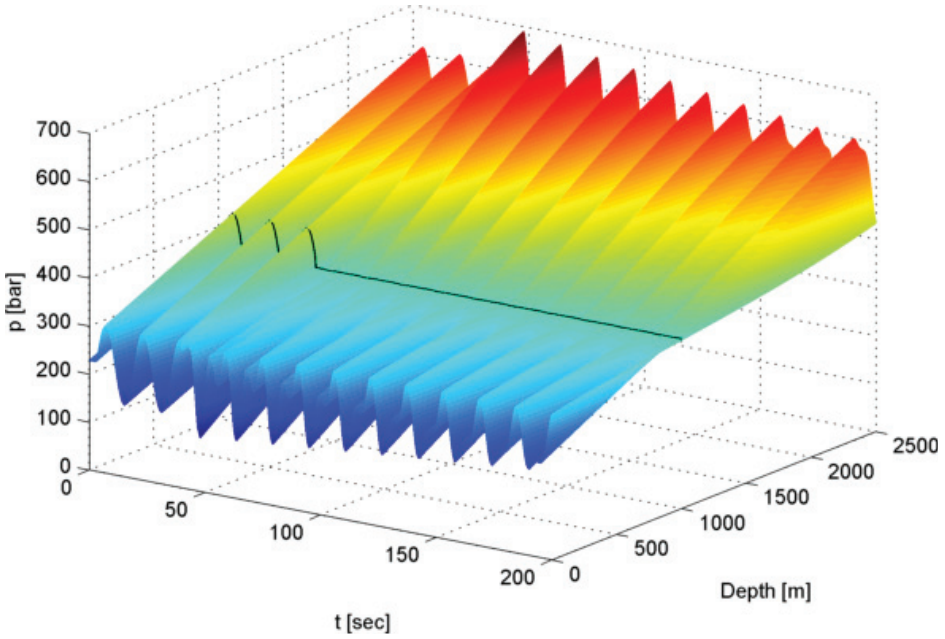

(a) Pressure distribution when using state feedback.

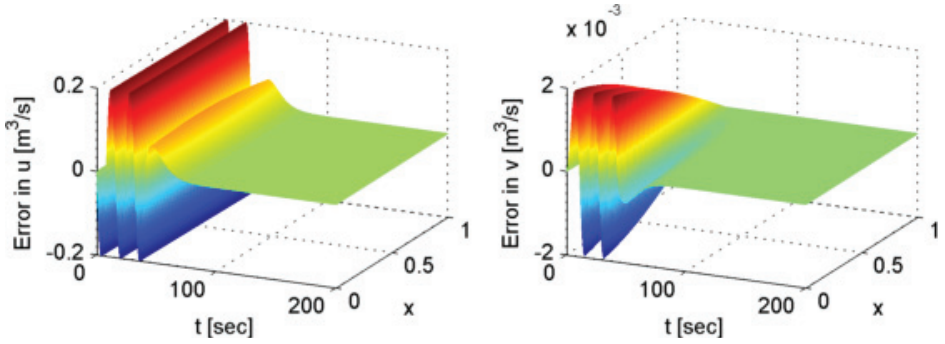

(b) System state estimation error.

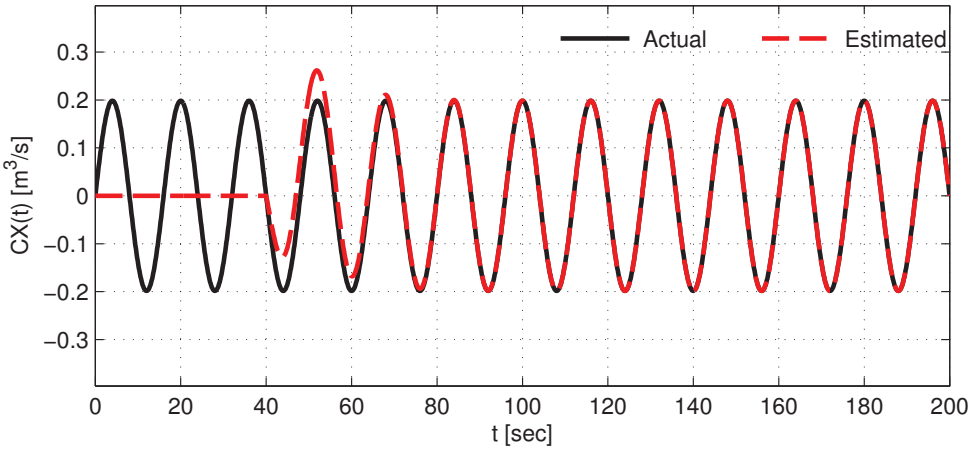

(c) Disturbance with estimated disturbance.

Figure 8.24: Case 2: P.s.f. controller: Disturbance and observer states.

8.3.2.2 Recursive controller

The recursive controller of Theorem 3.2 was implemented, as well as the rational approximation found in Section 8.3.1.2. The simulation results can be found in figures 8.25–8.28 on pages 127-130. The controller of Theorem 3.2 was fed with both the observer generated states and the actual states.

This controller suffers very much from transients and initial conditions present in the system when the controller is turned on. This is clearly observed from figures 8.25a and 8.25b. However, the amplitude of pressure fluctuations is reduced to only 0.2, slightly better than the pure state feedback controller, and additionally, is seems to still be improving when the simulation ends. The pressure distribution in the well is also suffering from the initial conditions, with the BHP exceeding 750 bar when the first applied pressure gradient reaches the bottom of the well. This is 150 bar more than the maximum pressure during open loop, as seen from Figure 8.27a. The output feedback implementation is slightly damped, however, as seen from Figure 8.27b. Additionally, the pressure at $z = \bar{z}$ does not meet its set point p_{sp} before the pressure gradient has reached the point on its way back up again, as observed from Figure 8.28b; a propagation time of 5.23 seconds according to (7.31). The control signals in figures 8.26a and 8.26b are more varying than for the pure state feedback case, but exhibit the same slowly varying bias as was observed from figures 8.21a and 8.21b.

This time, the pressure at the attenuation point exceeds the ± 2.5 bar limits, when using the reduced order controller, seen in Figure 8.25c. The amplitude of oscillations is about 3 bar. The manual modification of the poles had a larger impact on the frequency response than for the pure state feedback controller shown in the previous section. Also this time, however, the control signal is considerably smoother, as seen when comparing Figure 8.26c with figures 8.26a and 8.26b.

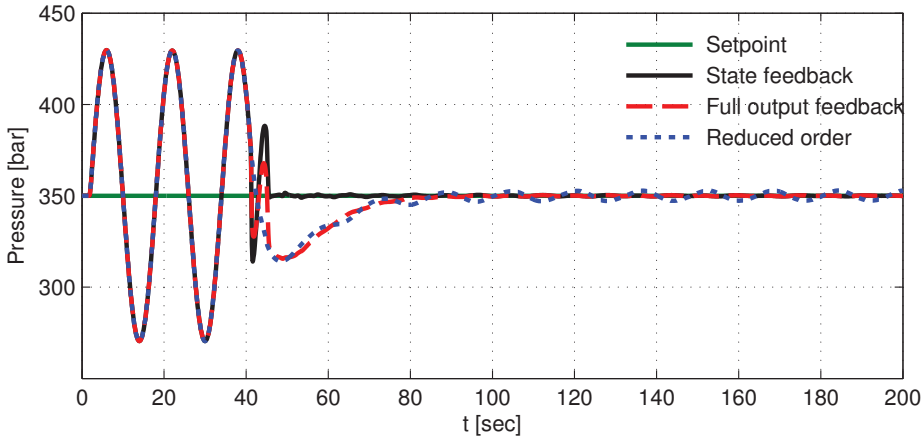

(a) Overview.

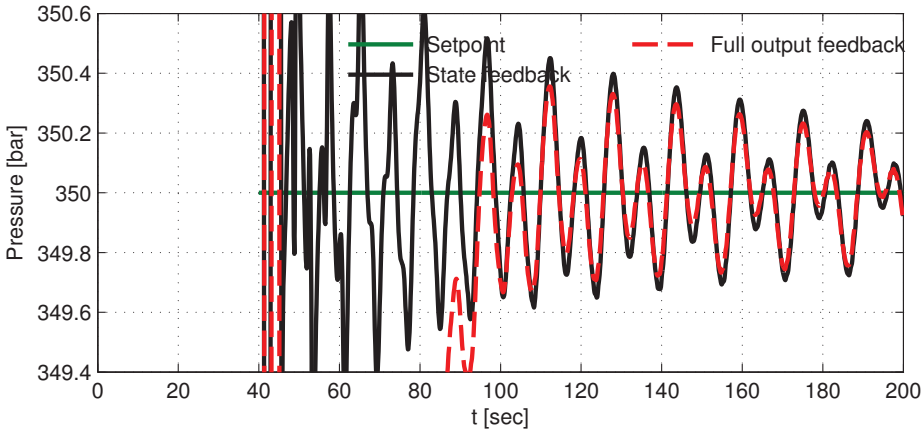

(b) State feedback vs full output feedback.

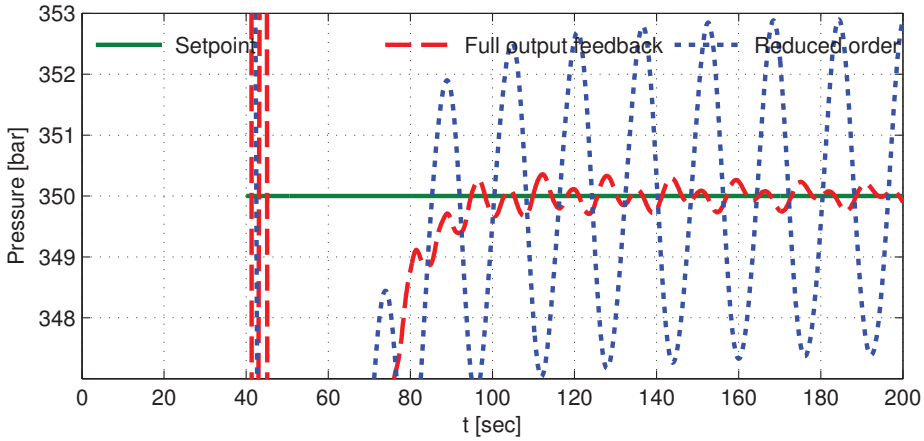

(c) Full vs reduced order output feedback.

Figure 8.25: Case 2: Recursive controller: Pressure at depth 1000 metres.

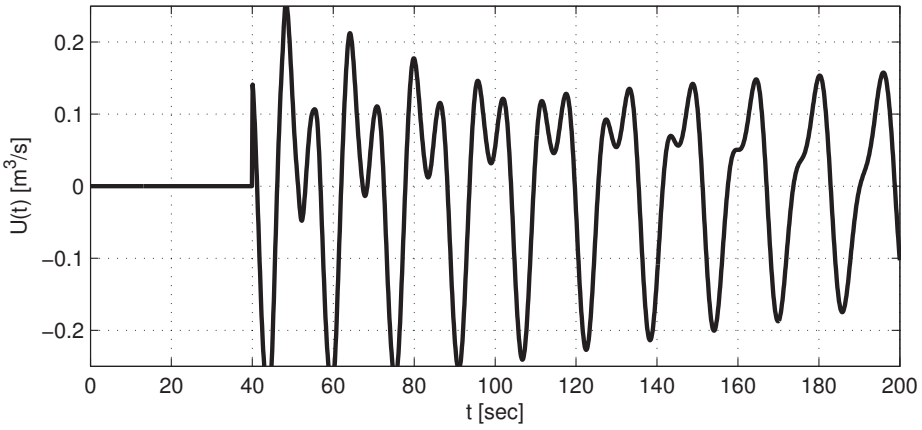

(a) State feedback.

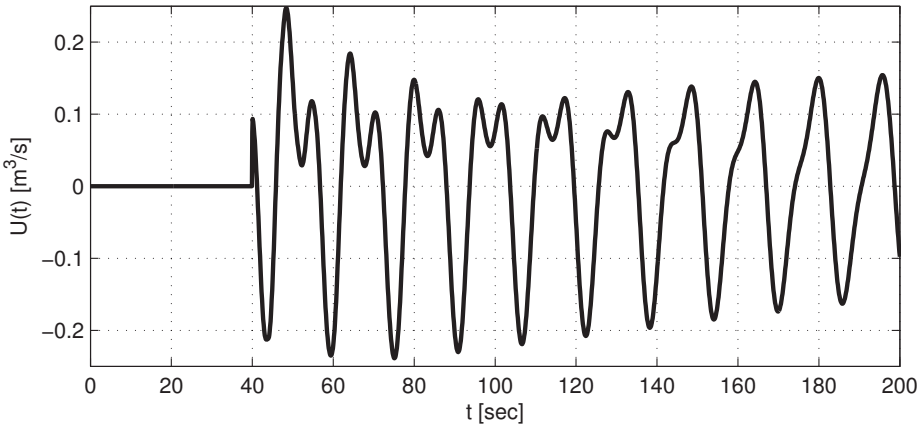

(b) Full order output feedback.

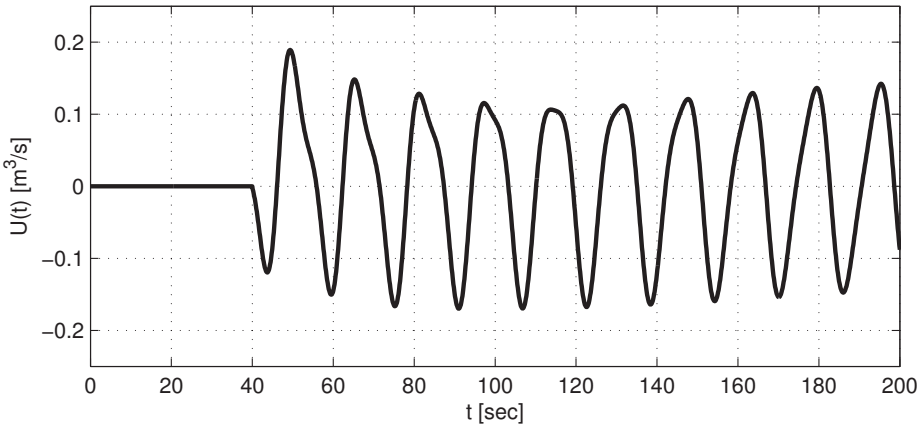

(c) Reduced order output feedback.

Figure 8.26: Case 2: Recursive controller: Applied controller signals.

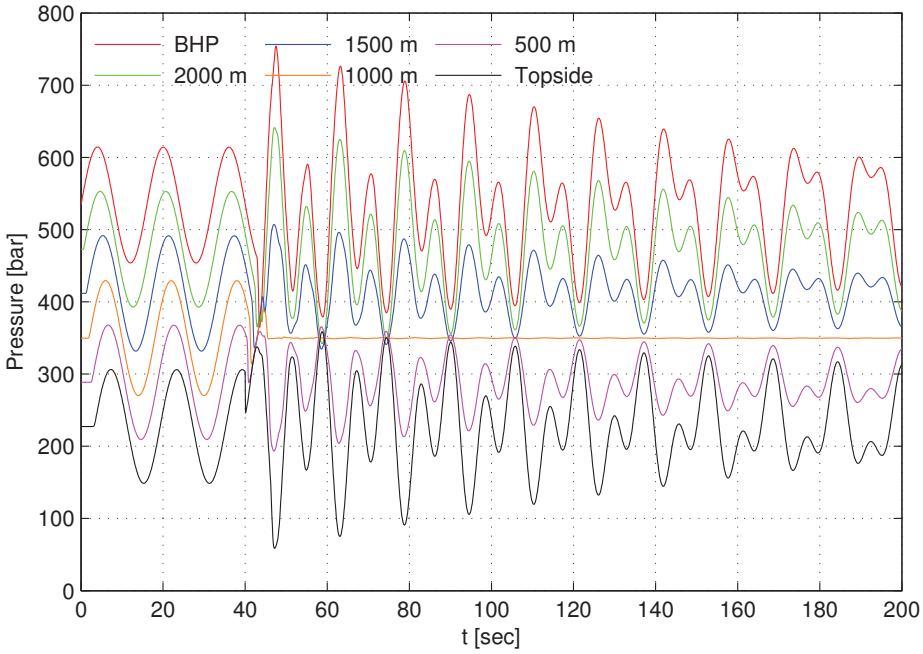

(a) State feedback.

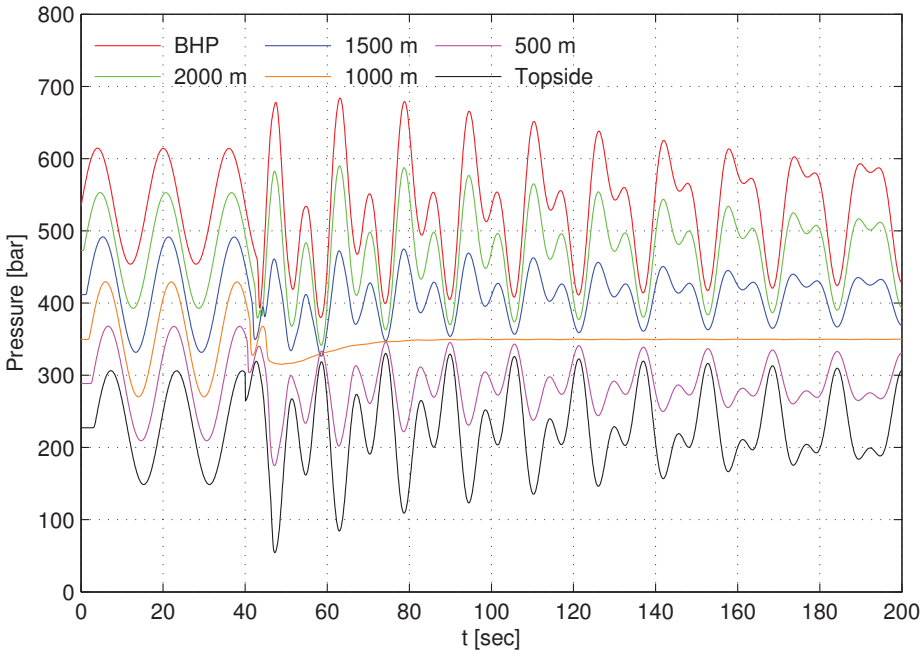

(b) Full order output feedback.

Figure 8.27: Case 2: Recursive controller: Pressure at selected depths.

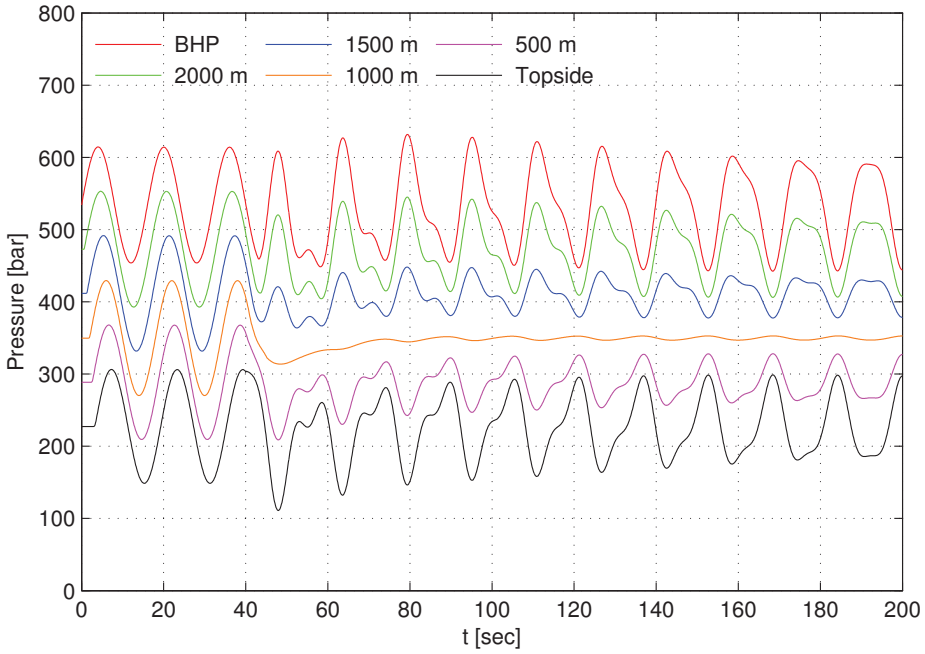

(a) Pressure at selected depths for reduced order controller.

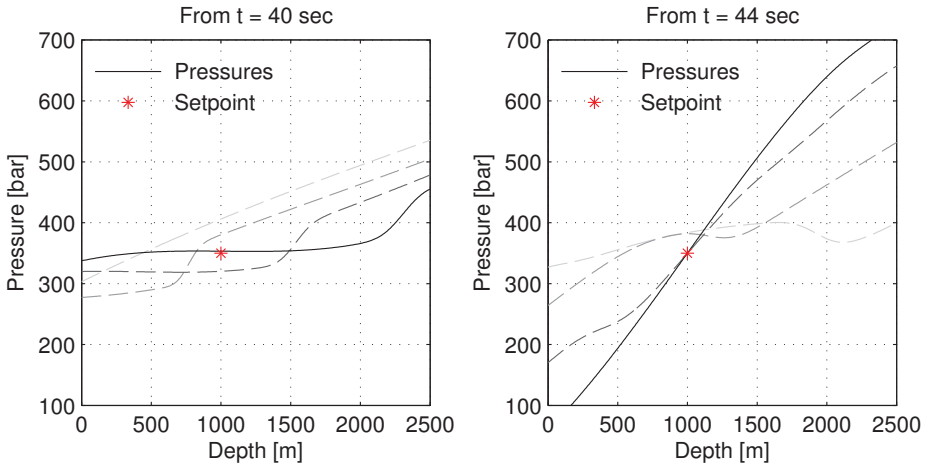

(b) Selected pressure profiles in the well, state feedback.

Figure 8.28: Case 2: Recursive controller: Pressure distribution in well.

8.3.2.3 Simplified controller

The simplified controller of Theorem 3.3 was implemented. Both the observer generated states and the actual states were fed to the controller. The rational approximation found in Section 8.3.1.2 was also implemented. The simulation results can be found in figures 8.29–8.32 on pages 132-135.

Clearly seen from the pressure fluctuation of only ± 0.12 bar observed from Figure 8.29b for both the state feedback and the output feedback case, the simplified controller actually performs better than the pure state feedback and recursive controllers in this simulation case. The pure state feedback and recursive controllers in the previous sections probably suffers more from the discretization method used. The pure state feedback controller suffers from discretization of the system states $u(x,t)$ and $v(x,t)$, while the recursive version additionally suffers from the discretization of the transmission line. A deterioration in the simplified controller's performance could certainly be expected if the magnitude of the kernels used in the integral terms (3.74) had been considerably larger. (Again; this is demonstrated in an additional simulation in appendix D.1.) From Figure 8.32b, it is once again observed that the applied pressure gradient needs to be propagated to $z = \bar{z}$ via $z = 0$ before the desired effect is achieved; a propagation time of more than 5 seconds.

The overall pressure distribution in the well and the applied control signals, are much more smooth and predictive, easily observed from figures 8.31, 8.30a and 8.30b, and particularly when comparing Figure 8.29b with Figure 8.20b and 8.25b. The reduced order controller achieved from sampling the simplified controller of Theorem 3.3 is once again superior to the other reduced order controllers, as observed when comparing Figure 8.29c with figures 8.20c and 8.25c. The amplitude of pressure fluctuations is only ± 0.4 when using this one.

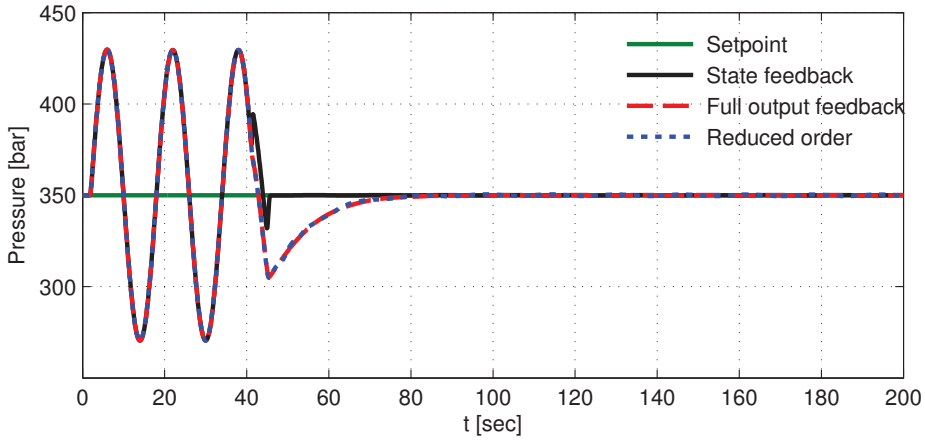

(a) Overview.

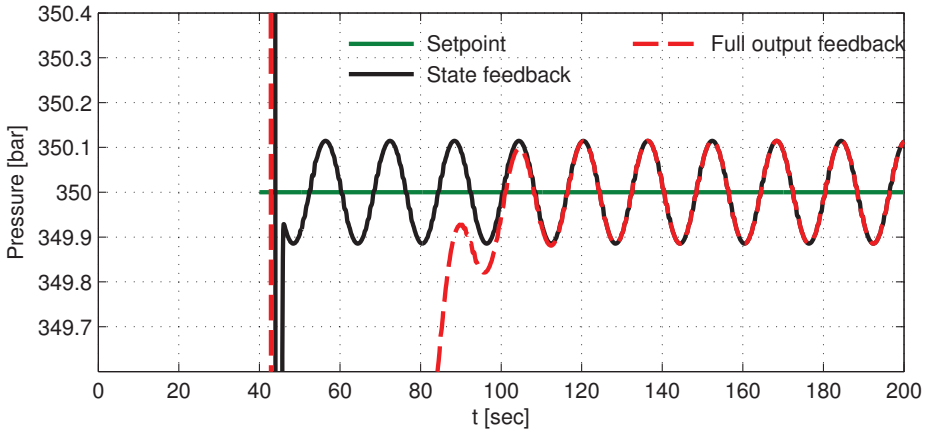

(b) State feedback vs full output feedback.

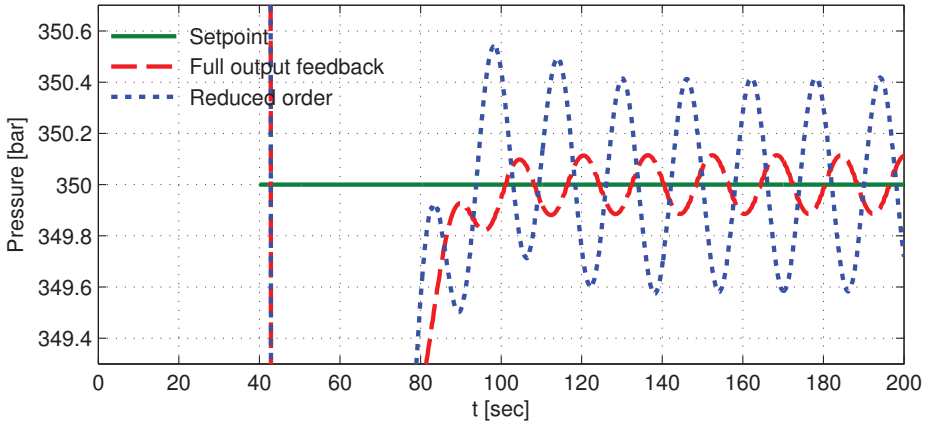

(c) Full vs reduced order output feedback.

Figure 8.29: Case 2: Simplified controller: Pressure at depth 2000 metres.

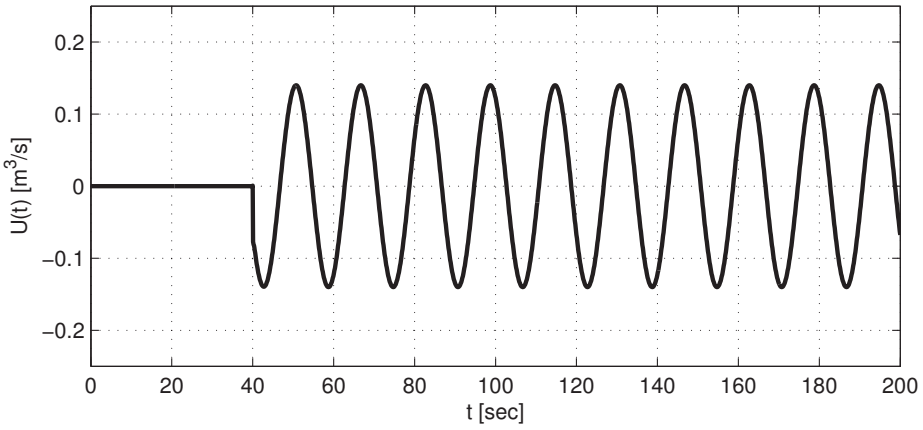

(a) State feedback.

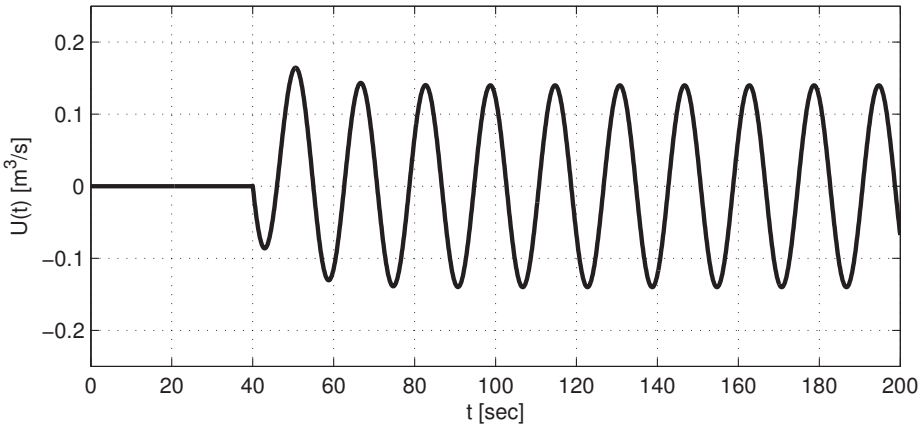

(b) Full order output feedback.

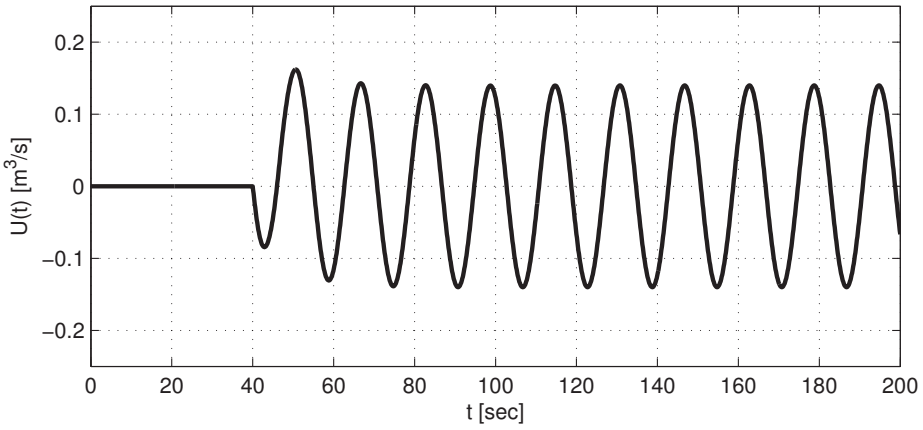

(c) Reduced order output feedback.

Figure 8.30: Case 2: Simplified controller: Applied controller signals.

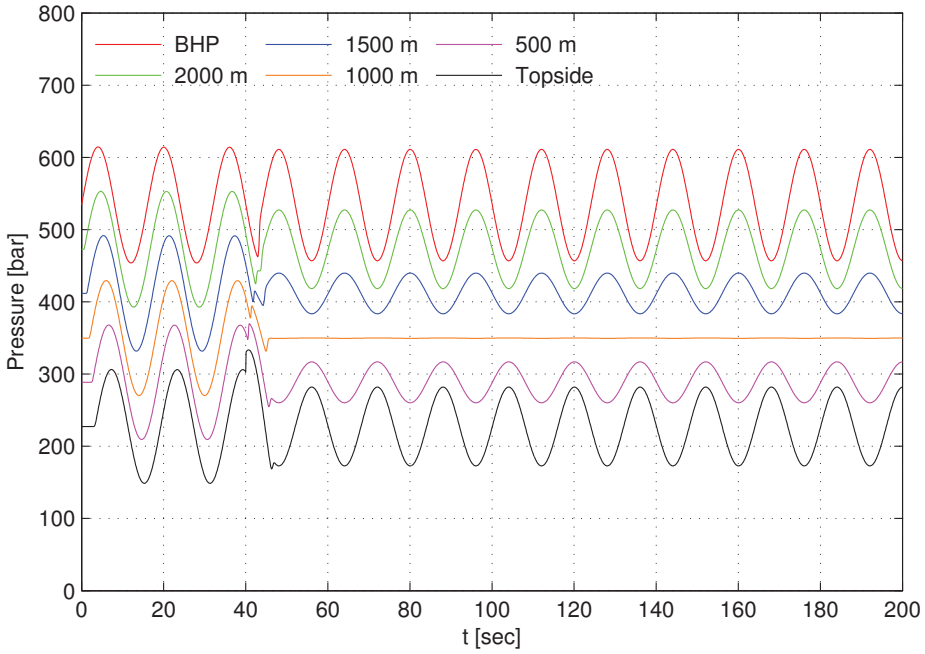

(a) State feedback.

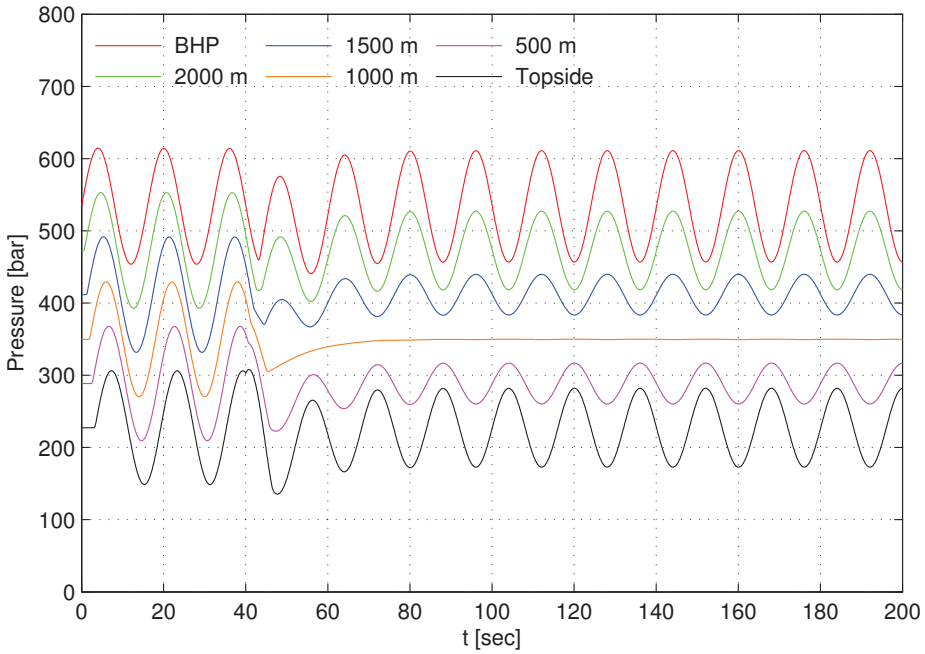

(b) Full order output feedback.

Figure 8.31: Case 2: Simplified controller: Pressure at selected depths.

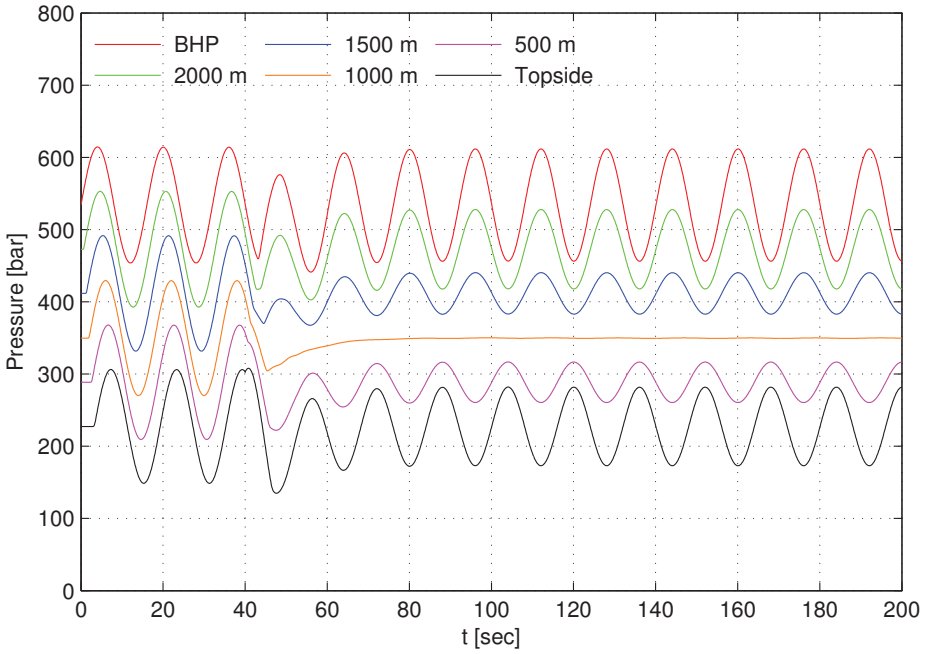

(a) Pressure at selected depths for reduced order controller.

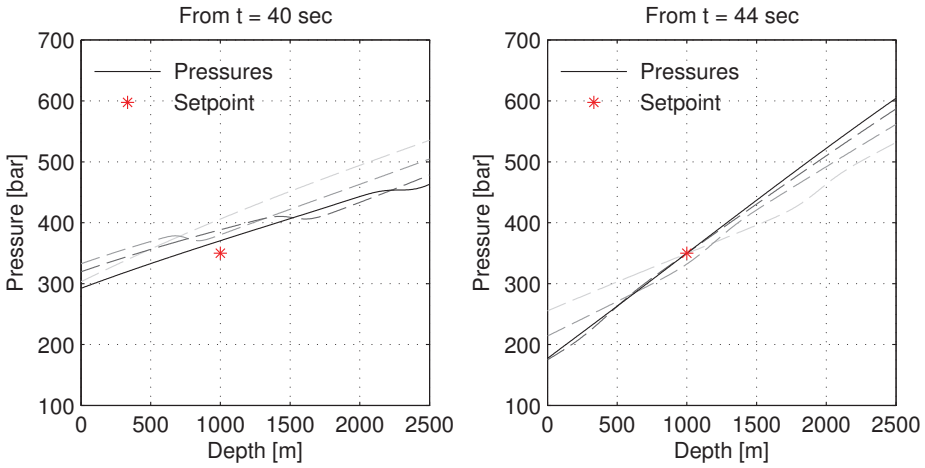

(b) Selected pressure profiles in the well, state feedback.

Figure 8.32: Case 2: Simplified controller: Pressure distribution in well.

Part IV

Conclusions

Chapter 9

Conclusions and further work

In this thesis, the results from Aamo (2013) have been generalized to achieve disturbance attenuation at an arbitrary point in the domain for a class of systems described by linear 2×2 partial differential equations of the hyperbolic type. The disturbance is modelled as an autonomous, finite dimensional linear system affecting the PDEs left boundary, and actuation is limited to the right boundary. Two controllers were derived; one is a function purely in the system states at the current time, while the other one is recursive and requires the controller to store the applied controller signal a finite length backwards in time. The latter controller is simpler and easier to derive, but the stored time-series of controller signals constitutes to an infinite amount of data on a continuous system. Additionally, the recursive controller relies on stored system states rather than the actual states, which is a potential robustness issue. However, its simplified structure facilitated for the derivation of a third controller, which was derived by neglecting some terms assumed to be small in magnitude. This controller had a significantly simpler structure than the other two, but its performance depends on the validity of the assumptions made. All the derived controllers can be combined with an observer generating full state and disturbance estimates from sensing co-located with the actuation.

Furthermore, the transfer functions of the observer combined with the controllers were derived. The resulting transfer functions were irrational, but a Laguerre-Gram based model order reduction technique was also presented for creating rational approximations from the irrational ones.

The derived theory was applied and tested through simulations on the heave problem from Managed Pressure Drilling. The full state controllers performed extremely well, both when using the system states directly and when using the observer generated states. An exponential convergence rate is observed in the latter case. As the terms neglected when deriving the

simplified controller were very small, the simplified controller performed surprisingly good as well and sometimes even better than the full controllers.

The attenuation properties of the reduced order transfer function approximations were also satisfactory in most cases. However, achieving a good transfer function match for the pure state feedback and recursive controllers deemed challenging, probably due to some resonance terms emerging for high frequencies. A good transfer function match was only achieved after some tuning, and often the resulting rational transfer function found by the Laguerre Gram based model order reduction algorithm contained at least one pair of unstable poles. This strongly indicates that overall system consisting of a the hyperbolic system, the recursive controller and an observer is, in fact, unstable for a certain set of system parameters. This is an open question, as no proofs of boundedness for the system states are given when using the observer generated states as input to the controllers. However, finding a good transfer function match when using the simplified controller was generally a lot easier, and a good match was quickly found without much tuning for both the test cases.

Suggested areas for further work are:

1. Further analyse the cause of the resonance terms in the derived transfer functions.
2. Consider weighting the frequencies of interest prior to performing the model reduction algorithm to the controller transfer functions, so that only the well-behaving frequency domain is approximated.
3. Extend the algorithm for determining the optimum set of parameters to optimize both of the free parameters used in the Laguerre Gram based model order reduction algorithm.
4. Prove boundedness of the system states when using the controller in conjunction with the observer, alternatively derive under which conditions the system states are bounded.
5. Analyse the robustness properties of the derived controllers. The controllers are heavily relying on having an exact mathematical model, and adaptations on some of the parameters may be necessary when the exact parameters are not known.
6. Test the controllers through lab experiments.

References

Ole Morten Aamo. Disturbance rejection in 2 x 2 linear hyperbolic systems. *IEEE Transactions on Automatic Control*, 58(5):1095–1106, 2013. xi, 4, 6, 21, 22, 24, 39, 40, 41, 67, 68, 89, 91, 98, 115, 139, 149

Ole Morten Aamo, Andrey Smyshlyaev, Miroslav Krstić, and Bjarne Anton Foss. Stabilization of a Ginzburg-Landau model of vortex shedding by output feedback boundary control. In *CDC. 43rd IEEE Conference on Decision and Control*, volume 3, pages 2409–2416, 2004. 6

Joseph Abate, Gagan L. Choudhury, and Ward Whitt. On the Laguerre method for numerically inverting Laplace transforms. *INFORMS Journal on Computing*, 8:413–427, 1996. 57, 60

Mark J. Ablowitz, Martin David Kruskal, and J. F. Ladik. Solitary wave collisions. *SIAM J. Applicat. Math.*, 36:428–437, 1979. 75

Milton Abramowitz and Irene Anne Stegun, editors. *Handbook of Mathematical Functions with Formulas, Graphs, and Mathematical Tables*. Dover Publications Inc., 1975. 55

Ahmed Amghayrir, Noël Tanguy, Pascal Bréhonnet, Pierre Vilbé, and Léon-Claude Calvez. Laguerre-Gram reduced-order modeling. *IEEE Transactions on Automatic Control*, 50(9):1432–1435, September 2005. 55, 56, 57, 58, 59, 60, 62

Karl Johan Åström. Adaptive control around 1960. *IEEE Control Systems*, 16(3):44–49, 1996. 39

Sheldon Axler. *Linear Algebra Done Right (2nd ed)*. Springer, 1997. 56, 58

Esmail Babolian, Zahra Masouri, and Saeed Hatamzadeh-Varmazyar. A direct method for numerically solving integral equations system using orthogonal triangular functions. *International Journal of Industrial Mathematics*, 1(2):135–145, 2009. 15

Ivo Babuška, Uday Banerjee, and John E. Osborn. Generalized finite element methods: Main ideas, results, and perspective. *International Journal of Computational Methods*, 1(1):67–103, June 2004. 16

Andras Balogh and Miroslav Krstić. Infinite-dimensional backstepping-style feedback transformations for a heat equation with an arbitrary level of instability. *European Journal of Control*, 8:165–177, 2002. 5, 75

Stefan Banach. Sur les opérations dans les ensembles abstraits et leur application aux équations intégrales. *Fundamenta Mathematicae*, 3:133–181, 1922. 15

Dario Bini. Toeplitz matrices, algorithms and applications. ECRIM News Online Edition, No. 22, 1995. URL `http://www.ercim.org/publication/Ercim_News/enw22/toeplitz.html`. 88

Dejan M. Bosković, Miroslav Krstić, and Weijiu Liu. Boundary control of an unstable heat equation via measurement of domain-averaged temperature. *IEEE Transactions on Automatic Control*, 46(12):2022 –2028, dec 2001. ISSN 0018-9286. 5

Helen Byrne. Applied partial differential equations. Lecture notes in course *B5b: Applied Partial Differential Equations*, Mathematical Institute, University of Oxford, 2012. URL `http://www.maths.ox.ac.uk/courses/course/19560/material`. 13

Chi-Tsong Chen. *Linear System Theory and Design*. Oxford University Press, international third edition, 2009. 153

Krzysztof Ciesielski. On Stefan Banach and some of his results. *Banach Journal of Mathematical Analysis*, 1(1):1–10, 2007. 15

Jean-Michel Coron, Brigitte d'Andrea Novel, and Georges Bastin. A strict lyapunov function for boundary control of hyperbolic systems of conservation laws. *IEEE Transactions on Automatic Control*, 52(1):2–11, 2007. 5

Cristina Cunha and Fermin Viloche. The Laguerre functions in the inversion of the Laplace transform. *Inverse Problems*, 9(1):57–68, 1992. 55

C. Curró, D. Fusco, and N. Manganaro. A reduction procedure for generalized Riemann problems with application to nonlinear transmission lines. *Journal of Physics A: Mathematical and Theoretical*, 44(33):335205, 2011. 3

Jonathan de Halleux, Christophe Prieur, Jean-Michel Coron, Brigitte d'Andrea Novel, and Georges Bastin. Boundary feedback control in networks of open channels. *Automatica*, 39(8):1365–1376, 2003. 3

Lokenath Debnath and Piotr Mikusinski. *Introduction to Hilbert Spaces with Applications*. Boston: Academic Press, 1990. 58

Thor Inge Fossen. *Handbook of Marine Craft Hydrodynamics and Motion Control*. John Wiley & Sons, 2011. 89

B. S. Garbow, G. Giunta, and J. N. Lynessand A. Murli. Software for an implementation of Weeks' method for the inverse of the Laplace transform. *ACM Transactions on Mathematical Software (TOMS)*, 14:163–170, 1988. 60

Majed Ghasemi, Majid Tavassoli Kajani, and Esmail Babolian. Numerical solution of the nonlinear Volterra-Fredholm integral equations by using homotopy perturbation method. *Applied Mathematics and Computation*, 188:446–449, 2007. 15

Paula Goatin. The aw-rascle vehicular traffic flow model with phase transitions. *Mathematical and Computer Modelling*, 44:287–303, 2006. 3

John Morten Godhavn. Control requirements for automatic managed pressure drilling system. In *SPE Drilling Completion*, pages 336–345, September 2010. 4

J. M. Greenberg and Li Ta Tsien. The effect of boundary damping for the quasilinear wave equation. *Journal of Differential Equations*, 52(1):66–75, 1984. 5

Martin Gugat and Markus Dick. Time-delayed boundary feedback stabilization of the isothermal Euler equations with friction. *Mathematical Control and Related Fields*, 1(4):469–491, 2011. 3

Martin Gugat and G. Leugering. Global boundary controllability of the de St. Venant equations between steady states. *Annales de l'Institut Henri Poincare*, 20(1):1–11, 2003. 3

Samir Hamdi, William E. Schiesser, and Graham W. Griffiths. Method of lines. *Scholarpedia*, 2:2859, 2007. 17

Don Hannegan. Case studies-offshore managed pressure drilling. In *SPE Annual Technical Conference and Exhibition, 24-27 September 2006, San Antonio, Texas, USA*, 2006. 3

Urs W. Hochstrasser. Orthogonal polynomials. In Milton Abramowitz and Irene Anne Stegun, editors, *Handbook of Mathematical Functions with Formulas, Graphs, and Mathematical Tables*, chapter 22, pages 771–792. Dover Publications Inc., 1975. 57

Zhihua Jiang and Walter Schaufelberger. *Block Pulse Functions and Their Applications in Control Systems*. Springer, 1992. 15

Patrick Kano, Moysey Brio, and Jerome V. Moloney. Application of Weeks method for the numerical inversion of the Laplace transform to the matrix exponential. *Communications in Mathematical Sciences*, 3:335–372, September 2005. 57, 60

Hassan K. Khalil. *Nonlinear Systems*. Prentice Hall, Inc, 2002. 5

Donald Knuth. Big Omicron and big Omega and big Theta. *ACM SIGACT News*, 8(2):18–24, 1976. 87

Petar V. Kokotović. The joy of feedback: nonlinear and adaptive. *Control Systems, IEEE*, 12(3):7–17, June 1992. 5

Erwin Kreyszig. *Advanced Engineering Mathematics*. John Wiley & Sons, 2010. 9, 10, 12, 13, 15, 56, 60, 62, 151, 155, 156

Miroslav Krstić and Andrey Smyshlyaev. Backstepping boundary control for first-order hyperbolic PDEs and application to systems with actuator and sensor delays. *Systems & Control Letters*, 57(9):750–758, 2008. 5, 6, 90

Ingar Skyberg Landet, Alexey Pavlov, and Ole Morten Aamo. Modeling and control of heave-induced pressure fluctuations in managed pressure drilling. *IEEE Transactions on Control Systems and Technoloy*, Preprint: Accepted for inclusion in a future issue, 2013. 6, 68

Xavier Litrico and Vincent Fromion. Boundary control of hyperbolic conservation laws with a frequency domain approach. In *Proceedings of the 45th IEEE Conference on Decision & Control, Manchester Grand Hyatt Hotel, San Diego, CA, USA, Dember 13-15*, 2006. 5

Weijiu Liu. Boundary feedback stabilization of an unstable heat equation. *SIAM Journal on Control and Optimization*, 42:1033–1043, 2003. 5

J. N. Lyness and G. Giunta. A modification of the Weeks method for numerical inversion of the Laplace transform. *Mathematics and Computation*, 47 (175):313–322, 1986. 61

Hessam Mahdianfar, Ole Morten Aamo, and Alexey Pavlov. Attenuation of heave-induced pressure oscillations in offshore drilling systems. In *Proceedings of the 2012 American Control Conference*, 2012. 6, 56

Rachid Malti, Didier Maquin, and José Ragot. Some results on the convergence of transfer function expansions on the Laguerre series. In *5th European Control Conference, ECC'99*, 1999. 57

Cleve Barry Moler. A balancing act for the matrix exponential. Blog post, July 23rd 2012. URL `http://blogs.mathworks.com/cleve/2012/07/23/a-balancing-act-for-the-matrix-exponential/`. 92

Peter J. Olver. *Introduction to Partial Differential Equations*. In preparation for publication. Available online at http://www.math.umn.edu/~olver/pdn.html, 2013. 11

Michael Renardy and Robert C. Rogers. *An Introduction to Partial Differential Equations*. Springer, second edition, 2004. 10

David L. Russell. Controllability and stabilizability theory for linear partial differential equations: Recent progress and open questions. *SIAM Review*, 20(4):639–739, 1978. 21

William E. Schiesser. *The Numerical Method of Lines: Integration of Partial Differential Equations*. Academic Press, 1991. 17

Andrey Smyshlyaev and Miroslav Krstić. Closed form boundary state feedbacks for a class of 1D partial integro-differential equations. *IEEE Transactions on Automatic Control*, 49:2185–2202, 2004. 75

Andrey Smyshlyaev and Miroslav Krstić. *Adaptive Control of Parabolic PDEs*. Princeton University Press, 2010. 6

Andrey Smyshlyaev, Eduardo Cerpa, and Miroslav Krstić. Boundary stabilization of a 1-d wave equation with in-domain antidamping. *SIAM Journal on Control and Optimization*, 48(6):4014–4031, May 2010. 6

Kenneth Steiglitz. Rational transform approximation via the Laguerre spectrum. *Journal of The Franklin Institute*, 280:387–394, 1965. 57, 60

John C. Strikwerda. *Finite Difference Schemes and Partial Differential Equations*. Society for Industrial & Applied Mathematics, 2004. 17

Noël Tanguy, Pierre Vilbé, and Léon-Claude Calvez. Optimum choice of free parameter in orthonormal approximations. *IEEE Transactions on Automatic Control*, 40(10):1811–1813, October 1995. 62, 63

Francesco Tricomi. Transformazione di Laplace e polinami di Laguerre (in italian). *R. C. Accademia nazionale dei Lincei*, 21:232–239, 1935. 55

Francesco Tricomi. *Integral Equations*. Courier Dover Publications, 1957. 15

Rafael Vazquez. Personal correspondence. E-mail sent to author on February 15. 2013, at 11:16 as a reply to *Kernel equations solver for the Backstepping method*, February 2013. 75

Rafael Vazquez and Miroslav Krstić. Control of 1-D parabolic PDEs with Volterra nonlinearities, Part I: Design. *Automatica*, 44:2778–2790, 2008a. 6

Rafael Vazquez and Miroslav Krstić. Control of 1-D parabolic PDEs with Volterra nonlinearities, Part II: Analysis. *Automatica*, 44:2791–2803, 2008b. 6

Rafael Vazquez and Miroslav Krstić. Marcum q-functions and explicit kernels for stabilization of 2 x 2 linear hyperbolic systems with constant coefficients. Submitted for publication to Systems and Control Letters on February 15, 2013, 2 2013. 75

Rafael Vazquez, Jean-Michel Coron, Miroslav Krstić, and Georges Bastin. Local exponential H^2 stabilization of a 2 x 2 quasilinear hyperbolic system using backstepping. In *Proceedings of the 50th IEEE Conference on Decision and Control and European Control Conference, Orlando, FL, USA*, pages 1329–1334, 2011a. 15

Rafael Vazquez, Miroslav Krstić, and Jean-Michel Coron. Backstepping boundary stabilization and state estimation of a 2 x 2 linear hyperbolic system. In *Decision and Control and European Control Conference (CDC-ECC), 2011 50th IEEE Conference on*, pages 4937 – 4942, December 2011b. 6, 23, 24, 39, 40, 41, 76

William T. Weeks. Numerical inversion of Laplace transforms using Laguerre functions. *Journal of the ACM*, 13:419–429, 1966. 60

Jacob Andre C. Weideman. Algorithms for parameter selection in the Weeks method for inverting the Laplace transform. *SIAM Journal on Scientific Computing*, 21:111–128, 1999. 57, 60, 61

Frank M. White. *Fluid Mechanics (SI units)*. McGraw-Hill, 2012. 73

David Vernon Widder. An application of Laguerre polynomials. *Duke Mathematical Journal*, 162:126–136, 1935. 55

Kan Wu. Why use fftshift(fft(fftshift(x))) in Matlab instead of fft(x)? File Exchange at the MATLABCentral, October 2009. URL http://www.mathworks.com/matlabcentral/fileexchange/25473-why-use-fftshiftfftfftshiftx-in-matlab-instead-of-fftx. 183

Salih Yalçinbaş. Taylor polynomial solutions of nonlinear Volterra-Fredholm integral equations. *Applied Mathematics and Computation*, 127(2-3):195–206, 2002. 15

Appendix A

Additional lemmas

A.1 Lemma 2 from Aamo (2013)

This lemma, with accompanying proof, was first stated in Aamo (2013) as his *Lemma 2*.

Lemma A.1. *Consider the system*

$$u_t(x,t) + \epsilon(x)u_x(x,t) = f(x)g(t) \tag{A.1}$$

for $x \in (-\infty, \infty)$, $t \geq 0$, *where* $\epsilon(x) > 0$, $\forall x$, *and* $u(x,0) = u_0(x)$. *Its solution is*

$$u(x,t) = u_0(\phi^{-1}(t+\phi(x))) + \int_0^t (\phi^{-1}(t-\gamma+\phi(x)))g(\gamma)d\gamma \tag{A.2}$$

where

$$\phi(z) = \int_z^1 \frac{d\gamma}{\epsilon(\gamma)}. \tag{A.3}$$

Proof. Consider a change of variables $(x,t) \leftrightarrow (\xi,\tau)$ and define

$$v(\xi,\tau) := u(x,t). \tag{A.4}$$

Let $\tau = t$ and x be chosen so that

$$\frac{\partial x}{\partial \tau}(\xi,\tau) = \epsilon(x), \quad x(\xi,0) = \xi. \tag{A.5}$$

Then by the chain rule, we have

$$\frac{\partial v}{\partial \tau} = u_t\frac{\partial t}{\partial \tau} + u_x\frac{\partial x}{\partial \tau} = u_t(x,t) + \epsilon(x)u_x(x,t) = f(x(\xi,\tau))g(\tau) \tag{A.6}$$

with

$$v(\xi, 0) = u(x(\xi, 0), 0). \tag{A.7}$$

Integration with respect to τ from 0 to τ yields

$$v(\xi, \tau) = v(\xi, 0) + \int_0^\tau f(x(\xi, \gamma))g(\gamma)d\gamma \tag{A.8}$$

From (A.5), we have

$$\frac{\partial x}{\epsilon(x)} = \partial\tau. \tag{A.9}$$

Integration with respect to τ from 0 to τ, remembering that $x(\xi, 0) = \xi$ yields

$$\int_\xi^{x(\xi,\tau)} \frac{d\gamma}{\epsilon(\gamma)} = \tau = t \tag{A.10}$$

By using the strictly increasing and hence invertible function (A.3), (A.10) can be written

$$\phi(\xi) - \phi(x) = t \tag{A.11}$$

solving this for x, and inserting into (A.8), we find

$$v(\xi, \tau) = v(\xi, 0) + \int_0^\tau f(\phi^{-1}(\phi(\xi) - \gamma))g(\gamma)d\gamma. \tag{A.12}$$

Now substituting for $\xi = \phi^{-1}(\phi(x) + t)$ obtain from (A.11) yields

$$v(\xi, \tau) = v(\xi, 0) + \int_0^\tau f(\phi^{-1}(\phi(x) + t - \gamma))g(\gamma)d\gamma. \tag{A.13}$$

Finally, from (A.13), (A.4) and (A.7) we find

$$u(x, t) = u(x, 0) + \int_0^t f(\phi^{-1}(t - \gamma + \phi(x)))g(\gamma)d\gamma. \tag{A.14}$$

□

A.2 Exact solution of a convergent matrix exponential series

Lemma A.2. *Consider a convergent infinite matrix series*

$$M = \sum_{k=0}^{\infty} B^k \tag{A.15}$$

for some square matrix B. Under the assumption of having $I-B$ nonsingular, M can explicitly be stated as

$$M = (I - B)^{-1} \tag{A.16}$$

Proof. Consider the truncated partial sum

$$M_N = \sum_{k=0}^{N} B^k \tag{A.17}$$

for which clearly

$$M = \lim_{N\to\infty} M_N. \tag{A.18}$$

The difference between M_N and the product BM_N is

$$M_N - BM_N = \sum_{k=0}^{N} B^k - B\sum_{k=0}^{N} B^k = \sum_{k=0}^{N} B^k - \sum_{k=1}^{N+1} B^k = I - B^{N+1}. \tag{A.19}$$

Or, by extracting the common term to the left

$$(I - B)M_N = I - B^{N+1}. \tag{A.20}$$

Under the assumption of having $I - B$ nonsingular, the inverse of $I - B$ exists, and we find

$$M_N = (I - B)^{-1}(I - B^{N+1}). \tag{A.21}$$

If we now let $N \to \infty$, and utilize that $B^{N+1} \to 0$ as $N \to \infty$ since (A.15) is convergent, we land on the desired result

$$M = (I - B)^{-1}. \tag{A.22}$$

□

A.3 Contour integral in the complex plane

This lemma is based on Example 6 from Section 14.1 in Kreyszig (2010).

Lemma A.3. *Consider a curve C in the complex plane constituting of a circle of radius R, centred at the origin. Then for some integer $n \in \mathbb{Z}$ we have*

$$\oint_C \frac{1}{z^n} dz = \begin{cases} 2\pi j & \text{for } n = 1 \\ 0 & \text{otherwise} \end{cases}. \tag{A.23}$$

Proof. We parametrize the curve C as

$$z = z(\theta) = Re^{j\theta}. \tag{A.24}$$

with θ spanning $[-\pi,\ \pi]$ (or $[0,\ 2\pi]$). Then

$$\frac{1}{z^n} = z^{-n} = R^{-n}e^{-jn\theta}, \quad dz = Rje^{j\theta}d\theta. \tag{A.25}$$

Inserting this, we find

$$\oint_C \frac{1}{z^n}dz = \int_{-\pi}^{\pi} R^{-n}e^{-jn\theta}Rje^{j\theta}d\theta = jR^{1-n}\int_{-\pi}^{\pi} e^{j\theta(1-n)}d\theta \tag{A.26}$$

if $n = 1$, then

$$\oint_C \frac{1}{z^n}dz = jR^{1-1}\int_{-\pi}^{\pi} e^{j\theta(1-1)}d\theta = j\int_{-\pi}^{\pi} d\theta = j(\pi+\pi) = 2\pi j \tag{A.27}$$

if $n \neq 1$, we perform the integration to obtain

$$\oint_C \frac{1}{z^n}dz = \frac{R^{n-1}}{1-n}[e^{j\theta(1-n)}]_{-\pi}^{\pi} = \frac{R^{n-1}}{1-n}[e^{j\pi(1-n)} - e^{-j\pi(1-n)}]. \tag{A.28}$$

As $n-1$ are integers, the exponents are multiples of $j\pi$, and hence the exponential expressions are always 1 and cancel out. The lemma is verified. □

A.4 Variation of constants

The following lemma gives the explicit solution to a linear, possibly time variant system of ODEs.

Lemma A.4. *Consider a system on the form*

$$\dot{x}(t) = A(t)x(t) + B(t)u(t) \tag{A.29}$$

for a vector $x \in \mathbb{C}$ of signals, matrices $A(t) \in \mathbb{C}^{n\times n}$, $B(t) \in \mathbb{C}^{n\times m}$, some vector of known signals $u(t) \in \mathbb{C}^m$. Assume there exists a matrix $\Xi(t, t_0)$, known as a fundamental matrix, with the following properties:

1. $\dfrac{d}{dt}\Xi(t, t_0) = A(t)\Xi(t, t_0)$

2. $\Xi(t,t) = I$

3. $\Xi^{-1}(t,t_0) = \Xi(t_0,t)$

4. $\Xi(t,t_0) = \Xi(t,t_1)\Xi(t_1,t_0)$

for any t, t_0 *and* t_1 *in the domain. Then the solution to* (A.29) *is*

$$x(t) = \Xi(t,t_0)x(t_0) + \int_{t_0}^{t} \Xi(t,\tau)B(\tau)u(\tau)d\tau. \tag{A.30}$$

Moreover, if $A(t) = A$ *is a constant matrix, the fundamental matrix can simply be taken as*

$$\Xi(t,t_0) = e^{A(t-t_0)} = \sum_{k=0}^{\infty} \frac{1}{k!} A^k (t-t_0)^k. \tag{A.31}$$

Proof. See e.g. Chen (2009, p. 108). □

A.5 Semigroup property

Lemma A.5. *Consider a linear, autonomous system of ODEs*

$$\dot{x}(t) = Ax(t). \tag{A.32}$$

for a vector $x(t) \in \mathbb{C}^n$ *and a matrix* $A \in \mathbb{C}^{n\times n}$*. Then for some constant* d *and a solution* $x(t)$ *of* (A.32)*, we have*

$$x(t-d) = e^{-Ad}x(t). \tag{A.33}$$

Proof. From Lemma A.4, we find the solution of (A.32) to be

$$x(t) = e^{A(t-t_0)}x(t_0) \tag{A.34}$$

from which is follows that

$$\begin{aligned} x(t-d) &= e^{A(t-d-t_0)}x(t_0) = e^{A(-d+t-t_0)}x(t_0) = e^{-Ad}e^{A(t-t_0)}x(t_0) \\ &= e^{-Ad}x(t) \end{aligned} \tag{A.35}$$

□

A. ADDITIONAL LEMMAS

Appendix B

Additional material

B.1 Integral equation types

Integral equations are equations in which an unknown function appears inside an integration. An example is

$$y(x) = f(x) + \int_{x_0}^{x} K(x, \xi) y(\xi) d\xi \tag{B.1}$$

for the unknown function $y(x)$, known functions $f(x)$ and $K(x, \xi)$ and some known constant x_0. Equations on the form (B.1) are generally termed *Volterra equations* (Kreyszig (2010, p. 236)). If the limits of integration are both fixed, the integral equation is termed a *Fredholm equation*. Additionally, the equation is said to be

1. Of the *first kind* if the unknown function does not appear outside the integral
2. Of the *second kind* if the unknown function does appear outside the integral

The equation is said to be

1. *Homogenous* if $f(x) \equiv 0$ in (B.1)
2. *Inhomogenous* otherwise

This means that the example equation (B.1), when assuming $f(x)$ and $K(x, \xi)$ are not identically zero, is an *inhomogenous Volterra equation of the second kind.*

B.2 Trapezoidal and midpoint rules

The trapezoidal rule (Kreyszig (2010, p. 828)) and midpoint rule are numerical integration schemes that splits the domain into a finite amount of intervals. The integral is the approximated by respectively trapezoids and rectangles. If we split the domain into $N-1$ equally spaced subintervals and denote $\Delta = (b-a)/(N-1)$ as the length of each subinterval, the integral of some function $f(x)$ from a to b is approximated as

$$\int_a^b f(x)dx \approx \Delta \left[\frac{1}{2}f(x_0) + f(x_1) + \cdots + f(x_{N-2}) + \frac{1}{2}f(x_{N-1})\right] \tag{B.2}$$

where $x_n = a + \Delta n$ when using the trapezoidal rule, and as

$$\int_a^b f(x)dx \approx \Delta \left[f(x_0) + f(x_1) + \cdots + f(x_{N-3}) + f(x_{N-2})\right] \tag{B.3}$$

where $x_n = a + \Delta(n + \frac{1}{2})$ when using the midpoint rule.

Appendix C

Additional transfer function approximations

C.1 Case 1

C.1.1 Pure state feedback controller

The additional transfer function approximations for simulation case 1, using the transfer function of the pure state feedback controller as stated in Theorem 5.1 can be found in figures C.1–C.3 on pages 158–160.

C.1.2 Recursive controller

The additional transfer function approximations for simulation case 1, using the transfer function in Theorem 5.2 can be found in figures C.4–C.6 on pages 161–163.

C.1.3 Simplified controller

The additional transfer function approximations for simulation case 1, using the transfer function in Theorem 5.3 can be found in Figure C.7 on page 164.

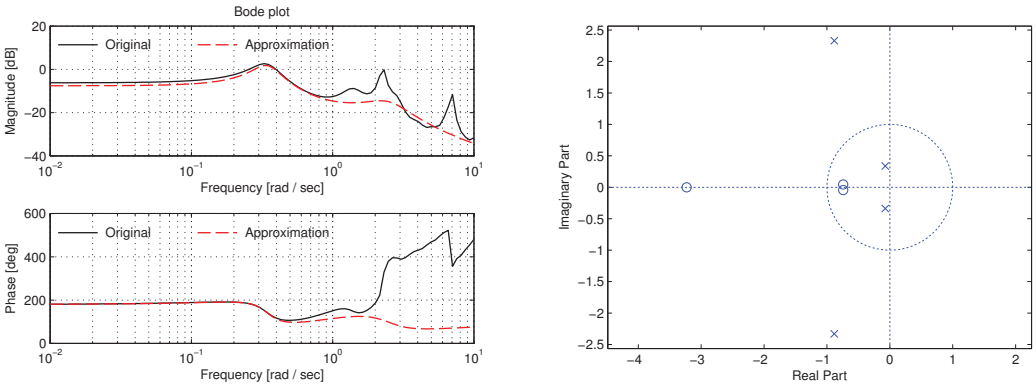

(a) Fourth order

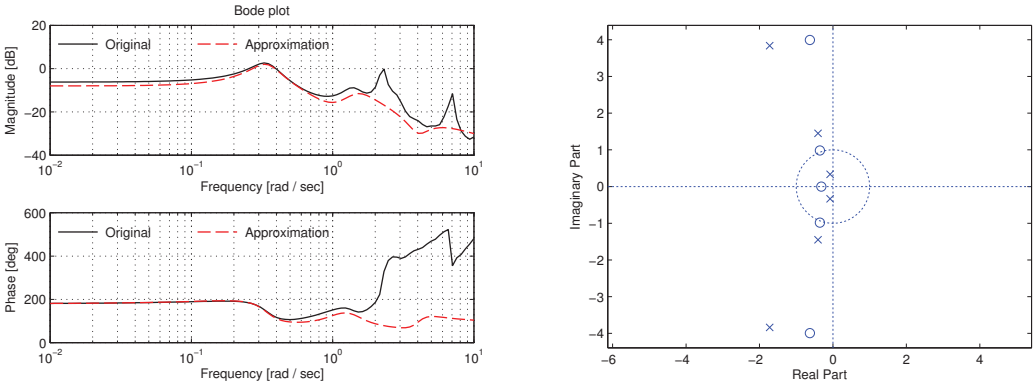

(b) Sixth order

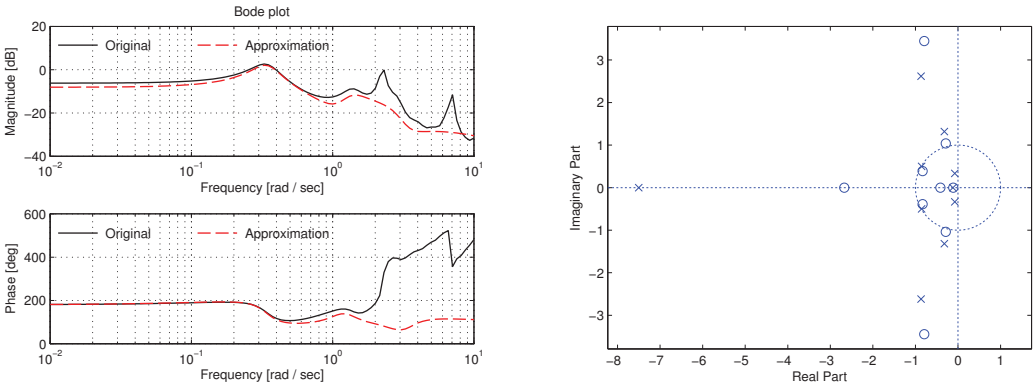

(c) Tenth order

Figure C.1: Case 1: P.s.f. controller: Approximations with $\sigma = 0.000$.

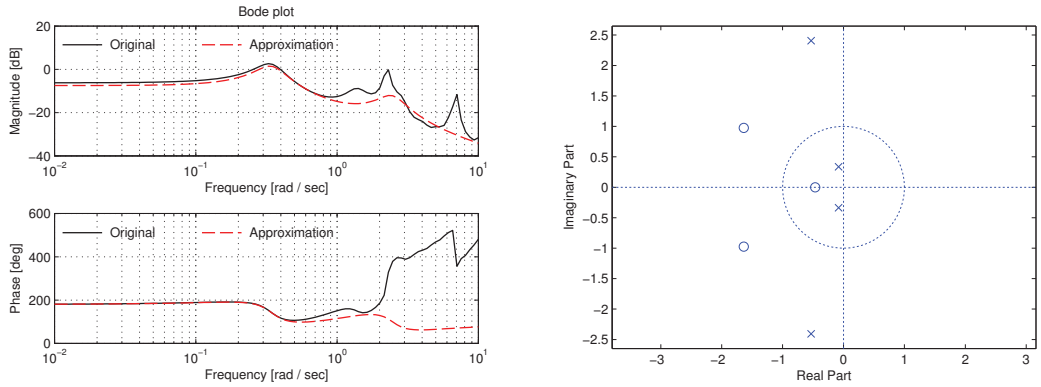

(a) Fourth order

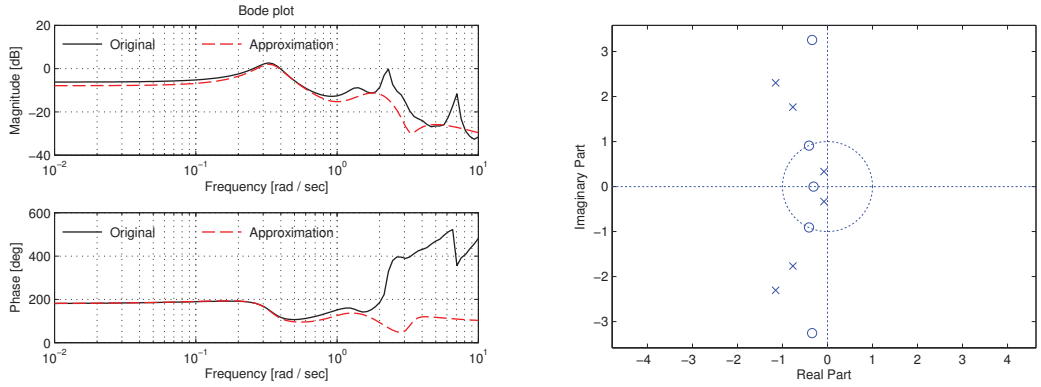

(b) Sixth order

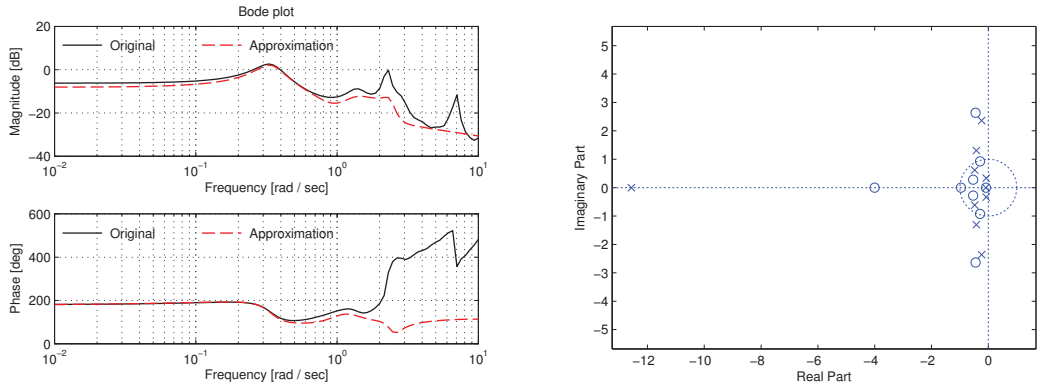

(c) Tenth order

Figure C.2: Case 1: P.s.f. controller: Approximations with $\sigma = 0.025$.

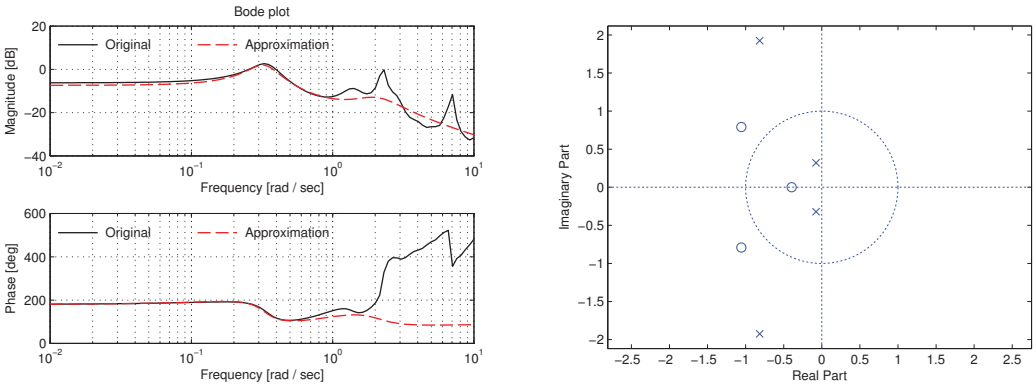

(a) Fourth order

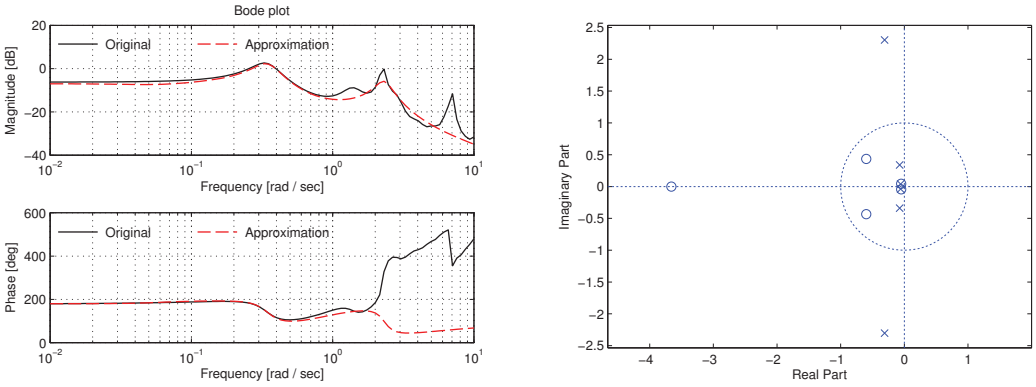

(b) Sixth order

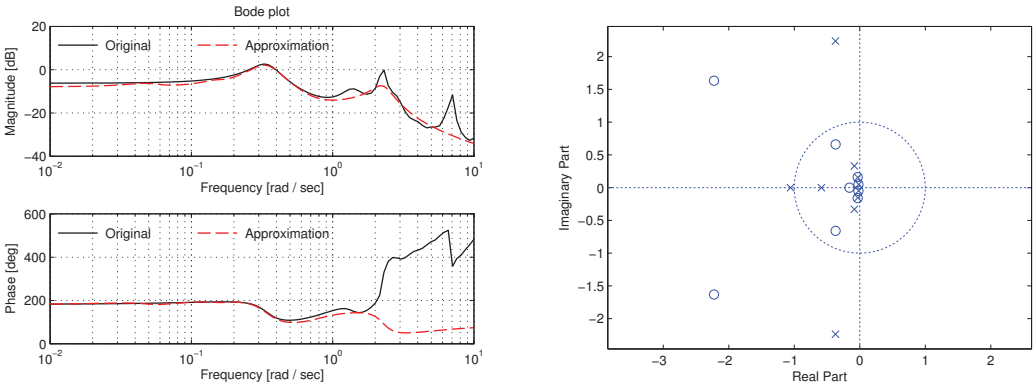

(c) Tenth order

Figure C.3: Case 1: P.s.f. controller: Approximations with $\sigma = 0.050$.

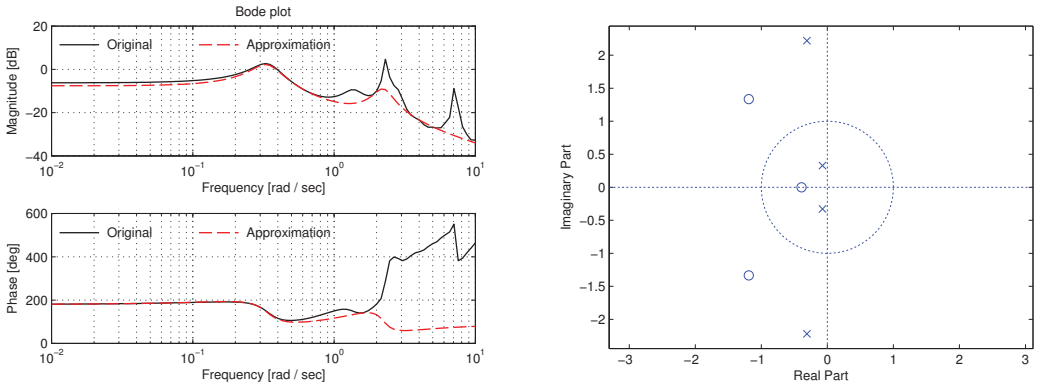

(a) Fourth order

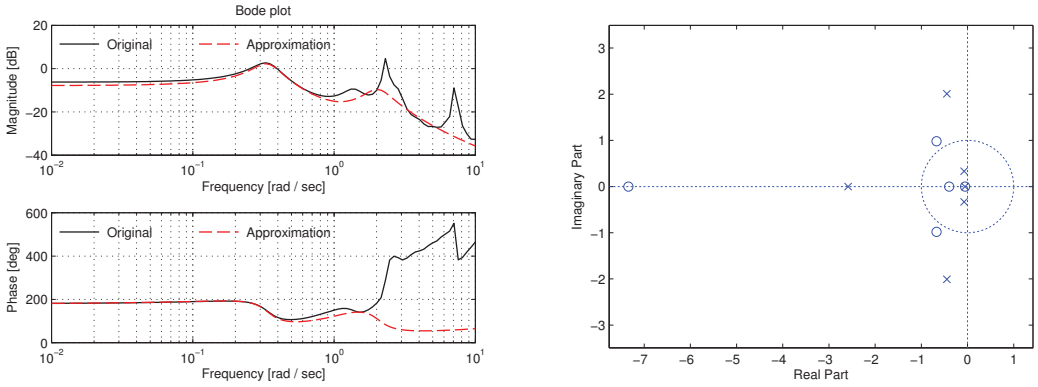

(b) Sixth order

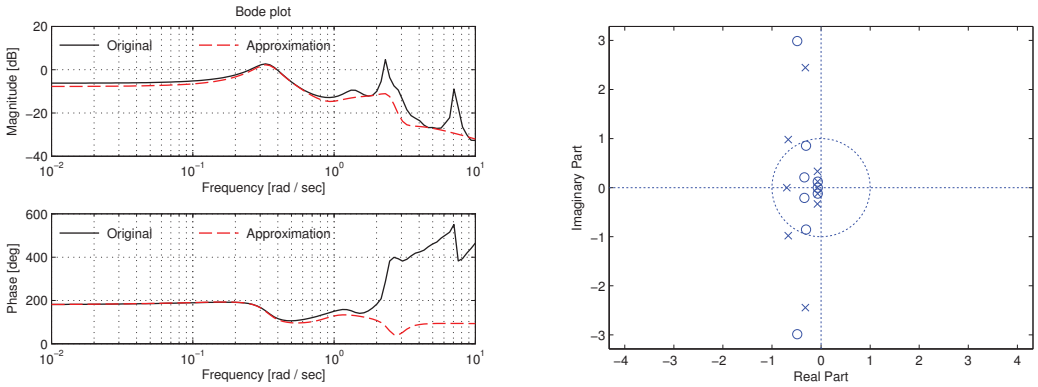

(c) Tenth order

Figure C.4: Case 1: Recursive controller: Approximations with $\sigma = 0.000$.

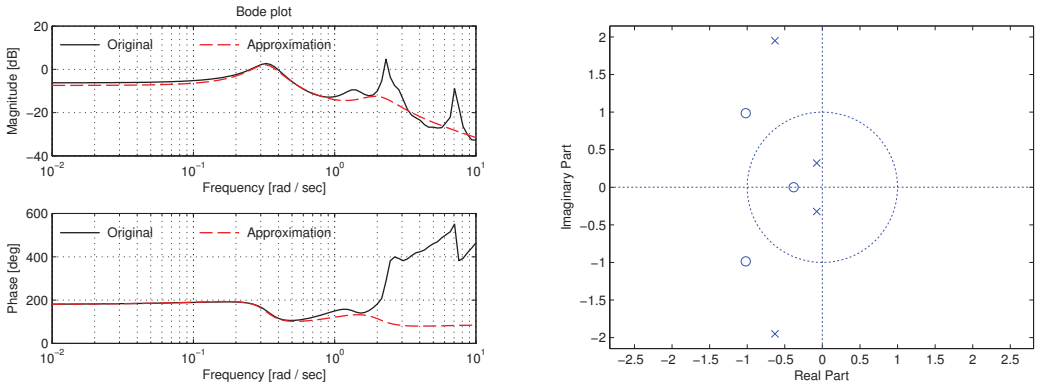

(a) Fourth order

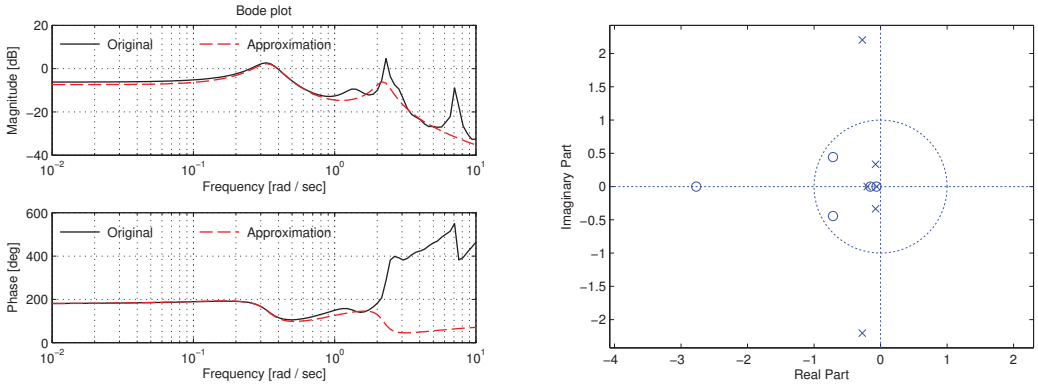

(b) Sixth order

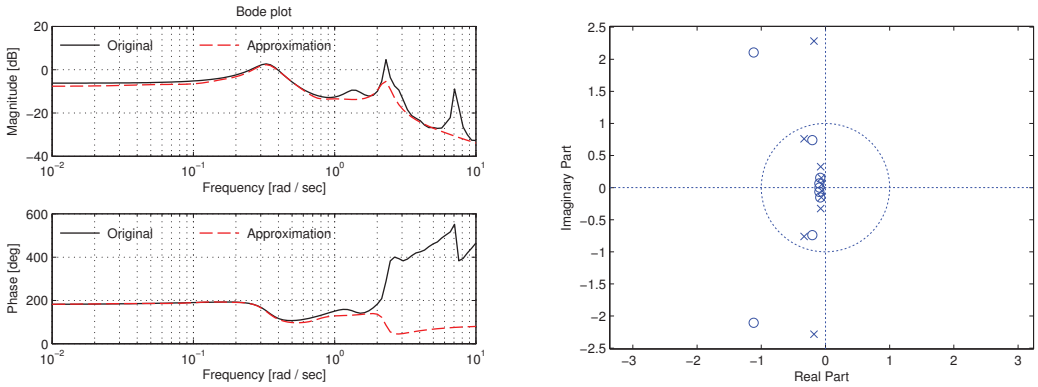

(c) Tenth order

Figure C.5: Case 1: Recursive controller: Approximations with $\sigma = 0.025$.

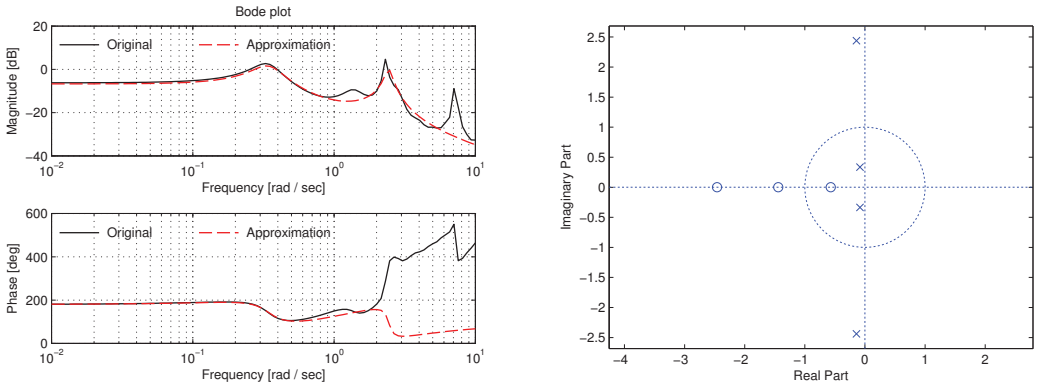

(a) Fourth order

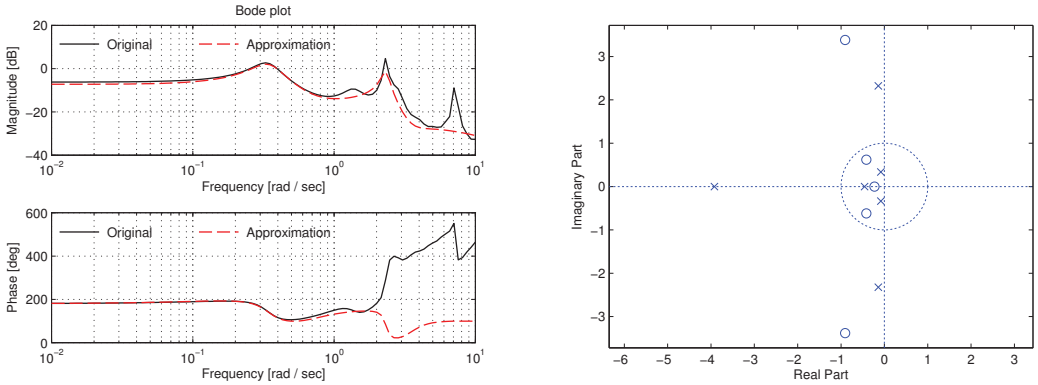

(b) Sixth order

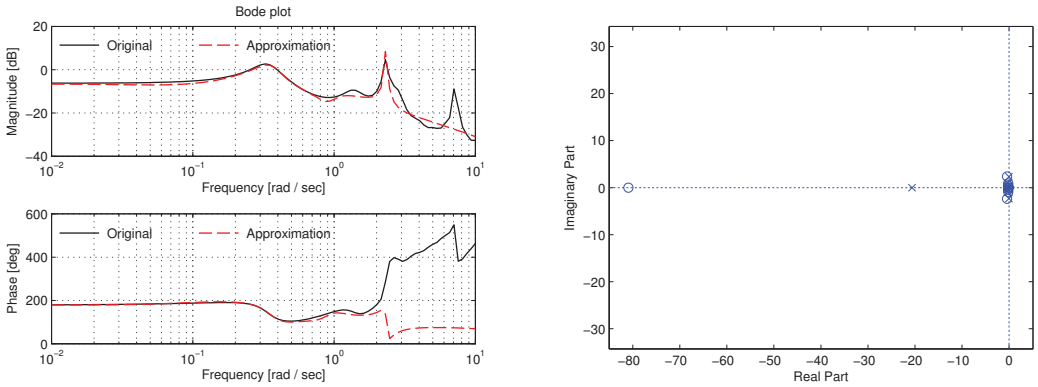

(c) Tenth order

Figure C.6: Case 1: Recursive controller: Approximations with $\sigma = 0.050$.

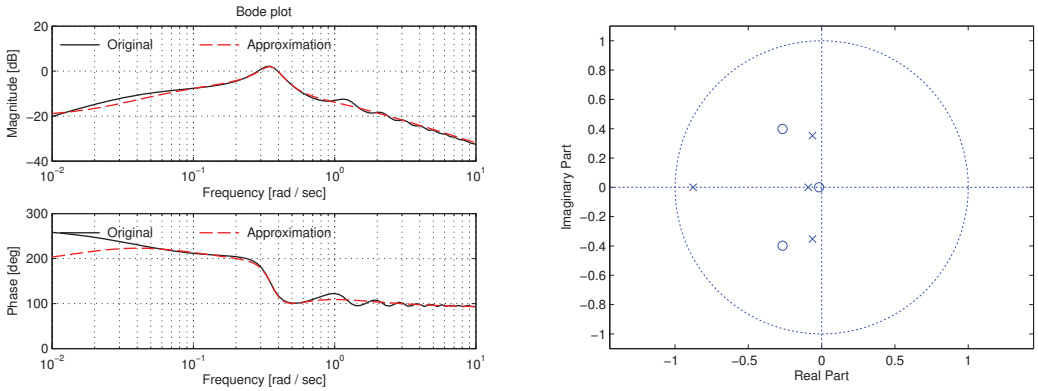

(a) Fourth order

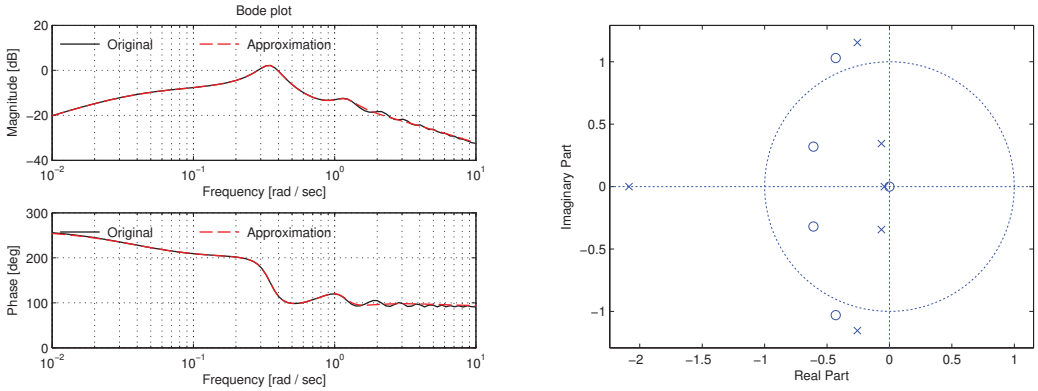

(b) Sixth order

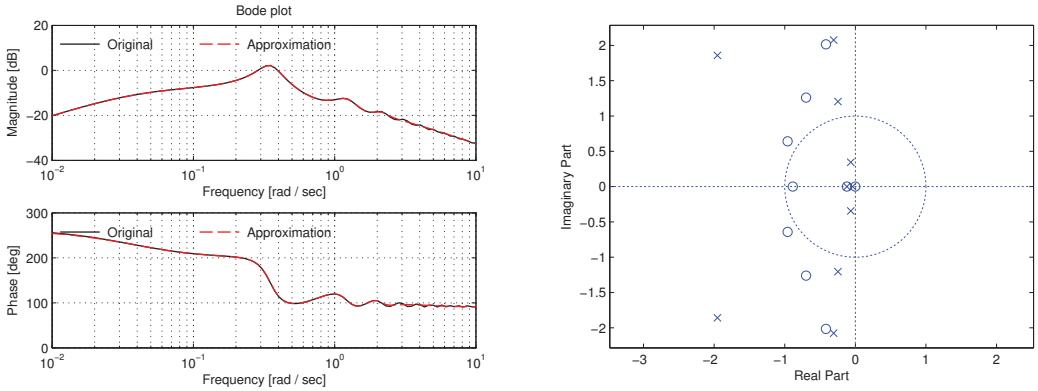

(c) Tenth order

Figure C.7: Case 1: Simplified controller: Approximations with $\sigma = 0.000$.

C.2 Case 2

C.2.1 Pure state feedback controller

The additional transfer function approximations for simulation case 2, using the transfer function of the pure state feedback controller as stated in Theorem 5.1 can be found in figures C.8–C.10 on pages 166–168.

C.2.2 Recursive controller

The additional transfer function approximations for simulation case 2, using the transfer function in Theorem 5.2 can be found in figures C.11–C.13 on pages 169–171.

C.2.3 Simplified controller

The additional transfer function approximations for simulation case 2, using the transfer function in Theorem 5.3 can be found in Figure C.14 on page 172.

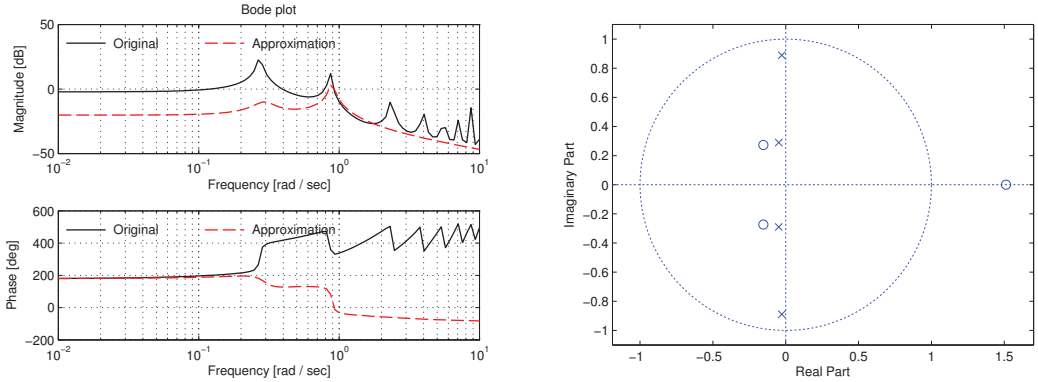

(a) Fourth order

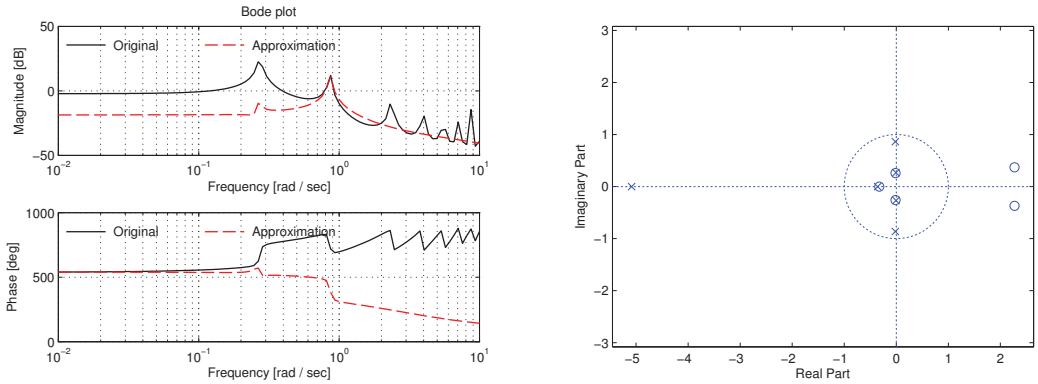

(b) Sixth order

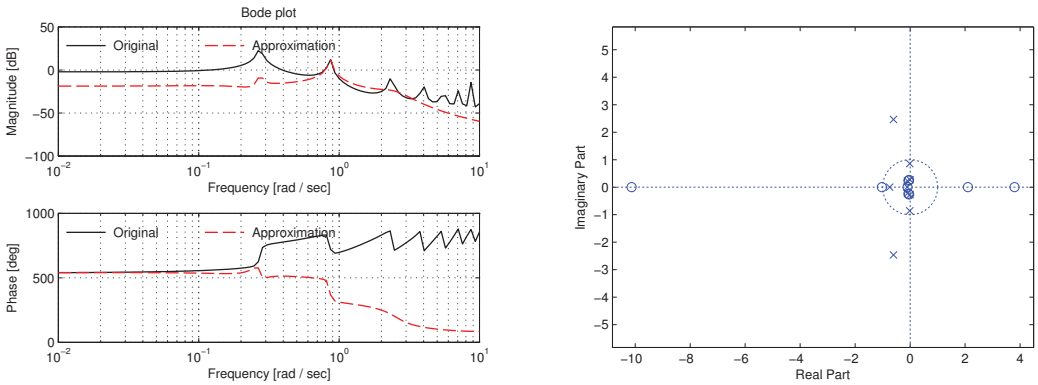

(c) Tenth order

Figure C.8: Case 2: P.s.f. controller: Approximations with $\sigma = 0.000$.

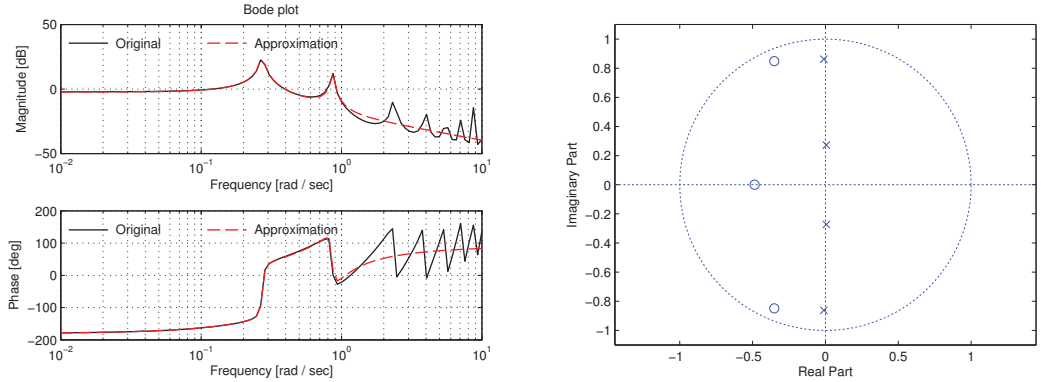

(a) Fourth order

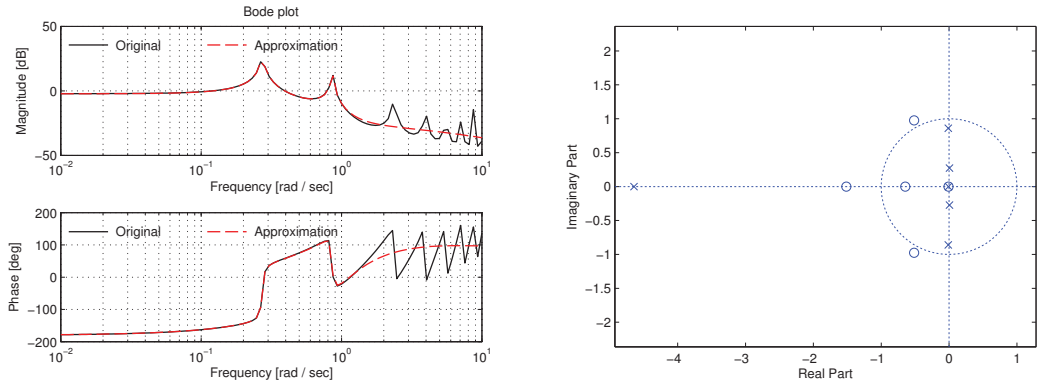

(b) Sixth order

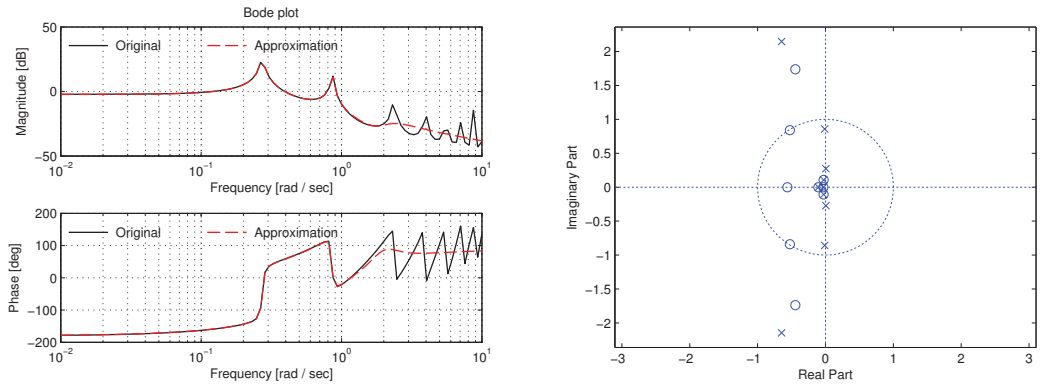

(c) Tenth order

Figure C.9: Case 2: P.s.f. controller: Approximations with $\sigma = 0.025$.

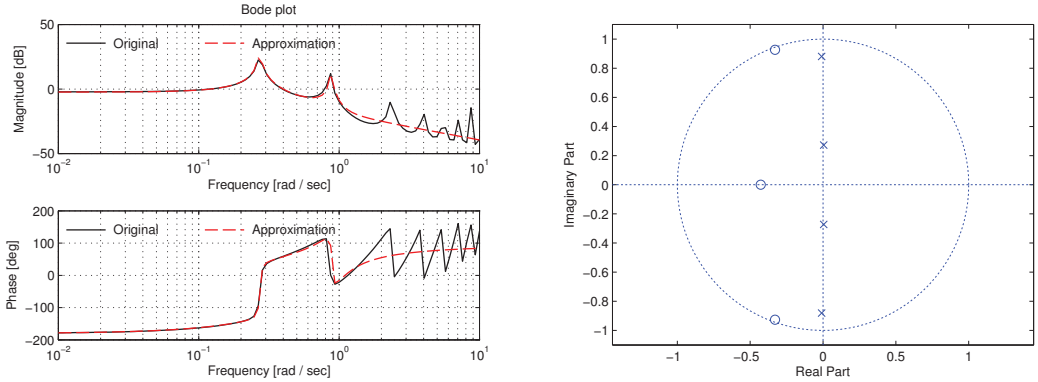

(a) Fourth order

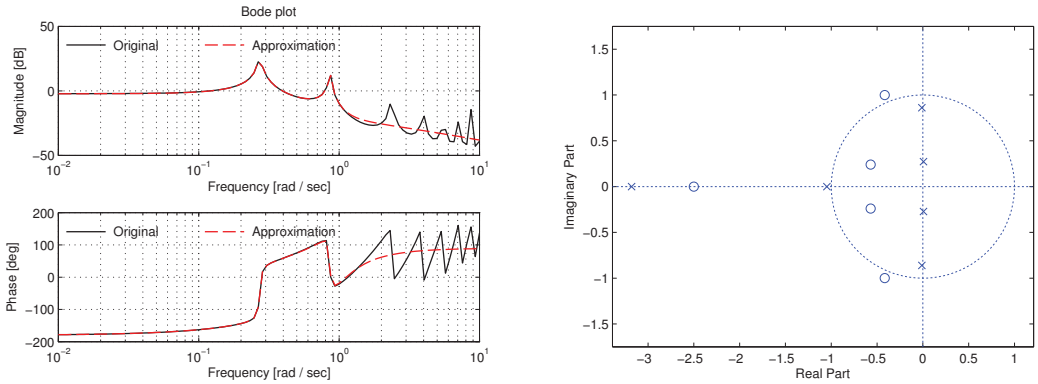

(b) Sixth order

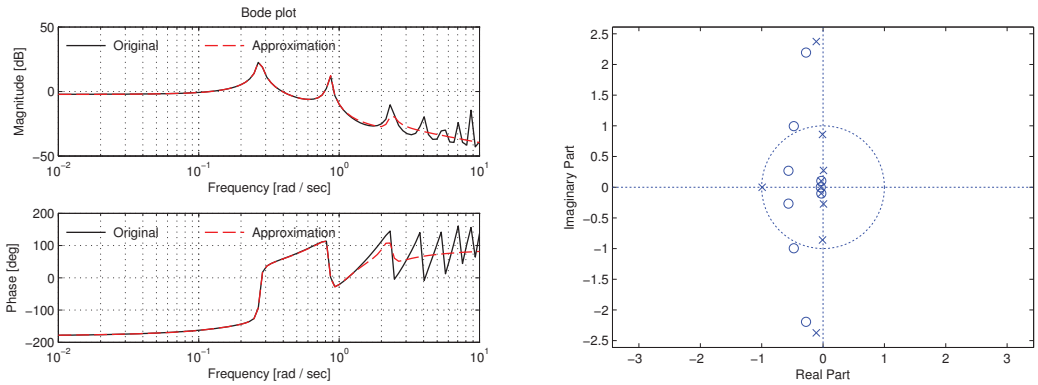

(c) Tenth order

Figure C.10: Case 2: P.s.f. controller: Approximations with $\sigma = 0.050$.

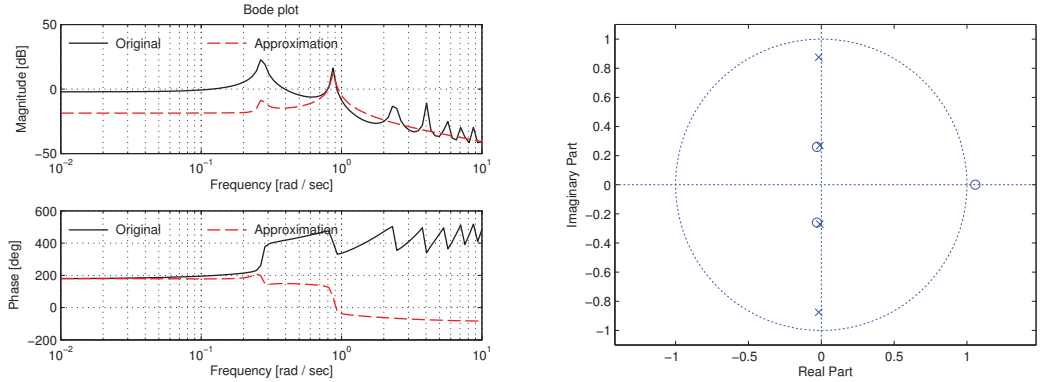

(a) Fourth order

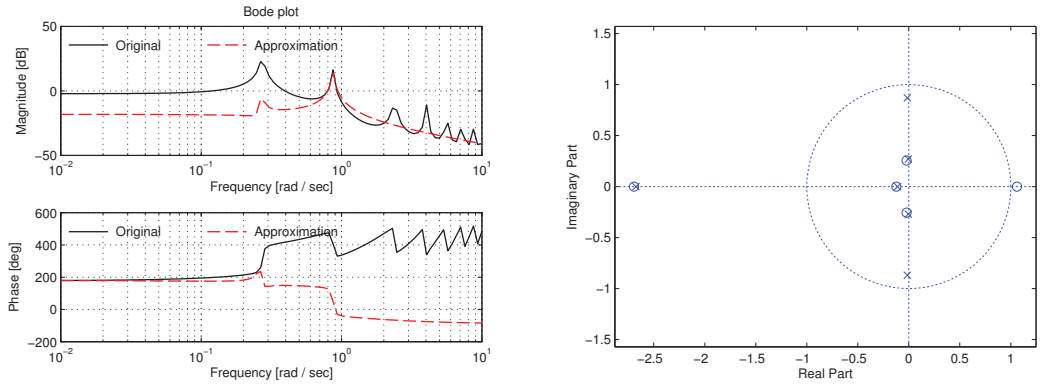

(b) Sixth order

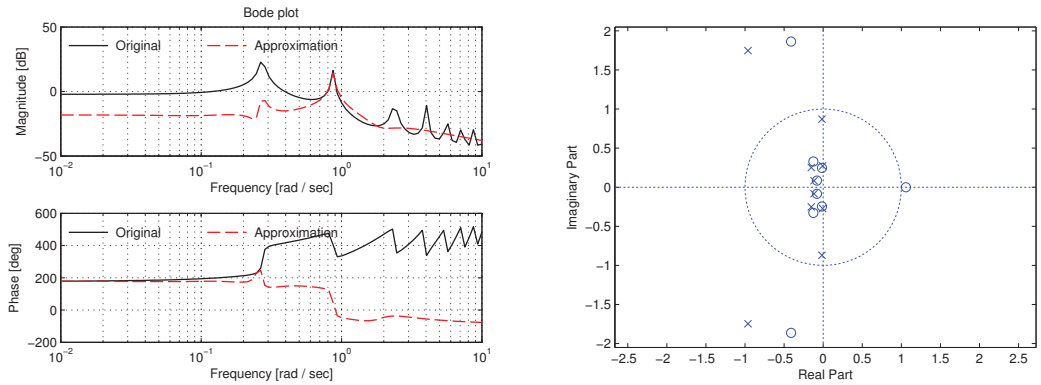

(c) Tenth order

Figure C.11: Case 2: Recursive controller: Approximations with $\sigma = 0.000$.

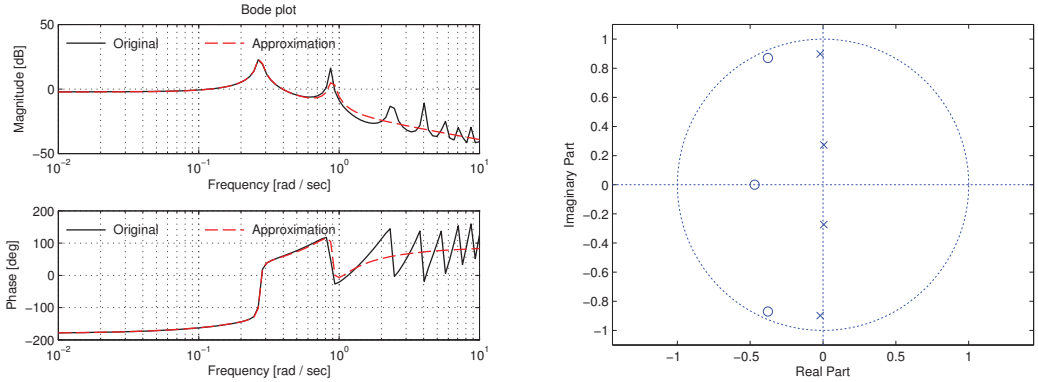

(a) Fourth order

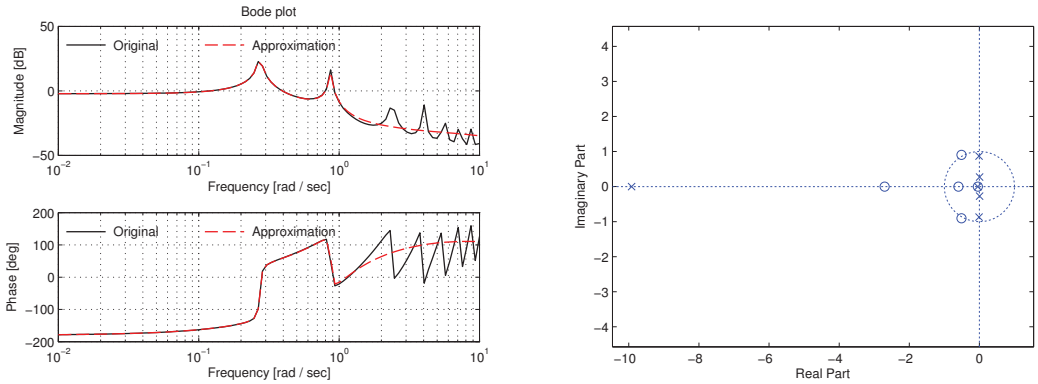

(b) Sixth order

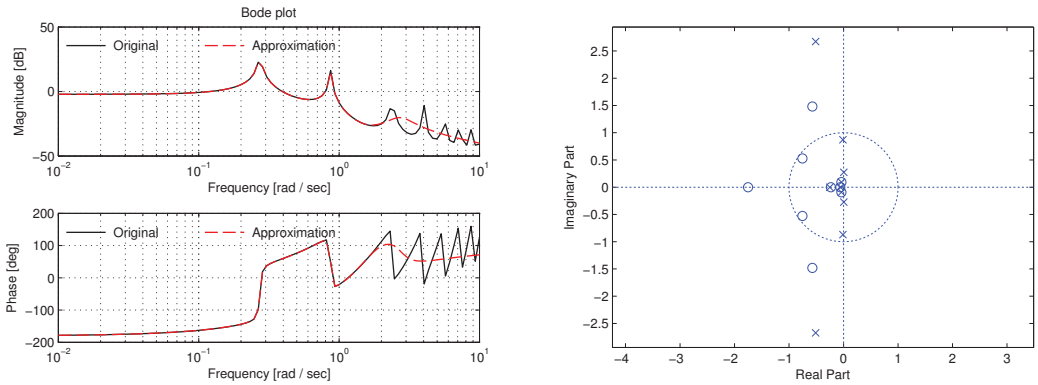

(c) Tenth order

Figure C.12: Case 2: Recursive controller: Approximations with $\sigma = 0.025$.

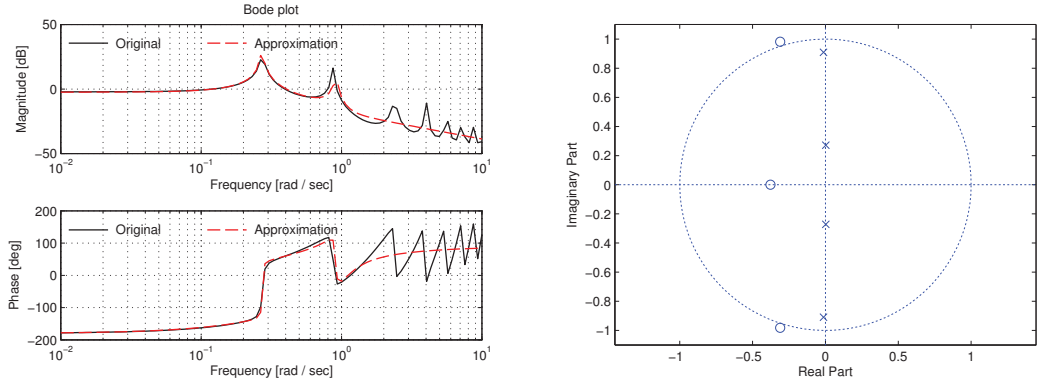

(a) Fourth order

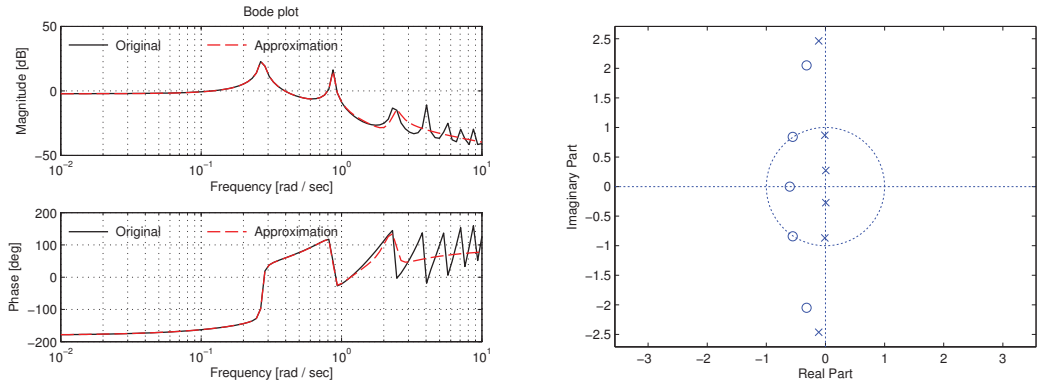

(b) Sixth order

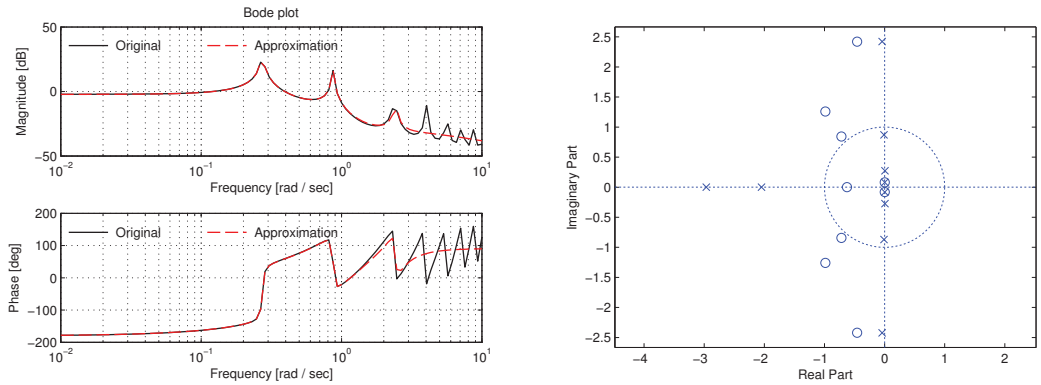

(c) Tenth order

Figure C.13: Case 2: Recursive controller: Approximations with $\sigma = 0.050$.

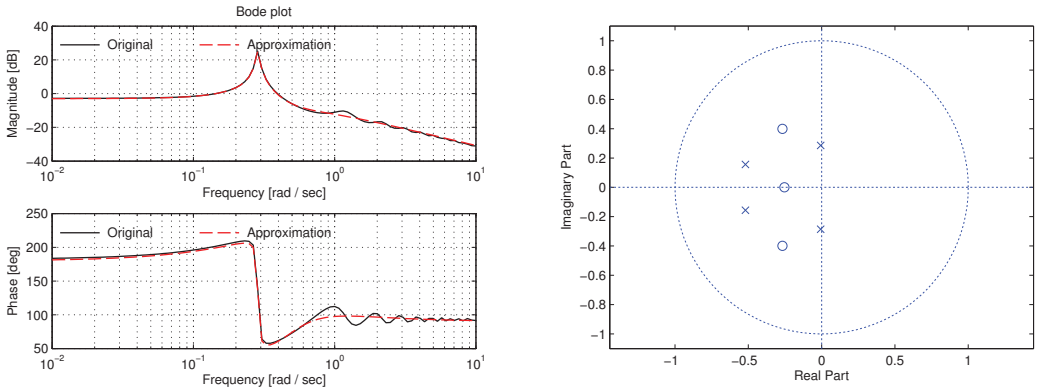

(a) Fourth order

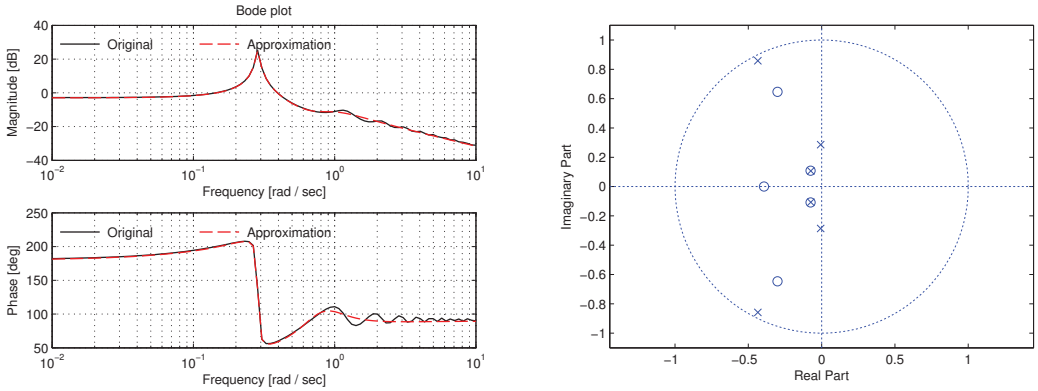

(b) Sixth order

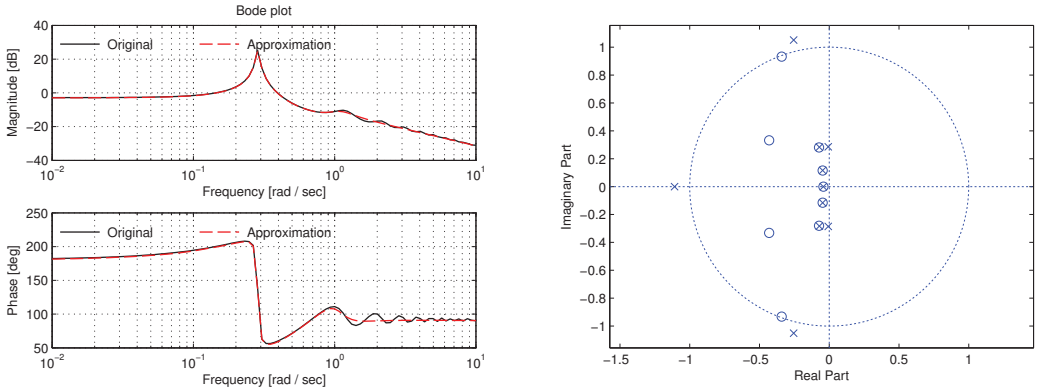

(c) Tenth order

Figure C.14: Case 2: Simplified controller: Approximations with $\sigma = 0.000$.

Appendix D

Additional simulations

D.1 Increased friction

We will in this additional simulation better demonstrate the strength of the pure state feedback controller compared to the other two controllers. The difference in performance for the three controllers is expected to be more evident now. The friction is multiplied by a factor of 100, resulting in $F_1 = 1000\ kg/m^3$. This is, of course, a highly non-physical MPD case, but it is constructed for illustrative purposes. The resulting terms $L^\alpha(\bar{x}, \xi)$ and $L^\beta(\bar{x}, \xi)$ in (3.52a)–(3.52b) now contain components with magnitude up to 2.48 and 0.61, respectively; and the terms added by the integrals in (3.74) are believed to be considerably larger. The simulation results are shown in figures D.1–D.2. Clearly seen from both figures, the performance is deteriorating for both the recursive and the simplified controllers. Notice the scales on the y-axes of Figure D.2. The pure state feedback controller still manages to achieve an attenuation resulting in pressure fluctuations with only 0.2 bar in magnitude, the recursive controller achieves 3 bar while the pressure fluctuations when using the simplified controller almost reaches 9 bar. This illustrates the cost of the assumption made when deriving the simplified controller, and also the robustness issues regarding the recursive controller.

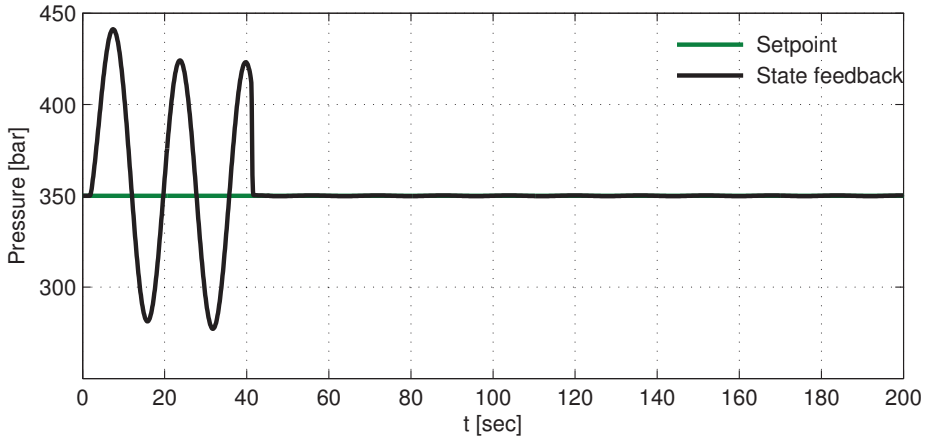

(a) Pure state feedback controller.

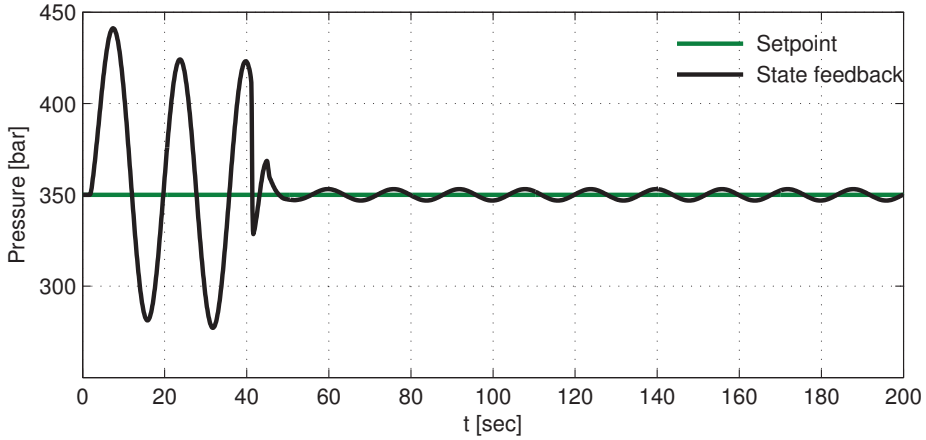

(b) Recursive controller.

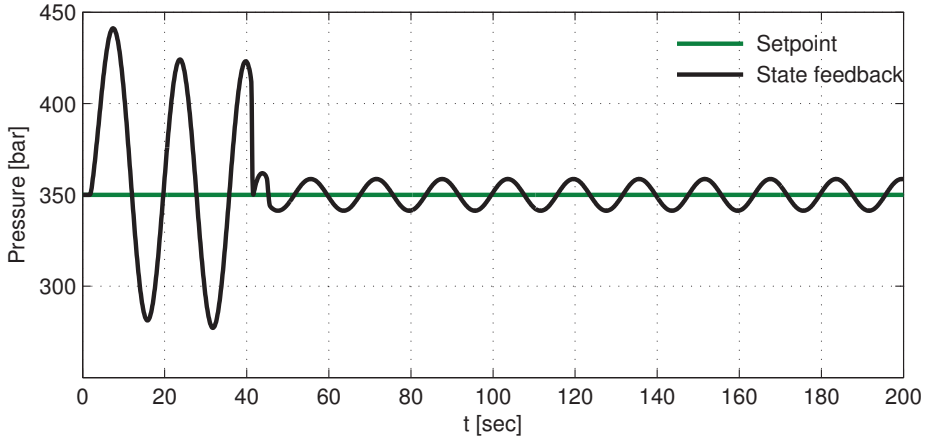

(c) Simplified controller.

Figure D.1: Increased friction: Pressure at depth 1000 metres.

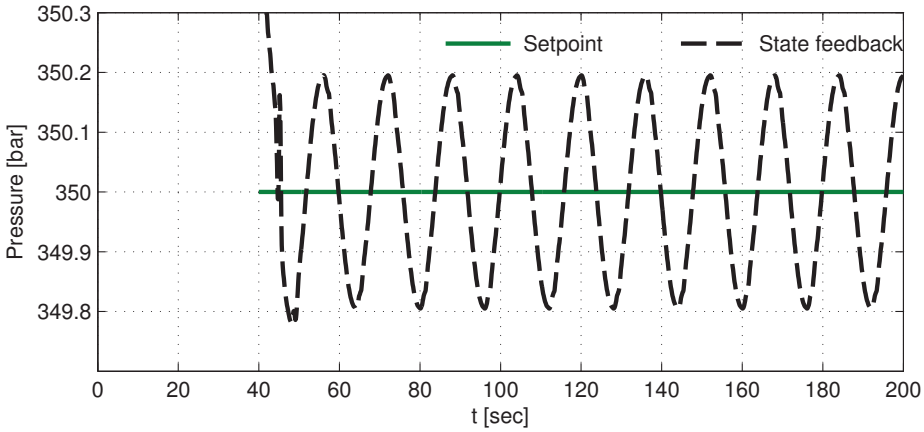

(a) Pure state feedback controller.

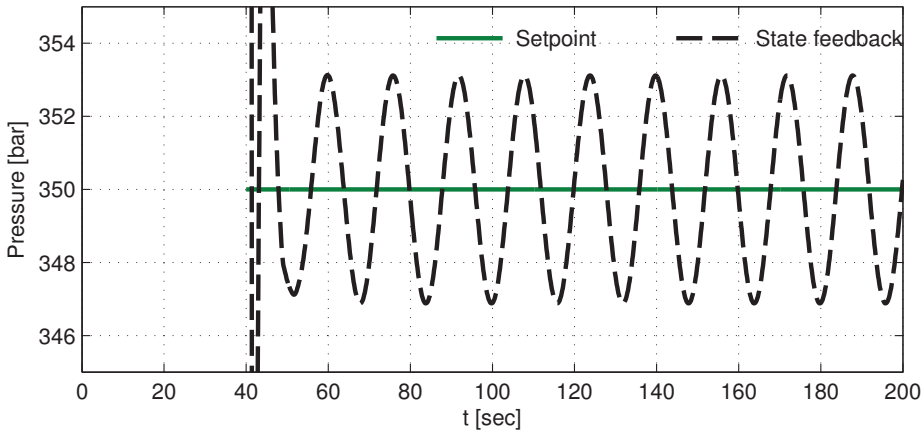

(b) Recursive controller.

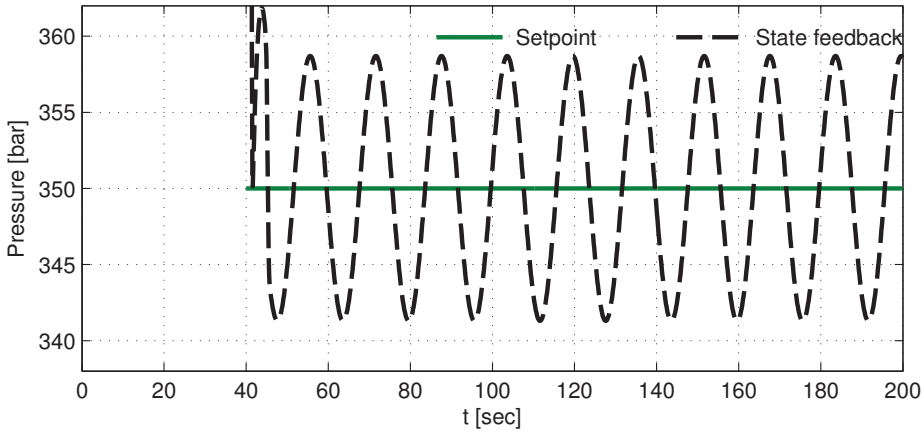

(c) Simplified controller.

Figure D.2: Increased friction: Pressure at depth 1000 metres.

D.2 The best fit, rational approximation of the recursive controller from Case 2

The sixth order reduced order controller with the original, unstable pair of poles as shown in Figure C.12b was here carefully simulated. The simulation results can be found in figures D.3–D.4 on pages 177–178. In Figure D.3, the pressure at depth 1000 meters when using the full output feedback implementation is plotted for comparison.

This time, the level of suppression is far better than the case where the poles were forced to the closed left half plane. The amplitude of fluctuations is about 0.5 bar, compared with the amplitude of 3 bars in Figure 8.25c on page 127.

However, the controller is internally unstable, and by simulating for a sufficiently long time, the internal controller will diverge.

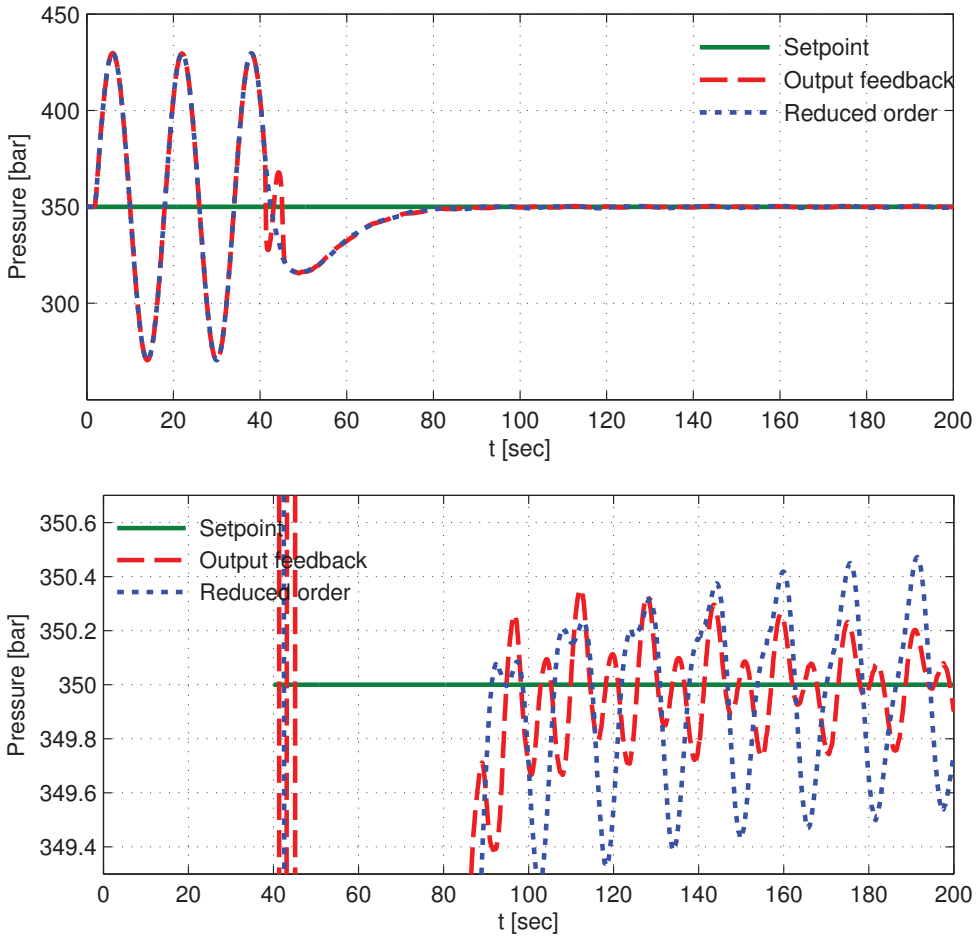

Figure D.3: The best fit rational approximation of the recursive controller from Case 2: Pressure at depth 1000 metres.

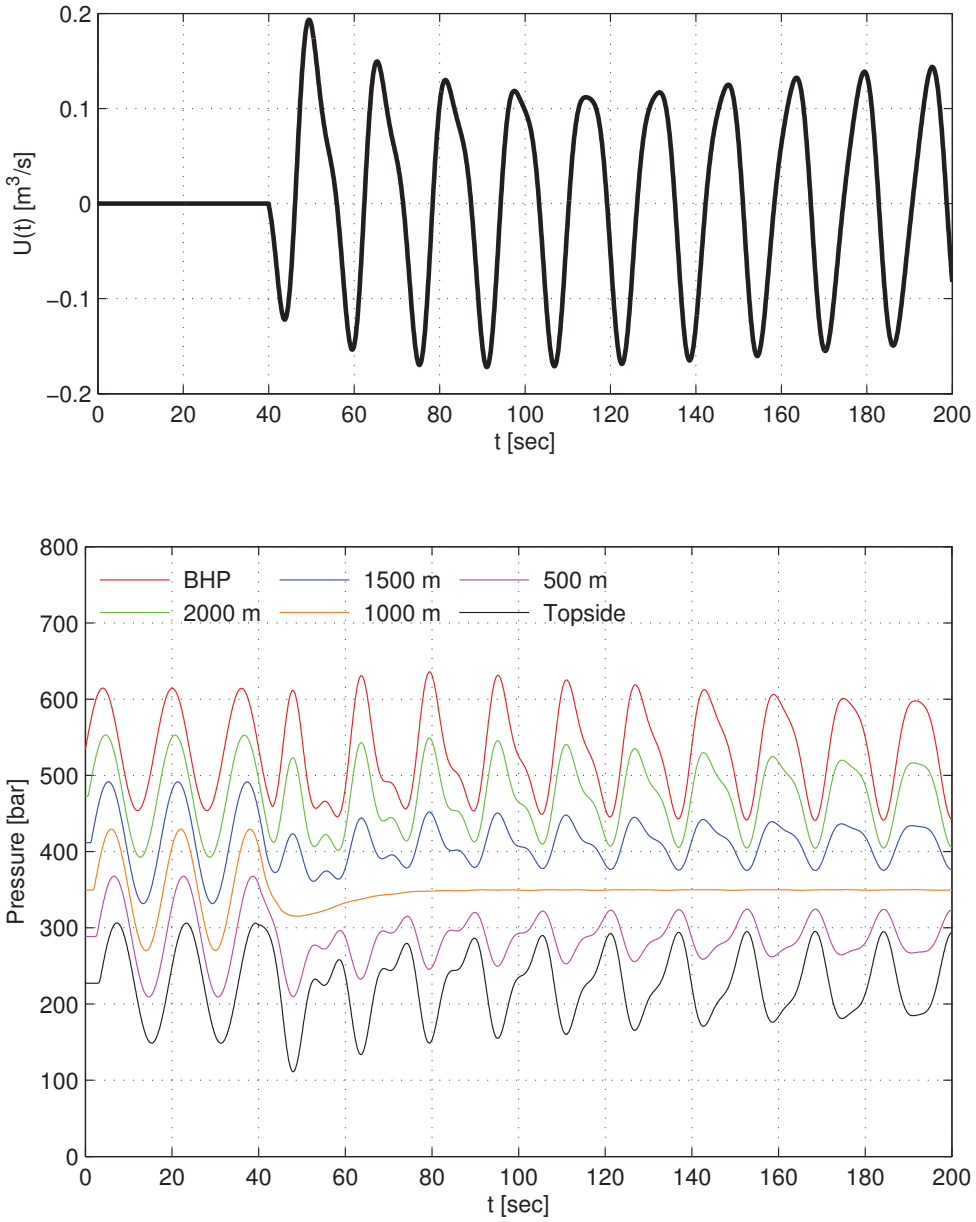

Figure D.4: The best fit rational approximation of the recursive controller from Case 2: Controller signal and pressure distribution.

Appendix E

Folder structure

This section contains descriptions of the folders and files on the accompanying disc. All scripts needed to run the simulations shown in the report are included. Prior to running any of the other scripts, the script *config_paths* has to be executed. This will add necessary folders containing shared scripts to the `MATLAB` path. In the following overview, folders are written in **boldface** with a preceding backslash, while files are written *italic*. A short descriptive comment written in plain style usually exceeds a folder or file.

\root

- *config_paths.m*
  This file adds the necessary folders an files to the `MATLAB` path required to run the other scripts in on the disc.
- **\Additional simulations**
  This subfolder contains the scripts simulating the additional simulations shown in Appendix D.
  - *run_K_inf_depth_1000_inc_fric.m*
    This script runs implementation with the simplified controller in Appendix D.1 and displays the results.
  - *run_psf_depth_1000_inc_fric.m*
    This script runs implementation with the pure state feedback controller in Appendix D.1 and displays the results.

- *run_rec_depth_1000_inc_fric.m*
  This script runs implementation with the recursive controller in Appendix D.1 and displays the results.
- *run_rec_depth_1000_tf_original.m*
  This script runs the implementation in Appendix D.2 and displays the results.

- **\Case_1**
  This implementations from Section 8.2 are found in this folder.

  - **\Pure_state_feedback**
    Contains scripts running and displaying the results for the implementations from Section 8.2.2.1.

    - *find_params_depth_2000_psf.m* Uses the method presented in Section 6.5 to find the optimal set of α and γ used in Section 8.2.1.1. Stores the result in the file *params_tf_psf_d2000.mat*.
    - *gen_tf_from_file_depth_2000_psf.m* Creates rational approximations using the parameters in the file *params_tf_psf_d2000.mat*, and stores the resulting transfer function coefficients in the file *tfs_psf_d2000.mat*.
    - *plot_approxes_depth_2000_psf.m* Plots the approximations in *tfs_psf_d2000.mat*, along with the original transfer function.
    - *run_psf_depth_2000.m* Runs the state feedback implementation.
    - *run_psf_depth_2000_obsv.m* Runs the output feedback implementation.
    - *run_psf_depth_2000_tf.m* Runs the implementation using the reduced order output feedback controller.
  - **\Recursive**
    This folder has the same structure at as the folder **\Pure_state_feedback**, containing scripts implementing the simulations and generating the transfer function approximations in Sections 8.2.1.2 and 8.2.2.2. All names have *rec* in place *psf*.

- **\Simplified**
  This folder has the same structure at as the folder **\Pure_state_feedback**, containing scripts implementing the simulations and generating the transfer function approximations in Sections 8.2.1.3 and 8.2.2.3. All names have *inf* in place *psf*.

- **\Case_2**
  This folder has exactly the same structure at as the folder **Case_1**, containing scripts implementing the simulations and generating the transfer function approximations in Section 8.3.

- **\drilling_system**
  This folder contains all the scripts used to implement the drilling system (7.1). To ease the implementation, was the hyperbolic system (3.1) implemented with the displayed pressures calculated by solving (7.5) for $p(xl, t)$, instead of implementing (7.1) directly.

  - **\controllers**
    Contains scripts implementing the different controllers.

    - *controller_K_inf.m* Implements the simplified controller from Theorem 3.3.
    - *controller_psf.m* Implements the pure state feedback controller from Theorem 3.1.
    - *controller_rec.m* Implements the recursive controller from Theorem 3.2.

  - **\coordinate_transforms**
    Contains different functions for coordinate transforms.

    - *alpha_from_u_and_v.m* Performs the backstepping transformation (3.3a).
    - *beta_from_u_and_v.m* Performs the backstepping transformation (3.3b).
    - *delta.m* Calculates the function $\delta(\xi, \bar{x}, t)$ in (3.48).

  - **\gains**
    Contains different functions for computations of gains.

- *controller_gains.m* Used to compute the controller gains used by the controllers derived in Chapter 3.
- *K_inf.m* Computes the gain $K_\infty(\bar{x})$, using (3.84).
- *K_psf.m* Computes the gain $K_{psf}(\bar{x})$, using (3.47).
- *K_rec.m* Computes the gain $K_{rec}(\bar{x})$, using (3.78).
- *observer_gains.m* Computes the observer gains needed by (4.1).

- **\kernel_solvers**
  - *K_kernel_solver.m* Solves (3.6)–(3.7) using the equations and methods derived in Section (7.5).
  - *L_kernel_solver.m* Solves (3.10)–(3.11).
  - *P_kernel_solver.m* Solves (4.4)–(4.5).
- **\model_reduction**

  Contains tools used to create the transfer function approximations found in Sections 8.2.1 and 8.3.1.
  - *error_fun.m* Evaluates the expression (6.48).
  - *find_params.m* Find the optimal set of parameters α and γ in (6.48) given a σ in (6.6) using the method described in Section 6.5.
  - *gen_tf.m* Generate a rational approximation from a given transfer function.
  - *gen_tf_from_file.m* Used *gen_tf.m* to generate transfer function approximations of different orders using from a set of α and γ read from a file.
  - *h_YU_inf_sampling.m* Samples the transfer function of Theorem 5.3. Does this by calling *h_YU_sampling.m*.
  - *h_YU_psf_sampling.m* Samples the transfer function of Theorem 5.1.
  - *h_YU_rec_sampling.m* Samples the transfer function of Theorem 5.2. Does this by calling *h_YU_sampling.m*.
  - *h_YU_sampling.m* Samples the transfer functions of Theorem 5.2 and 5.3.
  - *Laguerre_Gram.m* Generates a rational approximation from a given Laguerre spectrum using the method described in Section 6.3.

- *Laguerre_sampling_points.m* Returns the points in the complex plane where the transfer function samples needed by the Laguerre Gram algorithm are situated.That is; the points where F is evaluated in (6.33).
- *Laguerre_spectrum.m* Calculates the Laguerre spectrum from a series of transfer function samples using (6.35). The FFT algorithm is used. The samples are shifted using `fftshift()` before and after the FFT algorithm is applied, as the transform otherwise contains oscillatoric real components at the boundary. Thanks to Kan Wu for suggesting this (Wu (2009)). Note that the samples must be taken at the points given by *Laguerre_sampling_points.m* for the function to work properly.
- *setup_hypSys.m* A function created to ease the model reduction implementations. Configures a standard version of the hyperbolic system.

- **\setup**
  - *hypSys_from_well.m* Creates an hyperbolic system from a set of well parameters and calculates all the required parameters needed for simulations.
  - *well_02.m* Configurations of the well used in all simulations in this thesis, except the simulation in D.1 (which uses a modified friction factor F_1).
- **\shift_functions** Note that time-shift functions $d_\alpha(\bar{x}, \xi)$, $d_\beta(\bar{x}, \xi)$, $d_{rec}(\bar{x})$, $\kappa_\alpha(x, \xi)$, $\kappa_\beta(x, \xi)$, $\eta_\alpha(y)$, $\eta_\beta(y)$, as well as $\phi_\alpha(x)$, $\phi_\beta(x)$ and their inverses are all hard coded.
  - *Omega_alpha.m* Implements (3.50a).
  - *Omega_beta.m* Implements (3.50b).
  - *Phi_a.m* Implements (3.19a).
  - *Phi_b.m* Implements (3.19b).
  - *Psi_a.m* Implements (3.35a).
  - *Psi_b.m* Implements (3.35b).

  - *hyp_sys_dx.m* Returns the time derivatives of all the ODEs resulting from applying the Method of Lines to the hyperbolic system (3.1).
  - *hyp_sys_dx.m* Returns the time derivatives of all the ODEs resulting from applying the Method of Lines to the observer (4.1).
  - *hypSys_no_obsv_odefun.m* The function passed to the solver in `MATLAB` implementing the state feedback simulations.
  - *hypSys_w_obsv_odefun.m* The function passed to the solver in Matlab implementing the full output feedback simulations.
  - *hypSys_w_modReg_odefun.m* The function passed to the solver in Matlab implementing the reduced order controller simulations.

- **\plotfiles**

  - *plot_approxes.m* Used to plot the transfer function approximations in Sections 8.2.1 and 8.3.1.
  - *plotfile_no_observer.m* Plots the simulation results when no observer is used.
  - *plotfile_tf.m* Plots the simulation results when the reduced order controller is used.
  - *plotfile_tf_bode_and_zplane.m* A help function called by *plot_approxes.m*.
  - *plotfile_w_observer.m* Plots the simulation results when the full observer is used.

Appendix F

Journal paper

The following paper was submitted to *IEEE Transactions of Automatic Control* on May 7. 2013.

Disturbance Attenuation in the Interior Domain of Linear 2×2 Hyperbolic Systems

Henrik Anfinsen, Ole Morten Aamo, *Member, IEEE*

Abstract

In this paper, we develop a full state feedback law for disturbance attenuation in systems described by linear 2×2 partial differential equations of the hyperbolic type, with the disturbance modelled as an autonomous, finite dimensional linear system affecting the PDE's left boundary, and actuation limited to the right boundary. The effect of the disturbance is attenuated at an arbitrary point in the domain. The full state feedback law may be combined with an observer generating full state and disturbance estimates from sensing limited to the right boundary. The results are applied to the so-called heave problem from the oil and gas industry, and performance is demonstrated through simulations.

I. Introduction

IN THIS paper, we investigate the problem of disturbance rejection at an arbitrary point in the domain for systems described by linear 2×2 hyperbolic PDEs with spatially varying coefficients. We consider actuation and sensing on the right boundary with a disturbance entering on the left boundary.

This specific class of PDEs covers a wide range of physical systems, among them are open channels [1], gas flow pipelines [2], transmission lines [3], oil wells [4] and even road traffic [5]. Considering the wide range of practical applications, the act of stabilizing systems of this type has been subject to extensive research, and a number of techniques have been proposed in the literature.

A recently developed technique for control of PDEs is the backstepping method known from nonlinear control theory [6]. The backstepping method applied to partial differential equations was first developed for parabolic PDEs [7]. It was then used for stabilization of an unstable heat equation in [8], but this method was restricted to systems with a number of open-loop unstable eigenvalues no more than one. This was stressed further in [9] which allowed an arbitrary level of instability by using a backstepping method on a semi-discretized version of the system that made the closed-loop system stable. The method involved recursively solving a series of equations for the unknown kernels used in the backstepping transformation, but numerical computations showed that the kernel contained discontinuities as an artifact of the discretization method used. The number of discontinuities would tend to infinity when the discretization grid cell size approached zero.

This was improved in [10] by expressing the integration kernels as solutions to PDEs, giving the first solution of the problem in infinite-dimensional form. The method from [10] has since been applied to, among others, fluid flows [11], nonlinear parabolic equations [12]–[13] and has even been extended to adaptive versions [14].

The method has later been derived for application on hyperbolic systems: in [15] to first order hyperbolic systems; in [16] to second order systems, and; in [17] to two coupled first order equations. Most relevant to the present paper, are the results in [17] and [15], which were used in [18] to derive a full state feedback law for disturbance attenuation on the left boundary by control actuation from the right boundary, for the same type of systems considered in this paper. The full state feedback law was combined with a state observer to create an output feedback law, with sensing also limited to the right boundary. In this paper, we generalize these results to derive a full state feedback law for disturbance attenuation at an *arbitrary point in the domain*. While the state feedback law is the main contribution of this paper and the main

H. Anfinsen and O. M. Aamo are with the Department of Engineering Cybernetics, Norwegian University of Science and Technology, Trondheim N-7491, Norway (e-mail: henrik.anfinsen@gmail.com; aamo@ntnu.no)

object of interest in the simulations section, we also combine it with the state observer from [18] to create an output feedback law for comparison. The output feedback law is, of course, the more relevant controller from a practical point of view.

The disturbance attenuation problem - while posed in a general setting in the next section - is motivated by problems faced in the oil and gas industry. Typically, a disturbance enters at the inlet of a subsea pipeline, or at the bottom of an oil well, whereas sensing and actuation equipment is restricted to topside platforms or drilling rigs, potentially several kilometres away. Undesired influx into an oil well being drilled and undesired outflux of drilling mud and cuttings into the reservoir (known as kick and loss, respectively), are examples of problems that can be modelled using the type of systems investigated in this paper. Another application is the attenuation of pressure fluctuations due to undesired drill string motions caused by heaving when drilling offshore from a floating rig. This problem was addressed in [4] using a lumped model and simplifying assumptions with regards to available measurements, and in [19] where a linearization technique was used that neglected the friction terms, making the system decoupling a far simpler task. This problem is also our choice for a numerical demonstration of our theoretical results.

The paper is organized as follows. In Section II, we pose the disturbance attenuation problem. In Section III, we establish properties of system solutions and design a controller for disturbance attenuation at an arbitrary point in the domain assuming full state information is available. Two versions of the controller are derived. A state observer generating full state estimates and estimate of the disturbance, with co-located sensing and actuation restricted to the right boundary is given in Section IV. Both formulations of the controller are tested on the aforementioned problem from the oil and gas industry in Section V, before some concluding remarks are given in Section VI.

II. Problem statement

The type of systems to be considered in this paper are on the form

$$u_t(x,t) = -\epsilon_1(x)u_x(x,t) + c_1(x)v(x,t) \tag{1a}$$
$$v_t(x,t) = \epsilon_2(x)v_x(x,t) + c_2(x)u(x,t) \tag{1b}$$
$$u(0,t) = qv(0,t) + CX(t) \tag{1c}$$
$$v(1,t) = U(t) \tag{1d}$$
$$\dot{X}(t) = AX(t) \tag{1e}$$

propagating over the domain defined by $x \in [0,1]$ and $t \geq 0$. It is assumed that $\epsilon_1(x), \epsilon_2(x) > 0$ are $\mathcal{C}^1([0,1])$, and $c_1(x), c_2(x)$ are $\mathcal{C}([0,1])$. The disturbance term $X(t) \in \mathbb{R}^{n\times n}$ is parameterized by $A \in \mathbb{R}^{n\times n}$ and $C \in \mathbb{R}^{1\times n}$ with the pair (A,C) assumed observable. The parameter $q \neq 0$ is a constant, $U(t)$ is the controller input and $u(1,t)$ is assumed measured.

The objective is to design $U(t)$ such that

$$u(\bar{x},t) = rv(\bar{x},t) \tag{2}$$

is achieved for some given, fixed $\bar{x} \in (0,\ 1)$. This is a non-trivial generalization of the results from [18], where the control law achieving (2) for $\bar{x} = 0$ was derived.

III. Disturbance Attenuation

A. Previous results

In [18], the following backstepping transformation

$$\alpha(x,t) = u(x,t) - \int_0^x K^{uu}(x,\xi)u(\xi,t)d\xi - \int_0^x K^{uv}(x,\xi)v(\xi,t)d\xi \tag{3a}$$

$$\beta(x,t) = v(x,t) - \int_0^x K^{vu}(x,\xi)u(\xi,t)d\xi - \int_0^x K^{vv}(x,\xi)v(\xi,t)d\xi \tag{3b}$$

and the controller

$$U(t) = \int_0^1 K^{vu}(1,\xi)u(\xi,t)d\xi + \int_0^1 K^{vv}(1,\xi)v(\xi,t)d\xi + V(t) \tag{4}$$

were used to map the system (1) into the following decoupled form

$$\alpha_t(x,t) = -\epsilon_1(x)\alpha_x(x,t) - \epsilon_1(0)K^{uu}(x,0)CX(t) \tag{5a}$$

$$\beta_t(x,t) = \epsilon_2(x)\beta_x(x,t) - \epsilon_1(0)K^{vu}(x,0)CX(t) \tag{5b}$$

$$\alpha(0,t) = q\beta(0,t) + CX(t) \tag{5c}$$

$$\beta(1,t) = V(t) \tag{5d}$$

$$\dot{X}(t) = AX(t). \tag{5e}$$

The kernels in (3), (5a), (5b) were given as the solution to the following system of PDEs

$$\epsilon_1(x)K^{uu}_x(x,\xi) + \epsilon_1(\xi)K^{uu}_\xi(x,\xi) = -\epsilon_1'(\xi)K^{uu}(x,\xi) - c_2(\xi)K^{uv}(x,\xi) \tag{6a}$$

$$\epsilon_1(x)K^{uv}_x(x,\xi) - \epsilon_2(\xi)K^{uv}_\xi(x,\xi) = \epsilon_2'(\xi)K^{uv}(x,\xi) - c_1(\xi)K^{uu}(x,\xi) \tag{6b}$$

$$\epsilon_2(x)K^{vu}_x(x,\xi) - \epsilon_1(\xi)K^{vu}_\xi(x,\xi) = \epsilon_1'(\xi)K^{vu}(x,\xi) + c_2(\xi)K^{vv}(x,\xi) \tag{6c}$$

$$\epsilon_2(x)K^{vv}_x(x,\xi) + \epsilon_2(\xi)K^{vv}_\xi(x,\xi) = -\epsilon_2'(\xi)K^{vv}(x,\xi) + c_1(\xi)K^{vu}(x,\xi) \tag{6d}$$

with boundary conditions

$$K^{uu}(x,0) = \frac{\epsilon_2(0)}{q\epsilon_1(0)}K^{uv}(x,0) \tag{7a}$$

$$K^{uv}(x,x) = \frac{c_1(x)}{\epsilon_1(x)+\epsilon_2(x)} \tag{7b}$$

$$K^{vu}(x,x) = -\frac{c_2(x)}{\epsilon_1(x)+\epsilon_2(x)} \tag{7c}$$

$$K^{vv}(x,0) = \frac{q\epsilon_1(0)}{\epsilon_2(0)}K^{vu}(x,0) \tag{7d}$$

defined over the triangular domain

$$\mathcal{T} = \{(x, \xi) \ : \ 0 \leq \xi \leq x \leq 1\}. \tag{8}$$

The transformation (3) was originally derived in [17] and used for state feedback stabilization for (1) in the case without disturbance ($X(t) \equiv 0$). The inverse of (3) was also given in [17] as

$$\begin{aligned} u(x,t) = \alpha(x,t) &+ \int_0^x L^{\alpha\alpha}(x,\xi)\alpha(\xi,t)d\xi \\ &+ \int_0^x L^{\alpha\beta}(x,\xi)\beta(\xi,t)d\xi \end{aligned} \tag{9a}$$

$$\begin{aligned} v(x,t) = \beta(x,t) &+ \int_0^x L^{\beta\alpha}(x,\xi)\alpha(\xi,t)d\xi \\ &+ \int_0^x L^{\beta\beta}(x,\xi)\beta(\xi,t)d\xi \end{aligned} \tag{9b}$$

where the kernels are given as the solution to the system of PDEs

$$\begin{aligned} &\epsilon_1(x)L_x^{\alpha\alpha}(x,\xi) + \epsilon_1(\xi)L_\xi^{\alpha\alpha}(x,\xi) \\ &\qquad = -\epsilon_1'(\xi)L^{\alpha\alpha}(x,\xi) + c_1(x)L_\xi^{\beta\alpha}(x,\xi) \end{aligned} \tag{10a}$$

$$\begin{aligned} &\epsilon_1(x)L_x^{\alpha\beta}(x,\xi) - \epsilon_2(\xi)L_\xi^{\alpha\beta}(x,\xi) \\ &\qquad = \epsilon_2'(\xi)L^{\alpha\beta}(x,\xi) + c_1(x)L_\xi^{\beta\beta}(x,\xi) \end{aligned} \tag{10b}$$

$$\begin{aligned} &\epsilon_2(x)L_x^{\beta\alpha}(x,\xi) - \epsilon_1(\xi)L_\xi^{\beta\alpha}(x,\xi) \\ &\qquad = \epsilon_1'(\xi)L^{\beta\alpha}(x,\xi) - c_2(x)L_\xi^{\alpha\alpha}(x,\xi) \end{aligned} \tag{10c}$$

$$\begin{aligned} &\epsilon_2(x)L_x^{\alpha\beta}(x,\xi) + \epsilon_2(\xi)L_\xi^{\beta\beta}(x,\xi) \\ &\qquad = -\epsilon_2'(\xi)L^{\beta\beta}(x,\xi) - c_2(x)L_\xi^{\alpha\beta}(x,\xi) \end{aligned} \tag{10d}$$

with boundary conditions

$$L^{\alpha\alpha}(x,0) = \frac{\epsilon_2(0)}{q\epsilon_1(0)}L^{\alpha\beta}(x,0) \tag{11a}$$

$$L^{\alpha\beta}(x,x) = \frac{c_1(x)}{\epsilon_1(x)+\epsilon_1(x)} \tag{11b}$$

$$L^{\beta\alpha}(x,x) = -\frac{c_2(x)}{\epsilon_1(x)+\epsilon_1(x)} \tag{11c}$$

$$L^{\beta\beta}(x,0) = \frac{q\epsilon_1(0)}{\epsilon_2(0)}L^{\beta\alpha}(x,0) \tag{11d}$$

defined over the triangular domain (8). Proofs of existence and uniqueness for solutions of (6)-(7) and (10)-(11) were given in [17], and it was also proved that the solutions are continuous over $\mathcal{T}$. As the transform (3) is invertible, the stability properties of (1) and (5) are equivalent. This was utilized in [18] when deriving the controller achieving (2) for $\bar{x} = 0$, and will in this paper be utilized in a similar manner do derive a controller that achieves (2) some arbitrary $\bar{x} \in (0,\ 1)$.

B. Relationships in space and time

Lemma 1: For a PDE on the form

$$u_t + \epsilon(x)u_x = f(x)g(t), \quad x \in (-\infty, \infty),\ t \in [0, \infty) \tag{12}$$

with $\epsilon(x) > 0 \ \ \forall x$ and initial condition $u(x,0) = u_0(x)$, the following relationship apply to two arbitrary points $y, z \in (-\infty, \infty)$

$$\begin{aligned} u(y, t-\phi(y)) - u(z, t-\phi(z)) \\ = \int_{\phi(y)}^{\phi(z)} f(\phi^{-1}(\tau)) g(t-\tau) d\tau \end{aligned} \tag{13}$$

for $t \geq \max\{\phi(y), \phi(z)\}$, where

$$\phi(z) = \int_z^1 \frac{d\gamma}{\epsilon(\gamma)}. \tag{14}$$

Proof: Using Lemma 2 From [18], we derive the following relationships between two arbitrary points y and z

$$\begin{aligned} u(y,t) = u_0(\phi^{-1}(t+\phi(y))) \\ + \int_0^t f(\phi^{-1}(t-\gamma+\phi(y))) g(\gamma) d\gamma \end{aligned} \tag{15}$$

$$\begin{aligned} u(z,t) = u_0(\phi^{-1}(t+\phi(z))) \\ + \int_0^t f(\phi^{-1}(t-\gamma+\phi(z))) g(\gamma) d\gamma \end{aligned} \tag{16}$$

Assuming $t \geq \max\{\phi(y), \phi(z)\}$, we shift time in both equations to obtain

$$\begin{aligned} u(y, t-\phi(y)) = u_0(\phi^{-1}(t)) \\ + \int_0^{t-\phi(y)} f(\phi^{-1}(t-\gamma)) g(\gamma) d\gamma \end{aligned} \tag{17}$$

$$\begin{aligned} u(z, t-\phi(z)) = u_0(\phi^{-1}(t)) \\ + \int_0^{t-\phi(z)} f(\phi^{-1}(t-\gamma)) g(\gamma) d\gamma. \end{aligned} \tag{18}$$

Thus, the initial condition can be eliminated by subtracting (18) from (17), yielding

$$\begin{aligned} u(y, t-\phi(y)) - u(z, t-\phi(z)) \\ = \int_{t-\phi(z)}^{t-\phi(y)} f(\phi^{-1}(t-\gamma)) g(\gamma) d\gamma. \end{aligned} \tag{19}$$

An appropriate substitution $\tau = t - \gamma$ in the integral yields the desired result. ■

By using Lemma 1, we can characterize solutions α and β of (5) at two arbitrary points in the domain by time shifts as follows.

Lemma 2: For two arbitrary points $y, z \in [0,\ 1]$, solutions α and β of (5) satisfy

$$\alpha(y, t-\phi_\alpha(y)) - \alpha(z, t-\phi_\alpha(z)) = \Phi_\alpha(y,z) X(t) \tag{20a}$$

for $t \geq \max\{\phi_\alpha(y), \phi_\alpha(z)\}$ and

$$\beta(y, t-\phi_\beta(y)) - \beta(z, t-\phi_\beta(z)) = \Phi_\beta(y,z) X(t), \tag{20b}$$

for $t \geq \max\{\phi_\beta(y), \phi_\beta(z)\}$, where

$$\Phi_\alpha(y,z) = -\epsilon_1(0) \int_{\phi_\alpha(y)}^{\phi_\alpha(z)} K^{uu}(\phi_\alpha^{-1}(\tau), 0) C e^{-A\tau} d\tau \tag{21}$$

$$\Phi_\beta(y,z) = -\epsilon_1(0) \int_{\phi_\beta(y)}^{\phi_\beta(z)} K^{vu}(\phi_\beta^{-1}(\tau), 0) C e^{-A\tau} d\tau \tag{22}$$

with

$$\phi_\alpha(z) = \int_z^1 \frac{d\gamma}{\epsilon_1(\gamma)} \tag{23}$$

$$\phi_\beta(z) = \int_0^z \frac{d\gamma}{\epsilon_2(\gamma)}. \tag{24}$$

Proof: The proof for (20a) is independent from (20b), and for clarity of presentation, they will be proven separately.

The α-subsystem: The alpha-subsystem (5a) has the form required by Lemma 1 with $u(x,t) = \alpha(x,t)$, $\epsilon(x) = \epsilon_1(x)$, $f(x) = -\epsilon_1(0)K^{uu}(x,0)$ and $g(t) = CX(t)$. The result (20a) with (21) and (23) therefore follows by Lemma 1 and the semigroup property of (5e), i.e. $X(t-\tau) = e^{-A\tau}X(t)$.

The β-subsystem: Application of Lemma 1 is not straight forward to use on (5b) since the sign of $\epsilon_2(x)$ is not as required by Lemma 1. This is resolved by the change of variables

$$\bar{\beta}(x,t) := \beta(1-x,t) \Leftrightarrow \beta(x,t) = \bar{\beta}(1-x,t) \tag{25}$$

and

$$\bar{\epsilon}_2(x) := \epsilon_2(1-x) \tag{26}$$

so that (5b) becomes

$$\bar{\beta}_t(x,t) + \bar{\epsilon}_2(x)\bar{\beta}_x(x,t) = -\epsilon_1(0)K^{vu}(1-x,0)CX(t). \tag{27}$$

Lemma 1 may now be applied with $u(x,t) = \bar{\beta}(x,t)$, $\epsilon(x) = \bar{\epsilon}_2(x)$, and $f(x) = -\epsilon_1(0)K^{vu}(1-x,0)$ to achieve

$$\begin{aligned}&\bar{\beta}(y, t-h_\beta(y)) - \bar{\beta}(z, t-h_\beta(z)) \\ &\quad = -\epsilon_1(0) \int_{h_\beta(y)}^{h_\beta(z)} K^{vu}(1-h_\beta^{-1}(\tau)) C X(t-\tau) d\tau\end{aligned} \tag{28}$$

for $t \geq \max\{h_\beta(y), h_\beta(z)\}$ where

$$h_\beta(z) = \int_z^1 \frac{d\tau}{\bar{\epsilon}_2(\tau)}. \tag{29}$$

Inserting for β and substituting $y \to 1-y$ and $z \to 1-z$ yields

$$\begin{aligned}&\beta(y, t-h_\beta(1-y)) - \beta(z, t-h_\beta(1-z)) \\ &\quad = -\epsilon_1(0) \int_{h_\beta(1-y)}^{h_\beta(1-z)} K^{vu}(1-h_\beta^{-1}(\tau)) \\ &\quad \times CX(t-\tau) d\tau\end{aligned} \tag{30}$$

which is valid for $t \geq \max\{h_\beta(1-y), h_\beta(1-z)\}$. Comparing (24) and (29), we have $\phi_\beta(z) = h_\beta(1-z)$ and $\phi_\beta^{-1}(\tau) = 1 - h_\beta^{-1}(\tau)$, and (20b) with (22) and (24) follows. ■

C. Relationships to actuation

By utilizing the results in Lemma 2, we characterize the solutions α and β of (5) in terms of the actuation $V(t) = \beta(1,t)$ and disturbance $X(t)$.

Lemma 3: For every $y \in [0,\ 1]$, the solutions α and β of (5) satisfy

$$\alpha(y,t) = qV(t-\eta_\alpha(y)) + \Psi_\alpha(y)X(t) \tag{31a}$$

for $t \geq \eta_\alpha(y)$ and

$$\beta(y,t) = \ \ V(t-\eta_\beta(y)) + \Psi_\beta(y)X(t) \tag{31b}$$

for $t \geq \eta_\beta(y)$, where

$$\begin{aligned}\Psi_\alpha(y) &= \Phi_\alpha(y,0)e^{A\phi_\alpha(y)} \\ &\quad + (q\Phi_\beta(0,1)+C)e^{A(\phi_\alpha(y)-\phi_\alpha(0))} \end{aligned}\tag{32}$$

$$\Psi_\beta(y) = \Phi_\beta(y,1)e^{A\phi_\beta(y)} \tag{33}$$

and

$$\eta_\alpha(y) = \phi_\beta(1) + \phi_\alpha(0) - \phi_\alpha(y) \tag{34}$$

$$\eta_\beta(y) = \phi_\beta(1) - \phi_\beta(y). \tag{35}$$

Proof: Again, we'll split the proof into two parts, dealing with the α and β subsystems separately.

The α subsystem: From (20a), with $z = 0$ and time shifting $\phi_\alpha(y)$ units assuming $t \geq \phi_\alpha(0) - \phi_\alpha(y)$, we find

$$\begin{aligned}\alpha(y,t) &= \alpha(0, t-\phi_\alpha(0)+\phi_\alpha(y)) \\ &\quad + \Phi_\alpha(y,0)X(t+\phi_\alpha(y)).\end{aligned}\tag{36}$$

Inserting for the boundary condition (5c), we find

$$\begin{aligned}\alpha(y,t) &= q\beta(0, t-\phi_\alpha(0)+\phi_\alpha(y)) \\ &\quad + CX(t-\phi_\alpha(0)+\phi_\alpha(y)) \\ &\quad + \Phi_\alpha(y,0)X(t+\phi_\alpha(y)).\end{aligned}\tag{37}$$

From (20b), with $y = 0$, $z = 1$ and noticing that $\phi_\beta(0) = 0$, we find for $t \geq \phi_\beta(1)$

$$\beta(0,t) = \beta(1, t-\phi_\beta(1)) + \Phi_\beta(0,1)X(t). \tag{38}$$

Shifting time $\phi_\alpha(y) - \phi_\alpha(0)$ units assuming $t \geq \phi_\beta(1) + \phi_\alpha(0) - \phi_\alpha(y)$, we find

$$\begin{aligned}&\beta(0, t-\phi_\alpha(0)+\phi_\alpha(y)) \\ &\quad = \beta(1, t-\phi_\beta(1)-\phi_\alpha(0)+\phi_\alpha(y)) \\ &\quad + \Phi_\beta(0,1)X(t-\phi_\alpha(0)+\phi_\alpha(y)).\end{aligned}\tag{39}$$

Substituting (39) into (37), gives

$$\begin{aligned}\alpha(y,t) &= q\beta(1, t-\phi_\beta(1)-\phi_\alpha(0)+\phi_\alpha(y)) \\ &\quad + q\Phi_\beta(0,1)X(t-\phi_\alpha(0)+\phi_\alpha(y)), \\ &\quad + CX(t-\phi_\alpha(0)+\phi_\alpha(y)) \\ &\quad + \Phi_\alpha(y,0)X(t+\phi_\alpha(y))\end{aligned}\tag{40}$$

for $t \geq \phi_\beta(1) + \phi_\alpha(0) - \phi_\alpha(y)$. Using the semigroup property of (5e), results in

$$\begin{aligned}\alpha(y,t) &= q\beta(1, t - \phi_\beta(1) - \phi_\alpha(0) + \phi_\alpha(y)) \\ &\quad + q\Phi_\beta(0,1)e^{A(\phi_\alpha(y)-\phi_\alpha(0))}X(t) \\ &\quad + Ce^{A(\phi_\alpha(y)-\phi_\alpha(0))}X(t) \\ &\quad + \Phi_\alpha(y,0)e^{A\phi_\alpha(y)}X(t). \end{aligned} \tag{41}$$

By substituting for the boundary condition (5d), and $\Psi_\alpha(y)$ and $\eta_\alpha(y)$ as defined in (32) and (34), respectively, the first part of the lemma is verified.

The β subsystem: From (20b), with $z = 1$ and shifting time $\phi_\beta(y)$ units assuming $t \geq \phi_\beta(1) - \phi_\beta(y)$, we find

$$\begin{aligned}\beta(y,t) &= \beta(1, t - \phi_\beta(1) + \phi_\beta(y)) \\ &\quad + \Phi_\beta(y,1)X(t + \phi_\beta(y)). \end{aligned} \tag{42}$$

Substituting for the boundary condition (5d) and $\Psi_\beta(y)$ and $\eta_\beta(y)$ as defined in (33) and (35), respectively, and using the semigroup property of (5e), the lemma's second half is proven. ■

D. Control design

The lemmas derived above will be used to derive the control law achieving (2). Inserting (9) into (2), the controller objective is stated in terms of the α, β variables

$$\begin{aligned}&\alpha(\bar{x},t) + \int_0^{\bar{x}} L^{\alpha\alpha}(\bar{x},\xi)\alpha(\xi,t)d\xi \\ &\qquad + \int_0^{\bar{x}} L^{\alpha\beta}(\bar{x},\xi)\beta(\xi,t)d\xi \\ &= r\beta(\bar{x},t) + r\int_0^{\bar{x}} L^{\beta\alpha}(\bar{x},\xi)\alpha(\xi,t)d\xi \\ &\qquad + r\int_0^{\bar{x}} L^{\beta\beta}(\bar{x},\xi)\beta(\xi,t)d\xi. \end{aligned} \tag{43}$$

We seek a control signal $V(t)$ such that (43) is achieved. For completeness, we first state the result for the case $\bar{x} = 0$, which was given in [18].

Theorem 4: Suppose $q \neq 0$, $r \neq q$ and $V(t) = K_0 X(t)$, where

$$K_0 = \left(\frac{1}{r-q}C - \Phi_\beta(0,1)\right)e^{A\phi_\beta(1)}. \tag{44}$$

Then the control law (4) achieves (2) for all $t \geq \phi_\beta(1)$.

Proof: The result follows from letting $\bar{x} = 0$ in (55). ■

Next, we generalize the result by allowing $\bar{x} \in (0,1)$ and state two versions of the controller. The first version, referred to as the recursive controller, is simpler to derive but requires storage of past inputs. The second version is a pure state feedback controller that exploits the fact that past inputs are implicitly stored in the system states.

Theorem 5 (Recursive): Suppose $q \neq 0$, $r \neq 0$, $\bar{x} \in (0,1)$ and let

$$\begin{aligned} V(t) = \frac{q}{r}V(t-d_r(\bar{x})) + \frac{q}{r}\int_0^{\bar{x}} L^\alpha(\bar{x},\xi)V(t-d_\alpha(\xi,\bar{x}))d\xi \\ + \frac{1}{r}\int_0^{\bar{x}} L^\beta(\bar{x},\xi)V(t-d_\beta(\xi,\bar{x}))d\xi \\ + \frac{1}{r}K_r(\bar{x})X(t) \end{aligned} \tag{45}$$

where

$$d_\alpha(\xi,\bar{x}) = \eta_\alpha(\xi) - \eta_\beta(\bar{x}) \tag{46}$$

$$d_\beta(\xi,\bar{x}) = \eta_\beta(\xi) - \eta_\beta(\bar{x}) \tag{47}$$

$$d_r(\bar{x}) = d_\alpha(\bar{x},\bar{x}) \tag{48}$$

and

$$\begin{aligned} K_r(\bar{x}) = (\int_0^{\bar{x}} (L^\alpha(\bar{x},\xi)\Psi_\alpha(\xi) + L^\beta(\bar{x},\xi)\Psi_\beta(\xi))d\xi \\ + \Psi_\alpha(\bar{x}) - r\Psi_\beta(\bar{x}))e^{A\eta_\beta(\bar{x})} \end{aligned} \tag{49}$$

with

$$L^\alpha(\bar{x},\xi) = L^{\alpha\alpha}(\bar{x},\xi) - rL^{\beta\alpha}(\bar{x},\xi) \tag{50}$$

$$L^\beta(\bar{x},\xi) = L^{\alpha\beta}(\bar{x},\xi) - rL^{\beta\beta}(\bar{x},\xi) \tag{51}$$

and $L^{\alpha\alpha}(\bar{x},\xi), L^{\alpha\beta}(\bar{x},\xi), L^{\beta\alpha}(\bar{x},\xi), L^{\beta\beta}(\bar{x},\xi)$ is the solution to (10) and (11). Then the control law (4) achieves (2) for all $t \geq \eta_\alpha(\bar{x})$.

Proof: With the definitions (50) and (51), the controller objective (43), which is equivalent to (2), can be stated as

$$\begin{aligned} \alpha(\bar{x},t) - r\beta(\bar{x},t) = -\int_0^{\bar{x}} L^\alpha(\bar{x},\xi)\alpha(\xi,t)d\xi \\ - \int_0^{\bar{x}} L^\beta(\bar{x},\xi)\beta(\xi,t)d\xi. \end{aligned} \tag{52}$$

Using Lemma 3 successively with $y = \bar{x}$ and $y = \xi$, and inserting into (52) yields

$$\begin{aligned} qV(t-\eta_\alpha(\bar{x})) + \Psi_\alpha(\bar{x})X(t) - rV(t-\eta_\beta(\bar{x})) \\ - r\Psi_\beta(\bar{x})X(t) \\ = -\int_0^{\bar{x}} L^\alpha(\bar{x},\xi)(qV(t-\eta_\alpha(\xi)) \\ + \Psi_\alpha(\xi)X(t))d\xi \\ - \int_0^{\bar{x}} L^\beta(\bar{x},\xi)(V(t-\eta_\beta(\xi)) \\ + \Psi_\beta(\xi)X(t))d\xi \end{aligned} \tag{53}$$

which is valid for $t \geq \eta_\alpha(\bar{x})$. Rearranging (53) and time shifting $\eta_\beta(\bar{x})$ units, we find

$$\begin{aligned} rV(t) &= qV(t - \eta_\alpha(\bar{x}) + \eta_\beta(\bar{x})) \\ &\quad + (\Psi_\alpha(\bar{x}) - r\Psi_\beta(\bar{x}))X(t + \eta_\beta(\bar{x})) \\ &\quad + \int_0^{\bar{x}} L^\alpha(\bar{x}, \xi)(qV(t - \eta_\alpha(\xi) + \eta_\beta(\bar{x})) \\ &\quad + \Psi_\alpha(\xi)X(t + \eta_\beta(\bar{x})))d\xi \\ &\quad + \int_0^{\bar{x}} L^\beta(\bar{x}, \xi)(V(t - \eta_\beta(\xi) + \eta_\beta(\bar{x})) \\ &\quad + \Psi_\beta(\xi)X(t + \eta_\beta(\bar{x})))d\xi. \end{aligned} \tag{54}$$

A slight rearrangement of the terms in the integrals yields

$$\begin{aligned} rV(t) &= qV(t - \eta_\alpha(\bar{x}) + \eta_\beta(\bar{x})) \\ &\quad + (\Psi_\alpha(\bar{x}) - r\Psi_\beta(\bar{x}))X(t + \eta_\beta(\bar{x})) \\ &\quad + \int_0^{\bar{x}} (L^\alpha(\bar{x}, \xi)\Psi_\alpha(\xi) + L^\beta(\bar{x}, \xi)\Psi_\beta(\xi))d\xi \\ &\quad \times X(t + \eta_\beta(\bar{x})) \\ &\quad + \int_0^{\bar{x}} L^\alpha(\bar{x}, \xi)qV(t - \eta_\alpha(\xi) + \eta_\beta(\bar{x}))d\xi \\ &\quad + \int_0^{\bar{x}} L^\beta(\bar{x}, \xi)V(t - \eta_\beta(\xi) + \eta_\beta(\bar{x}))d\xi. \end{aligned} \tag{55}$$

The result now follows by using the semigroup property of (5e), replacing terms in (55) by the definitions (46)–(49), and dividing by r.

The control cancels the disturbance exactly in finite time, governed by the time of travel from $x = 1$ via $x = 0$ and back to $x = \bar{x}$, which equals $\eta_\alpha(\bar{x})$. ■

The controller of Theorem 5 has the disadvantage that it requires storage of past control inputs in the time interval $[t - d_r(\bar{x}), t]$. In addition, it has a pure feed forward structure relying on stored inputs rather than system states which presents a potential robustness issue. Using Lemma 3, which relates the system input to its states, it is possible to replace past inputs by states to form a state feedback controller that avoids these drawbacks.

Theorem 6 (Pure state feedback): Suppose $q \neq 0$, $r \neq 0$, $\bar{x} \in (0, 1)$ and let

$$\begin{aligned} V(t) &= \frac{1}{r}K_{psf}(\bar{x})X(t) + \frac{1}{r}\delta(\bar{x}, \bar{x}, t) \\ &\quad + \frac{1}{r}\int_0^{\bar{x}} L^\alpha(\bar{x}, \xi)\delta(\xi, \bar{x}, t)d\xi \\ &\quad + \frac{1}{r}\int_0^{\bar{x}} L^\beta(\bar{x}, \xi)\beta(\phi_\beta^{-1}(\kappa_\beta(\xi, \bar{x})), t)d\xi \end{aligned} \tag{56}$$

where

$$\begin{aligned} K_{psf}(\bar{x}) &= \Omega_\alpha(\bar{x}, \bar{x}) - r\Psi_\beta(\bar{x})e^{A\eta_\beta(\bar{x})} \\ &\quad + \int_0^{\bar{x}} L^\alpha(\bar{x}, \xi)\Omega_\alpha(\xi, \bar{x})d\xi \\ &\quad + \int_0^{\bar{x}} L^\beta(\bar{x}, \xi)\Omega_\beta(\xi, \bar{x})d\xi \end{aligned} \tag{57}$$

and

$$\delta(\xi,\bar{x},t)=\begin{cases}\delta_\alpha(\xi,\bar{x},t) & \text{if } \kappa_\alpha(\xi,\bar{x})\le\phi_\alpha(0)\\ \delta_\beta(\xi,\bar{x},t) & \text{otherwise}\end{cases} \tag{58}$$

$$\delta_\alpha(\xi,\bar{x},t)=\alpha(\phi_\alpha^{-1}(\kappa_\alpha(\xi,\bar{x})),t) \tag{59}$$
$$\delta_\beta(\xi,\bar{x},t)=q\beta(\phi_\beta^{-1}(\kappa_\alpha(\xi,\bar{x})-\phi_\alpha(0)),t) \tag{60}$$

with

$$\Omega_{\alpha\alpha}(\xi,\bar{x})=\Phi_\alpha(\xi,\phi_\alpha^{-1}(\kappa_\alpha(\xi,\bar{x})))e^{A\kappa_\alpha(\xi,\bar{x})} \tag{61}$$
$$\Omega_{\alpha\beta}(\xi,\bar{x})=(q\Phi_\beta(0,\phi_\beta^{-1}(\kappa_\alpha(\xi,\bar{x})-\phi_\alpha(0)))+C)e^{A\kappa_\beta(\xi,\bar{x})} + \Phi_\alpha(\xi,0)e^{A\kappa_\alpha(\xi,\bar{x})} \tag{62}$$
$$\Omega_\alpha(\xi,\bar{x})=\begin{cases}\Omega_{\alpha\alpha}(\xi,\bar{x}) & \text{if } \kappa_\alpha(\xi,\bar{x})\le\phi_\alpha(0)\\ \Omega_{\alpha\beta}(\xi,\bar{x}) & \text{otherwise}\end{cases} \tag{63}$$
$$\Omega_\beta(\xi,\bar{x})=\Phi_\beta(\xi,\phi_\beta^{-1}(\kappa_\beta(\xi,\bar{x})))e^{A\kappa_\beta(\xi,\bar{x})} \tag{64}$$

and

$$\kappa_\alpha(\xi,\bar{x})=\phi_\alpha(\xi)+\eta_\beta(\bar{x}) \tag{65}$$
$$\kappa_\beta(\xi,\bar{x})=\phi_\beta(\xi)+\eta_\beta(\bar{x}). \tag{66}$$

Then the control law (4) achieves (2) for all $t\ge\eta_\beta(\bar{x})$.

Remark 7: $\alpha(x,t)$ and $\beta(x,t)$ in (56) and (58) are obtained from the states $u(x,t)$ and $v(x,t)$ of system (1) by means of the transformation (3).

Proof: We start with a slightly rearranged version of (52)

$$r\beta(\bar{x},t)=\alpha(\bar{x},t)+\int_0^{\bar{x}}L^\alpha(\bar{x},\xi)\alpha(\xi,t)d\xi + \int_0^{\bar{x}}L^\beta(\bar{x},\xi)\beta(\xi,t)d\xi. \tag{67}$$

Using (31b) in Lemma 3, and inserting into (67), we arrive at

$$rV(t-\eta_\beta(\bar{x}))+r\Psi_\beta(\bar{x})X(t)=\alpha(\bar{x},t) + \int_0^{\bar{x}}L^\alpha(\bar{x},\xi)\alpha(\xi,t)d\xi + \int_0^{\bar{x}}L^\beta(\bar{x},\xi)\beta(\xi,t)d\xi \tag{68}$$

for $t\ge\eta_\beta(\bar{x})$. Time shifting $\eta_\beta(\bar{x})$ units and rearranging results in

$$rV(t)=-r\Psi_\beta(\bar{x})X(t+\eta_\beta(\bar{x}))+\alpha(\bar{x},t+\eta_\beta(\bar{x})) + \int_0^{\bar{x}}L^\alpha(\bar{x},\xi)\alpha(\xi,t+\eta_\beta(\bar{x}))d\xi + \int_0^{\bar{x}}L^\beta(\bar{x},\xi)\beta(\xi,t+\eta_\beta(\bar{x}))d\xi \tag{69}$$

which is valid for $t\ge0$. We will have to find expressions for $\alpha(\xi,t+\eta_\beta(\bar{x}))$ and $\beta(\xi,t+\eta_\beta(\bar{x}))$ that don't include time shifts.

The α-part: The α-part is a bit tricky, since the signal conditionally will have to be propagated through the boundary condition (5c), depending on the values of ξ and $\bar{x}$. From (20a), solutions to (5a) satisfy

$$\alpha(\xi, t - \phi_\alpha(\xi)) - \alpha(z, t - \phi_\alpha(z)) = \Phi_\alpha(\xi, z)X(t). \tag{70}$$

Shifting time by $\phi_\alpha(\xi) + \eta_\beta(\bar{x})$, we find

$$\begin{aligned}\alpha(\xi, t + \eta_\beta(\bar{x})) = \alpha(z, t - \phi_\alpha(z) + \kappa_\alpha(\xi, \bar{x})) \\ + \Phi_\alpha(\xi, z)X(t + \kappa_\alpha(\xi, \bar{x})),\end{aligned} \tag{71}$$

where (65) has been used. We would now like to select $z \in [0, 1]$ such that

$$\phi_\alpha(z) = \kappa_\alpha(\xi, \bar{x}). \tag{72}$$

Since the inverse of ϕ_α is defined on $[0, \phi_\alpha(0)]$, this is possible if

$$\kappa_\alpha(\xi, \bar{x}) \leq \phi_\alpha(0) \tag{73}$$

in which case we select $z = \phi_\alpha^{-1}(\kappa_\alpha(\xi, \bar{x}))$ and obtain

$$\begin{aligned}\alpha(\xi, t + \eta_\beta(\bar{x})) = \alpha(\phi_\alpha^{-1}(\kappa_\alpha(\xi, \bar{x})), t) \\ + \Phi_\alpha(\xi, \phi_\alpha^{-1}(\kappa_\alpha(\xi, \bar{x}))) \\ \times X(t + \kappa_\alpha(\xi, \bar{x})).\end{aligned} \tag{74}$$

Using the semigroup property of (5e) along with the definition (63), we obtain

$$\alpha(\xi, t + \eta_\beta(\bar{x})) = \alpha(\phi_\alpha^{-1}(\kappa_\alpha(\xi, \bar{x})), t) + \Omega_{\alpha\alpha}(\xi, \bar{x})X(t). \tag{75}$$

If (73) does not hold, the signal has to be propagated through the boundary condition (5c). In this case we select $z = 0$ and (71) becomes

$$\begin{aligned}\alpha(\xi, t + \eta_\beta(\bar{x})) = \alpha(0, t - \phi_\alpha(0) + \kappa_\alpha(\xi, \bar{x})) \\ + \Phi_\alpha(\xi, 0)X(t + \kappa_\alpha(\xi, \bar{x})).\end{aligned} \tag{76}$$

Substituting the boundary condition (5c) into (76) gives

$$\begin{aligned}\alpha(\xi, t + \eta_\beta(\bar{x})) = q\beta(0, t - \phi_\alpha(0) + \kappa_\alpha(\xi, \bar{x})) \\ + CX(t - \phi_\alpha(0) + \kappa_\alpha(\xi, \bar{x})) \\ + \Phi_\alpha(\xi, 0)X(t + \kappa_\alpha(\xi, \bar{x})).\end{aligned} \tag{77}$$

From (20b), solutions to (5b) satisfy

$$\beta(0, t) - \beta(z, t - \phi_\beta(z)) = \Phi_\beta(0, z)X(t). \tag{78}$$

Shifting time by $\kappa_\alpha(\xi, \bar{x}) - \phi_\alpha(0)$, we find

$$\begin{aligned}&\beta(0, t - \phi_\alpha(0) + \kappa_\alpha(\xi, \bar{x})) \\ &= \beta(z, t - \phi_\beta(z) - \phi_\alpha(0) + \kappa_\alpha(\xi, \bar{x})) \\ &+ \Phi_\beta(0, z)X(t - \phi_\alpha(0) + \kappa_\alpha(\xi, \bar{x})).\end{aligned} \tag{79}$$

Substituting (79) into (77) gives

$$\begin{aligned}\alpha(\xi, t + \eta_\beta(\bar{x})) = q\beta(z, t - \phi_\beta(z) - \phi_\alpha(0) + \kappa_\alpha(\xi, \bar{x})) \\ + q\Phi_\beta(0, z)X(t - \phi_\alpha(0) + \kappa_\alpha(\xi, \bar{x})) \\ + CX(t - \phi_\alpha(0) + \kappa_\alpha(\xi, \bar{x})) \\ + \Phi_\alpha(\xi, 0)X(t + \kappa_\alpha(\xi, \bar{x})).\end{aligned} \tag{80}$$

We now select $z = \phi_\beta^{-1}(\kappa_\alpha(\xi,\bar{x}) - \phi_\alpha(0))$, which is well defined since $0 < \kappa_\alpha(\xi,\bar{x}) - \phi_\alpha(0) \leq \phi_\beta(1)$. We find

$$\begin{aligned}\alpha(\xi, t+\eta_\beta(\bar{x})) = q\beta(\phi_\beta^{-1}(\kappa_\alpha(\xi,\bar{x}) - \phi_\alpha(0)), t) \\ + (q\Phi_\beta(0, \phi_\beta^{-1}(\kappa_\alpha(\xi,\bar{x}) - \phi_\alpha(0))) + C) \\ \times X(t - \phi_\alpha(0) + \kappa_\alpha(\xi,\bar{x})) \\ + \Phi_\alpha(\xi,0)X(t+\kappa_\alpha(\xi,\bar{x})).\end{aligned} \tag{81}$$

Using the semigroup property of (5e) along with the definition (64), we obtain

$$\begin{aligned}\alpha(\xi, t+\eta_\beta(\bar{x})) = q\beta(\phi_\beta^{-1}(\kappa_\alpha(\xi,\bar{x}) - \phi_\alpha(0)), t) \\ + \Omega_{\alpha\beta}(\xi,\bar{x})X(t).\end{aligned} \tag{82}$$

The above results (75) and (82) can be written more compactly by defining $\delta(\xi,\bar{x},t)$ and $\Omega_\alpha(\xi,\bar{x})$ as in (58)–(60) and (63), respectively, yielding

$$\alpha(\xi, t+\eta_\beta(\bar{x})) = \delta(\xi,\bar{x},t) + \Omega_\alpha(\xi,\bar{x})X(t). \tag{83}$$

The β-part: From (20b) in Lemma 2, solutions to (5b) satisfy

$$\beta(\xi, t-\phi_\beta(\xi)) - \beta(z, t-\phi_\beta(z)) = \Phi_\beta(\xi,z)X(t). \tag{84}$$

Shifting time by $\phi_\beta(\xi) + \eta_\beta(\bar{x})$, we find

$$\begin{aligned}\beta(\xi, t+\eta_\beta(\bar{x})) = \beta(z, t - \phi_\beta(z) + \kappa_\beta(\xi,\bar{x})) \\ + \Phi_\beta(\xi,z)X(t+\kappa_\beta(\xi,\bar{x})).\end{aligned} \tag{85}$$

where (66) has been used. We now select $z = \phi_\beta^{-1}(\kappa_\beta(\xi,\bar{x}))$, which is well defined since $0 < \kappa_\beta(\xi,\bar{x}) \leq \phi_\beta(1)$, and obtain

$$\begin{aligned}\beta(\xi, t+\eta_\beta(\bar{x})) = \beta(\phi_\beta^{-1}(\kappa_\beta(\xi,\bar{x})), t) \\ + \Phi_\beta(\xi, \phi_\beta^{-1}(\kappa_\beta(\xi,\bar{x})))X(t+\kappa_\beta(\xi,\bar{x})).\end{aligned} \tag{86}$$

Defining $\Omega_\beta(\xi,\bar{x})$ as in (64) we can write

$$\beta(\xi, t+\eta_\beta(\bar{x})) = \beta(\phi_\beta^{-1}(\kappa_\beta(\xi,\bar{x})), t) + \Omega_\beta(\xi,\bar{x})X(t). \tag{87}$$

The expression (56) now follows by substitution of (83) and (87) into (69) and using the definitions (57)–(66). The control law will cancel the disturbance exactly in finite time, governed by the time of travel from $x = 1$ to $x = \bar{x}$, which equals $\eta_\beta(\bar{x})$. ■

IV. State observer

The two versions of the control law derived in the previous section require full knowledge of the system states $u(x,t)$, $v(x,t)$ as well as the disturbance $X(t)$. While they constitute the main theoretical results of the present paper, and are verified in numerical simulations in the next Section, it is of interest to compare with the more realistic problem of output feedback control. In practical problems, measured signals are often limited to sensing at $x = 1$, a fact that requires the control laws to be modified. If we assume that estimates of $u(x,t)$, $v(x,t)$ and $X(t)$ are available and rely on the certainty equivalence principle, the controllers can be implemented by replacing states in the controller by their corresponding estimates. The estimates will have to be generated from the only signals available; the sensing at $x = 1$ and the generated controller input $U(t)$. Such an observer estimating the states of the system, was derived in [17], and a

proof of exponential convergence was also given. In fact, the estimates were proven to reach their real values in *finite* time.

A modification of the observer from [17] was done in [18] to accommodate the disturbance term entering at the boundary. The observer takes the applied input $U(t)$ and one measurement from the system as inputs, and estimates the system states as well as the disturbance. For completeness, we repeat here the governing equations for the observer developed in [18]. It is given as

$$\begin{aligned}\hat{u}_t(x,t) &= -\epsilon_1(x)\hat{u}_x(x,t) + c_1(x)\hat{v}(x,t) \\ &\quad + p_1(x)(y(t) - \hat{u}(1,t)) && \text{(88a)}\\ \hat{v}_t(x,t) &= \epsilon_2(x)\hat{v}_x(x,t) + c_2(x)\hat{u}(x,t) \\ &\quad + p_2(x)(y(t) - \hat{u}(1,t)) && \text{(88b)}\\ \hat{u}(0,t) &= q\hat{v}(0,t) + C\hat{X}(t) && \text{(88c)}\\ \hat{v}(1,t) &= U(t) && \text{(88d)}\\ \dot{\hat{X}} &= A\hat{X} + e^{A\phi_\alpha(0)}L(y(t) - \hat{u}(1,t)) && \text{(88e)}\end{aligned}$$

where

$$y(t) = u(1,t) \tag{89}$$

is the measurement. The matrix L is a gain matrix chosen such that $(A - LC)$ is Hurwitz. The functions $p_1(x)$ and $p_2(x)$ are injection gains, given as

$$\begin{aligned}p_1(x) &= Ce^{A\phi_\alpha(x)}L - \epsilon_1(1)P^{uu}(x,1) \\ &\quad - \int_x^1 P^{uu}(x,1)Ce^{A\phi_\alpha(\xi)}Ld\xi && \text{(90a)}\\ p_2(x) &= -\epsilon_1(1)P^{vu}(x,1) \\ &\quad - \int_x^1 P^{vu}(x,1)Ce^{A\phi_\alpha(\xi)}Ld\xi && \text{(90b)}\end{aligned}$$

where the kernels are the solution to[1]

$$\begin{aligned}&\epsilon_1(x)P^{uu}_x(x,\xi) + \epsilon_1(\xi)P^{uu}_\xi(x,\xi) \\ &\qquad = -\epsilon_1'(\xi)P^{uu}(x,\xi) + c_1(x)P^{vu}(x,\xi) && \text{(91a)}\\ &\epsilon_1(x)P^{uv}_x(x,\xi) - \epsilon_2(\xi)P^{uv}_\xi(x,\xi) \\ &\qquad = \epsilon_2'(\xi)P^{uv}(x,\xi) + c_1(x)P^{vv}(x,\xi) && \text{(91b)}\\ &\epsilon_2(x)P^{vu}_x(x,\xi) - \epsilon_1(\xi)P^{vu}_\xi(x,\xi) \\ &\qquad = \epsilon_1'(\xi)P^{vu}(x,\xi) - c_2(x)P^{uu}(x,\xi) && \text{(91c)}\\ &\epsilon_2(x)P^{vv}_x(x,\xi) + \epsilon_2(\xi)P^{uv}_\xi(x,\xi) \\ &\qquad = -\epsilon_2'(\xi)P^{vv}(x,\xi) - c_2(x)P^{uv}(x,\xi) && \text{(91d)}\end{aligned}$$

[1]Apparently, the original kernels equations stated in [17] contained some typos. The kernel equations stated here are the ones found in [18].

with boundary conditions

$$P^{uu}(0,\xi) = qP^{vu}(0,\xi) \tag{92a}$$

$$P^{uv}(x,x) = \frac{c_1(x)}{\epsilon_1(x)+\epsilon_2(x)} \tag{92b}$$

$$P^{vu}(x,x) = -\frac{c_2(x)}{\epsilon_1(x)+\epsilon_2(x)} \tag{92c}$$

$$P^{vv}(0,\xi) = \frac{1}{q}P^{uv}(0,\xi) \tag{92d}$$

defined over the triangular domain

$$\mathcal{T}_0 = \{(x,\xi) \ : \ 0 \leq x \leq \xi \leq 1\}. \tag{93}$$

It was proven in [17] that there exists a unique solution to (91)-(92), and that the solution is continuous over $\mathcal{T}_0$. For a proof of exponential convergence of the estimates, the interested reader is referred to [18].

V. Applications to the heave problem

A. Managed Pressure Drilling and the heave problem

During drilling operations, a drilling fluid called mud is pumped down through the drill string, through the drill bit at the bottom of the well, and up the annulus around the drill string. The mud serves several functions, like cooling down the drill bit and carrying cuttings out of the system. The mud also works to keep the pressure in the annulus at a desired level. This latter purpose is a crucial part of drilling, as the pressure needs to be kept within certain bounds to avoid fracturing of the formation or collapse of the well. Technologies developed with the aim of improving the pressure control throughout the well are often referred to as Managed Pressure Drilling (MPD).

The heave problem in MPD is a problem emerging when drilling offshore from a rig floating at the sea. The floating rig naturally moves up and down with the waves. During drilling, an active mechanism is used to keep the string from moving with the rig. However, every $27-29$ metres, it is necessary to stop the drilling to extend the drill string. During this procedure, the heave compensation mechanism is deactivated and the string is rigidly attached to the rig. The drill string then moves with the rig and acts as a piston on the mud in the well. Left uncompensated, this piston effect results in severe pressure fluctuations throughout the well, often exceeding the standard limits for pressure regulation accuracy in MPD, which are about ± 2.5 bar.

Traditional MPD has focused on maintaining a constant bottom hole pressure, but there may be situations where pressure regulation at other points in the well is preferable, e.g. at the bottom of a casing string (also known as a *casing-shoe*). Hence, the stage is set for application of the results of this paper.

B. Modelling

The following model was used in [18] to model the heave problem in MPD

$$p_t(z,t) = -\frac{\beta}{A_1}q_z(z,t) \tag{94a}$$

$$q_t(z,t) = -\frac{A_1}{\rho}p_z(z,t) - \frac{F_1}{\rho}q(z,t) - A_1 g \tag{94b}$$

$$q(0,t) = -A_2\bar{C}Z(t) \tag{94c}$$

$$p(l,t) = p_l(t) \tag{94d}$$

$$\dot{Z} = \bar{A}Z, \qquad Z(0) = Z_0 \tag{94e}$$

where l is the well depth, $z \in [0, l]$, $t \geq 0$, $p(z,t)$ is the pressure, $q(z,t)$ is the volumetric flow, β is the mud's bulk modulus, ρ is the mud density, A_1 is the cross sectional area of annulus, A_2 is the cross sectional area of the drill bit, F_1 is the friction factor and g is the gravity constant. $p_l(t)$ is the actuation, and its actuation device is assumed to have significantly faster dynamics than the rest of the system, so that actuator dynamics may be ignored. Also, $q(1,t)$ is assumed measured. A desired constant pressure at $z = \bar{z} \in (0, l)$ is stated as

$$p(\bar{z}, t) = p_{sp}. \tag{95}$$

The disturbance $Z(t)$ is assumed to be an autonomously driven harmonic oscillator, parametrized by a finite set $\{\omega_1, \omega_2, \ldots, \omega_n\}$ of known frequencies and

$$\bar{A} = \text{diag}\left(\begin{bmatrix} 0 & \omega_1 \\ -\omega_1 & 0 \end{bmatrix}, \ldots, \begin{bmatrix} 0 & \omega_n \\ -\omega_n & 0 \end{bmatrix}\right) \tag{96}$$

$$\bar{C} = \begin{bmatrix} 0 & 1 & 0 & 1 & \ldots & 0 & 1 \end{bmatrix} \tag{97}$$

with the pair $(\bar{A}, \bar{C})$ assumed observable. The model (94) was originally presented in [4], with the disturbance model (96)-(97) taken from [18].

C. Feasibility of design

System (94) will have to be mapped to the form (1) in order to use the results of the previous sections.

Lemma 8 (Modified from Lemma 10 in [18]): Assume $\bar{z} \in (0, l)$ and p_{sp} are given. Let

$$\bar{x} = \frac{\bar{z}}{l}, \tag{98}$$

then the transformation

$$u(x,t) = \frac{1}{2}\left[q(xl,t) + \frac{A_1}{\sqrt{\beta\rho}}\left(p(xl,t) - p_{sp} + \rho g l(x - \bar{x})\right)\right] \times e^{\frac{lF_1}{2\sqrt{\beta\rho}}(x-\bar{x})} \tag{99a}$$

$$v(x,t) = \frac{1}{2}\left[q(xl,t) - \frac{A_1}{\sqrt{\beta\rho}}\left(p(xl,t) - p_{sp} + \rho g l(x - \bar{x})\right)\right] \times e^{-\frac{lF_1}{2\sqrt{\beta\rho}}(x-\bar{x})} \tag{99b}$$

maps the system (94) to the form (1) with

$$X(t) = Z(t) \tag{100}$$

$$U(t) = \frac{1}{2}(q(l,t) - \frac{A_1}{\sqrt{\beta\rho}}(p_l(t) - p_{sp} + \rho g l(1 - \bar{x}))) \times e^{-\frac{lF_1}{2\sqrt{\beta\rho}}(1-\bar{x})} \tag{101}$$

$$\epsilon_1(x) = \epsilon_2(x) = \epsilon,\ c_1(x) = a_0 e^{\gamma x},\ c_2(x) = b_0 e^{-\gamma x} \tag{102}$$

$$q = -e^{-\gamma \bar{x}} \tag{103}$$

$$A = \bar{A}, \quad C = -e^{\frac{\gamma}{2}\bar{x}} A_2 \bar{C} \tag{104}$$

where

$$\epsilon = \frac{1}{l}\sqrt{\frac{\beta}{\rho}}, \quad \gamma = \frac{lF_1}{\sqrt{\beta\rho}} \tag{105}$$

$$a_0 = c_0 e^{-\gamma \bar{x}}, \quad b_0 = c_0 e^{\gamma \bar{x}}, \quad c_0 = -\frac{1}{2}\frac{F_1}{\rho}. \tag{106}$$

Moreover, the control objective (95) is transformed to (2) with $r = 1$.

Proof: We remove the constant term and shift the origin by defining

$$\bar{p}(z,t) = p(z,t) - p_{sp} + \rho g(z - \bar{z}) \tag{107}$$

from which we find

$$\bar{p}_z(z,t) = p_z(z,t) + \rho g \tag{108}$$

$$\bar{p}_t(z,t) = p_t(z,t). \tag{109}$$

This yields the following modified system

$$\bar{p}_t(z,t) = -\frac{\beta}{A_1} q_z(z,t) \tag{110a}$$

$$q_t(z,t) = -\frac{A_1}{\rho}\bar{p}_z(z,t) - \frac{F_1}{\rho} q(z,t) \tag{110b}$$

$$\bar{p}(l,t) = p_l(t) - p_{sp} + \rho g(l - \bar{z}). \tag{110c}$$

Consider now the diagonalizing change of variables

$$\bar{u}(z,t) = \frac{1}{2}\left(q(z,t) + \frac{A_1}{\sqrt{\beta\rho}}\bar{p}(z,t)\right) \tag{111a}$$

$$\bar{v}(z,t) = \frac{1}{2}\left(q(z,t) - \frac{A_1}{\sqrt{\beta\rho}}\bar{p}(z,t)\right) \tag{111b}$$

from which we find

$$\bar{u}_t(z,t) = -\sqrt{\frac{\beta}{\rho}}\bar{u}_z(z,t) - \frac{1}{2}\frac{F_1}{\rho}(\bar{u}(z,t) + \bar{v}(z,t)) \tag{112a}$$

$$\bar{v}_t(z,t) = \sqrt{\frac{\beta}{\rho}}\bar{v}_z(z,t) - \frac{1}{2}\frac{F_1}{\rho}(\bar{u}(z,t) + \bar{v}(z,t)). \tag{112b}$$

We scale the domain into $[0,1]$ by using $x = z/l$ and get rid of the terms $\bar{u}$ in (112a) and $\bar{v}$ in (112b) by defining

$$u(x,t) = \bar{u}(xl,t)e^{\frac{lF_1}{2\sqrt{\beta\rho}}(x-\bar{x})} \tag{113a}$$

$$v(x,t) = \bar{v}(xl,t)e^{-\frac{lF_1}{2\sqrt{\beta\rho}}(x-\bar{x})}, \tag{113b}$$

where (98) has been used. From (113) and (112), we obtain

$$u_t(x,t) = -\frac{1}{l}\sqrt{\frac{\beta}{\rho}}u_x(x,t) - \frac{1}{2}\frac{F_1}{\rho}v(z,t))e^{\frac{lF_1}{\sqrt{\beta\rho}}(x-\bar{x})} \tag{114}$$

$$v_t(x,t) = \frac{1}{l}\sqrt{\frac{\beta}{\rho}}v_x(x,t) - \frac{1}{2}\frac{F_1}{\rho}u(z,t))e^{-\frac{lF_1}{\sqrt{\beta\rho}}(x-\bar{x})} \tag{115}$$

which is on the form (1) with the coefficients given by (102) and (105)–(106). Composing the transformations (113), (111) and (107), we find (99).

The connection between $p_l(t)$ and $U(t)$ in (101) is verified by inserting $x = 1$ in (99b) and using (1d). The parameters in the boundary condition (1c) can be expressed by forming

$$u(0,t) + v(0,t)e^{-\frac{lF_1}{\sqrt{\beta\rho}}\bar{x}} = q(0,t)e^{-\frac{lF_1}{2\sqrt{\beta\rho}}\bar{x}} \tag{116}$$

and defining q, C as in (104) and (103), respectively. Lastly, by inserting $x = \bar{x} = \bar{z}/l$ into (99a) and (99b), we obtain

$$u(\bar{x},t) = \frac{1}{2}\left[q(\bar{x}l,t) + \frac{A_1}{\sqrt{\beta\rho}}\left(p(\bar{x}l,t) - p_{sp}\right)\right] \tag{117a}$$

$$v(\bar{x},t) = \frac{1}{2}\left[q(\bar{x}l,t) - \frac{A_1}{\sqrt{\beta\rho}}\left(p(\bar{x}l,t) - p_{sp}\right)\right]. \tag{117b}$$

Hence, the controller objective (95) is achieved if

$$u(\bar{x},t) = v(\bar{x},t), \tag{118}$$

thus, $r = 1$ in (2). ■

D. Simulations

We will test the controllers of Theorem 5 and 6 on the system (94). The system parameters used in the subsequent simulations are

$$\begin{aligned} \beta = 7317 \cdot 10^5 Pa,\ A_1 = 0.024\ m^2,\ \rho = 1250\ kg/m^3 \\ F_1 = 10\ kg/m^3 s,\ g = 9.81\ m/s^2,\ A_2 = 0.02\ m^2 \\ l = 3000\ m,\ p_{sp} = 350 \cdot 10^5\ Pa \\ \omega_1 = \frac{2\pi}{12}. \end{aligned} \tag{119}$$

Thus, the disturbance is a single harmonic of period 12 seconds. The chosen depth for pressure attenuation is 2000 m which corresponds to $\bar{x} = \frac{1}{3}$. The time-delayed control signal needed for the controller in Theorem 5 is generated using a transmission line. The observer poles were placed at $-0.15 \pm 0.02j$. To better see the effect of the controller, the system is initially left in open loop with the controller and observer switched on at $t = 40$.

Figure 1 shows the pressure distribution in the well for the recursive version of the controller in Theorem 5, with Figure 2 showing the pressure at the depth 2000 meters with a closer look from $t = 60$ seconds in Figure 2b. The applied controller inputs are shown in Figure 3. The equivalent plots for the pure state feedback version of the controller are given in Figures 4-6.

From Figure 2b and Figure 5b, it is seen that the effect of $Z(t)$ is strongly attenuated for both versions of the controller, with the amplitude of oscillations reduced from about 40 bar to about 0.7 bar for the recursive controller, and to approximately 0.1 bar for the pure state feedback controller. This constitutes to attenuation factors of approximately 60 and 400, respectively. The considerably improved level of attenuation for the pure state feedback version of the controller is justified by the robustness issues from using the recursive version of the controller, with the pure state feedback version relying on the actual system states rather than the stored inputs. The attenuation is extremely fast when using state feedback, and an exponential decay can be observed when using the observer generated states. This is in agreement with the theory that states attenuation in finite time for state feedback, while the observer provides exponentially converging state and disturbance estimates.

VI. Conclusions

We have generalized the results from [18], and derived a full state feedback law for disturbance attenuation at an arbitrary point in the domain for a class of systems described by linear 2×2 partial differential equations of the hyperbolic type, with the disturbance modelled as an autonomous, finite dimensional linear system affecting the PDE's left boundary, and actuation limited to the right boundary. The full state feedback law can be combined with an observer generating full state and disturbance estimates from sensing at the right boundary. The full state feedback law is formulated in two different

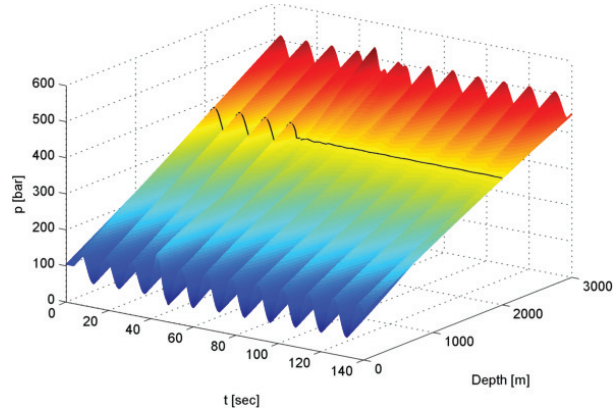

Fig. 1: Pressure distribution throughout the well for the recursive implementation using state feedback.

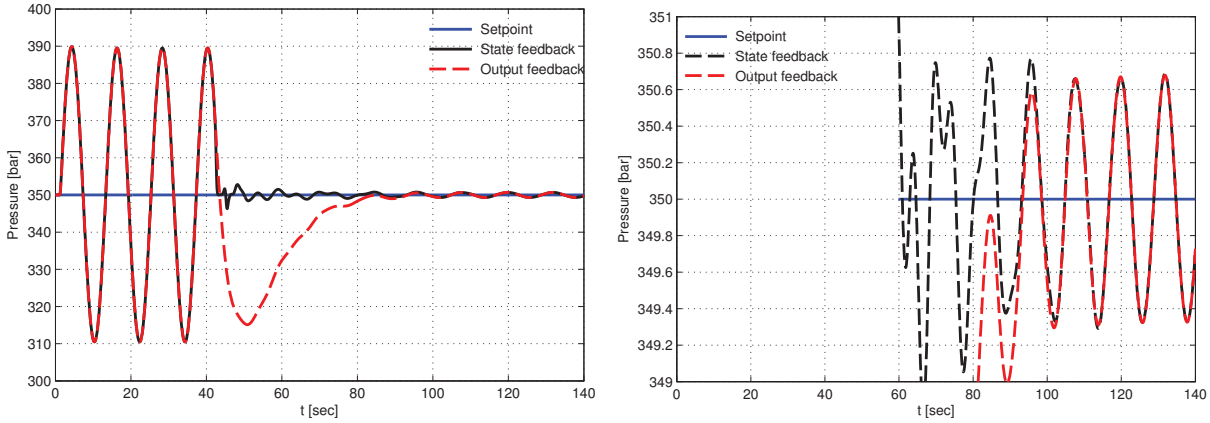

(a) Overview. (b) Zoomed in.

Fig. 2: Pressure at depth 2000 metres for the recursive implementation.

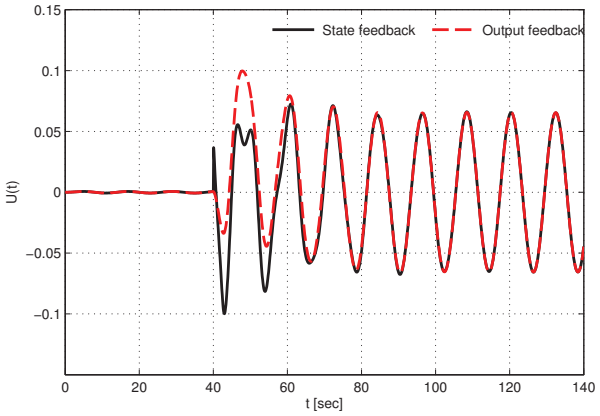

Fig. 3: Control input for the recursive implementation.

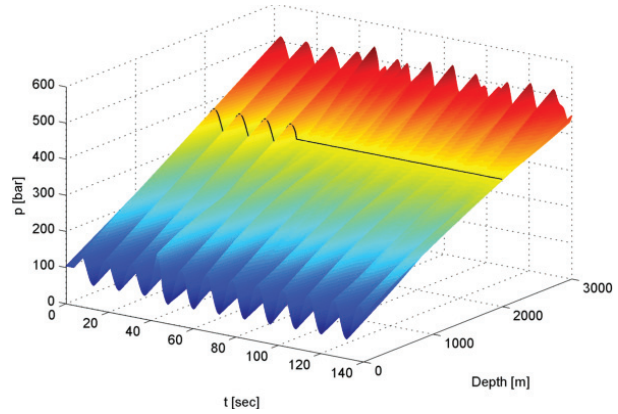

Fig. 4: Pressure distribution throughout the well for pure state feedback implementation using state feedback.

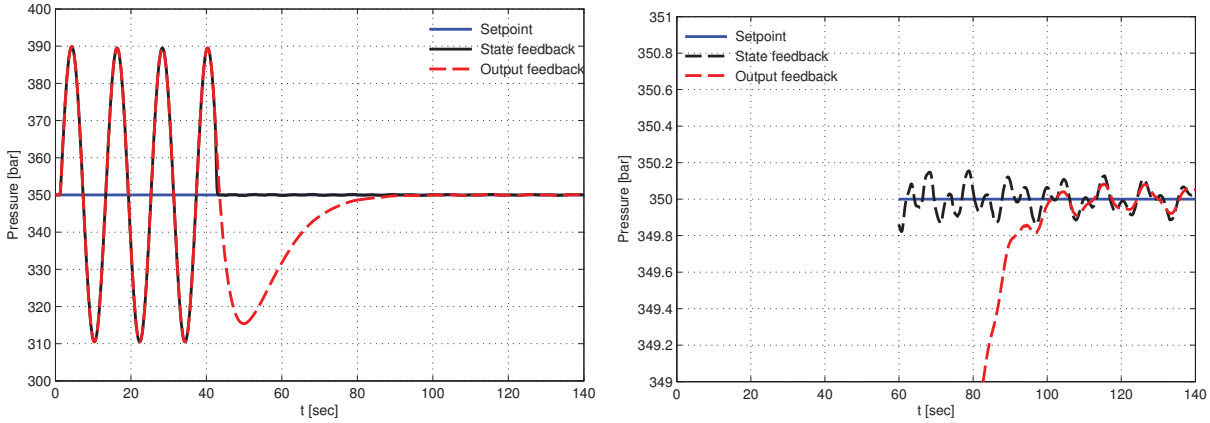

(a) Overview. (b) Zoomed in.

Fig. 5: Pressure at depth 2000 metres for the pure state feedback implementation.

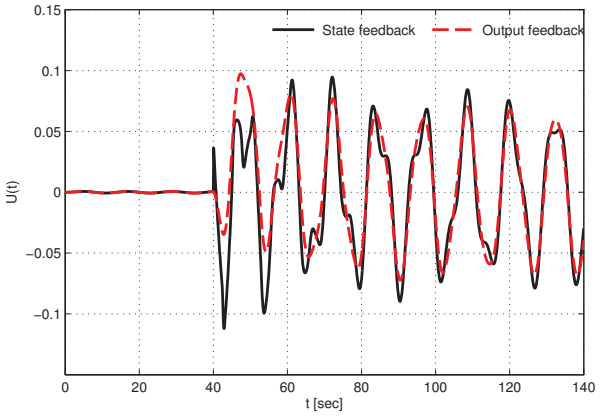

Fig. 6: Controller inputs for the pure state feedback implementation.

ways. One is recursive and requires storing a finite time-series of control inputs backwards in time, while the other one is a function purely in the system states at the current time.

Both formulations of the feedback law have been applied to the heave problem from the oil and gas industry, and showed significant attenuation properties.

REFERENCES

[1] M. Gugat and G. Leugering, "Global boundary controllability of the de St. Venant equations between steady states," *Annales de l'Institut Henri Poincare*, vol. 20, no. 1, pp. 1–11, 2003.

[2] M. Gugat and M. Dick, "Time-delayed boundary feedback stabilization of the isothermal Euler equations with friction," *Mathematical Control and Related Fields*, vol. 1, no. 4, pp. 469–491, 2011.

[3] C. Curró, D. Fusco, and N. Manganaro, "A reduction procedure for generalized Riemann problems with application to nonlinear transmission lines," *Journal of Physics A: Mathematical and Theoretical*, vol. 44, no. 33, p. 335205, 2011.

[4] I. S. Landet, A. Pavlov, and O. M. Aamo, "Modeling and control of heave-induced pressure fluctuations in managed pressure drilling," *IEEE Transactions on Control Systems and Technoloy*, vol. Preprint, p. Accepted for inclusion in a future issue, 2013.

[5] P. Goatin, "The aw-rascle vehicular traffic flow model with phase transitions," *Mathematical and Computer Modelling*, vol. 44, pp. 287–303, 2006.

[6] P. V. Kokotović, "The joy of feedback: nonlinear and adaptive," *Control Systems, IEEE*, vol. 12, no. 3, pp. 7–17, June 1992.

[7] M. Krstić and A. Smyshlyaev, *Boundary Control of PDEs*. Society for Industrial & Applied Mathematics, 2008.

[8] D. M. Bosković, M. Krstić, and W. Liu, "Boundary control of an unstable heat equation via measurement of domain-averaged temperature," *IEEE Transactions on Automatic Control*, vol. 46, no. 12, pp. 2022 –2028, dec 2001.

[9] A. Balogh and M. Krstić, "Infinite-dimensional backstepping-style feedback transformations for a heat equation with an arbitrary level of instability," *European Journal of Control*, vol. 8, pp. 165–177, 2002.

[10] W. Liu, "Boundary feedback stabilization of an unstable heat equation," *SIAM Journal on Control and Optimization*, vol. 42, pp. 1033–1043, 2003.

[11] O. M. Aamo, A. Smyshlyaev, M. Krstić, and B. A. Foss, "Stabilization of a Ginzburg-Landau model of vortex shedding by output feedback boundary control," in *CDC. 43rd IEEE Conference on Decision and Control*, vol. 3, 2004, pp. 2409–2416.

[12] R. Vazquez and M. Krstić, "Control of 1-D parabolic PDEs with Volterra nonlinearities, Part I: Design," *Automatica*, vol. 44, pp. 2778–2790, 2008.

[13] ——, "Control of 1-D parabolic PDEs with Volterra nonlinearities, Part II: Analysis," *Automatica*, vol. 44, pp. 2791–2803, 2008.

[14] A. Smyshlyaev and M. Krstić, *Adaptive Control of Parabolic PDEs*. Princeton University Press, 2010.

[15] M. Krstić and A. Smyshlyaev, "Backstepping boundary control for first-order hyperbolic PDEs and application to systems with actuator and sensor delays." *Systems & Control Letters*, vol. 57, no. 9, pp. 750–758, 2008.

[16] A. Smyshlyaev, E. Cerpa, and M. Krstic, "Boundary stabilization of a 1-d wave equation with in-domain antidamping," *SIAM Journal on Control and Optimization*, vol. 48, no. 6, pp. 4014–4031, May 2010.

[17] R. Vazquez, M. Krstić, and J.-M. Coron, "Backstepping boundary stabilization and state estimation of a 2x2 linear hyperbolic system," in *Decision and Control and European Control Conference (CDC-ECC), 2011 50th IEEE Conference on*, December 2011, pp. 4937 – 4942.

[18] O. M. Aamo, "Disturbance rejection in 2x2 linear hyperbolic systems," *IEEE Transactions on Automatic Control*, vol. 58, no. 5, pp. 1095–1106, 2013.

[19] H. Mahdianfar, O. M. Aamo, and A. Pavlov, "Attenuation of heave-induced pressure oscillations in offshore drilling systems," in *Proceedings of the 2012 American Control Conference*, 2012.